The Golgin GMAP-210
Functions and Mechanisms

Dissertation
der Fakultät für Biologie
der Ludwig-Maximilians-Universität München
Zur Erlangung des Doktorgrades der Naturwissenschaften
(Dr. rer. nat.)

vorgelegt von
Johannes Thilo Egerer
aus Marktredwitz

München am 25.März 2008

Rigorosum am Mittwoch 16.Juli 2008

Gutachter:

Prof. Nigg (Vorsitz)

Prof. MacWilliams

Prof. Boshart

Prof. Ackmann (Protokoll)

Prof. Soll

Prof. Jentsch

Ehrenwörtliche Versicherung und Erklärung über frühere Promotionsversuche

Hiermit versichere ich, Johannes Thilo Egerer, ehrenwörtlich, dass die vorgelegte Dissertation von mir selbständig und ohne unerlaubte Hilfe angefertigt ist. Des Weiteren erkläre ich, dass die vorgelegte Dissertation weder ganz noch in wesentlichen Teilen einer anderen Prüfungskommission vorgelegt wurde. Ich habe mich anderweitig keiner Doktorprüfung unterzogen.

München im Juli 2008

Johannes Egerer

Für meine Eltern, Rotraud und Gerhard Egerer

Zusammenfassung

Das Protein GMAP-210 (Golgi Mikrotubuli Assoziiertes Protein von 210 kDa) ist ein großes, Golgi lokalisiertes Protein mit ausgeprägten Doppelwendel Proteindomänen. Es ist Teil der lose definierten Proteinfamilie der Golgins, die an der Etablierung der Golgimorphologie und am vesikulären Transport im Bereich des Golgis beteiligt sind.

Unter Benutzung biochemischer, zellbiologischer und molekularbiologischer Methoden wurde GMAP-210 auf seine Golgilokalisierung, seine Interaktionspartner und seine Funktion im Aufbau und der Positionierung des Golgis untersucht.

In vitro und *in vivo* Experimente zeigten, dass GMAP-210 mittels seiner C-terminalen GRAB-Domäne an den Golgi bindet. Die vermutete Interaktion mit der kleinen GTPase Arf1 konnte, trotz überzeugender Hinweise, nicht abschließend geklärt werden. Die Bindung zwischen Arf1 und der GRAB-Domäne ist, bei Untersuchung des volllängen Proteins, nicht nachweisbar. Kurze C-terminale Fragmente, die die GRAB-Domäne enthalten, zeigen allerdings Interaktion mit Arf1. Dies deutet darauf hin, dass zur Bindung von GMAP-210 an den Golgi noch andere, regulierende Faktoren benötigt werden.

Ein Hefe 2-Hybrid Experiment, dass die gesamte Familie der kleinen Rab GTPasen auf Interaktion testete, konnte Rab1, dass am Golgi und im ER zu finden ist, als weiteren Interaktionspartner von GMAP-210 identifizieren. GMAP-210 wurde in Zellen auch an kleinen, vesikulären Strukturen gefunden, die zum Teil mit COPII und ERGIC53, Komponenten des frühen, sekretorischen Transportweges, überlappen. Dies ist ein weiterer wichtiger Hinweis darauf, dass GMAP-210 am Transport vom ER zum Golgi beteiligt ist, obwohl der Transport eines Modellsubstrats, des G-Proteins des vesikulären Stomatitis Virus (VSV-G), bei Abwesenheit von GMAP-210 nicht beeinträchtigt war. GMAP-210 funktioniert offenbar nur in spezialisierten, intrazellularen Transportwegen.

Reduzierung der GMAP-210 Proteinmenge in HeLa L Zellen mittels siRNA Technik veränderte die Golgimorphologie und führte dazu, dass der Golgi zu räumlich konzentrierten Ansammlungen von Vesikeln fragmentierte. Überexpression verursachte das Wachstum von langen, tubulären Strukturen aus dem Golgi. Beide morphologischen Effekte konnten allerdings nur in HeLa L Zellen beobachtet werden, nicht jedoch in *hTERT*-RPE1 Zellen. Da eine direkte Interaktion mit Mikrotubuli oder γ-Tubulin nicht gezeigt werden konnte, muss GMAP-210 die Golgimorphologie auf anderem Wege beeinflussen. Reduktion der GMAP-210 Menge durch siRNA zeigte ebenfalls, dass GMAP-210 mit dem intraflagellaren Transportprotein IFT20 interagiert. Das Protein befand sich nicht mehr am Golgiapparat, wenn die GMAP-210-Konzentration in der Zelle vermindert wurde. Die Interaktion beider Proteine ist direkt, GMAP-210 ist aber nicht an der Bildung des primären Ciliums in *hTERT*-RPE1 Zellen beteiligt, und der Verlust des Proteins IFT20 am Golgi verhinderte die Bildung des Ciliums ebenfalls nicht.

Diese Ergebnisse distinguieren GMAP-210 von den archetypischen Golgins, GM130 und p115, und lassen vermuten, dass GMAP-210 an einem hochspezialisierten Transportweg beteiligt ist, dabei aber trotzdem die Golgimorphologie in bestimmten Zelltypen beeinflussen kann.

Abstract

The protein GMAP-210 (Golgi Microtubule Associated Protein of 210 kDa) is a long coiled-coil protein, which localises to the Golgi apparatus. It is part of the loosely defined protein group of the golgins, which are involved in establishing the Golgi morphology and in vesicular trafficking around the Golgi.

By using biochemical, cell biological and molecular biological methods GMAP-210 was examined in regards to its Golgi targeting capability, its interaction partners and its function in establishing Golgi morphology and positioning.

In vitro and *in vivo* experiments showed that GMAP-210 targets to the Golgi via its C-terminal GRAB domain. Its proposed interaction with Arf1, however, could not be definitely determined, although there is strong evidence for it. Arf1 binding to the GRAB domain was hindered in the full-length protein, but not with short C-terminal fragments containing the minimal GRAB domain. This implies that additional factors are needed for GMAP-210 Golgi binding.

A yeast 2-hybrid screen of the entire family of small Rab GTPases identified the Golgi and ER localised Rab1 as a novel interaction partner of GMAP-210. GMAP-210 also labels vesicular tubular structures in the cell, which partially overlap with COPII and ERGIC53, components of the early secretory pathway. This gives additional evidence that GMAP-210 is involved in ER to Golgi transport. Trafficking of a model substrate, the vesicular stomatitis virus G-protein (VSV-G), however, was not impaired in the absence of GMAP-210. This indicates that GMAP-210 functions only in specialised transport pathways.

Knockdown of GMAP-210 in HeLa L cells by siRNA changed the Golgi morphology and the Golgi fragmented into a cluster of vesicles. Its overexpression caused the Golgi to grow long tubular structures. Both effects on morphology could only be observed in HeLa L cells, not in *hTERT*-RPE1 cells. As direct interaction with microtubules or γ-tubulin could not be detected, and GMAP-210 is therefore unlikely to affect Golgi morphology by directly perturbing microtubule function.

GMAP-210 knockdown by siRNA also showed its interaction with the intraflagellar transport protein IFT20. This protein lost its Golgi localisation when GMAP-210 was depleted. Both proteins interacted directly. GMAP-210, however, was not involved in primary cilium formation in *hTERT*-RPE1 cells and loss of IFT20 from the Golgi did not impair formation of the cilium, proposing that the Golgi pool of IFT20 had a function apart from intraflagellar transport and formation of the primary cilium.

These results set GMAP-210 apart from the archetypal golgins GM130 and p115 and indicate that GMAP-210 is involved in a highly specialised transport pathway, which could nevertheless influence the morphology of the Golgi apparatus in certain cell types.

Abbreviations

ADP	Adenosine 5'-Diphosphate
ALPS	ArfGAP1 lipid packing sensor
AMCA	6-((7-amino-4-methylcoumarin-3-acetyl)amino)hexanoic acid
Arf	ADP-ribosylation factor
Arl	ADP-ribosylation factor like
ATCC	American Type Culture Collection
ATP	Adenosine 5'-Triphosphate
BFA	Brefeldin A
cDNA	Complementary DNA
CGN	Cis-Golgi Network
CNAP	Chromosome Condensation-related SMC-associated Protein
COP	Coatomer Protein
DAPI	4',6-Diamidino-2-phenylindol
DNA	Deoxyribonucleic Acid
dNTP	Deoxynucleotide triphosphates
DMSO	Dimethylsulfoxide
E.coli	*Escherichia coli*
EDTA	Ethylenediamine Tetraacetic Acid
EEA	Early Endosome Antigen
EGFP	Enhanced Green Fluorescent Protein
EGTA	Ethylene Glycol Tetraacetic Acid
EM	Electron Microscope/-y
ER	Endoplasmic Reticulum
ERGIC	ER-Golgi Intermediate Compartment
FCS	Foetal Calf Serum
Fig.	Figure
GAP	GTPase Activating Protein
GDI	GDP Dissociation Inhibitor
GDP	Guanosine 5'-Diphosphate
GEP	Guanine Nucleotide Exchange Factor
GFP	Green Fluorescent Protein
GGA	Golgi-localising, γ-adaptin ear homology domain, Arf-binding protein

GL2	Firefly luciferase GL2
GM130	Golgi Matrix 130 kDa
GMAP-210	Golgi Microtubule Associated Protein of 210 kDa
GRASP	Golgi Reassembly and Stacking Protein
GRIP	Golgin-97 RanBP2alpha Imh1 p230/golgin-245
GRAB	GRIP Related Arf Binding
GS	Golgi SNARE
GST	Glutathione-S-Transferase
GTP	Guanosine 5'-Triphosphate
HeLa	Henrietta Lacks
6xHis	Histidine_6
HRP	Horseradish peroxidase
IFT	Intraflagellar Transport
IMAC	Immobilised Metal Affinity Chromatography
IP	Immunoprecipitation
IPTG	Isopropyl-β-D-thiogalactopyranoside
kb	kilobase
kDa	kilo Dalton
LAMP	Lysosome-associated Membrane Protein
LB	Luria-Bertani Broth
LiPEG	Lithium Polyethylene Glycol
MCS	Multiple Cloning Site
MES	2-(N-Morpholino)ethansulfonic acid
NEM	N-ethyl Maleimide
NLP	Ninein-like Protein
NSF	NEM Sensitive Factor
OD_{600}	Optical Density at 600 nm
PAGE	Polyacrylamide Gel Electrophoresis
PBS	Phosphate Buffered Saline
PCR	Polymerase Chain Reaction
PEG	Polyethylene Glycol
PFA	Paraformaldehyde
PMSF	Phenylmethylsulfonylfluorid

PIC	Protease Inhibitor Cocktail
Pipes	Piperazine-1,4-bis(2-ethanesulfonic acid)
PTEMF	Pipes Triton-X EDTA $MgCl_2$ Formaldehyde
RNA	Ribonucleic Acid
RPE1	Retina Pigment Epithelium 1
SC	Synthetic Complete
S.cerevisiae	Saccharomyces Cerevisiae
SDS	Sodium Dodecyl Sulphate
Sf9	Spodoptera frugiperda cell line 9
siRNA	Small interfering RNA
SMC	Structural Maintenance of Chromosomes
SNAP	Soluble NSF Attachment Protein
SNARE	SNAP Receptor
TCA	Trichloroacetic Acid
γTCC	γ-Tubulin Containing Complex
hTert	human Telomere reverse transcriptase
TE	10 mM Tris/HCl pH 7.5; 1 mM EDTA
Tev Protease	Tobacco etch virus Protease
TGN	Trans-Golgi Network
Tris	Trishydroxymethylaminomethane
γTuRC	γ-Tubulin Ring Complex
UTR	Untranslated Region
VSV-G	Vesicular Stomatitis Virus G-protein
Vti	Vps10p tail interacting
QDO	Quadruple Drop Out
YPDA	Yeast extract/Peptone/Dextrose/Adenine

Contents

1 Introduction **1**

1.1 The Mammalian Golgi Apparatus . . . 1

1.1.1 Golgi Morphology . . . 2

1.1.2 Golgi Matrix And Golgins . . . 2

Golgins . . . 2

GRASPs . . . 3

1.2 The Secretory Pathway . . . 4

1.2.1 ER To Golgi Transport . . . 4

1.2.2 Vesicular Traffic . . . 5

Coating . . . 5

Tethering . . . 7

SNAREs . . . 7

COPII-Coated Vesicles . . . 8

COPI-Coated Vesicles . . . 9

Cargo Receptor ERGIC-53 . . . 10

Cargo Receptor p24 Family . . . 10

1.3 Small GTPases . . . 10

1.3.1 Rab GTPases . . . 12

1.3.2 ADP-Ribosylation Factors . . . 13

ADP-Ribosylation Factor 1 . . . 14

ADP-Ribosylation Factor Like 1 And The GRIP Domain . . . 15

1.4 Golgi And The Cytoskeleton . . . 16

1.4.1 Microtubules, Dyneins And Kinesins . . . 16

1.4.2 Actin, Spectrin And Intermediate Filaments . . . 18

1.5 The Intraflagellar Transport System . . . 19

1.5.1 Cilia And Flagella: Morphology And Function . . . 19

1.5.2 Intraflagellar Transport . . . 21

1.5.3 Heterotrimeric Kinesin-II . . . 21

1.5.4 Intraflagellar Transport Protein of 20 kDa (IFT20) 22
1.6 Golgi-Microtubule Associated Protein 210kDa (GMAP-210) 22
1.6.1 General Aspects 22
1.6.2 Golgi Targeting 23
1.6.3 Function Of GMAP-210 As Microtubule Binding Protein 24
1.6.4 GMAP-210: GRIP Related Arf-Binding Domain 24
1.6.5 Overexpression And Knockdown: Effects On Transport 25
1.7 Aim Of This Work 26

2 Results **27**

2.1 GMAP-210 Is A Golgi Binding Protein 27
2.1.1 Tools For GMAP-210 Characterisation 27
Cloning Of GMAP-210 Full-Length, Fragments And Mutants 27
Polyclonal Antibodies Against GMAP-210 27
2.1.2 The C-Terminal GRAB Domain Of GMAP-210 Targets The Protein To The Golgi Apparatus 29
2.1.3 GMAP-210 N-terminus Does Not Target To The Golgi 32
2.1.4 Summary 33
2.2 The GMAP-210 GRIP Related ARF Binding Domain 35
2.2.1 GMAP-210 GRAB Domain Interacts With ADP-Ribosylation Factor Like 4A, C And D In A GTP Dependent Manner In Yeast 2-Hybrid Experiments 35
2.2.2 Transfected Arl4A, Arl4C And Arl4D Localise To The Plasma Membrane Of HeLa L Cells 39
2.2.3 Recombinant Arl4 Does Not Interact With Endogenous GMAP-210 In Pulldown Experiments 42
2.2.4 Arl4-GFP Does Not Co-Immunoprecipitate With Endogenous GMAP-210 From HeLa L Cells 42
2.2.5 *S.cerevisiae* Rud3p Also Interacts With *H.sapiens* Arl4 Family Members 45

2.2.6 The Small GTPase Arf1 Interacts With The GMAP-210 GRAB Domain . . . 46
2.2.7 Summary . . . 47
2.3 GMAP-210 siRNA Oligo Depletes Endogenous Protein And Causes Golgi Apparatus To Compact In HeLa L Cells . . . 48
2.3.1 Efficiency Of GMAP-210 3'-UTR siRNA Oligo Examined By Western Blot . . . 48
2.3.2 The Golgi Apparatus Compacts After GMAP-210 Knockdown . . . 49
2.3.3 Electron Microscopy Of HeLa L Golgi Apparatus After GMAP-210 Depletion . . . 51
2.3.4 After GMAP-210 Depletion, Expressed Protein Is Recruited To The Golgi Apparatus Independently Of GRAB Domain . . . 51
2.3.5 Summary . . . 54
2.4 GMAP-210 Co-Localises And Interacts With Markers From The ER-To-Golgi Pathway . . . 55
2.4.1 SNARES And Golgins Remain Localised To The Compacted Golgi Apparatus Upon GMAP-210 Knockdown . . . 56
2.4.2 GMAP-210 Interacts With The Rab GTPase Rab1 . . . 56
2.4.3 GMAP-210 Overlaps With The COPII Complex On A Subpopulation Of Vesicular Structures . . . 63
2.4.4 Peripheral GMAP-210 Signals Overlap With ERGIC53 . . . 63
2.4.5 Summary . . . 65
2.5 GMAP-210 siRNA Depletion Does Not Impair VSV-G Or Shiga Toxin B Subunit Trafficking . . . 67
2.5.1 Vesicular Stomatitis Viral G-Protein Is Transported To The Plasma Membrane At Normal Rates In GMAP-210 Knock-Down Cells . . . 67
2.5.2 Shiga Toxin B Subunit Is Internalised And Transported At Normal Rates In GMAP-210 siRNA Treated Cells . . . 68
2.5.3 Summary . . . 71
2.6 GMAP-210 Remains On Golgi Remnants After Brefeldin A Treatment And GMAP-210 Depletion Does Not Change Brefeldin A Effect On Cells . . . 71
2.6.1 Brefeldin A Effect On GMAP-210 Localisation . . . 71

2.6.2 Brefeldin A Induced Golgi Assembly and Disassembly After GMAP-210 Depletion . . . 73
2.6.3 Summary . . . 77
2.7 GMAP-210 Shows No Microtubule Interaction . . . 77
2.7.1 Transfection Of GMAP-210 Constructs Does Not Change The Microtubule Network In HeLa L . . . 77
2.7.2 GMAP-210 Depletion Does Not Disturb The Microtubule Network In HeLa L Cells . . . 79
2.7.3 GMAP-210 Does Not Interact With Taxol Stabilised Microtubules *in vitro* . . . 80
GMAP-210 N- And C-Terminus Do Not Bundle Microtubules *in vitro* 81
GMAP-210 Does Not Associate With Microtubules In Microtubule Spin-Down Assays . . . 82
2.7.4 GMAP-210 Has No Effect On Golgi Reassembly After Nocodazole Treatment . . . 83
2.7.5 GMAP-210 Is Not Associated With γ-Tubulin . . . 86
2.7.6 Summary . . . 88
2.8 GMAP-210 Recruits The Intraflagellar Transport Protein IFT20 To The Golgi Apparatus . . . 89
2.8.1 Tools For IFT20 . . . 89
IFT20: Cloning . . . 89
Database Information . . . 89
Polyclonal Antibodies Against IFT20 . . . 91
IFT20 siRNA And Antibody Specificity . . . 91
2.8.2 IFT20 Depletion Prevents Primary Cilium Formation . . . 93
2.8.3 GMAP-210 Depletion Prevents IFT20 Golgi Localisation . . . 94
2.8.4 GMAP-210 Does Not Localise On The Primary Cilium . . . 96
2.8.5 GMAP-210 siRNA Does Not Inhibit Primary Cilium Formation . . . 97
2.8.6 GMAP-210 Directly Interacts With IFT20 . . . 98
IFT20 Interacts With A Coiled-Coil Region Of GMAP-210 In Yeast 2-Hybrid . . . 99

IFT20 Co-Precipitates With GMAP-210 99

2.8.7 Heterotrimeric Kinesin II Is Not Associated With IFT20 On The Golgi Apparatus 100

Overexpressed Kif3B Does Not Localise To The Golgi Apparatus . 100

Kif3B Depletion Does Not Change Golgi Morphology 101

2.8.8 Summary 104

3 Discussion **105**

3.1 GMAP-210 Localises To The Golgi Apparatus And Vesicular Tubular Structures Of The Early Secretory Pathway 105

3.1.1 The C-Terminal GRAB Domain Is The Golgi Targeting Domain Of GMAP-210 105

3.1.2 GMAP-210 Localises To Vesicular Tubular Structures 107

3.1.3 Conclusion 107

3.2 GMAP-210 Depletion Does Not Block Intracellular Transport 108

3.3 GMAP-210 And The Microtubule Network 108

3.3.1 GMAP-210 Does Not Bind Directly To Microtubules 108

3.3.2 Nocodazole Induced Disassembly Of The Golgi Is Only Slightly Altered By GMAP-210 Depletion 109

3.3.3 GMAP-210 Is Not A γ-Tubulin Binding Protein 109

3.3.4 Conclusion 110

3.4 GMAP-210 Shows Interaction With Several Golgi Localised Proteins . . . 110

3.4.1 Binding Of The GRAB Domain To Arf1 Is Regulated 110

3.4.2 GMAP-210 Interacts With The Small GTPase Rab1 111

3.4.3 Conclusion 112

3.5 IFT20: An Unexpected GMAP-210 Interactor 113

3.5.1 GMAP-210 Interacts With IFT20 But Is Not Involved in Primary Cilium Formation 113

3.5.2 Conclusion 114

3.6 GMAP-210 And Golgi Morphology 116

3.6.1 Golgi Grows Tubules Upon GMAP-210 Overexpression 116
3.6.2 GMAP-210 Depletion Shrinks Golgi In HeLa L 116
3.6.3 Conclusion 117
3.7 Outlook 119

4 Materials And Methods 120

4.1 Materials And Reagents 120
4.1.1 Vectors And Plasmids 121
Parental Vectors 121
Plasmids 122
4.1.2 siRNA Oligos 122
4.1.3 Antibodies 122
Primary Antibodies 122
Secondary Antibodies 125
4.2 Bacterial Methods 126
4.2.1 Growth And Maintenance Of *E.coli* Bacteria 126
4.2.2 Bacteria Strains 126
4.2.3 Expression And Purification of Recombinant Protein From *E.coli* . 126
Culturing Of *E.coli* 126
Purification Of Recombinant, His-Tagged Protein Under Native Conditions 126
Purification Of Recombinant, His-Tagged Protein Under Denaturing Conditions 128
Purification of Recombinant Protein With GST- Or MBP-Tag . . . 128
4.3 Yeast Methods 129
4.3.1 Yeast Strain, Growth Medium and Culture 129
4.3.2 Transformation Of Yeast By The Frozen Cell Method 129
4.3.3 Yeast 2-Hybrid Method 130
4.4 DNA Methods 130
4.4.1 Cloning Strategies 130

4.4.2 Polymerase Chain Reaction (PCR) . . . 131
4.4.3 TA-TOPO Cloning . . . 132
4.4.4 Site-Specific Mutagenesis . . . 132
4.5 Protein Methods . . . 133
4.5.1 Determination of Protein Concentration . . . 133
4.5.2 Protein Precipitation . . . 133
4.5.3 SDS-PAGE (Polyacrylamide Gel Electrophoresis) . . . 134
4.5.4 Coomassie Staining of SDS-PAGE Gels . . . 134
4.5.5 Western Blotting . . . 134
4.5.6 Antibody Production And Purification . . . 135
4.6 Cell Culture Methods And Microscopy . . . 135
4.6.1 Mammalian Cell Culture . . . 135
Cell Lines . . . 135
Cell Growth Conditions And Growth Media . . . 136
4.6.2 Transient Transfection Of DNA Into Mammalian Cells . . . 136
4.6.3 RNA Interference . . . 136
4.6.4 Indirect Immunofluorescence . . . 137
Paraformaldehyde Fixation . . . 137
Methanol Fixation . . . 138
PTEMF Fixation . . . 138
Antibody Labelling Of Fixed Cells . . . 138
Immunofluorescence Microscopy . . . 138
Delta Vision Microscope . . . 139
4.6.5 Electron Microscopy . . . 139
4.6.6 Transport Assays . . . 139
VSV-G Transport Assay . . . 139
Shiga Toxin Uptake . . . 140
4.6.7 Drug Treatment . . . 140
4.7 Mammalian Biochemical Methods . . . 141

4.7.1 Protein Expression And Purification From Sf9 Cells With The Baculovirus System . . . 141
4.7.2 Preparation Of Rat Liver Golgi Membranes . . . 142
4.7.3 Preparation Of Mammalian Cell Extracts . . . 143
4.7.4 Preparation Of Tubulin From Pig Brain . . . 144
4.8 General Biochemical Methods . . . 144
4.8.1 Small GTPase Effector Pulldown From Cell Extracts . . . 144
Rab Effector Pulldown . . . 145
Arf-/Arl-Effector Pulldown . . . 145
4.8.2 Co-Immunoprecipitation From Cell Extracts . . . 146
4.8.3 Microtubule Assays . . . 146
In vitro Preparation Of Microtubules . . . 146
Microtubule Bundling . . . 146
Microtubule Spin-Down Assays . . . 147

A Plasmids Used **148**

1 Introduction

Eukaryotic cells are highly compartmentalised, which is one of the main features setting them apart from prokaryotes. These compartments are formed by membrane boundaries and are defined by unique lipid and protein composition They thus provide unique environments within the cell. Compartmentalisation gives the cell the ability to conduct a great variety of different processes necessary for cell survival and function. It allows for basic functions like protein and lipid synthesis, modification, degradation and transport to take place in a coordinated fashion.
Proteins and lipids have to be specifically distributed to the respective compartment, where they are further processed or fulfil their biological function. The distribution of proteins within the cell is orchestrated in a tightly controlled series of steps in transport pathways, which bridge specific donor and acceptor compartments. The transport pathways make use of vesicles, themselves small membrane compartments usually less than 100 nm in size (Palade, 1975; Dunphy and Rothman, 1985). The formation, loading, locomotion and incorporation of cargo into these compartments is regulated by proteins and lipids.
Although this complex web of interacting molecular mechanisms and pathways was studied intensively in the last years, a great amount of questions and problems still remain to be solved.

1.1 The Mammalian Golgi Apparatus

The Golgi apparatus in mammalian cells is a membrane structure composed of stacked cisternae, which are linked into ribbons. It is situated in the perinuclear region of the cell (Palade, 1975). The Golgi apparatus is the central organelle of intracellular transport. Proteins are post-translationally modified, while transported through the Golgi, before they are sorted and transported to the plasma membrane or their destination in the endosomal and lysosomal system (Farquhar and Palade, 1998).
As the central hub for transport, the Golgi receives a constant influx and efflux of proteins and it is clear, that the Golgi is not a static organelle, but highly dynamic (Barr and Warren, 1996). That it nevertheless keeps its size, position and composition is a hint at the immense amount of control that is exerted on intracellular trafficking, which unavoidably passes through the Golgi (Rothman *et al.*, 1982).

1.1.1 Golgi Morphology

The Golgi was discovered by Camillo Golgi in the year 1898 (Golgi, 1898) as a reticulate structure in silver stained Purkinje cells. Since then, and especially in the recent years, much has been discovered about Golgi morphology, structure and function.
The stacked Golgi is polarised along the vector of intracellular traffic. Its stacked cisternae can be subdivided into three regions (Schweizer *et al.*, 1988; Griffiths and Simons, 1986). The side, which receives synthesised material from the endoplasmic reticulum is called cis-Golgi, followed by the medial and the trans-Golgi. Beyond the trans-Golgi is a system of tubular Golgi membranes, called the trans-Golgi network (TGN) where secreted material is sorted and transported to the respective target compartment. A similar structure is observed at the cis-face, which is accordingly called cis-Golgi network (CGN). The CGN is also called the Vesicular Tubular Compartment (VTC) or ER-Golgi-Intermediate Compartment (ERGIC) (Appenzeller-Herzog and Hauri, 2006).

1.1.2 Golgi Matrix And Golgins

The Golgi is composed of membranous flattened cisternae, which are stacked onto each other. These stacks stay attached when Golgi membranes are purified (Morre and Mollenhauer, 1964; Morre *et al.*, 1970), indicating anchors, which tether the cisternae together. Additionally, detergent extraction of these isolated membranes leaves a proteinaceous exoskeleton with the characteristic organisation of Golgi cisternae (Slusarewicz *et al.*, 1994). Members of this putative Golgi matrix behave in a special way upon disassembly of the Golgi. After inhibition of ER-to-Golgi transport by the fungal compound Brefeldin A or overexpression of the dominant negative form of the small GTPase Sar1, most Golgi resident enzymes redistribute back to the ER. Golgi matrix proteins, however, were found attached to small Golgi remnants, which are distributed near the ER-exit-sites (Seemann *et al.*, 2000; Ward *et al.*, 2001) throughout the cell.
Two classes of proteins are implied in Golgi matrix formation, the Golgi Reassembly and Stacking Proteins (GRASP) and the golgins.

Golgins Golgins have initially been identified as cause for a variety of autoimmune diseases. Their tertiary structure contains long coiled-coil stretches, giving them a rod-like structure (Barr and Short, 2003; Gillingham and Munro, 2003). Furthermore, most of them interact with small Ras-like GTPases (Short *et al.*, 2005) of the Rab or ADP-ribosylation factor families (see 1.3, p.10*ff*). Golgins are not only responsible for maintenance of the Golgi matrix but also for several other functions (Barr and Short, 2003;

Gillingham and Munro, 2003).
GM130, p115 and giantin are believed to be central players in establishing Golgi structure by tethering arriving vesicles to cisternae (Cao *et al.*, 1998; Seemann *et al.*, 2000; Sonnichsen *et al.*, 1998). GM130 is linked to the Golgi cis-face by GRASP65 and is the acceptor for vesicle-bound p115 or a complex made up of p115 and the type II transmembrane golgin giantin.
p115 is a myosin shaped homodimer with an N-terminal globular head domain, a coiled-coil tail and a short acidic domain in the C-terminus (Sapperstein *et al.*, 1995). It acts in tethering in the early secretory pathway and it is necessary for proper SNAREpin formation during vesicle fusion (Shorter *et al.*, 2002). It binds the GTPase Rab1 with its globular head domain. Its acidic C-terminus interacts with the basic N-terminal motif of GM130 (Sonnichsen *et al.*, 1998). GM130 forms a homodimer (Nakamura *et al.*, 1997) and interacts with the Golgi localised GRASP65 by a C-terminal motif (Barr *et al.*, 1998). It also binds to the small GTPases Rab1, Rab2 and Rab33b (Barr and Short, 2003). Giantin is a 400 kDa transmembrane protein with a large N-terminal, cytosolic coiled-coil domain (Linstedt and Hauri, 1993). Giantin localises mainly at the edges of the Golgi stack and binds p115 by its N-terminus just like GM130 (Sonnichsen *et al.*, 1998). The cis-Golgi localised type II transmembrane protein Golgin-84 has also been proposed to be involved in Golgi structure maintenance, although it does not behave like Golgi matrix proteins in respect to Brefeldin A treatment, as Golgin-84 redistributes to the endoplasmic reticulum (Diao *et al.*, 2003). While the Golgi matrix proteins described above influence Golgi cisternae stacking, Golgin-84 is involved in lateral Golgi organisation (Diao *et al.*, 2003; Satoh *et al.*, 2003). Overexpression and depletion of the protein cause fragmentation of the Golgi ribbon (Diao *et al.*, 2003). Depletion also reduces ER-to-Golgi transport and increases the ER volume (Diao *et al.*, 2003). Interaction of Golgin-84 with the small GTPase Rab1 gives further evidence that Golgin-84 is involved in ER-to-Golgi trafficking (Satoh *et al.*, 2003).

GRASPs In mammalian cells, two GRASP proteins exist, GRASP65 and GRASP55 (Barr *et al.*, 1997; Shorter *et al.*, 1999). GRASP65 is located on the cis-Golgi where it recruits GM130 to the membrane surface (Barr *et al.*, 1998), GRASP55 at the medial-Golgi recruits Golgin-45 (Short *et al.*, 2001). GRASPs are peripheral membrane proteins targeted to the membrane by N-terminal myristoylation (Short *et al.*, 2005). Both proteins are required for Golgi stacking and their phosphorylation is involved in Golgi fragmentation during mitosis (Sutterlin *et al.*, 2002; Preisinger *et al.*, 2005).

1.2 The Secretory Pathway

1.2.1 ER To Golgi Transport

The Golgi is the central organelle in intracellular transport and secretion (Palade, 1975) (Fig.1). Membrane and lumenal proteins are synthesised by ribosomes, which are located on the nuclear envelope and the rough ER (Shibata *et al.*, 2006). The newly synthesised polypeptide is, most of the time co-translationally, translocated into the ER lumen. They fold into their native conformation most often by the help of chaperons like calnexin and calreticulin (Nehls *et al.*, 2000). Properly folded proteins are labelled by the quality control machinery in the ER for export. Golgi-bound vesicles are formed in the transitional part of the smooth ER at so-called ER exit sites (ERES) (Bannykh *et al.*, 1996). Cargo is recruited into vesicles, which are formed by the COPII coat machinery (Fig.2, p.6). COPII coated vesicles undergo homotypic fusion and form the ERGIC (Appenzeller-Herzog and Hauri, 2006). These ER-Golgi-intermediate compartments are transported by microtubule based motors to the cis-face of the Golgi apparatus and fuse (Allan *et al.*, 2002). Cargo escaped from the ER or cargo receptors ready to be recycled for another round of ER export are transported back to the ER in COPI-coated vesicles (Wieland and Harter, 1999).

The mechanism by which transport from the ERGIC to the TGN happens is still controversial. One model is the cisternal maturation model (Allan and Balch, 1999). ERGICs travel to the cis-face of the Golgi and undergo homotypic fusion in order to form new cis-Golgi cisternae. At the same time COPI coated vesicles travel in retrograde direction, not only to recycle proteins to the ER, but also to retrieve proteins from the medial and trans-Golgi cisternae. Thus, cis-Golgi cisternae mature gradually to medial and trans cisternae.

In the stable cisternae model (Rothman, 1994), cisternae remain unchanged. ERGIC fuses with the cis-Golgi or sends forth anterograde transport vesicles. At cis-Golgi proteins are modified and transferred to medial- and trans-Golgi cisternae by anterograde, COPII coated vesicles. COPI coated retrograde transport vesicles would then be responsible for retrieval of escaped early Golgi and ER-resident proteins.

Whichever is the mode of Golgi transition, proteins are then packaged into clathrin coated vesicles at the trans-Golgi network (TGN) and exported to endosomes and lysosomes or into exocytic transporters, which are destined directly to the plasma membrane for exocytosis (Maxfield and McGraw, 2004).

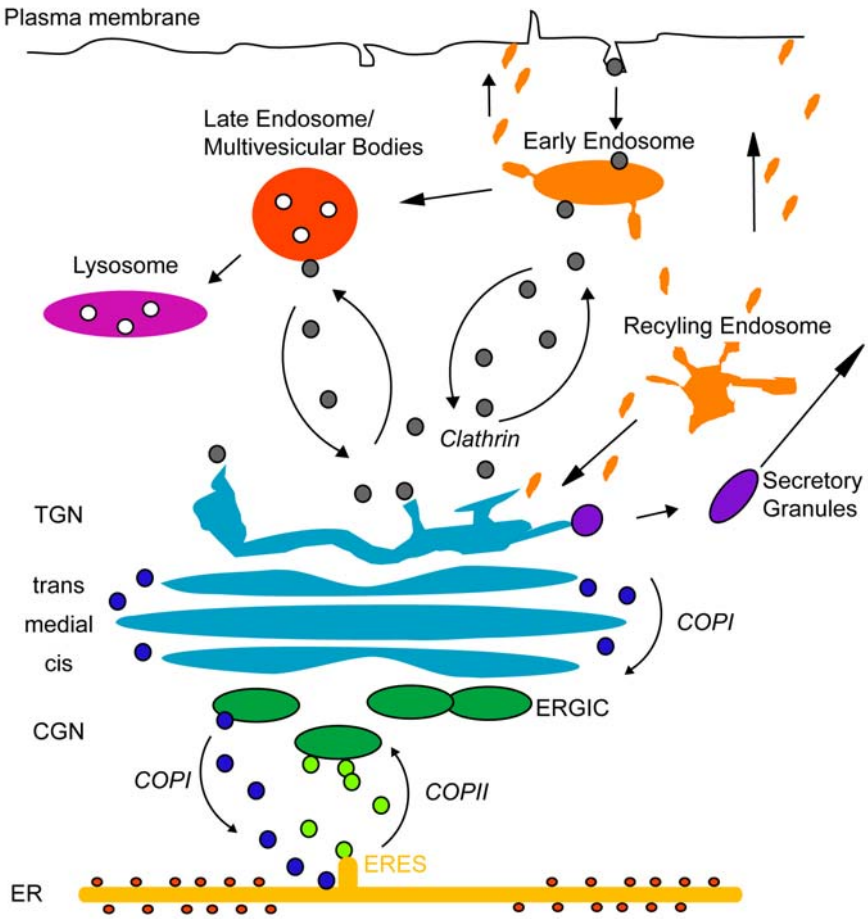

Figure 1: **Schematic View Of Intracellular Traffic.** Schematic view of compartments and cargo carriers of the secretory and endocytic pathway; dark blue: COPI vesicles; light green: COPII vesicles; grey: clathrin coated vesicles; orange: endocytic carriers; white: internal vesicles of multivesicular bodies; arrows specify routes of transport; not drawn to scale.

1.2.2 Vesicular Traffic

Intracellular traffic is performed in vesicular cargo carriers (Palade, 1975; Novick *et al.*, 1980; Balch *et al.*, 1984). These carriers form from donor membranes, travel to the acceptor membrane and fuse with it (Fig.2). These events follow the same principle irrespective of the donor and acceptor membranes. However, the proteins and protein complexes involved in these processes are mostly different.

Coating Biogenesis of vesicles occurs by a process called coating (Kirchhausen, 2000; Bonifacino and Lippincott-Schwartz, 2003). In the region of the donor membrane where vesicles bud off, the coat complexes are recruited by activated, small GTPases and assemble into a cage-like structure (Fig.2A and B) which deforms the membrane into a vesicle bud and eventually pinches off the membrane (Fig.2B). However, the structural

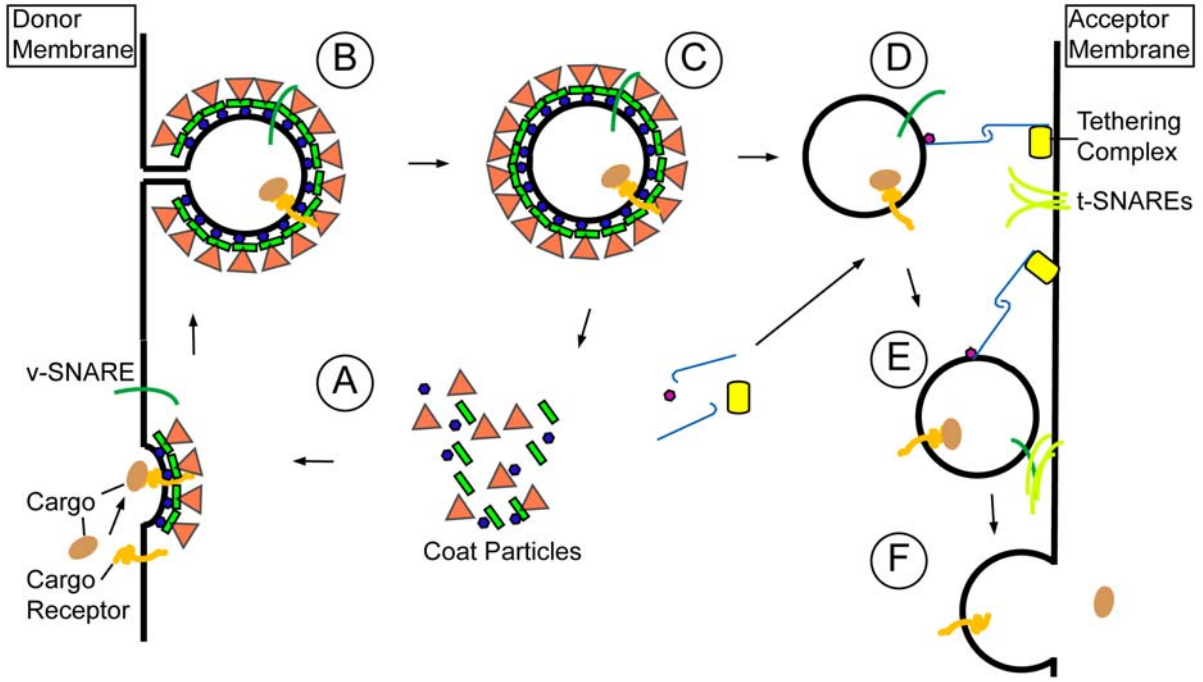

Figure 2: **Schematic Summary Of Vesicular Transport From Budding To Fusion.** The Schematic shows the principle of vesicle biogenesis at the donor membrane and fusion with the acceptor membrane as described in the text; A: Bud Initiation; B: Pinch-off; C: Uncoating; D: Tethering; E: Docking; F: Fusion; v-SNAREs are mostly R-SNAREs, t-SNAREs mostly Q-SNAREs; not drawn to scale; inspired by Bonifacino and Glick (2004)

deformation of membranes is not the only function of coat proteins. They also interact with recognition motives in cargo proteins and concentrate them in the budding vesicle. These cargo proteins are often transmembrane proteins that interact with coat proteins by their cytoplasmic domain (Fig.2A and B). They themselves may be cargo receptor proteins, which bind soluble proteins in the lumen of the compartment and thus recruit them specifically to the carrier vesicle (e.g. the lectin ERGIC53, (Hauri *et al.*, 2000)). Another functional class of proteins, the SNAREs (SNAP receptors), are also recruited to the membrane of the budding vesicle and are necessary for vesicle fusion with the target membrane (Sollner *et al.*, 1993; Short and Barr, 2004). Furthermore, molecular motors and their cargo adaptors are often needed on the vesicle to give them directed motility. They are recruited from the cytosol after coat disassembly (Allan *et al.*, 2002).
At some point in the budding process, the GTP hydrolysing activity of the coat initiating small GTPase is triggered by a GTPase activating protein (GAP) and the coat disassembles (Kirchhausen, 2000). Subsequently, the vesicle is prepared for fusion with the target membrane by recruiting additional factors for tethering and priming the SNAREs (see Fig.2 A, B and C).

Tethering When reaching the acceptor membrane, vesicles undergo a process called tethering (Fig.2D), in which long coiled-coil proteins, so-called golgins, and protein complexes (e.g. TRAPP, Exocyst, VFT, HOPS) establish long-range contact between the membranes (Shorter and Warren, 1999; Sonnichsen *et al.*, 1998). These tethers are often recruited to donor and acceptor domains by small, Ras-like GTPases. In the case of the Golgin p115 (Uso1p in *S.cerevisiae*) this is Rab1 (Ypt1 in *S.cerevisiae*) (Allan *et al.*, 2000; Cao *et al.*, 1998). Other golgins have also been reported to bind to Golgi-Reassembly-and-Stacking-Proteins (GRASPs), like GM130, which binds to GRASP65 (Barr *et al.*, 1998). After establishing a first contact between vesicle and acceptor membrane, vesicle diffusion is limited. The tether collapses the vesicle onto the target membrane to reduce the distance between the surface of the two bilayers and the actual fusion is initiated by the SNARE proteins (Fig.2 E and F).

SNAREs SNAREs are proteins with a C-terminal α-helical transmembrane anchor, or, as in the example of Ykt6 or SNAP-25, with a C-terminal lipid moiety for membrane insertion (Nichols and Pelham, 1997). The N-terminus is variable and the middle part consists of heptad repeats of hydrophobic amino acids. This allows the protein to form coiled-coils of α-helices, which are able to form a bundle of four parallel helices with other SNARE proteins (Weber *et al.*, 1998). This finally drives merging of the membranes and the fusion of the vesicle with the target membrane (Weber *et al.*, 1998). SNAREs are divided into four classes: R-SNAREs with an arginine residue in the centre of the SNARE domain and Q_a-, Q_b-, Q_c-SNAREs with a glutamine instead of arginine. Each SNARE bundle, also called SNAREpin, consists of one of each R-, Q_a-, Q_b- and Q_c-SNARE (Weimbs *et al.*, 1997; Fasshauer *et al.*, 1998; Bock *et al.*, 2001).
SNAREs localised to the same membrane compartment are found assembled into cis-SNARE complexes and would thus be unable to drive membrane fusion. They have to be primed, which is done by the cytosolic NSF (N-ethylmaleimide sensitive fusion protein) (Hanson *et al.*, 1995, 1997). This is an ATPase associated with diverse cellular activities (AAA), which is recruited to SNARE bundles by a second soluble factor: SNAP (α-, β- or γ-soluble NSF attachment proteins)(Clary *et al.*, 1990). NSF is inactivated by N-ethylmaleimide's cysteine alkylating activity, thus its name. NSF hydrolyses ATP, delivering the needed energy to unravel the SNARE bundle leaving the single SNAREs in an energy rich state (Wilson *et al.*, 1992; Whiteheart *et al.*, 1992). This is believed to overcome the energy barrier of membrane fusion. How specificity of SNARE bundling is achieved is still unknown, but it is suspected, that the factor Sec1/Munc18 (SM proteins)

could interact with SNAREs (Nichols and Pelham, 1997), probably on their N-terminus and act as fusion inhibitor until the vesicle reaches the proper target membrane. Vesicle tethers, like p115, are also supposed to prevent premature SNAREpin formation (Shorter *et al.*, 2002).

COPII-Coated Vesicles COPII-coated vesicles are carriers of the anterograde transport from the ER to the ER-Golgi-Intermediate Compartment (ERGIC) (Barlowe *et al.*, 1994). They might also be involved in the anterograde transport of cargo from cis-Golgi to later Golgi cisternae. The 60-100 nm sized COPII vesicles form at ER exit sites (ERES), stable membrane domains on the smooth ER (Murshid and Presley, 2004).
COPII-coat formation is initiated by the GTP-bound Ras-like GTPase Sar1. This GTPase recruits the coat complex Sec23/24 from the cytosol to the endoplasmic reticulum membrane to form the "pre-budding complex" (Bonifacino and Glick, 2004). Prior to this, Sar1 is activated by the guanine nucleotide exchange factor (GEF) Sec12 by inducing the exchange of GDP to GTP in the centre of Sar1 (Barlowe and Schekman, 1993). The pre-budding complex recruits a heterotetramer, containing two Sec13 and two Sec31 subunits, which form a mesh-like scaffold on top of the Sar1-Sec23/24 coat (Lederkremer *et al.*, 2001). The polymerising coat deforms the membrane to form a bud, which eventually pinches off the membrane. Whether the neck of the nascent vesicle is closed by coat protein or if there is a factor, which helps this process is presently unknown (Bonifacino and Glick, 2004).
The hydrolysis of Sar1 is activated by the Sec23 subunit of the coat complex. Additionally, Sec13/31 improve the GAP-activity of Sec23 (Bi *et al.*, 2002). Inactivation of Sar1 leads to uncoating of the vesicles. How this is coordinated on a temporal scale, so that the nascent vesicle is not uncoated too early, is still subject of speculation.
While the vesicle is formed it is loaded with cargo at the same time. Transmembrane cargo proteins bind directly to the COPII coat, whereas soluble cargo binds indirectly by the means of cargo receptors (Appenzeller *et al.*, 1999; Muniz *et al.*, 2000; Powers and Barlowe, 2002). The receptors unload their cargo at the target compartment. Cargo and cargo receptors show specific recruitment signals in their cytoplasmic tail. Most common motifs are di-acidic ([DE]X[DE]) (Nishimura and Balch, 1997) or short hydrophobic sequences (FF, YYM, FY, LL, IL) (Kappeler *et al.*, 1997; Nakamura *et al.*, 1998). For ER export signal recognition the Sec24 component is the major player (Barlowe, 2003). In humans there are four Sec24 isoforms, each of, which show three different cargo binding sites. As there are also two isoforms of Sar1 and two Sec23 isoforms, it is likely that specificity of cargo recruitment can be regulated and that specialised COPII vesicles exist for different species of cargo (Fromme and Schekman, 2005). Important cargo receptors

like p24 and ERGIC-53 are discussed below. After uncoating, the COPII vesicles are tethered to each other and undergo homotypic fusion to form the ERGIC. The tethering agents are p115/Uso1p and Rab1 (Cao *et al.*, 1998; Allan *et al.*, 2000). Rab1 is activated by its GEF (Allan *et al.*, 2000; Cao *et al.*, 1998), which is in fact a component of the seven subunit comprising complex called "transport protein particle I" (TRAPPI)(Wang *et al.*, 2000), and recruited to the COPII vesicle by the Sec23 COPII subunit (Cai *et al.*, 2007). Vesicle fusion is driven by the SNAREs, which form SNAREpins of three Q-SNAREs and one R-SNARE (see 1.2.2, p.7)(Fasshauer *et al.*, 1998). In the early secretory pathway five SNAREs have been identified, which are Syntaxin5 (Sed5p), Ykt6 (Ykt6p) as Q-SNAREs and Sec22 (Sec22p), Bet1 (Bet1p) and Membrin (Bos1p) as R-SNAREs (Nichols and Pelham, 1997).

COPI-Coated Vesicles COPI coatomer vesicles are also part of the early secretory pathway. They are important for retrograde traffic from Golgi-to-VTC-to-ER, but also for retrograde traffic within the Golgi, where it recycles early Golgi proteins back to further cis-localised cisternae (Kirchhausen, 2000; Murshid and Presley, 2004). Transport from Golgi to ER or VTC to ER is especially needed to recycle cargo receptors of the anterograde pathway, like p24 or ERGIC-53 (Letourneur *et al.*, 1994; Fiedler *et al.*, 1996). Cargo is recruited by the γCOP subunit, which recognizes a di-lysine (KKXX, KXKXX) signal (Harter *et al.*, 1996). The multi-spanning membrane protein KDEL receptor retrieves proteins by their lumenal KDEL signal and recruits them to the COPI vesicles (Pellham, 1990).

COPI is a seven subunit complex (α, β, β', γ, δ, ϵ, ζ) (Kirchhausen, 2000). COPI formation is initiated by the GTP-bound, active Arf1 GTPase. This GTPase is activated by its early Golgi localised guanine nucleotide exchange factor (GEF) GBF1 (Kawamoto *et al.*, 2002; Zhao *et al.*, 2002; Garcia-Mata *et al.*, 2003). Arf1 binds directly to the β- and γ-subunit (Majoul *et al.*, 2001; Zhao *et al.*, 1999). The remaining components are then recruited to the complex, together with cargo, cargo receptors and the Arf1 GTPase activating protein ARFGAP (Goldberg, 1999). COPI and ARFGAP stimulate hydrolysis of Arf1 bound GTP and thus inactivation, which leads to subsequent uncoating of vesicles (Kirchhausen, 2000).

Tethering of retrograde intra-Golgi transport vesicles happens most probably by the interaction of giantin and p115 with GM130 (Sonnichsen *et al.*, 1998). Another tethering complex implied in COPI retrograde trafficking is the COG complex, which is composed of eight subunits (Ungar *et al.*, 2006). Whether it is a tether for specific COPI vesicles or co-acts with the p115-GM130-Giantin tether is yet unknown.

Cargo Receptor ERGIC-53 One important cargo receptor incorporated into COPII vesicles is the lectin ERGIC-53 (ER-Golgi-Intermediate Compartment Protein of 53kDa; p58 in rat) (Hauri *et al.*, 2000). This type I transmembrane protein is most concentrated in the vesicular-tubular clusters, but could also be found in the ER and cis-Golgi. ERGIC-53 contains a CRD (carbo-hydrate recognition domain) in its N-terminal, lumenal domain. It binds soluble D-Mannose glycoproteins from the ER lumen and recruits them into the nascent vesicle. ERGIC-53 forms homodimers and homohexamers (Schweizer *et al.*, 1988; Lahtinen *et al.*, 1992) by disulfide bridging.
In its cytosolic C-terminus, ERGIC-53 also shows a di-lysine KKXX signal, which allows it to be sorted back to the ER by the COPI vesicle coat (Schindler *et al.*, 1993). Thus ERGIC-53 cycles from the ER to the ERGIC and cis-Golgi by the anterograde transport machinery and is retrieved to the ER by retrograde transport.

Cargo Receptor p24 Family Members of the p24 cargo receptor family are transmembrane proteins with a short C-terminal stretch, which contains recognition signals for COPI- and COPII-coat recruiting (Dominguez *et al.*, 1998; Stamnes *et al.*, 1995; Rojo *et al.*, 1997). p24 family members cycle between ER and Golgi, transporting lumenal cargo (Muniz *et al.*, 2000; Dominguez *et al.*, 1998). It has been found that oligomers of some p24 family members interact with GRASPs (see 1.1.2, p.2) by their cytoplasmic domain and that this interactions prevents p24 export to the cell surface (Barr *et al.*, 2001).

1.3 Small GTPases

Rab- and Arf-Proteins are small monomeric GTPases or guanine nucleotide binding proteins (GNBPs). They are part of the Ras superfamily (Pereira-Leal and Seabra, 2000; Burd *et al.*, 2004), which also includes Ras, Rho/Rac and Ran. They are 20 to 25 kDa in size and regulate growth, motility and trafficking by acting as molecular switches. They change from an inactive, GDP-bound to an active, GTP-bound state in a regulated and timed manner.
All small G-proteins (which also include the α subunit of the heterotrimeric G-Protein and factors of protein synthesis) have a common structural feature, the G-domain (Vetter and Wittinghofer, 2001). The G-domain is a α-β-structure made from a mixed 6-stranded beta sheet and five helices located on both sides. The catalytic centre contains a Mg^{2+} ion and the guanosine nucleotide, which is bound between the P-loop and the two switch regions, switch I and II. In the active form, the switch regions build hydrogen bonds to the γ-phosphate of GTP by conserved threonine and glycine residues. The conformation

is often compared to a loaded spring mechanism, as hydrolysis of the GTP releases the two switch regions and leads to profound conformational changes.

As both, the GDP to GTP exchange and the GTP hydrolysis are rather slow, accessory proteins are needed to accelerate the processes. For activation GNBPs interact with guanine nucleotide exchange factors (GEFs) (Klebe *et al.*, 1995), for inactivation they depend on the GTPase activating proteins (GAPs) (Scheffzek *et al.*, 1998). The conformational change during activation of the GTPase allows effectors to bind with the GTPase and form an active complex.

Mutations in two conserved residues of Ras have been found to lock the protein in one of the two conformations, active or inactive. Mutation of threonine 35 to asparagine keeps

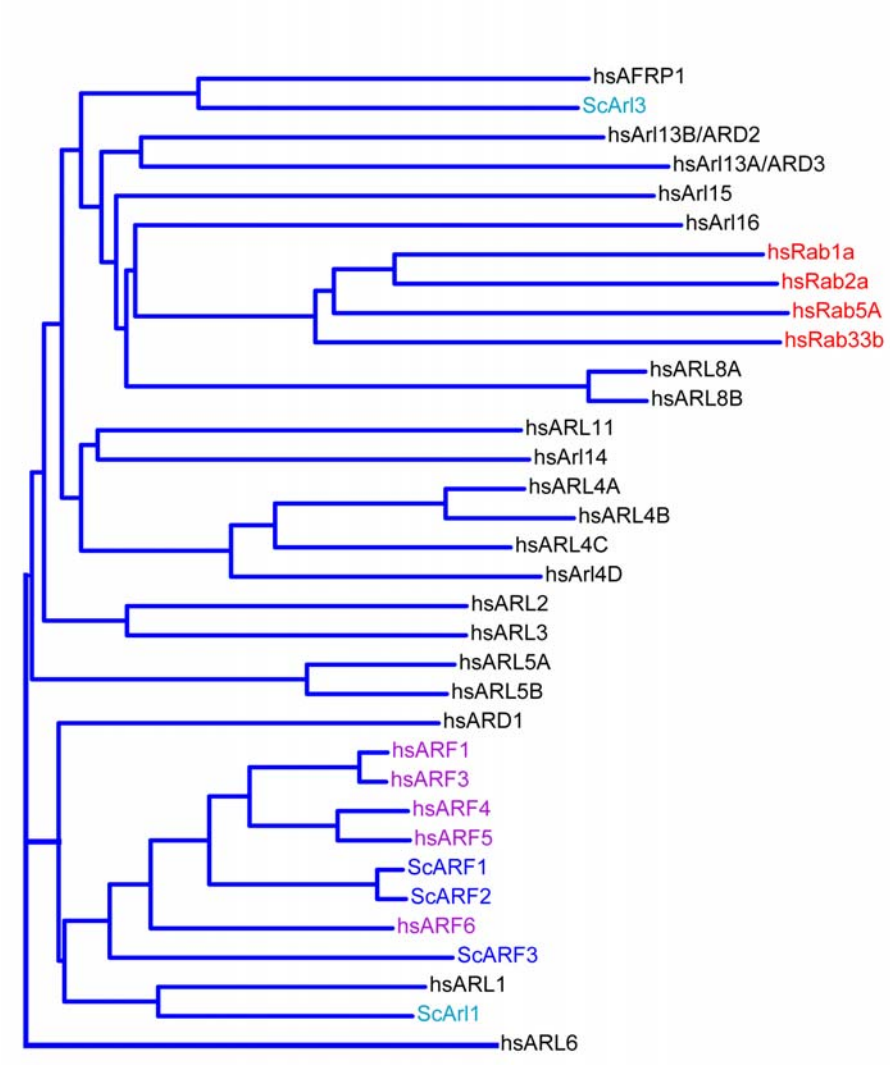

Figure 3: **Phylogenetic Tree Of The Rab-, Arf- And Arl-Family.** Phylogenetic tree of the human and *S.cerevisiae* Arf- and Arl-family, compared to selected members of Rab-GTPases involved in membrane trafficking; black: human Arl; violet: human Arf; red: human Rab, blue: *S.cerevisiae* Arf; light blue: *S.cerevisiae* Arl; generated with VectorNTI 10 (Invitrogen).

the GTPase in its inactive, GDP-locked conformation, mutation of a catalytic glutamine to leucine or alanine (Haas *et al.*, 2005) prevents the GTPase from hydrolysing the GTP to GDP and thus remains constitutively active.
For intracellular transport three families of the Ras superfamily are of special importance (Fig.3): the Rabs, the ADP-ribosylation factor (Arf) and ADP-ribosylation factor like (Arl) proteins.

1.3.1 Rab GTPases

The Rab family is one of the biggest of the Ras-superfamily. It consists of more than 60 members (Short *et al.*, 2005). Rabs contain the G-domain as a basic unit, but some features are specific for Rab GTPases and set them apart from other members of the superfamily (Vetter and Wittinghofer, 2001). They have a highly flexible C-terminus with a double cysteine prenylation signal. This lipid tail is inserted into the target membrane (Rak *et al.*, 2003; Sivars *et al.*, 2003). In their inactive form, Rabs are found soluble in the cytosol, which makes it necessary for the hydrophobic prenylated tail to be protected by GDIs (guanine nucleotide dissociation inhibitors), which shield the hydrophobic lipid moiety against the hydrophilic environment.
Thus, Rab GTPases cycle between the cytosol and the target membrane. GDP-bound, inactive Rab is associated with GDI in the cytosol, gets delivered to the target membrane, binds its GEF and gets activated. After interacting with its effectors, Rabs subsequently are deactivated by their specific GAP and leave the membrane, again bound to the GDI (Pfeffer and Aivazian, 2004; Short *et al.*, 2005).
Rab GTPases are involved in many different processes. They give identity to the membranes of organelles of the endocytic and secretory pathway (Pfeffer, 2001; Short *et al.*, 2005; Zerial and McBride, 2001), like Rab5 (early endosomes) and Rab7 (late endosomes) (Miaczynska and Zerial, 2002; Maxfield and McGraw, 2004). Rabs are involved in vesicle tethering, like Rab1 (Allan *et al.*, 2000; Moyer *et al.*, 2001) and Rab2 (Short *et al.*, 2001), and vesicle motility, like Rab6 (Short *et al.*, 2002; Matanis *et al.*, 2002). A recent finding by Yoshimura *et al.* (2007); Nachury *et al.* (2007) showed that Rab8a is involved in primary cilium formation and that loss of Rab8a prevents cilium growth, whereas Rab8a overexpression provokes formation of an exaggerated primary cilium.
When Rabs are targeted to the membrane they recruit their effectors either from the cytosol or from the pool of membrane bound proteins. In this process, many Rabs bind to golgins and other proteins with coiled-coil structures and may change their conformation (Short *et al.*, 2005; Pfeffer, 2001). The Rab GTPase family is one of the most important regulators of intracellular traffic and a number of Rab proteins still has no function

assigned to them.

1.3.2 ADP-Ribosylation Factors

Another class of small G-proteins involved in membrane trafficking are the ADP-ribosylation factor proteins (Chavrier and Goud, 1999). They were initially discovered as cofactors in the cholera toxin induced ADP-ribosylation of the G_s-subunit of the heterotrimeric G-proteins (Kahn and Gilman, 1986). In human cells five members of the Arf family are expressed. They are divided into three groups: class I containing Arf1 and Arf3 (some mammals like mouse and rat also have Arf2), class II containing Arf4 and Arf5 and class III containing Arf6. Arf1 and Arf3 might be redundant, although most experimental results were achieved with Arf1. Arf4 and Arf5 have partially overlapping functions with class I Arfs. The most divergent member is Arf6, which is not Golgi localised but is found at the plasma membrane (Gillingham and Munro, 2007).
By sequence homology another subgroup of Arfs, termed Arf-like (Arl) proteins, has been found (human Arl1 shares 56% identity and 76% similarity with human Arf1) (Burd *et al.*, 2004). The main difference in comparison to Arf is that Arf-like proteins cannot function as cofactors for cholera toxin (Tamkun *et al.*, 1991). The Arl protein family consists of about 20 members (Fig.3, p.11). Most Arl proteins have unknown functions. The small GTPase Sar1 (see 1.2.2, p.8) is also a distant Arf-family member (Munro, 2005).
Arf proteins feature a G-domain (Vetter and Wittinghofer, 2001), but instead of a flexible C-terminal tail with a prenyl anchor, like in Rab proteins, they have an N-terminal amphipathic helix by which they bind to membranes (Amor *et al.*, 1994). This amphipathic helix is myristoylated in most Arfs. Exceptions are Sar1, the acetylated Arls, like AFRP1/Arl3p (Behnia *et al.*, 2004; Setty *et al.*, 2004), Arl8A/B (Hofmann and Munro, 2006) and Arls with a myristoylation signal, which is probably not myristoylated (Arl2 and Arl3) (Sharer *et al.*, 2002).
Additionally, Arf proteins have a unique structural feature in comparison to all other small G-proteins (Pasqualato *et al.*, 2002), the interswitch toggle. The loop connecting switch I and switch II of the nucleotide binding domain forms a hydrophobic pocket in the GDP-bound conformation. This hydrophobic pocket can accommodate the amphipathic helix with its hydrophobic myristoyl moiety. Upon nucleotide exchange, the interswitch toggle undergoes a two-residue register shift, which causes the hydrophobic pocket to vanish. The amphipathic helix is released and ready for membrane binding. This has two consequences: first, in the Arf family, activation and membrane binding are tightly linked and, second, Arf family members do not need GDP-dissociation inhibitors (GDI) to travel through the cytosol (Gillingham and Munro, 2007), as the hydrophobic membrane anchor

is secured within the interswitch pocket. Additionally, the amphipathic helix is short in comparison to the Rab C-terminus, which brings the Arf GTPase and its effectors closer to the membrane (Neu *et al.*, 1997).
Two of the best studied Arf GTPases are the Golgi localised Arf1 and Arl1.

ADP-Ribosylation Factor 1 Arf1 is crucial in intracellular transport and in organelle organisation (Bonifacino and Lippincott-Schwartz, 2003). The key function of Arf1 is twofold. First, it initiates Golgi-to-ER retrograde trafficking by assembling the COPI coat (see 1.2.2, p.9). Second, it is required for TGN-to-endosome trafficking as it regulates assembly of the clathrin coat at both compartments, TGN and endosomes. Thus, Arf1 can be found on all Golgi cisternae, its spacial specificity regulated by different factors. The most important regulator is the guanine nucleotide exchange factor, which activates the GTPase by replacing GDP for GTP. There are a total of 7 Arf GEF families. They are peripheral membrane proteins with a central, conserved 200 residue domain, the Sec7 domain (Chardin *et al.*, 1996). The seven families are GBF (Golgi specific Brefeldin A resistance factor), BIG (BFA Inhibited GEF), PSD (PH and Sec7 domain), IQSEC (IQ and Sec7), cytohesin and FBXO8. For most of them substrate specificity is not entirely clear, but it is proposed that GBF1 acts on cis-Golgi localised Arf1 and is involved in COPI vesicle formation (Gillingham and Munro, 2007). BIG is trans-Golgi localised and acts in clathrin coated vesicle formation (Shinotsuka *et al.*, 2002).
Arf1 activation can be blocked by the fungal compound Brefeldin A. Brefeldin A binds at the interface between Arf1 and its GEF and forms a stable Arf1-GDP-GEF complex. All available GEF protein is sequestered and Arf1 cannot be activated, Arf1-dependent transport is inhibited and Golgi proteins redistribute to the ER (Sciaky *et al.*, 1997).
The GTPase activating proteins (GAPs) of Arf1 have a 140 residue domain in common. It was discovered in ArfGAP1 and DDEF1 (Goldberg, 1999; Mandiyan *et al.*, 1999). The 24 known ArfGAPs can be divided into 10 families: ArfGAP1, ArfGAP3, SMAP, Hrb, Git, Centaurin α, β, γ and δ and DDEF1 (Gillingham and Munro, 2007). Furthermore, it is proposed that in COPI-assembly the coatomer Sec23 subunit greatly stimulates the ArfGAP activity and may, in fact, even be more important for Arf inactivation (Goldberg, 1999).
Two more functions of Arf1 will be discussed briefly. First, Arf1 influences the lipid composition of membranes by recruiting and/or activating phospholipase D (PLD) (Brown *et al.*, 1993) and Phosphatidylinositol 4-kinase (PI4K) Type IIIβ (Haynes *et al.*, 2005). Second, in *S.cerevisiae*, Arf1p recruits the golgin Rud3p to the cis-Golgi (Gillingham *et al.*, 2004).

ADP-Ribosylation Factor Like 1 And The GRIP Domain Arl1 is a trans-Golgi localised small GTPase (Munro, 2005). Although its GEF is still elusive, it is known to be recruited to the Golgi apparatus by a cascade of signals, which involves the small Arl GTPase AFRP1 (Arf related protein 1)/Arl3p (Behnia *et al.*, 2004; Setty *et al.*, 2004). AFRP1 is rather divergent from the Arl family (Fig.3, p.11). This becomes most obvious by the fact that it is not myristoylated on its N-terminal amphipathic helix, but acetylated (Behnia *et al.*, 2004; Setty *et al.*, 2004). Upon activation AFRP1 binds to the four transmembrane protein Sys1 (Fig.4). The following steps in the cascade are unknown, but in this process Arl1 is recruited to the trans-Golgi membrane and activated (Behnia *et al.*, 2004; Setty *et al.*, 2004).
Arl1 itself is necessary to bind a special class of golgins to the trans-Golgi membrane (Munro and Nichols, 1999; Gangi-Setty *et al.*, 2003; Panic *et al.*, 2003a; Wu *et al.*, 2004). These golgins have a conserved 50 amino acid motif at their C-terminus, the GRIP domain (**G**olgin-97, **R**abBP2α, **I**mh1p, **p**230). The first two helices of the GRIP domain interact mainly with the switch II region, but also partially switch I and the interswitch region of Arl1 (Wu *et al.*, 2004).

The GRIP domain protein binds as a homodimer and needs two active Arl1 molecules. A conserved tyrosine residue is absolutely necessary for Golgi binding (Y697 in Golgin-97 (Barr, 1999), Y2185 in Golgi-245 (Panic *et al.*, 2003b)). It is proposed that residues at the C-terminus of the GRIP domain protein are inserted into the membrane.
In mammals there are four proteins, which comprise a GRIP domain: Golgin-97, p230/golgin-245, GCC185 and GCC88 (Barr and Short, 2003; Gillingham and Munro, 2003). In yeast there is only one, Imh1p. They are all involved in endosome to TGN trafficking

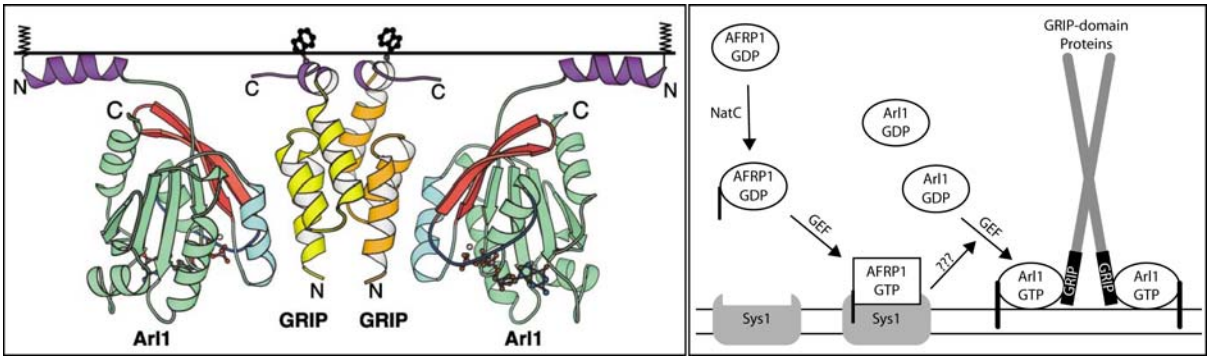

Figure 4: **Binding Of GRIP Domain Proteins To ADP-Ribosylation Factor Like 1.**
Left: Structure of the Arl1/GRIP complex; N-terminal myristoyl group and GRIP domain tryptophanes are inserted into the membrane; adapted from Panic *et al.* (2003b). Right: Schematic steps of Arl GTPase cascade necessary for GRIP protein recruitment to the Golgi; AFRP1 is activated and binds to the transmembrane protein Sys1; this activates and recruits Arl1 from the cytosol to the membrane, where two molecules Arl1 bind to a GRIP domain protein dimer; not drawn to scale.

(Lu *et al.*, 2004; Yoshino *et al.*, 2003). Deletion of Arl1 or competing for Arl1 binding by overexpressing a GRIP domain-only construct, removes Golgin-97 and Golgi-245 from the Golgi and inhibits Shiga-toxin transport to Golgi and TGN46 recycling (Lu *et al.*, 2004; Yoshino *et al.*, 2003). Recent evidence shows that the golgin GCC185 may participate in the docking of late endosome-derived, Rab9-bearing transport vesicles at the TGN (Reddy *et al.*, 2006).

1.4 Golgi And The Cytoskeleton

1.4.1 Microtubules, Dyneins And Kinesins

Microtubules form a major part of the cytoskeleton. In fibroblasts microtubules originate from the microtubule organising centre (MTOC) or centrosome and radiate out to the cell periphery (Hirokawa and Takemura, 2004). They are the main component of the mitotic spindle and are necessary for separating the homolog chromosomes in mitosis, but are also necessary for organelle movement in interphase cells (Raynaud-Messina and Merdes, 2007).

Microtubules are built of α- and β-tubulin, which polymerise to form thirteen parallel protofilaments of linearly arranged heterodimers (Hirokawa, 1998). For nucleation, microtubules need a third tubulin, γ-tubulin, which forms, together with accessory proteins, γ-tubulin small complexes (γ-TuSC) or bigger γ-tubulin ring complexes (γ-TuRCs) (Raynaud-Messina and Merdes, 2007). The Microtubules are 25 nm in diameter and have a fast growing end, the microtubule plus-end, and a slow growing end, the microtubule minus end. Building blocks are constantly dissociating from microtubules and it depends on the rate of assembly versus disassembly whether microtubules grow on the plus-end or shrink. This mechanism is called "tread-milling" and allows the microtubule network to scan the cell's interior for binding partners (Vaughan, 2005).

The microtubules form "rails" for microtubule motors (Hirokawa, 1998), but can also anchor structures to their ends, like the kinetochore of chromosomes. This allows the cell to organise its interior by active transport and anchoring.

In most cell lines, the Golgi apparatus is situated near the microtubule organising centre (MTOC) (Allan *et al.*, 2002). Microtubule depolymerising drugs, like nocodazole, cause the Golgi apparatus to fragment into mini-stacks near the ER-exit sites (Thyberg and Moskalewski, 1999) and to reform into a normal Golgi ribbon near the MTOC upon washout of the drug (Ho *et al.*, 1989). This clearly shows that the microtubule network and its molecular motors are essential for Golgi morphology and positioning.

An effect similar to the one caused by microtubule depolymerisation could be achieved

by inactivation or depletion of cytoplasmic dynein (Burkhardt *et al.*, 1997). Dynein is a microtubule minus-end directed, molecular motor, which is attached to Golgi or vesicle membranes by the protein complex dynactin. Dynactin localisation at membranes is dependent on the small GTPase Rab6, which recruits the dynactin subunit $p150^{glued}$ (Matanis *et al.*, 2002; Short *et al.*, 2002) and the golgin Bicaudal-D (Hoogenraad *et al.*, 2001). As dynactin binds to microtubule plus-ends, a search and capture mechanism for microtubule-membrane interaction is proposed (Vaughan, 2005): microtubules grow from the MTOC and "search" the cytoplasm for membrane bound dynactin. After establishing contact, dynein is recruited and the captured membranes start travelling to the microtubule minus-ends. By this mechanism, dynein brings ER-Golgi-intermediate compartments (see 1.2.2, p.8) to the Golgi cis-face or aid in recycling protein from the trans-Golgi to the ER, independent of COPI (Young *et al.*, 2005). Distribution of endocytic cargo carriers is also influenced by dynein/dynactin and interaction of the late endosomal Rab, Rab7, with dynein/dynactin has been proposed (Murshid and Presley, 2004). This would enable directed transport of vesicles from late endosomes to the TGN. In contrast to dynein-bound vesicles, vesicles leaving the Golgi apparatus travel in the opposite direction. Kinesins are molecular motors directed to the microtubule plus-ends (Hirokawa, 1998). In humans, like in mouse, there are 45 kinesins (Miki *et al.*, 2001) and many of them are thought to be involved in intracellular trafficking. The isoform Kif5B has been found at the Golgi apparatus (Gyoeva *et al.*, 2000) and knockdown by siRNA caused the Golgi to acquire a compact structure (Feiguin *et al.*, 1994). Several other kinesins are supposed to be involved in transport away from the Golgi to the microtubule plus-ends and thus may bring exocytic vesicles from the Golgi to the plasma membrane (Hirokawa, 1998). This is especially true in neurons, where the localisation of cargo is more specialised and it is likely that more and different kinesins are involved (Hirokawa and Takemura, 2004). Notably, in polarised epithelial cells the Golgi is positioned at the microtubule plus-ends and thus directions of transport are reversed (Hirokawa and Takemura, 2004).

Apart from centrosomally anchored microtubules, microtubules could origin from the cis-Golgi (Chabin-Brion *et al.*, 2001; Marsh *et al.*, 2001). Here the golgin GMAP-210 is implied (Infante *et al.*, 1999) as anchoring agent. CLASP (Clip-associating protein) is another protein, which binds to microtubule plus-ends and stabilises them at the cell cortex (Mimori-Kiyosue *et al.*, 2005). It also localises to the Golgi apparatus, but its function there is not yet clear. The microtubule binding protein Hook3 is also localised on cis-Golgi membranes and is supposed to anchor the Golgi apparatus near the centrosome (Walenta *et al.*, 2001).

Considering all this, the importance of the microtubule cytoskeleton for Golgi positioning,

maintenance and morphology becomes obvious.

1.4.2 Actin, Spectrin And Intermediate Filaments

The second big cytoskeletal system is the actin network. Actin fibres are nucleated at different places in the cell. The most prominent place is the plasma membrane (Wang, 1985; Svitkina *et al.*, 1986), where actin is involved in endocytosis and cell motility. Actin filaments are built of actin monomers (G-actin) and have, like microtubules, a plus-end (barbed end) and a minus-end (pointed end). The cortical actin network is most often of mixed polarity (Lewis and Bridgeman, 1992). Actin filaments also form stress fibres, lamellipodia and filopodia (DePina and Langford, 1999) and are found in the cytosol interacting with organelles and microtubules.
The Golgi apparatus is linked to the actin meshwork and it is implied in different functions of transport and Golgi morphology. The actin associated motor protein Myosin Va is in complex with the small GTPase Rab27a and melanophilin on melanosomes and is involved in their trafficking to the plasma membrane (Fukuda *et al.*, 2002; Wu *et al.*, 2002). Other Myosin motors, like Myosin VI, or the propelling force of assembling actin comets could transport vesicles away from Golgi membranes nearer to microtubule based motors where vesicles are captured for long range transport (Egea *et al.*, 2006).
Additionally, actin is not only involved in vesicle budding and transport, but also in maintenance of Golgi morphology. Disruption of the actin network by drugs like latrunculin, causes the Golgi cisternae to fragment, swell (Lazaro-Dieguez *et al.*, 2006) and increase their intra cisternal pH. Microtubules had no influence in this morphological change.
It is also interesting to note that the small GTPase Arf1 (1.3.2, p.14), which is involved in initiation of clathrin and COPI coat formation (see 1.2.2, p.9), also recruits the Rho-GTPase Cdc42 to the Golgi and thus induces actin polymerisation (Stamnes, 2002). Cdc42 binds to γCOP, but competes with the p23 cargo receptor. Furthermore the Golgi bound Cdc42-GAP, ARHGAP10, is dependent on Arf1 (Dubois *et al.*, 2005). Actin nucleation and polymerisation need the effectors WASP (Wiskott-Aldrich syndrome protein) and Arp2/3 (Matas *et al.*, 2004). Cdc42 bound to coatomer recruits these actin nucleators and prevents dynein binding to the nascent vesicle (Chen *et al.*, 2005). Hehnly and Stamnes (2007) propose that Cdc42 prevents premature dynein driven transport of the forming vesicle.
The actin network interacts also with the spectrin network. Spectrin was identified in erythrocytes on the cytosolic face of the plasma membrane. It gives structure to these cells (Luna and Hitt, 1992). On the Golgi apparatus special isoforms of spectrin and its adaptors the ankyrins have been identified, which have links to every cytoskeletal net-

work, especially to the actin meshwork (DeMatteis and Morrow, 2000). Spectrin anchors the dynactin complex to the membrane and thus is necessary for microtubule minus-end directed transport (Holleran *et al.*, 1996). Its localisation to the Golgi is dependent on Arf1 function and it is removed immediately by BFA treatment (DeMatteis and Morrow, 2000). Its function in Golgi morphology and transport, however, is still not clear.
The third network of cytoskeletal structures in eukaryotic cells are the intermediate filaments. IFs are different, depending on cell type, and consist of keratins, neurofilament-like proteins, lamins or the vimentin-related proteins (desmins, glial fibrillary acid proteins, peripherins)(Gao and Sztul, 2001). Vimentin IFs have also been shown to interact with Golgi localised proteins, although the function is not known yet.

1.5 The Intraflagellar Transport System

Cilia and flagella are organelles found in many cells and organisms. They function in cell mobility or for sensory reception (Scholey, 2003) and are formed of a microtubular axoneme (Fig.5), protruding from the basal body and sheathed by plasma membrane (Rosenbaum and Witman, 2002). This complex structure is built by a unique machinery, which transports axonemal building blocks from the cytoplasm to the distal tip of the cilium or flagellum. The transport within the cilium is independent of vesicular membrane carriers, but relies on a unique proteinaceous particle complex, the intraflagellar transport (IFT) machinery (Koeminski *et al.*, 1993; Qin *et al.*, 2004).
Many studies about the intraflagellar transport system were performed in *Chlamydomonas reinhardtii* and *Caenorhabditis elegans*, but most findings also apply to mammals.

1.5.1 Cilia And Flagella: Morphology And Function

Cilia and flagella are cylindrous protrusions from the plasma membrane, which contain an axoneme (Johnson, 1995; Porter and Sale, 2000). In motile cilia and flagella, this structure is built in a 9+2 conformation (Fig.5), which means 9 microtubule doublets surround a central microtubule doublet. The outer doublets are linked by inner and outer dynein arms and are connected to the central doublet by radial spokes. The dyneins cause sliding of microtubules against each other, while radial spokes, nexins and the central microtubule pair transform the movement into coordinated cilium beating (Scholey, 2003). Non-motile cilia, so-called primary cilia, have a simpler composition, as the axoneme is missing dynein, nexin arms, radial spokes and the central doublet (9+0) (Perkins *et al.*, 1986). In both types, the axoneme grows directly from the basal body, which moved into the vicinity of the plasma membrane upon cilium formation. The basal body is built

from a ring of triplet microtubules and is attached to the plasma membrane by transition fibres (Rosenbaum and Witman, 2002), which separate the space within the cilium from the cytoplasm (Witman, 1990) (Fig.5). Although primary cilia were considered immotile, it has become clear that at least cilia on embryonic nodal cells are motile (Nonaka *et al.*, 1998). Their beating is necessary for establishing left-right asymmetry in the embryo (Nonaka *et al.*, 2002).

Flagella are necessary for cell motility, but also for signalling as has been shown in mating *Chlamydomonas* (Wang *et al.*, 2006). One example for specialised, immotile, primary cilia is the vertebrate photoreceptor. These polarised sensory neurons consist of the cell body (called inner segment IS) and the outer segment (OS), which contains discs of membranes where opsin, a photosensitive protein, can be found. The OS is formed from a primary cilium (DeRobertis, 1958; Tokuyasu and Yamada, 1959) and a small 9+0 connection still exists in adult vertebrates. By this bridge protein is shuttled from the IS, where it is synthesised, to the OS. Failure by the cell to do so causes rapid degeneration of the photosensitive stacks and destruction of the outer segment, which leads to blindness (Sung and Tai, 2000). Primary cilia also function as chemical sensors in

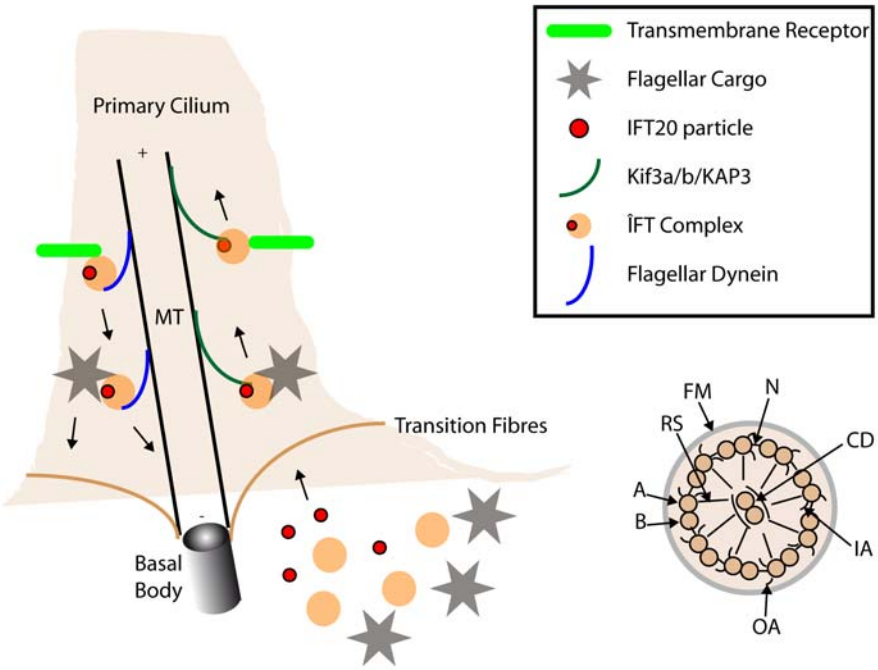

Figure 5: **Intraflagellar Transport And Cilium with 9+2 Morphology.** Left: Schematic overview of the intraflagellar transport of cargo from the cytoplasm to the cilium tip and retrograde transport to the base; arrows indicate movement direction; cilium is simplified and not to scale; Right: section of cilium; 9+2 structure with outer and inner microtubule doublets; A: A-fibre of outer microtubules; B: B-fibre of outer microtubules; CD: central microtubule doublet with sheath; FM: flagellar membrane; IA: inner dynein arms; OA: outer dynein arms; N: nexins; RS: radial spokes; not to scale.

olfactory and auditory sensory cells, mechanosensors in bone and kidney and are vital for signal transduction, providing a platform where membrane receptors can be concentrated (Scholey, 2003; Rosenbaum and Witman, 2002; Scholey and Anderson, 2006).

1.5.2 Intraflagellar Transport

Cilia and flagella are assembled by the intraflagellar transport machinery (Qin *et al.*, 2004). This machinery consists of several proteins organised in two complexes or lobes. Lobe A consists of about 4-6 polypeptides and is supposed to bind to a version of flagellar transport specific, cytoplasmic dynein (Dhc1b/Dhc2) (Cole *et al.*, 1998; Pazour *et al.*, 1998, 1999). It is involved in retrograde transport from the cilium tip to the basal body. Lobe B consists of about 11-13 proteins (Cole *et al.*, 1998; Piperno *et al.*, 1998) and binds to heterotrimeric kinesin-II (Cole *et al.*, 1998). The IFT-machinery was observed by electron microscopy and formed readily visible rafts, which travel on the B fibre of the outer microtubule doublets of the axoneme, directly underneath the plasma membrane sheath of the cilium (Ringo, 1967)(Fig.5). After reaching the distal tip with the help of MT-plus-end directed kinesin-II, cargo is unloaded, kinesin deactivated and minus-end directed dynein activated. The IFT particle travels back to the basal body (Koeminski *et al.*, 1993). Apart from transporting building blocks for the axonemes, it is proposed that the IFT machinery also helps to bring cilium-localised receptors to the cilium membrane compartment. Thus, it not only builds the cilium but is also necessary for its function (Scholey and Anderson, 2006; Qin *et al.*, 2005; Pan and Snell, 2003).
Defects of the IFT machinery cause severe diseases like blindness, deafness, polycystic kidney disease and situs inversus amongst others (Bisgrove and Yost, 2006).

1.5.3 Heterotrimeric Kinesin-II

Heterotrimeric kinesin-II consists of two motor proteins, Kif3A and Kif3B, and a non-motor accessory protein KAP3 (kinesin accessory protein 3) (Marszalek and Goldstein, 2000). The two motor monomers dimerise by a 35 nm long coiled-coil rod (DeMarco *et al.*, 2001). KAP3 is associated with the tail domain of the Kif-subunits (Wedaman *et al.*, 1996). As an N-kinesin it performs ATP-dependent microtubule plus-end directed transport and was shown to be involved in intraflagellar trafficking (Walther *et al.*, 1994; Kozminski *et al.*, 1995). Kif3 is also proposed in ER-to-Golgi transport (LeBot *et al.*, 1998), although this has only been seen in *X.laevis* with the Kif3 homologue Xklp3.

1.5.4 Intraflagellar Transport Protein of 20 kDa (IFT20)

Human IFT20 is the homologue of the *Chlamydomonas* IFT20. The protein is 158 amino acids long, has a molecular mass of 18.1 kDa and an isoelectric point of 4.95 (Yin *et al.*, 2003). It is expressed in a wide array of tissues.
IFT20 is part of Lobe B of the IFT particle (Rosenbaum and Witman, 2002) and interacts with IFT57 (Baker *et al.*, 2003). Furthermore, it directly binds to the Kif3B component of the heterotrimeric kinesin-II. Depletion of IFT20 from cells prevents primary cilium formation (Follit *et al.*, 2006). The most surprising feature of IFT20, however, is its localisation. As expected, it can be found at the basal body and faintly at the primary cilium, but also shows a clear presence in the perinuclear region, co-localising with different Golgi markers (Follit *et al.*, 2006). A faint stream of IFT20 signals has been reported in cells where cilium and Golgi apparatus are separated. IFT20's function on the Golgi is still unknown, but it is suspected that it is involved in transport of newly synthesised material from the Golgi to the cilium, which is needed for cilium assembly and function (Follit *et al.*, 2006). At the cilium IFT20 and its cargo would then be incorporated into the IFT particle and transported into the cilium.

1.6 Golgi-Microtubule Associated Protein 210kDa (GMAP-210)

1.6.1 General Aspects

GMAP-210 was found independently by two groups with different experimental approaches. Durfee *et al.* (1993) found GMAP-210 cDNA in a Yeast 2-Hybrid screen as an interactor of the retinoblastoma protein and named it Trip-230, whereas Rios *et al.* (1994) found GMAP-210 in a screen with the serum of patients with the Sjoegren's autoimmune disorder and named it p210. The same group renamed it some years later to GMAP-210 (Golgi Microtubule Associated Protein of 210 kD) as they found it to not only localise to the Golgi apparatus (Rios *et al.*, 1994; Chen *et al.*, 1999), but also to interact with short, stable microtubules (Infante *et al.*, 1999).
GMAP-210 is a 1979 amino acids long protein with an apparent molecular weight of 210 kDa (Rios *et al.*, 1994), a calculated molecular weight of 224 kDa and a pI of 5.1 (Infante *et al.*, 1999). It has long stretches of coiled-coil and localises peripherally to the cis-Golgi as shown by staining with antisera from Sjoegren's disease patients, electron microscopy studies (Rios *et al.*, 1994) and transfection of tagged recombinant protein (Infante *et al.*, 1999; Gillingham *et al.*, 2004). Its coiled-coil structural elements, its Golgi localisation and its behaviour in cells treated with Brefeldin A qualify GMAP-210 as po-

tential Golgi matrix protein (Barr and Short, 2003; Gillingham and Munro, 2003). Upon Brefeldin A treatment GMAP-210 does not recycle to the ER, but localises to the same Golgi remnants as does the Golgi matrix protein GM130 (Rios *et al.*, 1994).

1.6.2 Golgi Targeting

Without doubt GMAP-210 localises to the Golgi apparatus (Rios *et al.*, 1994; Infante *et al.*, 1999; Chen *et al.*, 1999; Gillingham *et al.*, 2004). The targeting motif is, however, not clear. Infante *et al.* (1999) map the Golgi interacting domain to the N-terminal 375 amino acids (Fig. 6). The theory of N-terminal membrane binding is supported by a finding, which identifies an amphipathic α-helical ALPS motif (ArfGAP1 lipid packing sensor) in the first 38 amino acids of GMAP-210. This domain binds membranes with a high degree of positive membrane curvature, similar to that found in 50 nm vesicles (Drin *et al.*, 2007). Infante *et al.* (1999) also show that the GMAP-210 C-terminal GFP-fusion protein targets to the centrosome and displaces CTR453, a marker for the pericentriolar material. This is however in contrast to publications by Chen *et al.* (1999) and Gillingham *et al.* (2004) which showed that binding of GMAP-210 is mediated by the C-terminus.

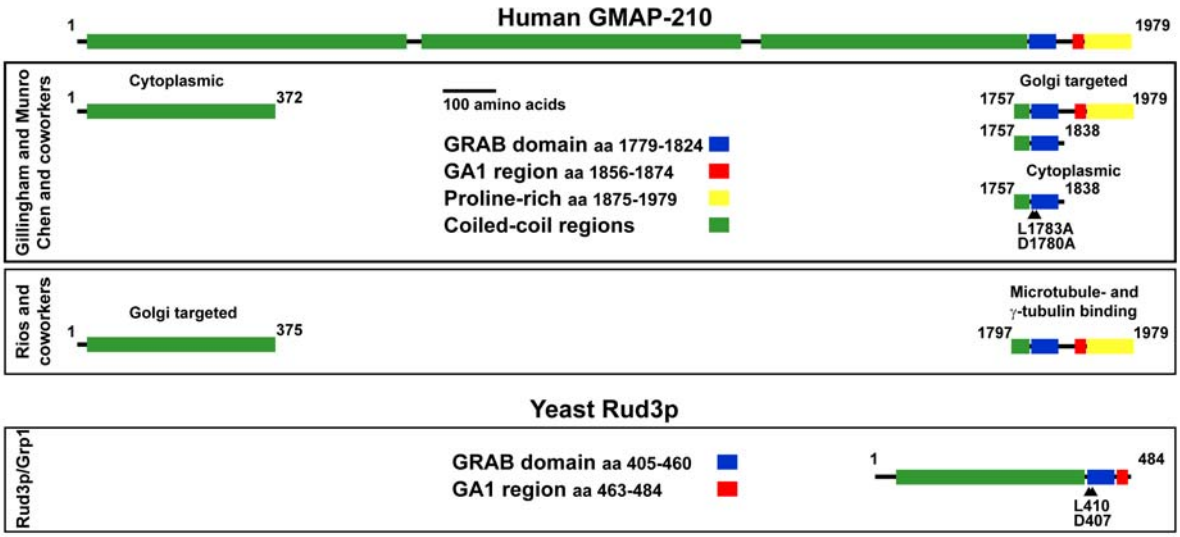

Figure 6: **GMAP-210 And Rud3p Domain Structure.** Domains of GMAP-210 and their proposed function as described by either Infante *et al.* (1999) or Gillingham *et al.* (2004); Chen *et al.* (1999). Modified from Barr and Egerer (2005).

1.6.3 Function Of GMAP-210 As Microtubule Binding Protein

Infante *et al.* (1999) also claimed that the C-terminus of GMAP-210 is responsible for binding GMAP-210 to short stable microtubules and co-sediments with them from cold calcium washed cells. Overexpression of GMAP-210 showed that the microtubules, normally radiating from the centrosome, became less focused, attributing this to recruitment of microtubule minus-ends to Golgi localised GMAP-210 (Infante *et al.*, 1999). This finding was further supported in Rios *et al.* (2004), where GMAP-210 was found to bind γ-TCCs (γ-Tubulin Containing Complexes) and to recruit them to the Golgi apparatus upon overexpression of GMAP-210. This is consistent with the need of γ-TuRCs for microtubule nucleation and their attachment to the centrosome (Rios *et al.*, 2004; Barr and Egerer, 2005). It has also been found that microtubules could nucleate from the Golgi apparatus (Marsh *et al.*, 2001; Efimov *et al.*, 2007) and GMAP-210 would be predestined to function as nucleator of these non-centrosomal microtubules (Efimov *et al.*, 2007).

1.6.4 GMAP-210: GRIP Related Arf-Binding Domain

This would all be very compelling except that microtubule interaction of the GMAP-210 C-terminus contradicts with observations by Gillingham *et al.* (2004); Chen *et al.* (1999), which localise the Golgi binding domain to the same region. Additionally, Gillingham *et al.* (2004) could specify a distinct Golgi binding motif and interaction protein for the *S.cerevisiae* homologue of GMAP-210, Rud3p or Grp1p (golgin-160-related protein).
Rud3p was discovered by a high copy suppressor screen with *sec34-2*, a temperature-sensitive mutant defective in the late stages of ER to Golgi transport (Kim, 2003). Rud3p is a 484 amino acids long, peripheral, cis-Golgi localised protein with coiled-coil structures (Fig.6), which does not redistribute back to the ER upon block of ER export by Brefeldin A or by transfection of the Sar1p dominant negative mutant (Kim, 2003).
Gillingham *et al.* (2004) also found an analogy between the GRIP domain of trans-Golgi localised golgins (see 1.3.2, p.14) and a 80 residues long domain in the C-terminus of Rud3p. GRIP interacts with Arl1p in a GTP-dependent manner (Panic *et al.*, 2003b; Wu *et al.*, 2004). Rud3p GRAB domain likewise binds to Arf1p and is thus targeted to the Golgi apparatus (Gillingham *et al.*, 2004). Like the essential tyrosine residue in the GRIP domain (Barr, 1999), GRAB domain-Arf1p interaction is disturbed by mutation of conserved residues. In Rud3p GRAB domain these residues are leucine 410 and, to a lesser degree, aspartate 407 (Gillingham *et al.*, 2004).
It was further shown that a ER-to-Golgi cargo receptor Erv14p, which is found on COPII vesicles, is necessary for Golgi targeting of Rud3p, but not for *in vitro* binding of Arf1p

with Rud3p (Gillingham *et al.*, 2004). Erv14 is involved in transport of the Axl2p plasma membrane protein (Powers and Barlowe, 2002). Rud3p, however, does not bind directly to Erv14p (Gillingham *et al.*, 2004) and after deletion of Rud3p, Axl2p is still transported to the plasma membrane, although it shows defects in post-translational glycan modification (Powers and Barlowe, 1998; Gillingham *et al.*, 2004).
A simple bioinformatical search for GRAB domain relatives revealed that this is a motif found in proteins of all eukaryotes. Normally one protein with this feature is found per organism, in *A.thaliana* there are two (Gillingham *et al.*, 2004). The homologue of Rud3p in humans is, although essentially bigger in size, GMAP-210. The minimum domain necessary to target GMAP-210 to the Golgi apparatus proved to be amino acids 1757 to 1838. The mutation of the residues aspartate 1780 and leucine 1783 abolished Golgi localisation (Gillingham *et al.*, 2004). Nevertheless, human Arf1 shows no interaction with the GMAP-210 GRAB.
The C-terminus of GRAB-domain golgins has a second feature, which Gillingham *et al.* (2004) termed GA1. It has no influence on Rud3p targeting, but seems to be necessary for Rud3p function.

1.6.5 Overexpression And Knockdown: Effects On Transport

GMAP-210 has been shown to bind to microtubule minus-ends, the Golgi apparatus and centrosome (Rios *et al.*, 1994; Chen *et al.*, 1999; Infante *et al.*, 1999; Pernet-Gallay *et al.*, 2002) and to interact with γ-tubulin, proposing it to be responsible for microtubule nucleation. Although some of these points are still debatable (Gillingham *et al.*, 2004; Barr and Egerer, 2005), further studies have been performed to elucidate GMAP-210 function, especially in regards to its role at the Golgi apparatus of mammalian cells (Infante *et al.*, 1999; Pernet-Gallay *et al.*, 2002). Depletion of GMAP-210 fragments the Golgi ribbons dramatically (Rios *et al.*, 2004). Overexpression of GMAP-210 not only disturbs the microtubule network, but enlarges and fragments the Golgi apparatus (Rios *et al.*, 2004; Pernet-Gallay *et al.*, 2002). GMAP-210 also seems to have a function in intracellular protein transport, as overexpression disrupts anterograde transport from ER to cis-/medial-Golgi (Pernet-Gallay *et al.*, 2002) and blocks retrograde transport of the shiga toxin B-subunit from Golgi-to-ER.

1.7 Aim Of This Work

The golgin GMAP-210 has been identified as a homologue of *S.cerevisiae* Rud3p, which localises to the Golgi apparatus by its conserved GRAB domain. This domain is present in proteins throughout the realm of eukaryotes (Gillingham *et al.*, 2004). Rud3p GRAB domain has been shown to interact with the small GTPase Arf1p, which is necessary for Rud3p to localise to the Golgi apparatus. Human GMAP-210 also localises to the Golgi membranes in a GRAB domain dependent fashion, although involvement of Arf1 could not be shown yet (Gillingham *et al.*, 2004). Nevertheless, involvement of a small, Golgi-localised GTPase is very likely. Finding a GTPase, which recruits GMAP-210 to Golgi apparatus by its GRAB domain will enable us to deduce the function of GMAP-210 in the secretory pathway. This information will also settle the dispute about the Golgi localising region of GMAP-210, may it be the N-terminus (Infante *et al.*, 1999) or the C-terminus (Chen *et al.*, 1999; Gillingham *et al.*, 2004).

Furthermore, various functions have already been proposed for GMAP-210. GMAP-210 was shown to bind to microtubules and might even be involved in their nucleation by recruiting γ-TCCs (Infante *et al.*, 1999; Rios *et al.*, 2004). Other publications show GMAP-210's involvement in anterograde and retrograde trafficking (Pernet-Gallay *et al.*, 2002), whereas it is also discussed that GMAP-210 might be similar to Rud3p and is rather necessary for proper Golgi function, influencing glycosylation (Kim, 2003; Gillingham *et al.*, 2004; Barr and Egerer, 2005). GMAP-210 is also proposed to be involved in maintenance of Golgi morphology, either by interaction with the cytoskeleton (Infante *et al.*, 1999) or by acting as a Golgi matrix protein (Barr and Egerer, 2005).

This work will deal with the ambiguous findings about GMAP-210, its localisation and function. Furthermore, it will study the interaction partners and mechanisms in which this elusive, but interesting, protein may be involved.

2 Results

2.1 GMAP-210 Is A Golgi Binding Protein

The protein GMAP-210 was found at the Golgi apparatus (Rios *et al.*, 1994; Chen *et al.*, 1999). It has long stretches of coiled-coil and behaves like a Golgi matrix protein (Rios *et al.*, 1994; Barr and Short, 2003; Gillingham and Munro, 2003). Nevertheless, the exact Golgi binding domain of GMAP-210 is disputed (Infante *et al.*, 1999; Chen *et al.*, 1999; Gillingham *et al.*, 2004). To settle this dispute the full length coding sequence of GMAP-210 and various N- and C-terminal truncation constructs were cloned and antibodies against an N-terminal, recombinant fragment prepared. With these tools, localisation of GMAP-210 in cells stained with the antibody or transfected with GFP-tagged constructs was studied by immunofluorescence microscopy.

2.1.1 Tools For GMAP-210 Characterisation

First, various tools for studying the golgin GMAP-210 were produced.

Cloning Of GMAP-210 Full-Length, Fragments And Mutants The full-length coding sequence of GMAP-210 was cloned from a human liver cDNA library (Becton-Dickinson, Heidelberg) by standard polymerase chain reaction. Following the shortway system cloning strategy a BamHI and a XhoI restriction sites were added to the 5'- and 3'-end, respectively. Thus, the cloned DNA construct could be subcloned in any shortway compatible vector. The tags provided by the vector were in frame at the 5'- or the 3'-end. For easier subcloning a silent adenosine to thymidine mutation was inserted at position 2924 of the GMAP-210 coding sequence in order to disrupt a BamHI restriction site, which would interfere with the chosen cloning strategy. N- and C-terminal truncation constructs and GRAB domain mutations were derived by using the full-length clone as template in a standard PCR (see Table 13, p.148*ff.*). For the D1780A L1783A mutation of the GRAB domain a special, 42 base pairs long quickchange primer was designed, which changed both codons at the same time (GAC to GCC$^{bp:5338-5340}$ and CTA to GCA$^{bp:5347-5349}$). Before subcloning, all DNA constructs were sequenced and checked for compliance with the data base sequence.

Polyclonal Antibodies Against GMAP-210 In order to detect endogenous GMAP-210 in immunofluorescence and Western blot experiments and for use in co-immunoprecipitations, an antibody to the N-terminus of GMAP-210 (amino acids 1 to 375 with

6xHis-tag) was raised by Biogenes in two rabbits (#6129 and #6130) with a total of 2 mg recombinant protein (see 4.5.6, p.135). Testbleeds were evaluated approximately 1 month after initial immunisation and boost injections. Bleedout of rabbits was performed 1 month after the 2^{nd} testbleed.

Antibodies were affinity purified from rabbit #6130 bleedout with the GST-6xHis-tagged version of the initial antigen.

Antibody specificity was tested in immunofluorescence and Western blot and for both methods a concentration of 1:500 proved to be optimum. In immunofluorescence, that antibody stained a structure in the perinuclear region and co-localised with the Golgi marker GM130 (Fig.7). The antibody also showed staining on small vesicular tubular structures in the cell periphery, which did not co-stain for GM130. After knockdown of GMAP-210 with a specific siRNA oligo, the signal in the perinuclear region and on the vesicular tubular structures vanished (Fig.24, p.49). In Western blot experiments, the antibody revealed a single band at 210 kDa, which also disappeared after siRNA knockdown (Fig.23, p.49). The antibody against the N-terminal 375 amino acids of GMAP-210 specifically and exclusively recognised endogenous protein in immunofluorescence and Western blotting.

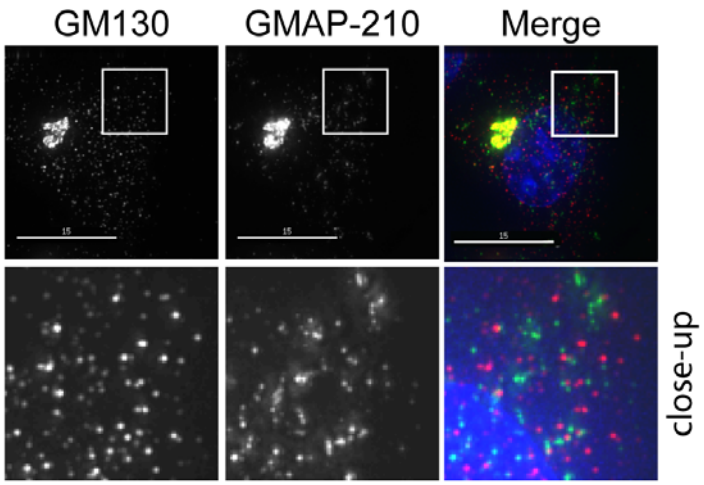

Figure 7: **GMAP-210 Localisation In HeLa L Cells.** HeLa L cells were fixed with paraformaldehyde and stained with mouse anti GM130 (red, 1:500) and rabbit anti GMAP-210 (green, 1:500) primary antibodies; lower pictures show a contrast and brightness enhanced close-up of the region indicated in the upper pictures, box=10 μm; pictures were acquired by delta vision microscopy and image stacks were subsequently deconvolved and merged into one picture; blue channel: DAPI staining; Bar=15 μm.

2.1.2 The C-Terminal GRAB Domain Of GMAP-210 Targets The Protein To The Golgi Apparatus

Although GMAP-210 localises undoubtedly to the Golgi apparatus, it is still debatable whether GMAP-210 targets to the Golgi via its N- or C-terminus (Infante *et al.*, 1999; Chen *et al.*, 1999). In order to solve this contradiction, the behaviour of several N- and C-terminal, GFP-tagged constructs was tested in HeLa cells.

First the localisation of endogenous GMAP-210 was elucidated in greater detail by staining untreated cells with the polyclonal antibody and examining them by delta vision microscopy.

For this end, HeLa L cells were fixed with paraformaldehyde and stained for GMAP-210 and the cis-Golgi marker GM130 (Fig.7). GMAP-210, stained by polyclonal antibody, was localised mainly in a juxtanuclear region and co-localised partially with the signal of GM130 staining, although not completely. Thus, GMAP-210 is at the cis-Golgi compartment as described before (Rios *et al.*, 1994). Additionally, vesicular tubular structures could be observed in the periphery of the cell, stained for GMAP-210, but not GM130. As Gillingham *et al.* (2004) described, a domain in the C-terminus is responsible for target-

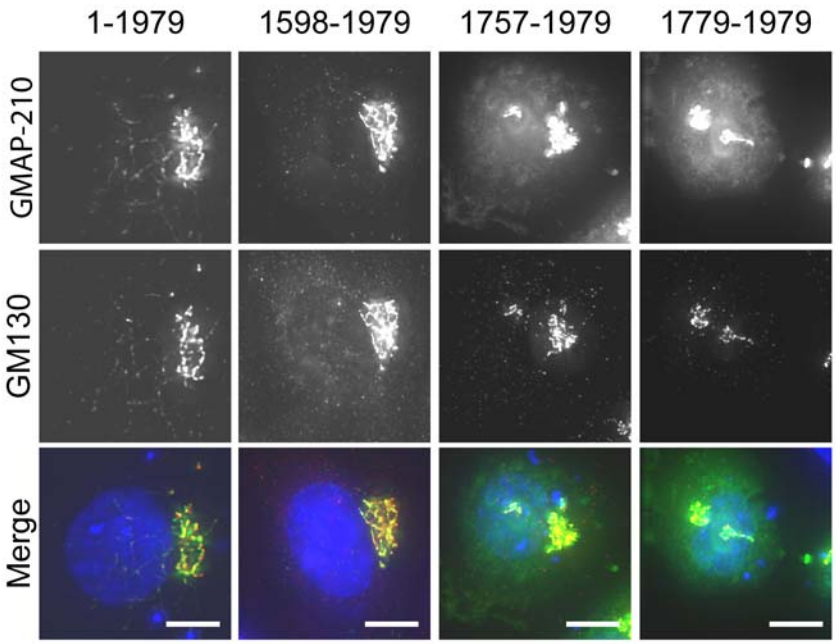

Figure 8: **Localisation Of GMAP-210 C-Terminus In HeLa L Cells.** Heal L cells were transfected with the indicated full-length or C-terminal GMAP-210 constructs (green) for 24 h and fixed with paraformaldehyde; cells were stained with mouse anti GM130 (red, 1:500); pictures were acquired by delta vision microscopy and image stacks subsequently deconvolved and merged into one picture. For better visibility of fine structures, contrast and brightness were enhanced by the same values in each picture and channel; blue channel: DAPI staining; Bar=5 μm.

ing GMAP-210 to the Golgi. In order to test this, GFP-tagged constructs of GMAP-210 full-length and the C-terminal 382, 223 and 201 amino acids were transfected into HeLa L cells. After fixation with paraformaldehyde and co-staining for the golgin GM130, cells were analysed by delta vision microscopy (Fig.8). Expressed GFP-tagged full-length GMAP-210 localised to the Golgi just like antibody staining had shown for the endogenous protein (Fig.7, p.28). The C-terminal 382 amino acids (pEGFPC2-GMAP-210 1598-1979) also decorated the Golgi apparatus and even as few as the C-terminal 201 amino acids (pEGFPC2-GMAP210 1779-1979) were enough for Golgi targeting. The two shorter fragments, however, showed a diffuse cytosolic pool in addition to Golgi targeting instead of staining vesicular tubular structures. This showed, that the C-terminus of GMAP-210 can target to the Golgi. Closer examination of Fig.8 showed, that overexpression of full-length GMAP-210 caused the Golgi to grow out into long "spider-leg"-like tubules, which can also be observed with GM130 staining. A similar effect was not seen by overexpressing

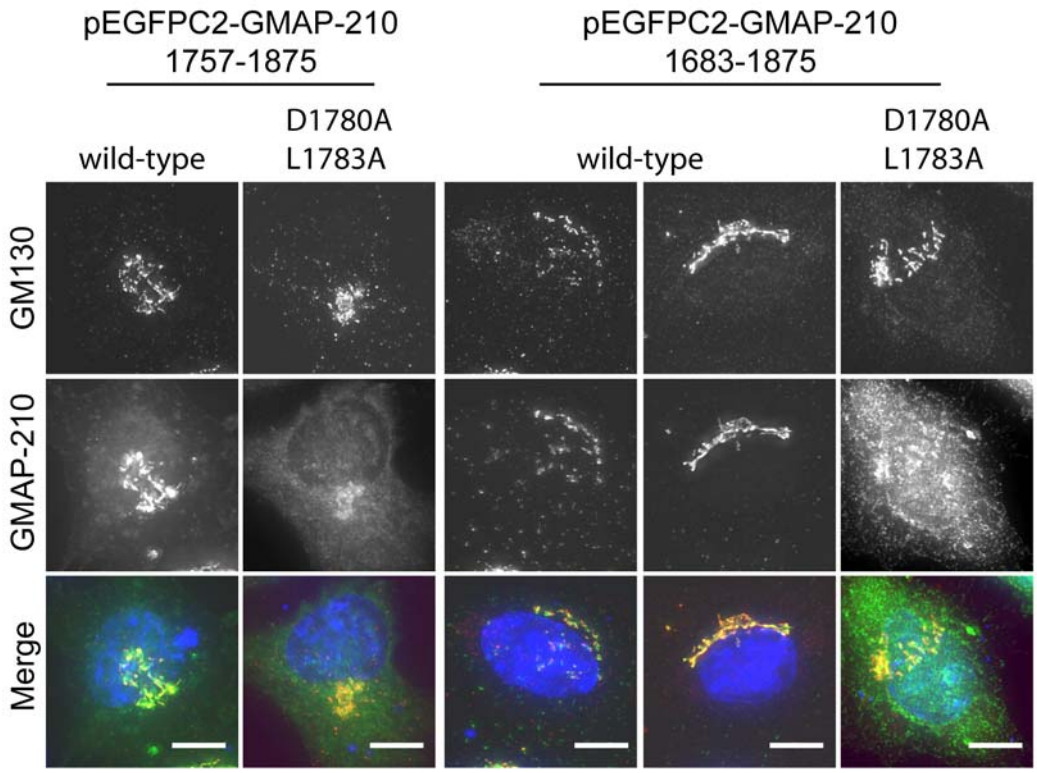

Figure 9: **GRAB Domain And GRAB Domain Mutants In HeLa L Cells.** HeLa L cells were transfected for 24 h with constructs for expression of GMAP-210 GRAB domain (amino acids 1757-1875) or GRAB domain plus the C-terminally adjacent coiled-coil region (amino acids 1683-1875) in wild-type or GRAB mutant form (D1780A L1783A) as indicated (green); cells were fixed with paraformaldehyde and stained with mouse anti GM130 (red, 1:500); pictures were acquired by delta vision microscopy and the attained image stacks deconvolved and merged into a single picture; blue channel: DAPI staining; Bar=5 μm.

any of the other
C-terminal constructs.
To further narrow down the domain, which recruits GMAP-210 C-terminus to the Golgi, the GRAB (**G**RIP **R**elated **A**rf **B**inding) domain described by Gillingham *et al.* (2004) was transfected into HeLa L cells (Fig.9), fixed with paraformaldehyde and co-stained with an antibody against GM130. Two different constructs were used. One expressed the minimal GRAB domain (pEGFPC2-GMAP-210 1757-1875), the second the GRAB domain with the N-terminally adjacent coiled-coil region (1683-1875), which should enable dimerisation (Panic *et al.*, 2003b). Both constructs localised to the Golgi. The shorter construct, however, also showed a diffuse cytosolic signal, whereas the construct comprising the coiled-coil region, showed distinct vesicular structures in the cell periphery. Neither construct had an effect on Golgi morphology. As Gillingham *et al.* (2004) discovered the GRAB domain by an analogy to the GRIP domain (Barr, 1999), they could identify conserved residues, aspartate at position 1780 and leucine at position 1783, which were necessary for Golgi targeting. Mutation of the two amino acids to alanine should abolish Golgi localisation.
First GRAB domain mutants were made by quickchange mutagenesis and then transfected into HeLa as GFP-tagged constructs (Fig.9; pEGFPC2-GMAP-210 1757-1875 D1780A L1783A and pEGFPC2-GMAP-210 1683-1875 D1780A L1783A). Both constructs showed strongly reduced Golgi localisation in HeLa L cells. This was especially visible from the diffuse cytosolic distribution of mutant GRAB domain (GMAP-210 1683-1875 D1780A L1783A), when compared to wild-type (GMAP-210 1683-1875). Some protein was still present at the Golgi.
As a next step, the targeting of longer GMAP-210 constructs with disturbed GRAB domain targeting was tested. Three different constructs were transfected into HeLa L cells, fixed, co-stained with an antibody against GM130 and analysed by delta vision microscopy (Fig.10). Two of these constructs, full-length GMAP-210 and a C-terminal construct of GMAP-210 (pEGFPC2-GMAP-210 1598-1997 D1780A L1783A) were double mutants, replacing the essential aspartate 1780 and leucine 1783 with alanine, whereas the third construct was completely missing the GRAB domain (pEGFPN3-GMAP-210 1-1712). Mutant GMAP-210 C-terminus (pEGFPC2-GMAP-210 1598-1997 D1780A L1783A) showed reduced binding affinity to the Golgi apparatus. A diffuse cytosolic pool of GFP appeared in cells expressing this construct. Full-length GMAP-210 with the D1780A L1783A mutation was still localised on the Golgi (upper row in Fig.10), although the vesicular-tubular structures became much more prominent in comparison to transfection of wild-type GFP-tagged GMAP-210. When the GRAB domain was removed entirely from the protein (pEGFPN3-GMAP-210 1-1712), the construct no longer localised at the Golgi,

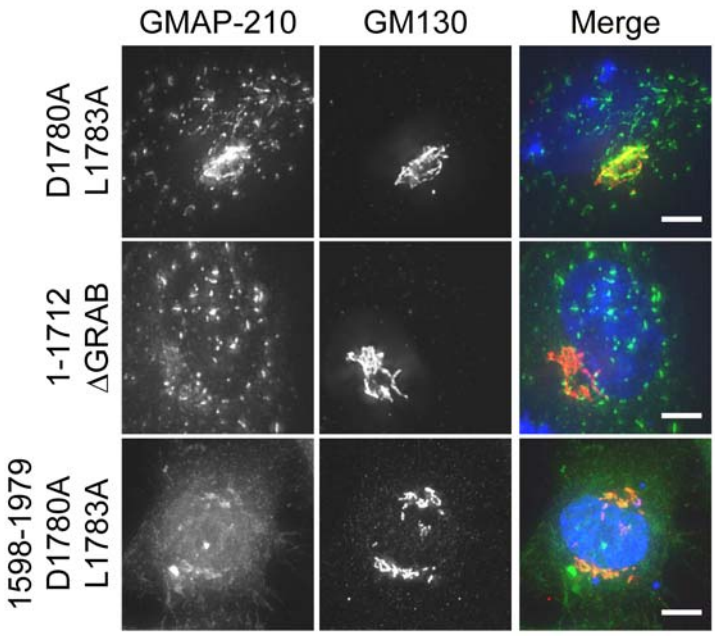

Figure 10: **Localisation Of GRAB Domain Mutants In HeLa L Cells.** HeLa L cells were transfected for 24 h with constructs for expression of GMAP-210, which either lacked GRAB domain (amino acids 1-1712) or were mutated in the GRAB domain (D1780A L1783A) as indicated (green); cells were fixed with paraformaldehyde and stained with mouse anti GM130 (red, 1:500); pictures were acquired by delta vision microscopy and the attained image stacks deconvolved and merged into one picture; blue channel: DAPI staining; Bar=5 μm.

but showed very pronounced vesicular tubular structures. Some of those clustered in a juxtanuclear region, overlapping with the Golgi localised GM130. With all three constructs, Golgi morphology was not changed in comparison to untransfected cells.
Transfection of various C-terminal constructs into HeLa L cells showed, that the C-terminus of GMAP-210 localises to the Golgi apparatus. The GRAB domain described by Gillingham *et al.* (2004) could be identified as minimal Golgi targeting motif and mutation of its two essential residues, aspartate 1780 and leucine 1783, reduced the Golgi targeting capability strongly. Full-length constructs with the GRAB mutation or without a GRAB domain localised more and more prominently to the vesicular tubular structures, on which endogenous, full-length GMAP-210 could also be seen.

2.1.3 GMAP-210 N-terminus Does Not Target To The Golgi

The GMAP-210 N-terminus was described as sole Golgi targeting domain by Infante *et al.* (1999). Although, the C-terminal GRAB domain has already been shown to target to the Golgi apparatus, Golgi binding of the N-terminus had to be ruled out.

Several GFP-tagged N-terminal constructs of GMAP-210 were transfected into HeLa L cells. Cells were fixed, co-stained for GM130 and analysed by epifluorescence (Fig.11). The transfected constructs did not have an effect on Golgi morphology. The construct comprising amino acids 1 to 375 (pEGFPC2-GMAP-210 1-375) weakly overlapped with the GM130 signal, but most of it showed a diffuse cytosolic localisation. A longer N-terminal construct, GMAP-210 amino acids 1 to 1332 (pEGFPC2-GMAP-210 1-1332), had stronger localisation to Golgi, but still high cytosolic background. When GMAP-210 is broken down further, a construct comprising amino acids 618 to 803 (pEGFPC2-GMAP-210 618-803) had some juxtanuclear concentration around the signal for GM130, but was very diffuse and most GFP signal could be found in the cytosol. Amino acids 855 to 1332 (pEGFPC2-GMAP-210 855-1332), however, showed a weak, but specific Golgi localisation. Amino acids 1332 to 1712 (pEGFPC2-GMAP-210 1333-1712) showed no Golgi localisation at all and a construct combining the latter two (pEGFPC2-GMAP-210 855-1712) had only a very weak Golgi localisation, with most protein going to the nucleus. Amino acids 1598 to 1778 (pEGFPC2-GMAP-210 1598-1778) were only found in the cytosol.
The N-terminus of GMAP-210 and constructs from the middle part, between amino acids 855 and 1333, showed some Golgi localisation, although much weaker than the GRAB domain targeted C-terminus (see 2.1.2, p.29*ff*).

2.1.4 Summary

Examining the localisation of GMAP-210, it became clear, that GMAP-210 is a cis-localised protein, which targets to the Golgi by its C-terminal GRAB domain, as described by Chen *et al.* (1999) and Gillingham *et al.* (2004). Mutation of the essential amino acids aspartate 1780 and leucine 1783 diminished Golgi binding of the GRAB domain greatly. However full-length constructs of GMAP-210 with GRAB mutation or with truncated C-terminus accumulated on small vesicular tubular structures. These also stained for endogenous GMAP-210 in untransfected cells but not for GM130. Overexpression of full-length GMAP-210 led to “spider-leg”-like outgrowth from the Golgi apparatus. The N-terminus showed little to no Golgi localisation. Fragments containing amino acid 855 to 1332 also targeted weakly to the Golgi.

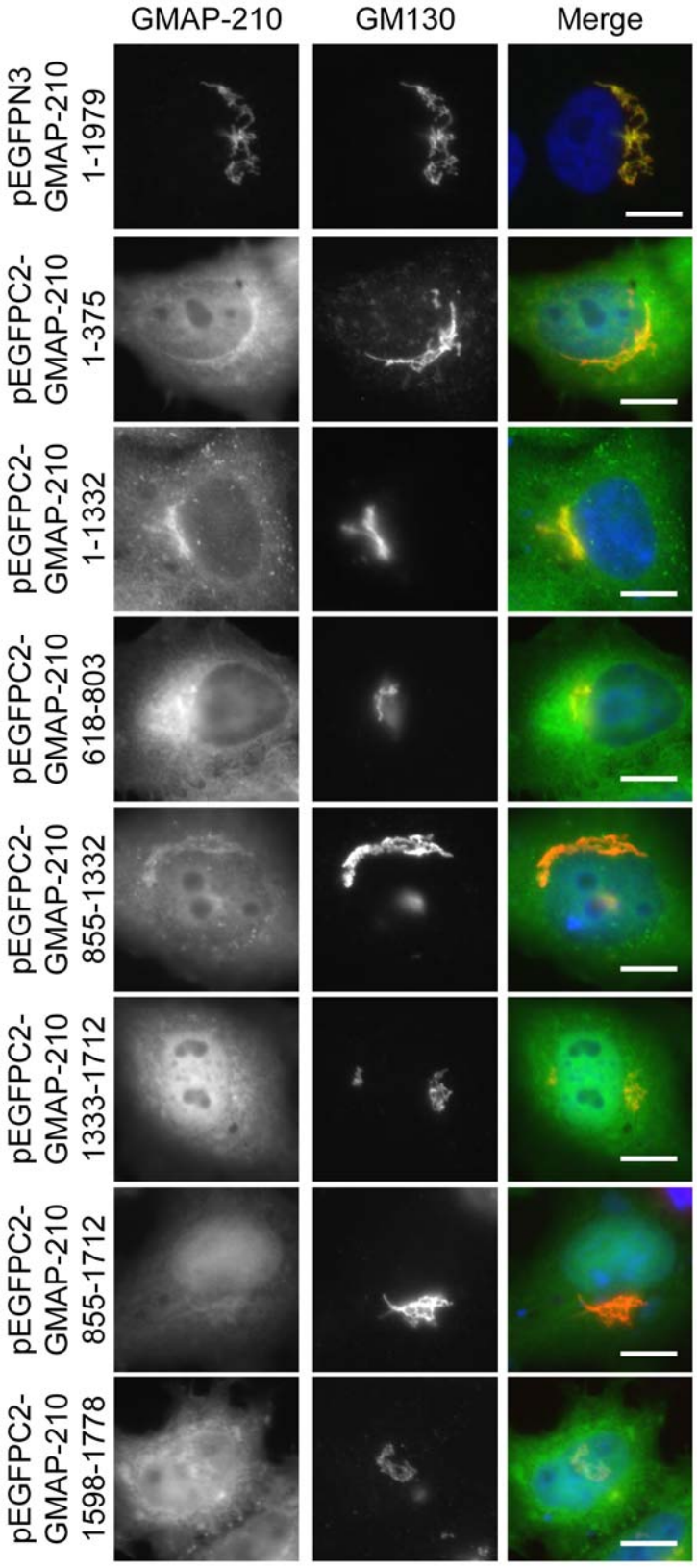

Figure 11: **Localisation Of Different GMAP-210 Fragments In HeLa L Cells.** HeLa L cells were transfected with various truncation constructs of GMAP-210 for 24 h; cells were fixed with paraformaldehyde and stained with mouse anti GM130 antibody (red, 1:500); blue channel: DAPI staining; Bar=5 μm.

2.2 The GMAP-210 GRIP Related ARF Binding Domain

As described by Gillingham *et al.* (2004), the *S.cerevisiae* homologue of mammalian GMAP-210, Rud3p, targets to the Golgi apparatus by its C-terminal GRAB domain. The binding is mediated by the ADP-ribosylation factor 1 (Arf1p), which binds Rud3p in a similarly to the way Golgin-97 and p230 GRIP domain targets to the trans-Golgi by Arl1p. It is likely, that GMAP-210 also interacts with a small GTPase, probably human Arf1.

2.2.1 GMAP-210 GRAB Domain Interacts With ADP-Ribosylation Factor Like 4A, C And D In A GTP Dependent Manner In Yeast 2-Hybrid Experiments

In analogy to Rud3p (Gillingham *et al.*, 2004) GRAB domain interaction with the small GTPase Arf1p, GMAP-210 should also bind a small GTPase by its GRAB domain.

This was first examined with yeast 2-hybrid interaction studies, testing GMAP-210 against human Arf1 and human ADP-ribosylation factor-like protein, Arl1 (Fig.12). Arf1 and Arl1 were used as bait in the pFBT9 vector with GMAP-210 and Golgin-97 as prey (in pAct2). The G-proteins were used in their wild-type and GTP-locked, active form. For Arl1 an N-terminally truncated construct was created, which was missing the N-terminal amphipathic helix, which often causes problems in interaction studies, due to its hydrophobic character (Gillingham and Munro, 2007). In yeast 2-hybrid, Golgin-97 interacted with Arl1 in its active, GTP-locked form, not with the wild-type. GMAP-210 did

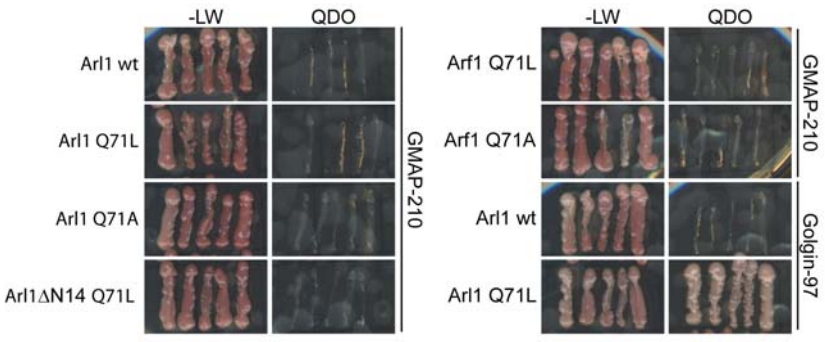

Figure 12: **Yeast 2-Hybrid Of GMAP-210 And ADP-ribosylation Factor.** Yeast 2-Hybrid interaction study of full-length GMAP-210 or Golgin-97 (fused to GAL4 transactivating domain; prey) and ADP-ribosylation factor 1 or ADP-ribosylation factor-like 1 as bait (fused to GAL4 binding domain) either in wild-type, GTP-bound, active (Q-L or Q-A) or N-terminally truncated form (ΔN14; without amphipathic helix); -LW: leucine and tryptophane deficient medium (growth control); QDO: quadruple drop out medium; leucine, tryptophane, alanine and histidine deficient medium.

not interact with any protein tested, neither Arf1 nor Arl1, independently of nucleotide state or truncations.

In human cells nearly 30 members of the Arf/Arl family are know, but only 6 in *S.cerevisiae*. This makes it possible, that mammalian GMAP-210 interacts with another member of the ADP-ribosylation factor family apart from Arf1. Thus, all members from this family were cloned from human cDNA libraries and subcloned into the pFBT9 vector for testing against full-length GMAP-210 in yeast 2-hybrid interaction studies (Fig.13). In yeast 2-hybrid experiments full-length GMAP-210 interacted with three out of four members of the Arl4 group (isoforms A, C, D) and with Arl16. Arl11 showed unspecific self-activation. The Arl8A result was ambiguous and further experiments showed, that Arl8A is unlikely to interact with GMAP-210. No member of the Arf family showed a positive signal, nor did the Arl-related protein Sar1 or any of the Arf-domain proteins (ARD1-3).

As the Golgi binding capability of GMAP-210 is mediated by the GRAB domain, the Arl-family members, positive in the yeast 2-hybrid screen, also had to interact with only the GRAB domain of GMAP-210 rather than the full-length protein.

Thus, the GMAP-210 GRAB domain in wild-type and GRAB mutant form (GMAP-210 1683-1875 D1780A L1783A) was tested against Arl4A and Arl4C in GDP- and GTP-locked conformation, Arl16 wild-type and Arf1/Arl1 in wild-type and GTP-locked form (Fig. 14, p.38). Wild-type and active-mutant Arl4A and Arl4C interacted with wild-type GRAB domain, but not with the GRAB domain mutant. Inactive Arl4 showed no reaction with any GRAB construct. Arl16 did not show any interaction with GMAP-210 GRAB domain. Interestingly, GTP-locked, active Arf1 (Arf1Q71L) and Arl1 (Arl1Q71L) reacted with the GRAB domain construct, while showing dependency on the GRAB mutation. This result was in contrast to experiments with full-length GMAP-210 and Arf1/Arl1 (Fig.12).

GMAP-210 GRAB domain interacts with members from the Arl4 group of Arl-GTPases in a nucleotide-state-dependant manner.

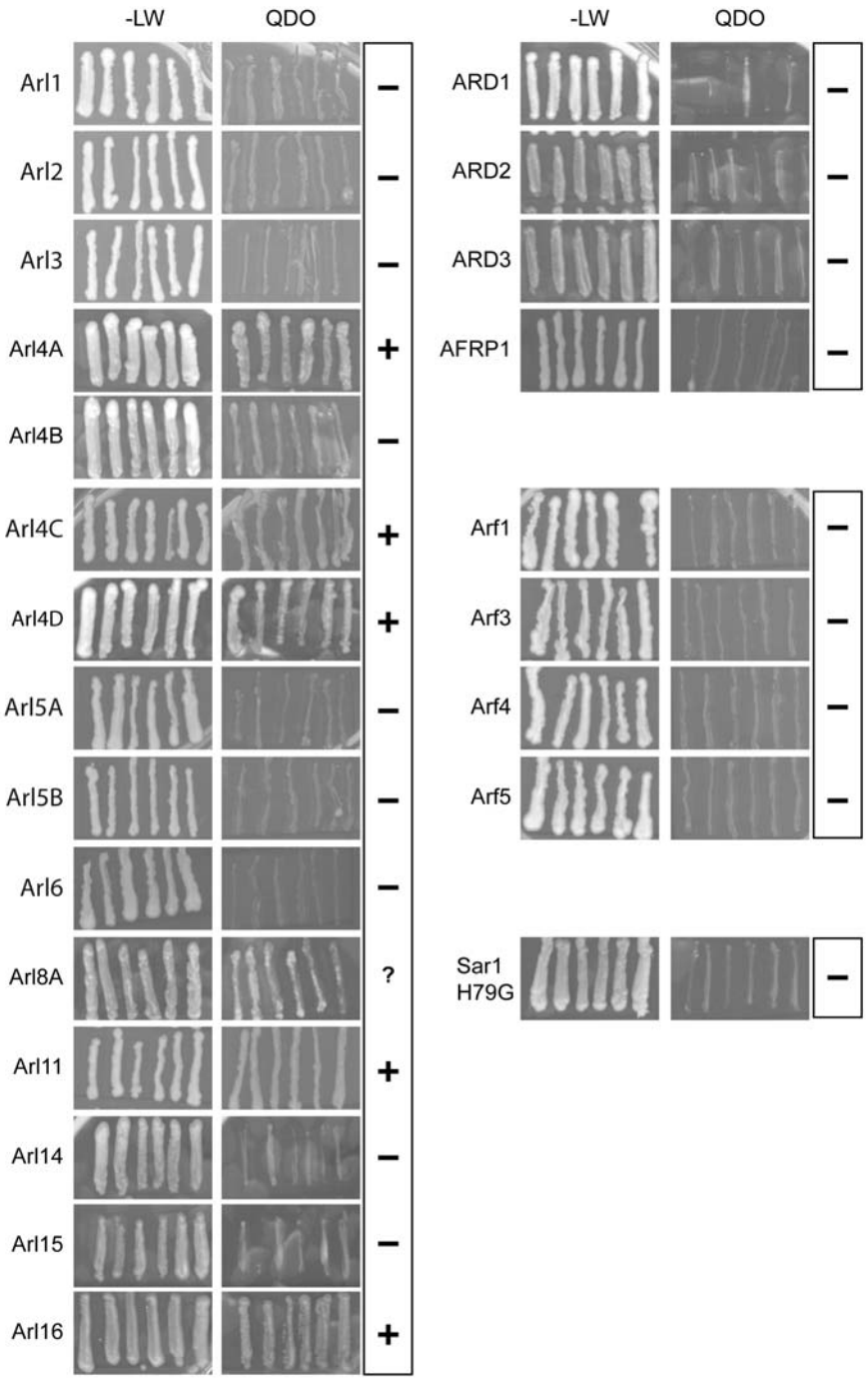

Figure 13: **Yeast 2-Hybrid Screen For GMAP-210 Interaction Partners In The Arf- And Arl-Family.** Yeast 2-Hybrid interaction study of full-length GMAP-210 (fused to GAL4 transactivating domain; prey) and ADP-ribosylation factor family, ADP-ribosylation factor-like family or Sar1 (GTP-locked, active form) as bait (fused to GAL4 binding domain); "+" and "-" indicate positive and negative interaction results; "?" indicates ambiguous result; -LW: leucine and tryptophane deficient medium (growth control); QDO: quadruple drop out medium; leucine, tryptophane, alanine and histidine deficient medium.

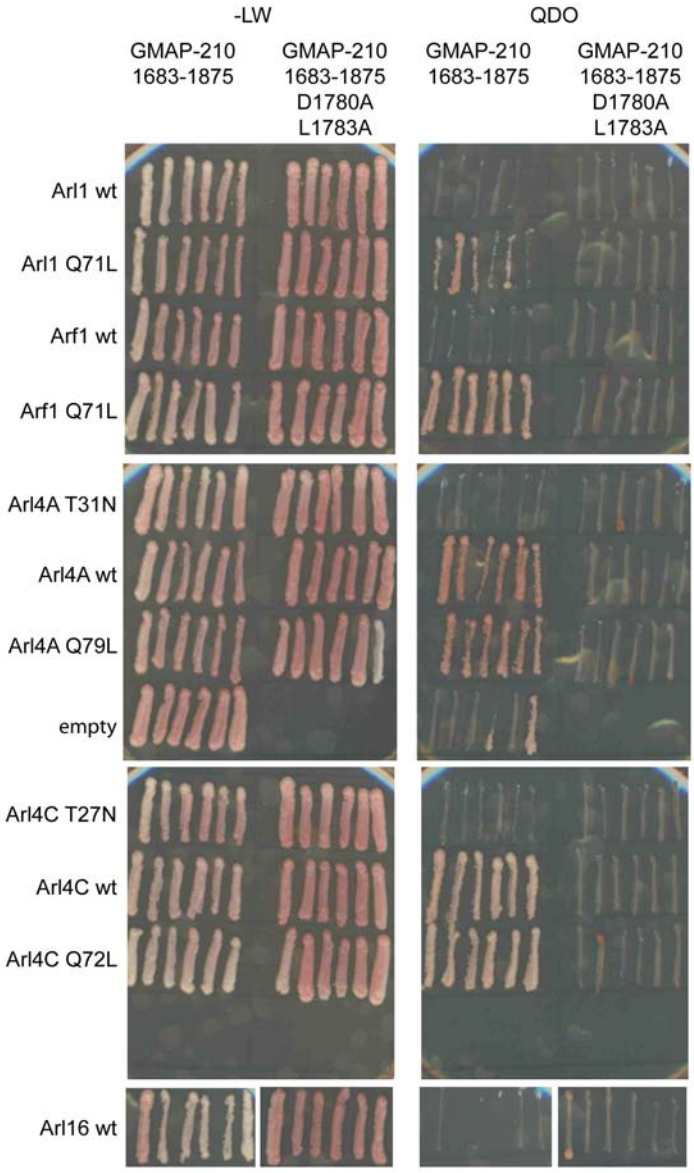

Figure 14: **GRAB Domain Interaction With Arf1 And Arl4A/C.** Yeast 2-Hybrid interaction study of wild-type and GRAB mutant (D1780A L1783A) GMAP-210 GRAB domain (amino acids 1683-1875) (fused to GAL4 transactivating domain as prey) and ADP-ribosylation factor 1 or ADP-ribosylation factor-like 4 family as bait (fused to GAL4 binding domain), either in wild-type, GTP-bound active (Q-L) or GDP-bound inactive (T-N) form as indicated; -LW: leucine and tryptophane deficient medium (growth control); QDO: quadruple drop out medium; leucine, tryptophane, alanine and histidine deficient medium.

2.2.2 Transfected Arl4A, Arl4C And Arl4D Localise To The Plasma Membrane Of HeLa L Cells

To show that the Arl-GTPases, which were found to interact with GMAP-210 in yeast 2-hybrid, also co-localise on the Golgi apparatus, their localisation had to be shown in living cells. To this end, all members of the ADP-ribosylation factor and ADP-ribosylation factor like family were transfected into HeLa L cells and *in vivo* localisation was studied by epifluorescence microscopy (Fig.15 and Fig.16). The cells were co-stained with an antibody against GMAP-210. Arf1-GFP showed localisation in a juxtanuclear position and overlapped with the signal of the GMAP-210 antibody at the Golgi complex (Steams *et al.*, 1990). Some nuclear localisation could be seen, depending on expression levels. Arf3-, Arf4- and Arf5-GFP had weak Golgi staining, but most of the protein was present in the cytosol. Arf6 was localised in the cytosol, although it also was concentrated at the mid-body of dividing cells. The Arl-family of small GTPases localised to a greater variety of compartments when transfected into HeLa L cells. Interesting in the context

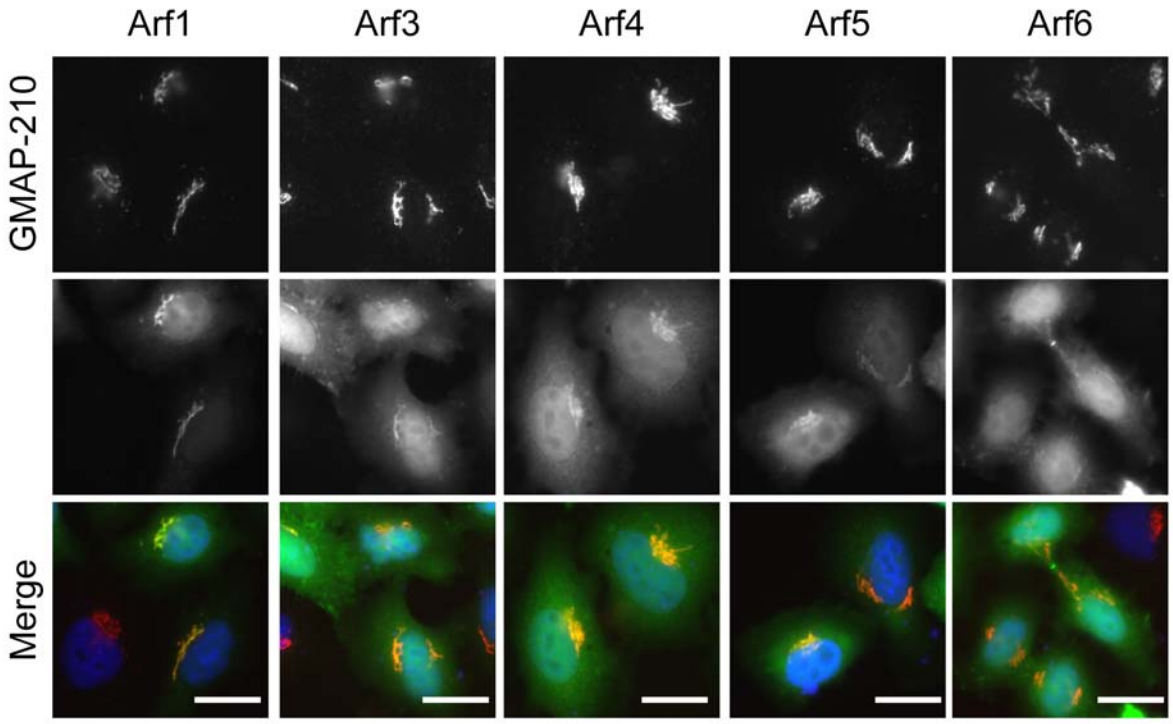

Figure 15: **Localisation Of The Arf Family Members In HeLa L Cells.** HeLa L cells transfected for 24 hours with a construct for expression of the the indicated member of the ADP-ribosylation factor family with an enhanced GFP-Tag on the C-terminal end (green) were fixed with paraformaldehyde and stained with the rabbit anti GMAP-210 antibody (red, 1:500); blue channel: DAPI staining; Bar=10 μm.

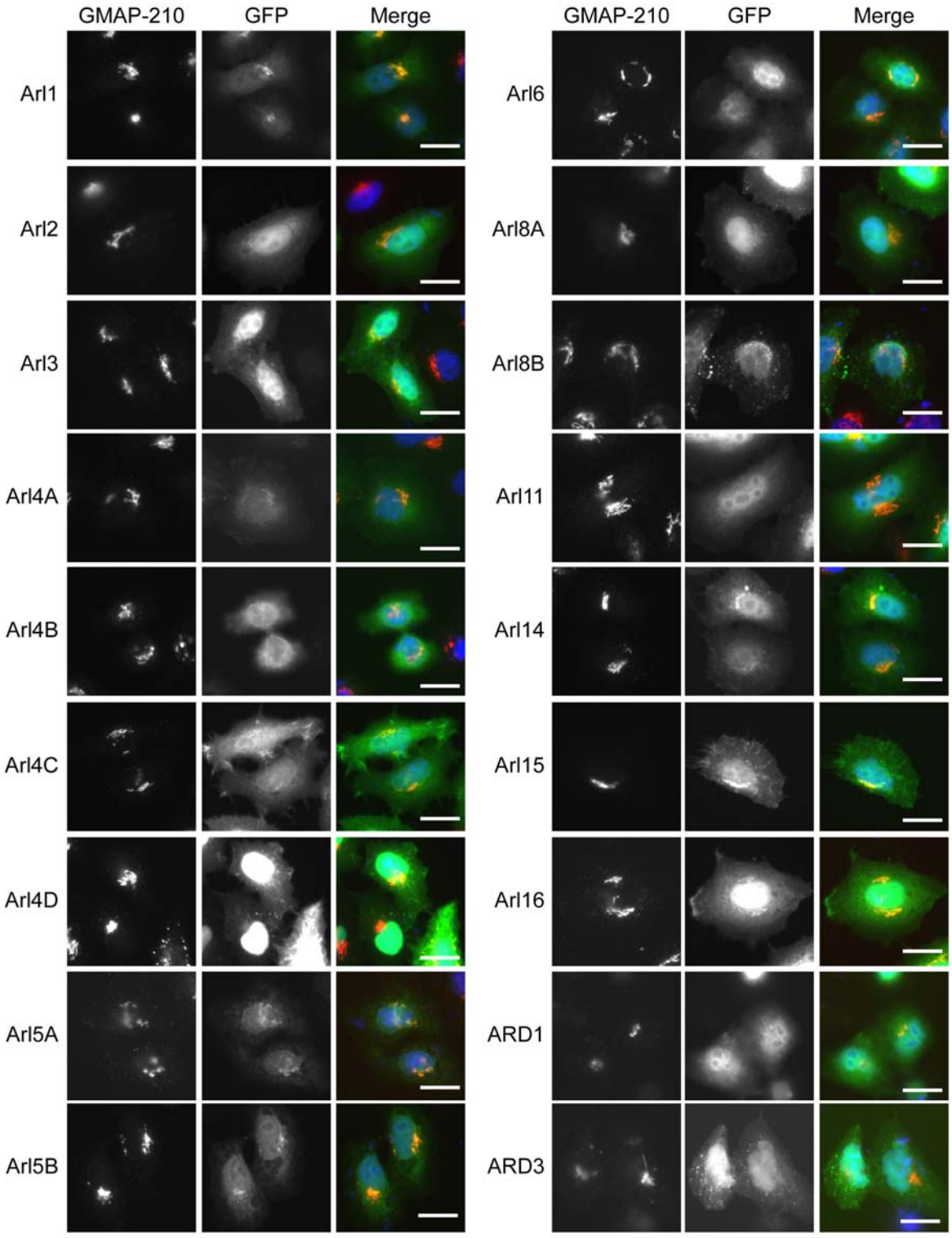

Figure 16: **Localisation Of The Arl Family Members In HeLa L Cells.** HeLa L cells transfected for 24 hours with a construct for expression of the indicated member of the ADP-ribosylation factor-like family with an enhanced GFP-Tag on the C-terminal end (green) were fixed with paraformaldehyde and stained with the rabbit anti GMAP-210 antibody (red, 1:500); blue channel: DAPI staining; Bar=10 μm.

of this study were only Arl-proteins localising to the Golgi complex. These were Arl1-GFP, Arl5-GFP (isoforms A and B) and Arl15-GFP. Arl16-GFP could be found mainly in the nucleus and cytosol; plasma membrane ruffles were also stained by Arl16-GFP. The Arl4 group, which interacted with the GMAP-210 GRAB domain in yeast 2-hybrid experiments (see 2.1.2, p.29*ff*), localised to the plasma membrane of HeLa L cells.
The Ratio of GTPases in active, GTP-bound form in comparison to inactive GDP-bound form is rather low in cells. Localisation of transfected wild-type protein, hence, could be difficult to distinguish from a high background signal. Better targeting of small GTPases could be achieved by transfection of GTP-locked mutants. Thus, selected members of the Arf and Arl family, in their constitutively active mutant form, were transfected into HeLa L cells and their localisation examined (Fig.17). GTP-locked Arl2-, Arl3- and Arl6-

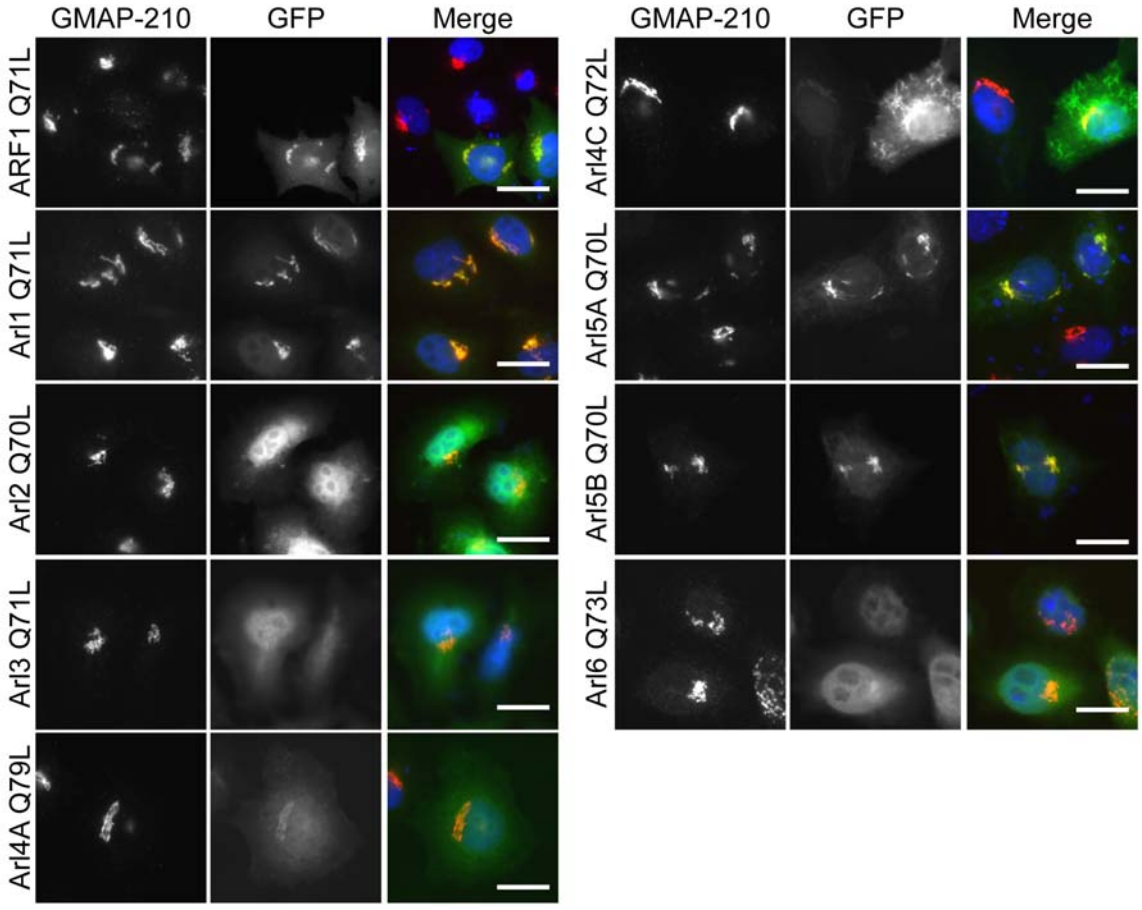

Figure 17: **Localisation Of The Arf and Arl Family Members As GTP-Locked Mutants.** HeLa L cells transfected for 24 hours with a construct for expression of the indicated member of the ADP-ribosylation factor or ADP-ribosylation factor-like family with an enhanced GFP-Tag on the C-terminal end (green); the catalytic glutamine was mutated to leucine thus the GTPase was locked in a GTP-binding, active conformation; the cells were fixed with paraformaldehyde and stained with the rabbit anti GMAP-210 antibody (red, 1:500); blue channel: DAPI staining; Bar=10 μm.

GFP could be observed only in the cytosol of HeLa L cells, Arl1Q71L (GTP-locked) and Arf1Q71L (GTP-locked) localised to the Golgi complex, as did Arl5A and Arl5B. The putative GRAB domain interactors Arl4A and Arl4C still localised at the plasma membrane. Only some weak Golgi targeting was observable.
So neither wild-type nor GTP-locked, active Arl4 shows a distinct targeting to the Golgi apparatus and no co-localisation with GMAP-210.

2.2.3 Recombinant Arl4 Does Not Interact With Endogenous GMAP-210 In Pulldown Experiments

The Arl4 group of the ADP-ribosylation factor family showed GRAB-domain dependent binding to GMAP-210, but did not co-localise with GMAP-210 on the Golgi apparatus. As transfection of tagged proteins could sometimes lead to mis-localisation, a biochemical approach was used to prove the results found in yeast 2-hybrid.
The interaction of GMAP-210 and ADP-ribosylation factor-like 4 was tested in pulldown experiments. Recombinant GST-tagged Arl-proteins (Arl1ΔN14, Arl3, Arl4AΔN14, Arl4CΔN14 and Arf1ΔN14) were incubated with HeLa L cytosol from cells transfected with pEGFPN3-GMAP210 or pEGFPC2-GMAP-210 1683-1875, both as wild-type or D1780A L1783A GRAB mutants. Bound proteins were analysed by Western blotting and identified with antibodies against GFP, GMAP-210 or p230 (Fig.18). Staining for p230 would show binding of endogenous p230 GRIP domain to Arl1ΔN14 under the experimental conditions, and served as positive control. Staining for GFP showed binding of exogenously expressed GMAP-210 full-length or GRAB domain, GMAP-210 staining compared endogenous against exogenous GMAP-210 binding to the GTPases.
Arl1 pulled down Golgin-245/p230 and no other GTPase tested showed any signal. Under no conditions binding of GMAP-210 was visible (weak signal of wild-type GMAP-210-GFP with Arl4AΔN14 is not mirrored by GMAP-210 antibody staining; signal is due to spill-over during gel loading process).
Also in pulldown experiments, Arl4 interaction with GMAP-210 could not be proven.

2.2.4 Arl4-GFP Does Not Co-Immunoprecipitate With Endogenous GMAP-210 From HeLa L Cells

Co-immunoprecipitation experiments were also performed to examine GMAP-210 interaction with Arl-GTPases. HeLa L cells were transfected with pEGFPN3-Arl4A, pEGFPN3-Arl4C or pEGFPN3-Arl1 and a lysate produced. The lysates were incubated with anti GFP or rabbit anti GMAP-210 antibody and Protein G sepharose. Antibody free beads

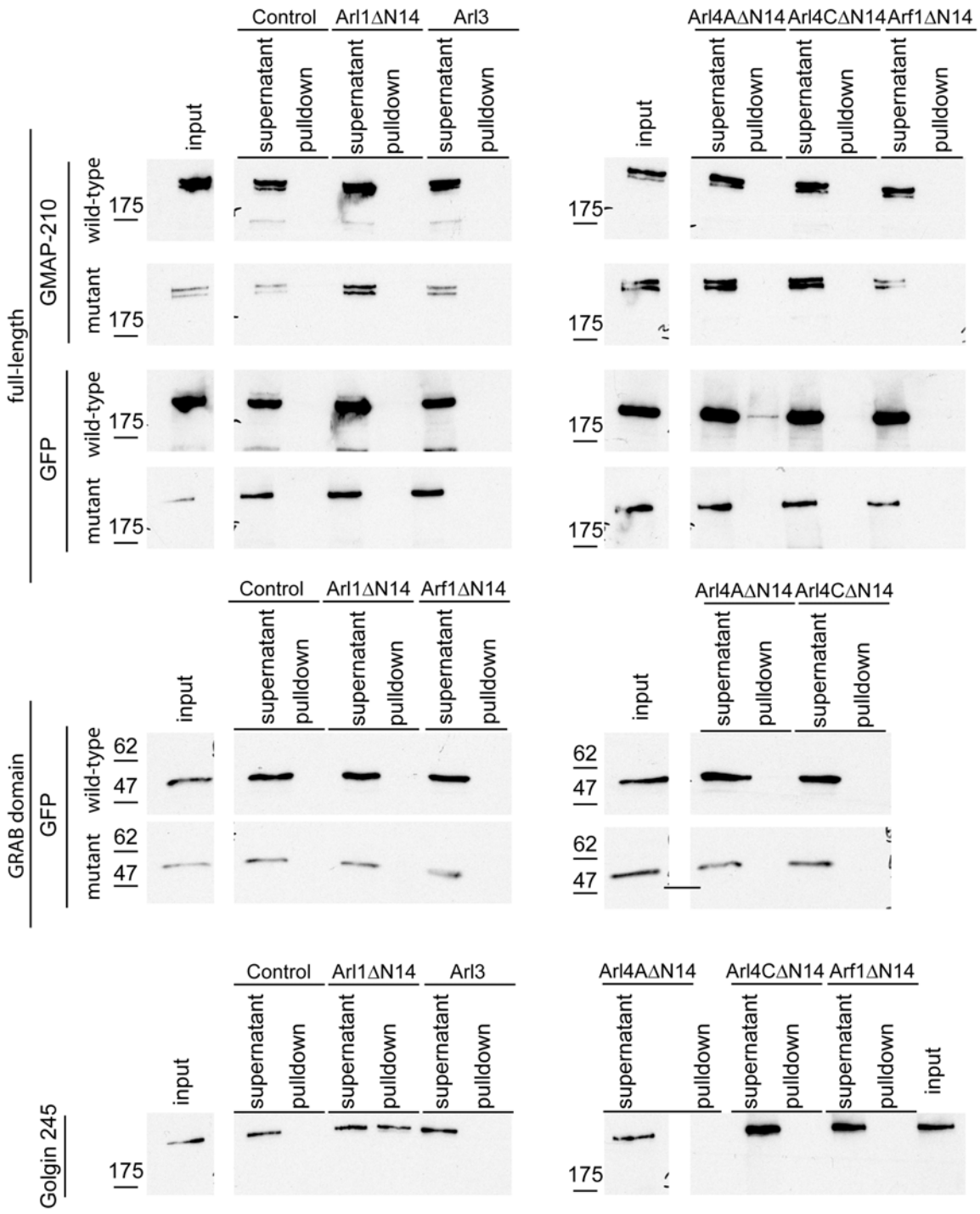

Figure 18: **Pulldown of GMAP-210 From HeLa Cell Extract With Recombinant Arl GTPases.** HeLa L cells were transfected with constructs for expression of wild-type GMAP-210 or GRAB mutant GMAP-210 D1780A L1783A (top); wild-type GRAB domain (amino acids 1683-1875) or mutant GRAB domain (1683-1875; D1780A L1783A) (middle); HeLa L cytosol was prepared in TMK buffer and incubated with GST-proteins produced on the same day and coupled to glutathione-sepharose; 0.05% Triton-X100 and 100 μM GTP were added for incubation; beads were boiled in SDS sample buffer and analysed by Western blotting from 6% or 12.5% SDS-PAGE gels; proteins were detected with either rabbit anti GMAP-210 (1:500, top), goat anti GFP (1:1000, top and middle) or mouse anti Golgin-245 (1:250, bottom) antibodies.

were used as control. Precipitated proteins were analysed by SDS-PAGE and Western blotting (Fig.19). Detection of proteins was done with sheep anti GFP and rabbit anti GMAP-210 antibodies. Exogenously expressed, GFP-tagged Arl1, Arl4A and Arl4C were precipitated efficiently by the sheep anti GFP antibody but no endogenous GMAP-210 was co-immunoprecipitated from the extract. GMAP-210 was efficiently precipitated from the extract, without co-purifying transfected GFP-tagged GTPases. Therefore, GMAP-210 and Arl4 do not interact *in vivo*.

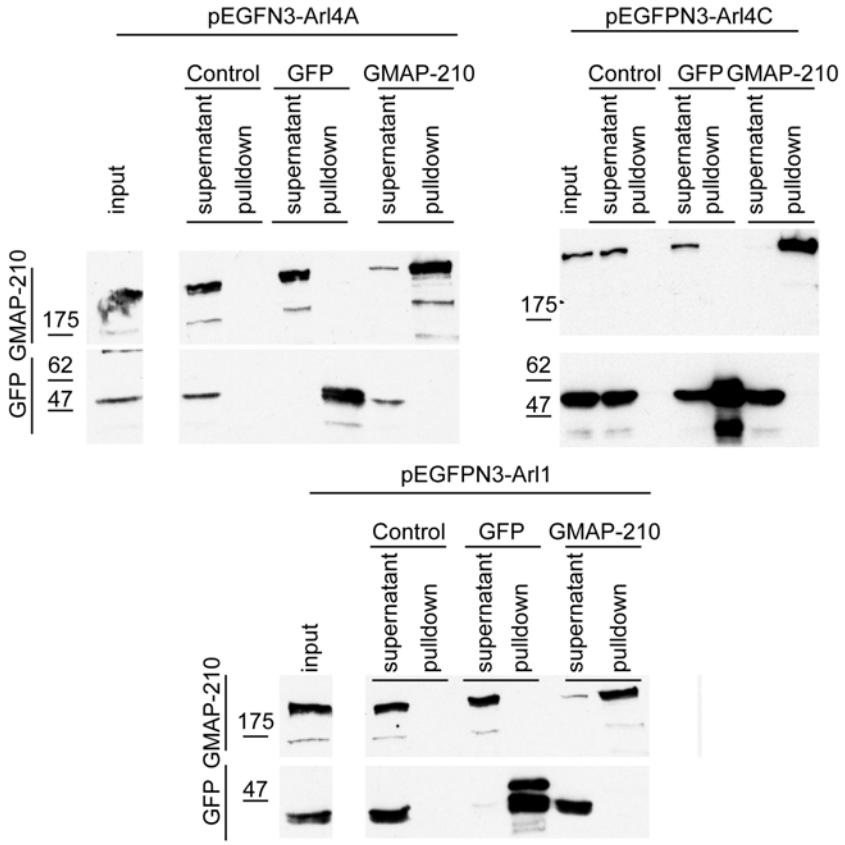

Figure 19: **Immunoprecipitation Of GMAP-210 And GFP-Tagged Arl Family Members.** HeLa L cells were transfected for 24 hours with the indicated constructs; a cell lysate was produced in NL100 buffer and incubated with rabbit anti GMAP-210, goat anti GFP or no antibody and protein-G sepharose; bound protein was extracted from beads by boiling in SDS sample buffer and analysed on 6% (GMAP-210) or 10% (GFP) SDS-PAGE gels and subjected to Western blotting; membranes from 6% gels were analysed with rabbit anti GMAP-210 (1:500), membranes from 10% with goat anti GFP (1:1000) antibodies.

2.2.5 *S.cerevisiae* Rud3p Also Interacts With *H.sapiens* Arl4 Family Members

As there is no evidence for GMAP-210 interaction with ADP-ribosylation factor family proteins so far, the original results, which describes *S.cerevisiae* Rud3p and Arf1p interaction were analysed with a different approach than presented in Gillingham *et al.* (2004). First, yeast 2-hybrid interaction studies were done with *S.cerevisiae* Arf1p (ScArf1) as bait in the pFBT9 vector and Rud3p and human GMAP-210 in the prey pAct2 vector (Fig.20). Neither Rud3p full-length nor GMAP-210 full-length interacted with ScArf1 in yeast 2-hybrid experiments. The nucleotide state of the GTPase was of no consequence as shown by use of the GTP-locked, active mutant ScArf1Q71L. Tested against human Arl-family members, however, Rud3p interacted with Arl4A and Arl4C in yeast 2-hybrid interaction screening just like GMAP-210 (2.2.1, p.35). Gillingham *et al.* (2004) showed yeast 2-hybrid interaction of Rud3p and Arf1p, however.
Next, ScArf1 was transfected into human HeLa L cells to see if it would localise to the Golgi as in *S.cerevisiae*. Fig.21 (upper panel) showed, that GFP-tagged Arf1p from *S.cerevisiae* co-localised with GM130 in perinuclear region, thus targeted to the mammalian Golgi. The lower row, however, makes clear, that Rud3p did not localise to the

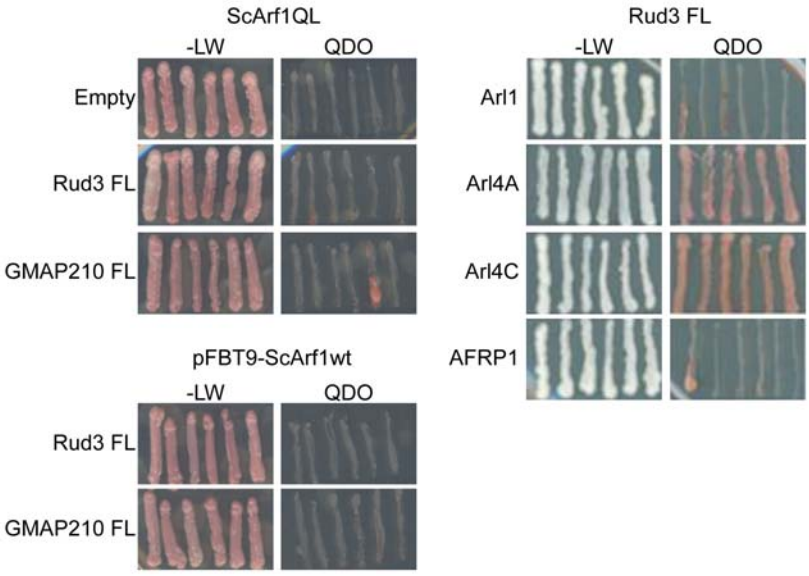

Figure 20: **Interaction Studies For GMAP-210 or Rud3p Against Arf1p,** *homo sapiens* **Arl1 and Arl4.** Yeast 2-Hybrid interaction study of full-length GMAP-210 or full-length *S.cerevisiae* Rud3p (fused to GAL4 transactivating domain; prey) against *S. cerevisiae* ADP-ribosylation factor 1 (fused to GAL4 binding domain) either in wild-type or GTP-bound, active form (Q71) (left) and ADP-ribosylation factor like 1, 4 and AFRP1 (right); -LW: leucine and tryptophane deficient medium (growth control); QDO: quadruple drop out medium; leucine, tryptophane, alanine and histidine deficient medium.

Golgi of HeLa L cells, even if they were co-transfected with Arf1p-GFP, which should have provided the proper interaction partner. In yeast 2-hybrid, Rud3p showed interaction with the same Arf/Arl-GTPases as GMAP-210. Furthermore, Rud3p could not target to the Golgi apparatus if transfected into mammalian cells, even not when *S.cerevisiae* Arf1p was present.

2.2.6 The Small GTPase Arf1 Interacts With The GMAP-210 GRAB Domain

As the most likely candidate for GRAB domain interaction, Arf1 did not interact with full-length GMAP-210 (Fig.12, p.35), the whole Arl and Arf family was tested for binding partners of GMAP-210. The Arl-GTPases, which interacted with GMAP-210 in yeast 2-hybrid, Arl4A, B and C (Fig.13, p.37) did not co-localise with GMAP-210 *in vivo* (Fig.16, p.40) and showed no interaction in biochemical experiments (Fig.18,19, p.43,44). Arf1, however, interacted in yeast 2-hybrid with a fragment containing only the GRAB domain (aa 1683-1875) (Fig.14, p.38). Thus, several fragments of GMAP-210 were tested for their interaction capability with Arf1 in yeast 2-hybrid (Fig.22). Full-length GMAP-210 did not interact with Arf1, neither did fragments, which did not contain the GRAB domain. The minimal GRAB domain (aa 1779-1835) did also not interact with Arf1, probably due to missing dimerisation elements. The GRAB domain with a short stretch

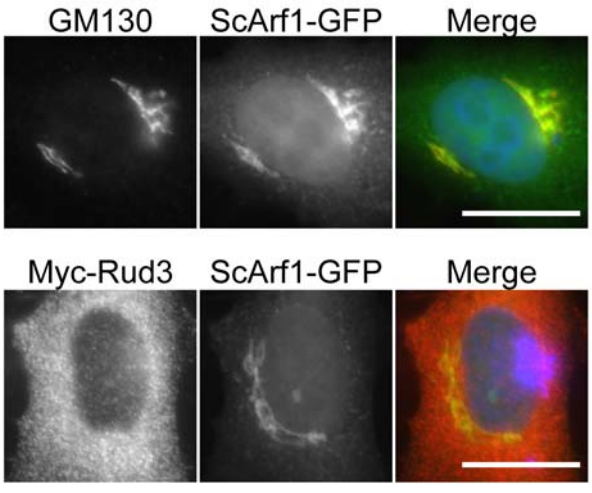

Figure 21: **Localisation of Arf1p and Rud3p In HeLa L Cells.** HeLa L cells were transfected with *S.cerevisiae* pEGFPN3-Arf1p (top, green) or *S.cerevisiae* pMyc-Rud3p (bottom) and pEGFPN3-Arf1p (bottom green) for 24 hours and fixed with paraformaldehyde; cells were stained sheep anti GM130 (red, 1:500, top) or mouse anti c-myc (9E10, 1:1000, red, bottom); blue channel: DAPI staining; Bar=10 μm.

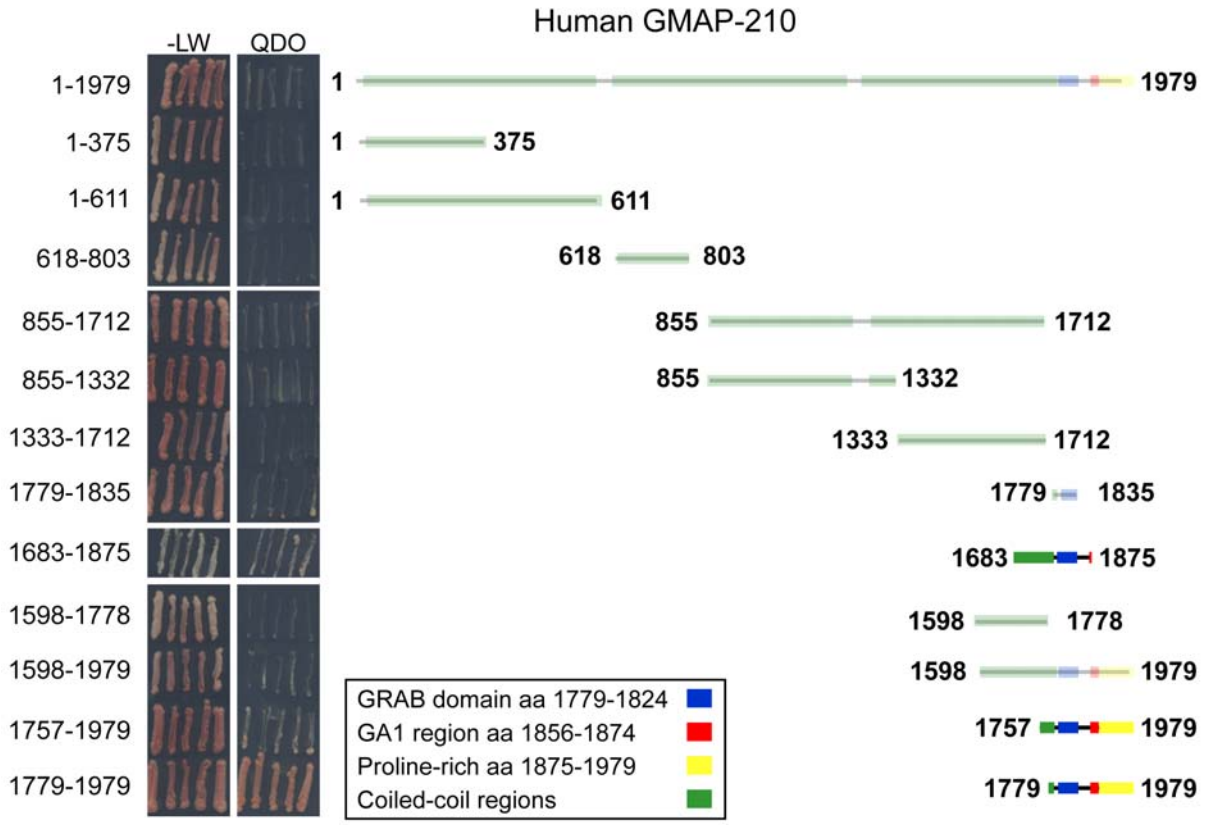

Figure 22: **Mapping Of GMAP-210 GRAB Domain Interaction With Arf1.** Yeast 2-Hybrid experiment testing Arf1 bait with GMAP-210 fragments as prey; cartoon shows tested fragments, transparent fragments are non-interacting; -LW: leucine and tryptophane deficient medium (growth control); QDO: quadruple drop out medium; leucine, tryptophane, alanine and histidine deficient medium.

of coiled-coil structure (aa 1683-1875) and C-terminal constructs comprising the GRAB domain on their N-terminus (aa 1757-1979 and aa 1779-1979) showed binding with Arf1. A C-terminal fragment (aa 1598-1979), which contained a longer stretch of coiled-coil, N-terminally to the GRAB domain, however, did not interact with Arf1. Some element within amino acids 1598 to 1682 is likely responsible for inhibiting Arf1 interaction with the GRAB domain of full-length GMAP-210.

2.2.7 Summary

The GMAP-210 homologue Rud3p interacts with the small GTPase Arf1p by its GRAB domain and is thus recruited to the Golgi apparatus. As the Arf/Arl-family in mammals is much bigger than in *S.cerevisiae*, GTPases apart from Arf1 could be possible interaction partners and recruiting factors for human GMAP-210. The whole family of Arf- and Arl-proteins was tested in yeast 2-hybrid and members of the Arl4 group showed positive

interaction with full-length GMAP-210, which was abolished by GRAB domain mutation and usage of the inactive mutant of Arl4. GFP-tagged Arl4 showed no co-localisation with GMAP-210 in HeLa L cells. Arl4-GFP targeted to the plasma membrane. Additionally, pulldown experiments with GST-tagged Arl4 and co-immunoprecipitation of Arl4-GFP with GMAP-210 gave no evidence for interaction. This makes it unlikely, that GMAP-210 and Arl4 are interaction partners *in vivo*. Arf1 did not interact with full-length GMAP-210, but interacted with GRAB domain containing fragments. Mapping of GMAP-210 showed, that inclusion of amino acids 1598 to 1682 in yeast 2-hybrid constructs abolished Arf1 interaction with the GMAP-210 GRAB domain.

2.3 GMAP-210 siRNA Oligo Depletes Endogenous Protein And Causes Golgi Apparatus To Compact In HeLa L Cells

Rios *et al.* (1994) showed, that depletion of GMAP-210 by siRNA fragments the Golgi apparatus. Knocking down GMAP-210 would prove a useful tool, not only to monitor morphology of the Golgi apparatus in absence of GMAP-210, but also to examine effects on the microtubule network, intracellular transport events and effects on localisation of various Golgi markers. For depletion of GMAP-210 from cultured human cells, an siRNA oligo was designed, which targets a sequence in the 3'-untranslated region of the GMAP-210 gene (see Table 5, p.122).

2.3.1 Efficiency Of GMAP-210 3'-UTR siRNA Oligo Examined By Western Blot

Depletion efficiency of the GMAP-210 siRNA oligo had to be tested by Western blotting. Extracts of HeLa L and *hTERT*-RPE1 cells treated for 72 h with the siRNA oligo against the GMAP-210 3'-UTR or the control oligos GL2 or Lamin A were subjected to Western blotting. Protein was detected with the affinity purified rabbit anti GMAP-210 antibody (Fig.23). The Western blot showed a single, specific band well above the 175 kDa marker in extracts from control HeLa L and *hTERT*-RPE1 cells. After 72 h of treatment with GMAP-210 siRNA oligo, the band disappeared completely. GMAP-210 was depleted by the chosen siRNA oligo.

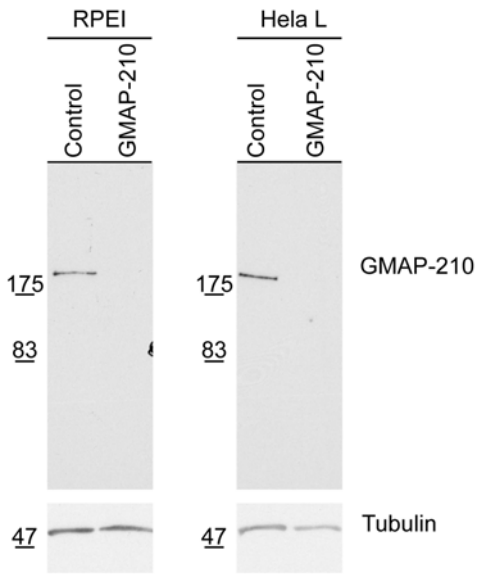

Figure 23: **GMAP-210-3'UTR siRNA Efficiency In *hTERT*-RPE1 and HeLa L.** HeLa L or *hTERT*-RPE1 cells were transfected with siRNA oligos against GL2 or Lamin A (control) or GMAP-210 3'-UTR for 72 h; cells were extracted in mammalian lysis buffer and 20 μg protein loaded onto 6% and 10% SDS-PAGE gels and subjected to Western blotting; proteins were detected with either rabbit anti GMAP-210 or mouse anti α-tubulin DM1A antibodies.

2.3.2 The Golgi Apparatus Compacts After GMAP-210 Knockdown

GL2, Lamin A or GMAP-210 siRNA oligos were transfected for 72 h into HeLa L and *hTERT*-RPE1 cells. After fixation and staining for GM130 and GMAP-210, cells were analysed by immunofluorescence microscopy (Fig.24). The signal for GMAP-210 was strongly reduced in both cell types after 72 h of treatment with the siRNA oligo against

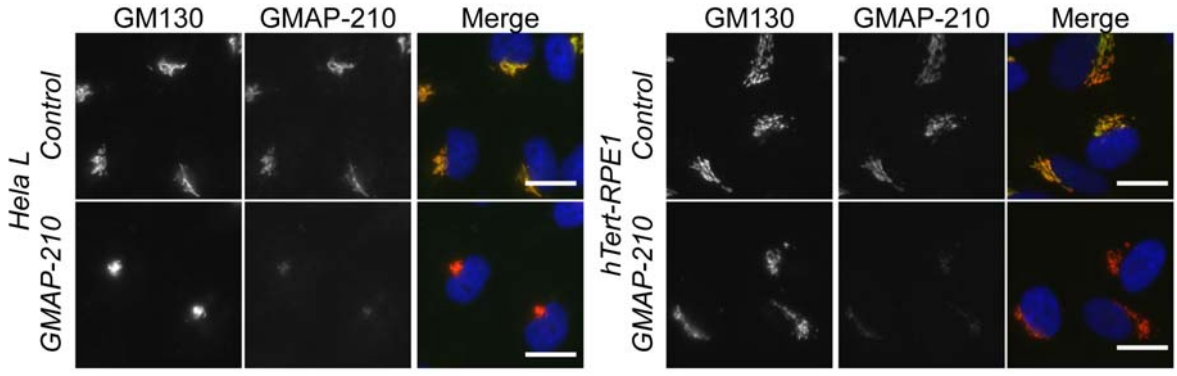

Figure 24: **GMAP-210 siRNA Effect On HeLa L And *hTERT*-RPE1 Cells.** HeLa L and *hTERT*-RPE1 cells were transfected for 72 h with siRNA oligos against GL2 (control) and GMAP-210 3'-UTR, fixed with paraformaldehyde and stained with mouse anti GM130 (red, 1:500) and rabbit anti GMAP-210 (green, 1:500) antibodies; blue channel: DAPI staining; Bar=10 μm.

GMAP-210 3'-UTR. While in *hTERT*-RPE1 cells no morphological change of the Golgi could be observed, the Golgi in HeLa L cells became small and rounded up upon depletion of GMAP-210 by siRNA. Furthermore, the signal intensity of GM130 became much brighter and remained on the Golgi, indicating a higher concentration of protein within a smaller area.

In order to quantify the observed Golgi shrinking in HeLa L and *hTERT*-RPE1 cells, cells from two independent experiments, performed as described above, were analysed and nuclear diameter compared to Golgi diameter. Long Golgi ribbons were measured from compartment tip to tip (Fig.25) using the Photoshop CS2 measuring tool. 15 to 25 cells were measured per experiment and condition. In HeLa L cells, nuclear diameter changed from 6.05(+/-0.17) to 5.41(+/-0.52), Golgi diameter changed from 4.78(+/-0.4) to 2.27(+/-0.52). Thus, Golgi diameter in HeLa L cells decreased to half the value of

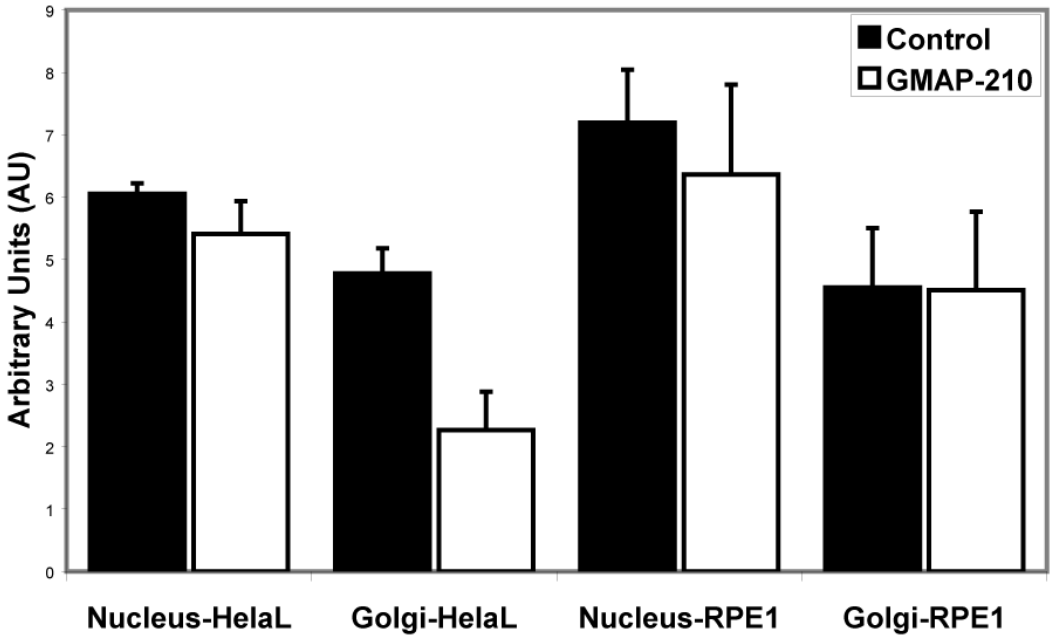

Figure 25: **Graphical Representation Of GMAP-210 siRNA Effect.** HeLa L or *hTERT*-RPE1 cells were transfected for 72 h with siRNA oligos against GL2 (control) and GMAP-210 3'-UTR, fixed with paraformaldehyde and stained with mouse anti GM130 (1:500) and rabbit anti GMAP-210 (1:500) antibodies (see Fig.24); measurement of nuclear and Golgi diameter was done with Adobe Photoshop measuring tool, measuring 15-25 individual cells per experiment (n=2); nuclear diameters in HeLa L cells are: GL2 6.05+/- 0.17; GMAP-210 5.41+/-0.52; Golgi length (maximum distance between endpoints): GL2 4.78+/-0.4; GMAP-210 2.27+/-0.62. In *hTERT*-RPE1 cells nuclear diameters were: GL2 7.19+/-0.85; GMAP-210 6.36+/-1.44; Golgi length: GL2 4.55+/-0.95; GMAP-210 4.51+/-1.26; all given in arbitrary units.

wild-type cells upon depletion of GMAP-210 by siRNA. In *hTERT*-RPE1 cells, nuclear diameter was 7.19(+/-0.85) and 6.36(+/-1.44), Golgi size changed from 4.55(+/-0.95) to 4.51(+/-1.26) for control and GMAP-210 siRNA, respectively. Golgi size did not change in *hTERT*-RPE1 cells after GMAP-210 depletion. In both cell types, however, overall cell size stayed approximately the same as monitored by nucleus diameter.
GMAP-210 depletion caused shrinking of the Golgi apparatus in HeLa L cells by approximately 50% whereas *hTERT*-RPE1 cells' Golgi did not change.

2.3.3 Electron Microscopy Of HeLa L Golgi Apparatus After GMAP-210 Depletion

For a closer examination of the changes in Golgi morphology caused by depletion of GMAP-210 in HeLa L cells, electron microscopy was performed (4.6.5, p.139). HeLa L cells were treated for 72 h with siRNA oligos against GL2 as control or GMAP-210 3'-UTR (Fig.26) and then processed for electron microscopy as described in 4.6.5 (p.139). In HeLa L control cells, the Golgi consisted of stacked cisternae, which formed ribbons in the perinuclear region (Fig.26; white arrowheads; pictures only show section of Golgi ribbon). In GMAP-210 depleted cells the Golgi ribbon structure broke down, stacks vanished and only oddly shaped, bloated vesicles of varying sizes remained (Fig.26; black arrowheads). In some cells, these vesicular structures clustered in a small area near the nucleus. This was reminiscent of the collapse effect observed in immunofluorescence of HeLa L cells (Fig.24, p.49).
GMAP-210 depletion in HeLa L by siRNA causes fragmentation of the Golgi apparatus and fragments cluster near the nucleus.

2.3.4 After GMAP-210 Depletion, Expressed Protein Is Recruited To The Golgi Apparatus Independently Of GRAB Domain

In order to examine whether the GMAP-210 siRNA phenotype (see 2.3, p.48) is reversible by transfection of GFP-tagged GMAP-210 constructs, HeLa L cells were transfected with GL2 control siRNA oligos or GMAP-210 3'-UTR siRNA oligos for 72 h. 48 hours after siRNA treatment, constructs for GMAP-210 expression with enhanced GFP-tags were transfected (Fig.27, p.53). The cells were fixed and stained for GM130. As can be seen in Fig.27, transfection of full-length GMAP-210 (pEGFPN3-GMAP-210) had little effect on the compacted Golgi, also transfection of GMAP-210 GRAB domain (pEGFPC2-GMAP-210 1683-1875) had no effect. Surprisingly enough, the GRAB mutant of full-length GMAP-210 (pEGFPC2-GMAP-210 D1780A L1783A), which showed only weak target-

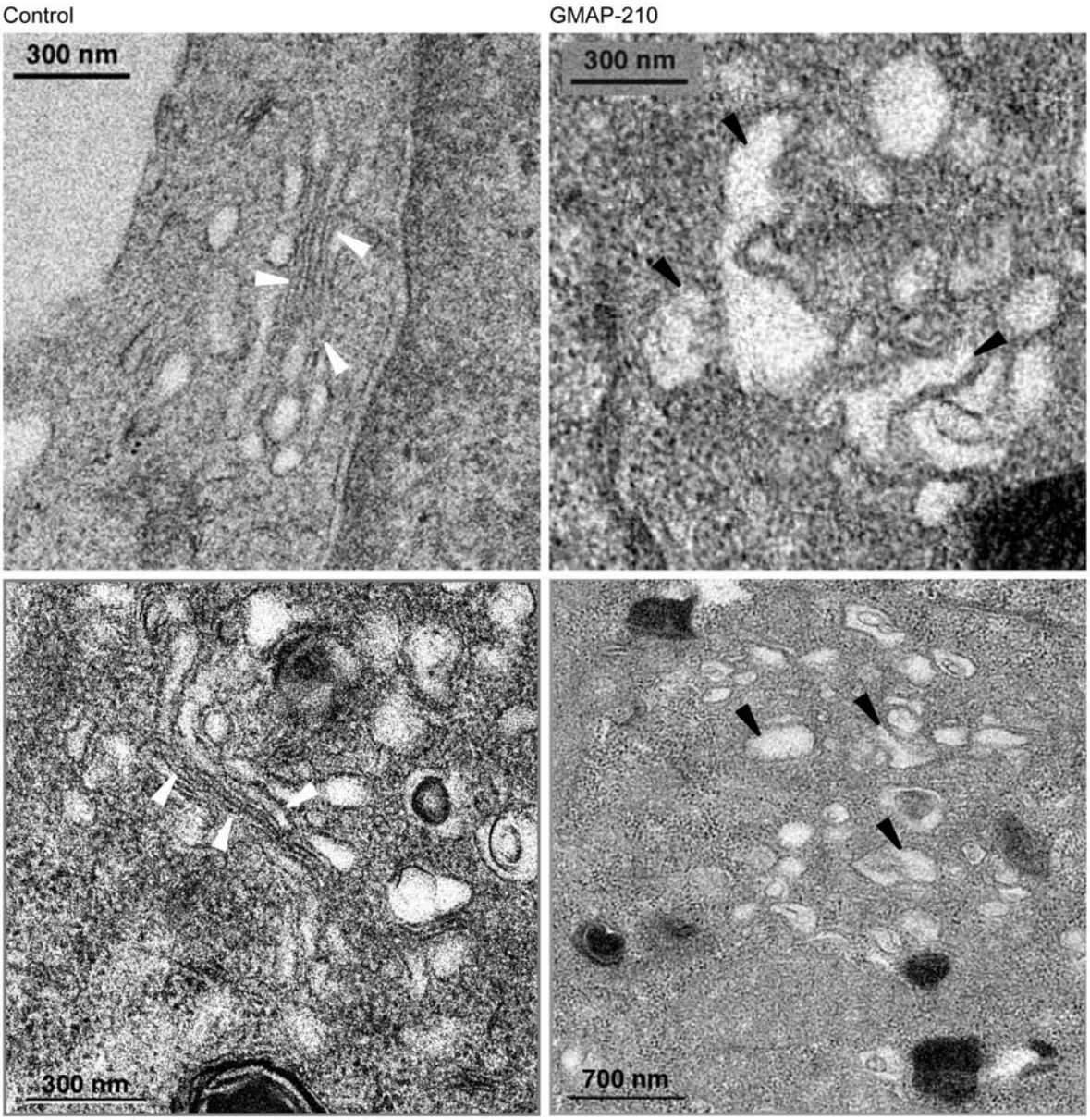

Figure 26: **Electron Microscopy Of HeLa L Golgi Apparatus.** HeLa L cells were transfected with siRNA oligo against GL2 control (left) or GMAP-210 3'-UTR (right) for 72 h and fixed in 2.5% glutaraldehyde in 0.1 M cacodylate buffer containing 5% sucrose, pH 7.1-7.2, at room temperature for 30-40 min, then in the same fixative containing 1% tannic acid at 4°C for 30-60 min, postfixed in 1% OsO_4 for 1-2 hrs, stained en bloc in 1% aqueous uranyl acetate at 60°C overnight, dehydrated in ethanol and embedded in Spurr's medium. Thin sections were taken on a Leica Ultracut with a Diatome diamond knife and investigated in a Philips (FEI) CM 12 electron microscope operated at 120 kV; white arrowheads: stacked Golgi cisternae in control cells; black arrowheads: Golgi fragments after GMAP-210 depletion; pictures by Dr. Thomas Keil.

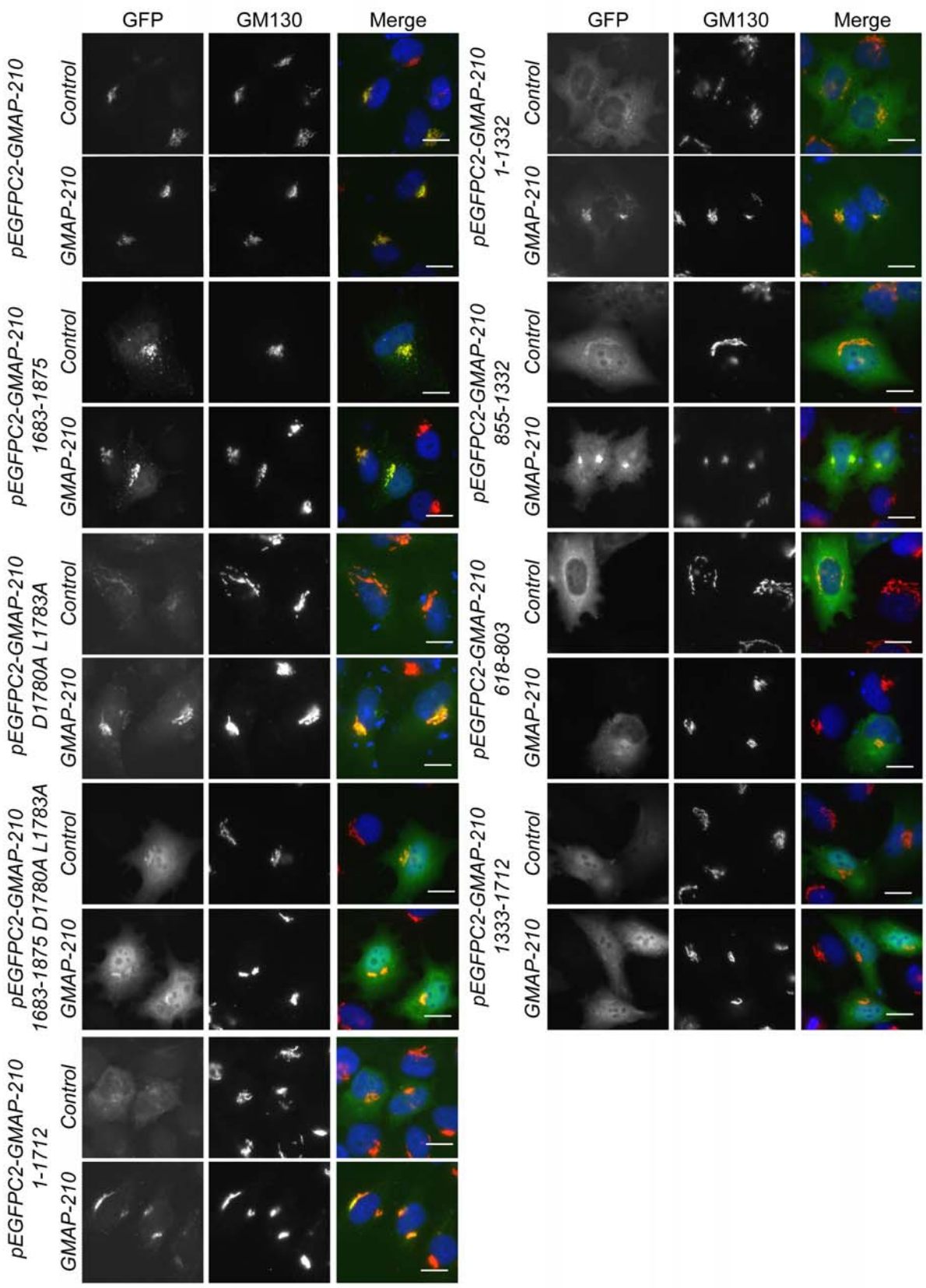

Figure 27: **GMAP-210 Fragments In GMAP-210 siRNA Background.** HeLa L cells were transfected for 72 h with an siRNA oligo against GMAP-210 3'-UTR or GL2 (control); after 48 h the cells were also transfected with the indicated GMAP-210 fragments for 24 h (green); cells were fixed with paraformaldehyde and stained with the mouse anti GM130 antibody (red, 1:500); blue channel: DAPI staining; Bar=10 μm.

ing to the Golgi in control cells, showed clear and distinct localisation to the Golgi after depletion of endogenous GMAP-210. In order to analyse this effect, more fragments of GMAP-210 were transfected. Transfection of the GRAB domain mutant (pEGFPC2-GMAP-210 1683-1875 D1780A L1783A) was mostly localised diffusely in the cytosol. The weak Golgi localisation was not changed after siRNA of GMAP-210. N-terminal constructs missing the GRAB domain like pEGFPC2-GMAP-210 1-1712 or pEGFPC2-GMAP-210 1-1332, however, showed a clear signal at the Golgi apparatus in absence of endogenous GMAP-210. This was in contrast to control cells. Further mapping for this putative Golgi targeting signal in GMAP-210 showed, that the region between amino acids 855 and 1332 got recruited to the Golgi apparatus after GMAP-210 siRNA treatment (pEGFPC2-GMAP-210 855-1332). Constructs comprising amino acids 618 to 803 or 1333 to 1712 remained diffusely localised in the cytosol (pEGFPC2-GMAP-210 618-803 and 1333-1712). This phenomenon will be further examined in 2.4.2 (p. 56).
As the observed siRNA phenotype (see 2.3, p.48) in HeLa L was different compared to the one observed in *hTERT*-RPE1 cells, it was necessary to check in *hTERT*-RPE1 cells if GFP-tagged GMAP-210 constructs were recruited to the Golgi upon depletion of endogenous GMAP-210.
hTERT-RPE1 cells were treated with GL2 control siRNA oligos or GMAP-210 siRNA oligos for 72 h. After 48 h they were also transfected with GFP-tagged constructs of GMAP-210 full-length, wild-type and GRAB domain mutant (D1780A L1783A) and GMAP-210 amino acids 1 to 1712. The cells were fixed and stained for GM130 as Golgi marker (Fig.28). Full-length GMAP-210 wild-type (pEGFPN3-GMAP-210) or GRAB mutant (pEGFPC2-GMAP-210 D1780A L1783A) co-localised with GM130 on the Golgi apparatus, independently of presence or absence of endogenous GMAP-210. The GMAP-210 construct without GRAB domain (pEGFPC2-GMAP-210 1-1712) could be found concentrated in the perinuclear region, but did not co-localise with GM130, neither in control nor in GMAP-210 depleted cells. Hence, *hTERT*-RPE1 cells behaved differently from HeLa L cells in relation to localisation of GMAP-210.
Depletion of GMAP-210 in HeLa L cells caused compaction of the Golgi. This effect was not reversed by overexpression of GFP-tagged GMAP-210, although GRAB domain mutant constructs of GMAP-210 were recruited to the Golgi after depletion of endogenous GMAP-210, an effect not seen in *hTERT*-RPE1 cells under the same conditions.

2.3.5 Summary

An siRNA oligo against the 3'-UTR of the human GMAP-210 gene was designed and tested for its efficiency. Endogenous GMAP-210 is depleted from HeLa L and *hTERT*-

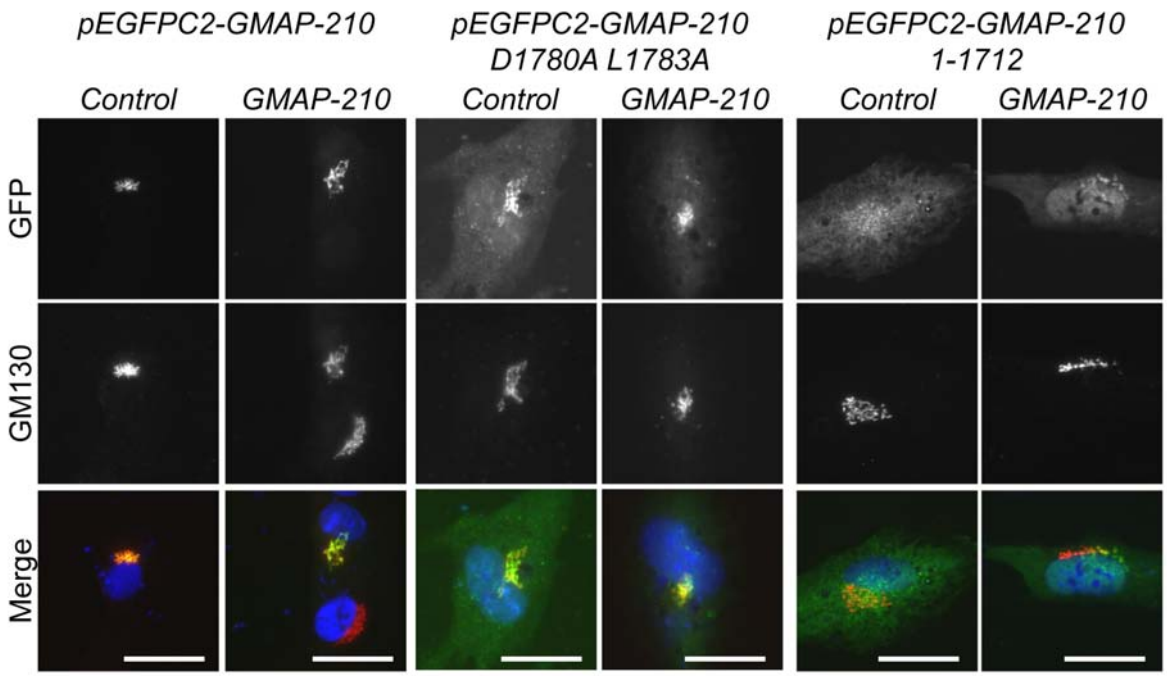

Figure 28: **GMAP-210 Fragments In GMAP-210 siRNA Background In *hTERT*-RPE1 Cells.** *hTERT*-RPE1 cells were transfected for 72 h with an siRNA oligo against GMAP-210 3'-UTR or GL2 (control); after 48 h the cells were also transfected with the indicated GMAP-210 fragments and mutant constructs for 24 h; cells were fixed with paraformaldehyde and stained with mouse anti GM130 antibody (red, 1:500); blue channel: DAPI staining; Bar=5 μm.

RPE1 cell extracts after 72 h as monitored by Western blotting. In immunofluorescence, Golgi staining by GMAP-210 antibodies vanished completely. In HeLa L cells, the Golgi apparatus showed a compacted morphology after depletion of GMAP-210, monitored by intensified GM130 staining on the smaller and round-up Golgi. Electron microscopy elucidated, that, on an ultrastructural level, the compacted Golgi was a cluster of swollen vesicular fragments.

Transfection of GMAP-210 GRAB domain mutants, which were unable to bind to Golgi in control cells, were suddenly recruited to Golgi membranes. Mapping revealed, that GMAP-210 amino acids 855 to 1332 were responsible for this. In *hTERT*-RPE1 cells a change in Golgi morphology could not be obtained.

2.4 GMAP-210 Co-Localises And Interacts With Markers From The ER-To-Golgi Pathway

Up to date, no interaction partners are known for GMAP-210, apart from the putative interaction with ADP-ribosylation factor 1 (Arf1), discovered with the *S.cerevisiae* homologue of GMAP-210 (Gillingham *et al.*, 2004). Thus, several components from the

secretory pathway of mammalian cells were tested for interaction and co-localisation with GMAP-210 or for specific changes in their distribution upon GMAP-210 depletion.

2.4.1 SNARES And Golgins Remain Localised To The Compacted Golgi Apparatus Upon GMAP-210 Knockdown

GMAP-210 is localised to the cis-Golgi (Rios *et al.*, 1994) and is a putative interaction partner of a small Arf-/Arl-GTPase, as shown in *S.cerevisiae* for Rud3p and Arf1p (Gillingham *et al.*, 2004). In order to find interaction partners of GMAP-210, which could elucidate its function on the Golgi apparatus, siRNA against GMAP-210 3'-UTR and subsequent co-staining with antibodies against a variety of Golgi markers was performed in HeLa L cells (Fig.29). The proteins tested were the SNAREs GS15, GS27, GS28, Vti1a and Vti1b, Golgi localised large coiled-coil proteins Golgin-245/p230, Golgin-84, TGN46 and GM130 and the cargo sorting KDEL-receptor. All these proteins had a pool on the Golgi apparatus. Upon depletion of GMAP-210 by siRNA, the Golgi collapsed while all examined proteins still localised to its membrane. The signal intensity for all markers became higher, indicating the same amount of protein within a smaller area of Golgi membranes. The only protein which showed a slightly weaker Golgi localised signal, in comparison to other tested markers, is the SNARE Vti1b. This might indicate a partial loss of Vti1b from the Golgi apparatus, when GMAP-210 was depleted. None of the tested proteins co-localised with GMAP-210 on the Golgi apparatus. This is expected and especially obvious for the trans-Golgi golgins p230 and TGN46.
None of the tested markers could be identified as candidates for GMAP-210 interaction and apart from Vti1b, Golgi localisation was not impaired by GMAP-210 depletion.

2.4.2 GMAP-210 Interacts With The Rab GTPase Rab1

Rab GTPases are involved in a great variety of intracellular transport steps (Pfeffer, 2001). Furthermore, Rab-GTPases have a propensity to bind to proteins with long coiled-coil regions (Short *et al.*, 2005).
To identify possible interaction partners for GMAP-210 amongst Rab proteins, GMAP-210 was screened in a yeast 2-hybrid assay against the complete Rab family available as a library in the laboratory. GMAP-210 was used as prey in the pAct2 vector, the Rab GTPases were used as bait in the pFBT9 vector. The GTPases were used as GTP-locked, active mutants (catalytic glutamine to alanine). The complete screen is given in Fig.30. The yeast 2-hybrid screening showed GMAP-210 interacting with Rab1a/1b, Rab2a/2b, Rab8a, Rab10, Rab14, Rab15, Rab35 and Rab39. Rab45 is self-activating and thus is

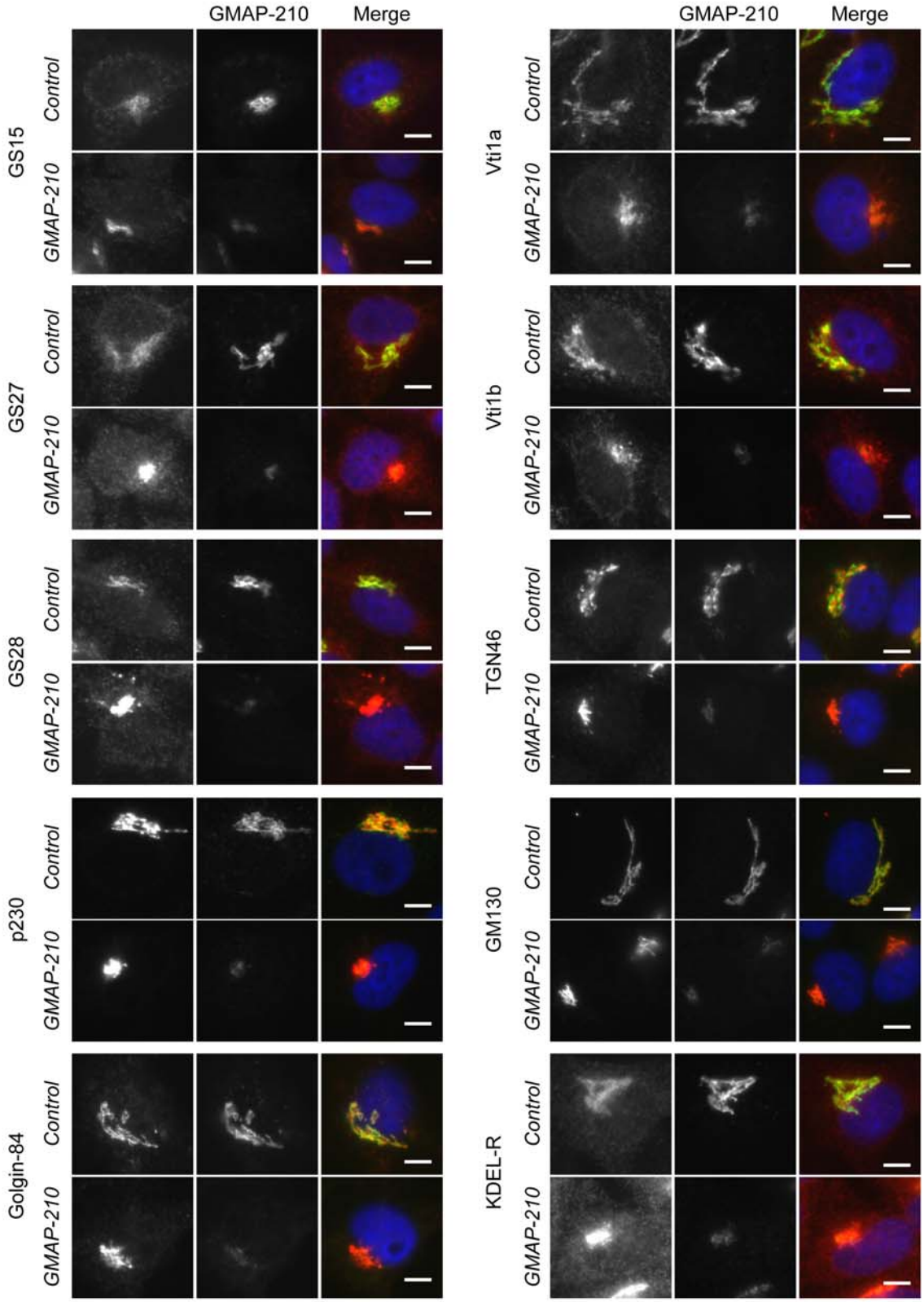

Figure 29: **Selected Golgi Markers And GMAP-210.** HeLa L cells were transfected with an siRNA oligo against GMAP-210 3'-UTR or GL2 (control) for 72 h and fixed with either methanol (KDEL-R) or paraformaldehyde (all others); cells were stained with rabbit anti GMAP210 (green, 1:500) antibody; for co-staining anti GS15 (1:100), anti GS27 (1:500), anti GS28 (1:500), anti Golgin-245/p230 (1:250), anti Vti1a (1:100), anti Vti1b (1:100), anti GM130 (1:500), anti KDEL R (1:500) (all mouse, red), anti Golgin-84 (1:500) or anti TGN46 (1:2000) (both sheep, red) antibodies were used; blue channel: DAPI staining; Bar=5 μm.

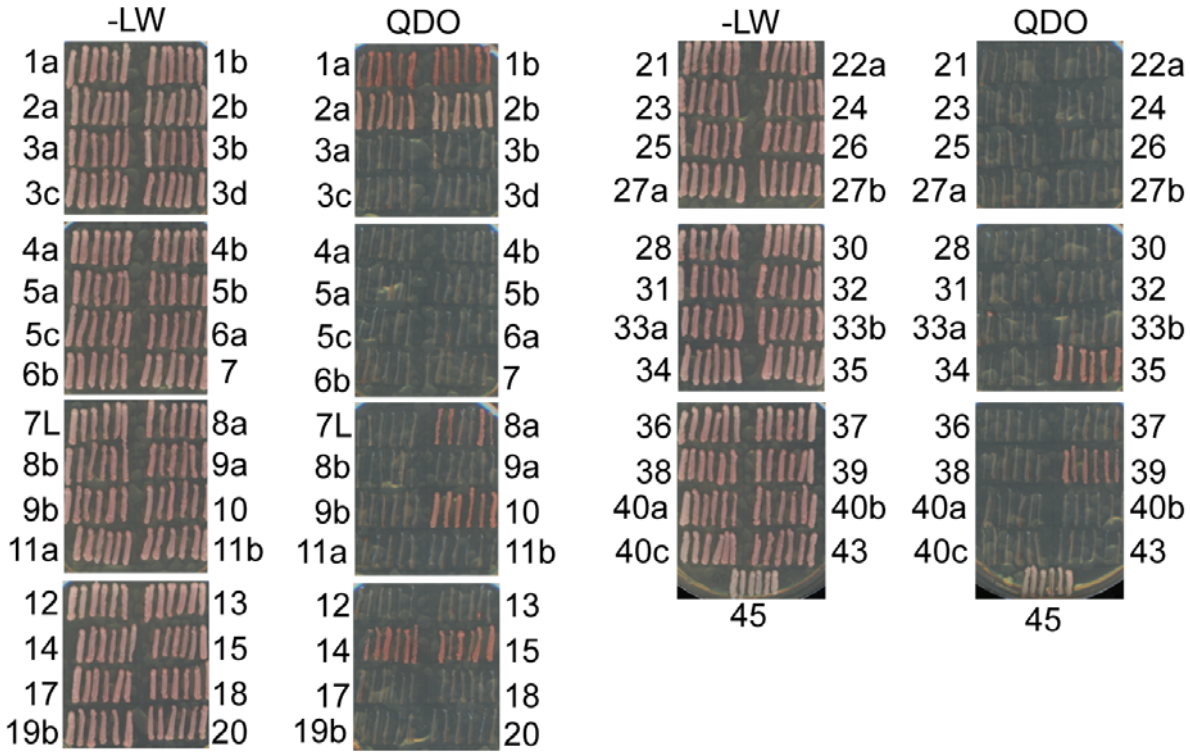

Figure 30: **Yeast 2-Hybrid Screen Of GMAP-210 Against The "Rabome".** Yeast 2-Hybrid interaction experiment, screening GMAP-210 full-length (prey in pAct2) against a complete collection of Rab GTPases (Rabome) in GTP-bound, active mutant form (Q-A) (bait in pFBT9) -LW: leucine and tryptophane deficient medium (growth control); QDO: leucine, tryptophane, histidine and alanine deficient medium; numbers indicate Rab GTPase number.

used as positive control.

Of these Rab proteins, Rab1 and Rab2 are Golgi localised and involved in ER to Golgi and intra-Golgi trafficking (Allan *et al.*, 2000; Moyer *et al.*, 2001; Short *et al.*, 2001). They have also been described to bind to several coiled-coil Golgi localised proteins (Short *et al.*, 2005). This made them possible candidates for further examination.

HeLa L cells were treated with GL2 control siRNA or GMAP-210 siRNA for 72 h, fixed and stained for Rab1 or Rab2 while co-stained with an antibody against the golgin GM130 (Fig.31) Rab1 and Rab2 localised to the same perinuclear structure like GM130. Rab1 also showed a web-like structure, which might represent its localisation to the endoplasmic reticulum. Upon GMAP-210 depletion, the Golgi became very compact and round-up. Still Rab1 and Rab2 co-localise with GM130 and Rab1 could still be found at the endoplasmic reticulum. Thus, neither Rab1 nor Rab2 changed localisation when GMAP-210 was depleted in HeLa L cells.

Rab1 and Rab2 interaction with GMAP-210 was further tested by mapping the interaction domain by the yeast 2-hybrid method (Fig.32). Rab1a and Rab2a were used as bait in the yeast 2-hybrid assay, whereas different GMAP-210 fragments were used as

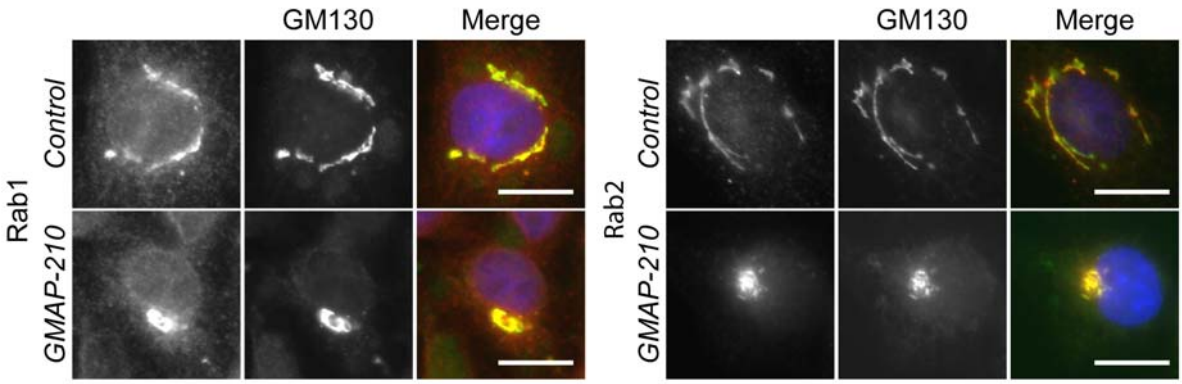

Figure 31: **GMAP-210 And The Small GTPases Rab1 And Rab2.** HeLa L cells were treated with an siRNA oligo against GMAP-210 3'-UTR or GL2 (control) for 72 h and fixed with paraformaldehyde; the cells were stained with mouse anti Rab1 (red, 1:5, top) or Rabbit anti Rab2 (red, 1:500, bottom) and sheep anti GM130 (green, 1:500) antibodies; blue channel: DAPI staining; Bar=10 μm.

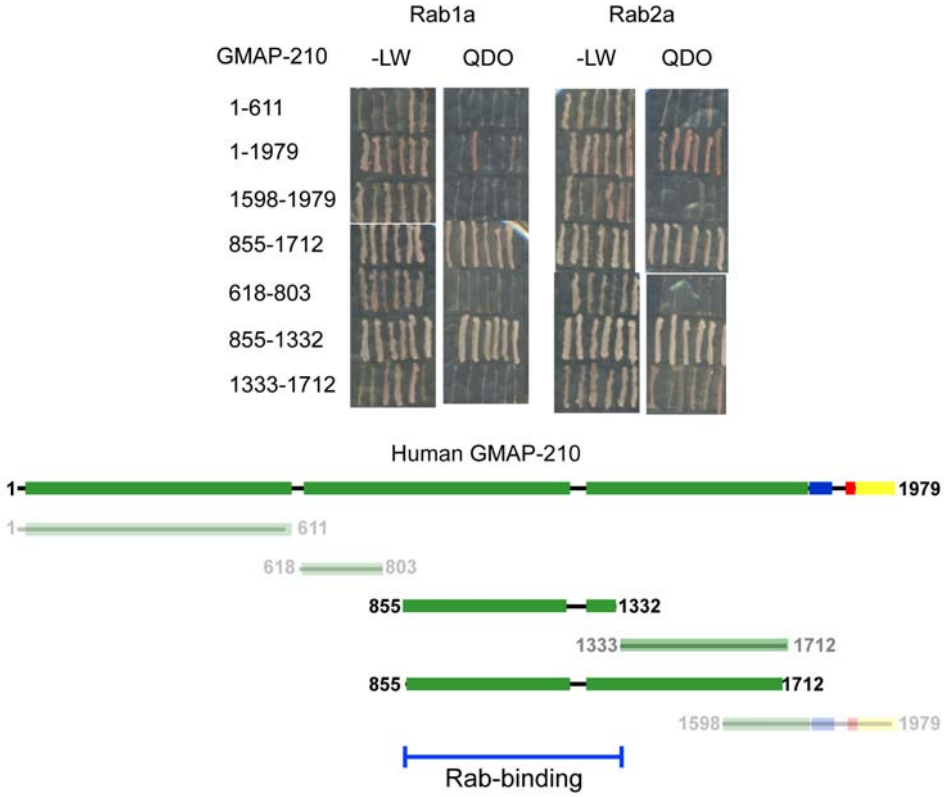

Figure 32: **Yeast 2-Hybrid Mapping for Rab1/Rab2 Interaction Site in GMAP-210.** Yeast 2-Hybrid interaction mapping experiment, testing indicated GMAP-210 fragments as prey in pAct2 vector against Rab1a and Rab2a wild-type in the pFBT9 vector; -LW: leucine and tryptophane deficient medium (growth control); cartoons indicate tested fragments, non-interacting fragments are depicted transparent; QDO: leucine, tryptophane, histidine and alanine deficient medium; numbers indicate amino acid range of fragment tested.

prey. In general Rab2a gave a stronger interaction than Rab1a. Full-length GMAP-210 interacted with both GTPases. Of the tested fragments only amino acids 855 to 1712 and the sub-fragment 855-1332 gave a signal. With Rab2a as bait, GMAP-210 amino acids 1333 to 1712 also reacted although weaker than with amino acids 855 to 1332.

This interaction still had to be proven by biochemical interaction studies. For this the Rab GTPases identified in yeast 2-hybrid as possible GMAP-210 partners were expressed in *E.coli* with an N-terminal glutathione-S-Transferase(GST)-tag and coupled to glutathione-S-sepharose loaded with GTP and incubated with HeLa L cell extract. Bound protein was examined by SDS-PAGE and Western blotting. Detection with anti GMAP-210 antibodies showed binding (Fig.33, top; p.61). Coupling of recombinant Rab proteins to beads was monitored by coomassie stained SDS-PAGE, comparing input to supernatant of the coupling reaction (Fig.33, bottom; p.61). All proteins except Rab39 coupled efficiently, although Rab39 coupling was still sufficient for the experiment. The Western blotting of eluted protein clearly showed binding of GMAP-210 to Rab1, but not to Rab2 and to none of the other tested Rab GTPases Rab8a, Rab10, Rab14, Rab15, Rab35 or Rab39.

As Rab effector, binding of GMAP-210 to Rab1 had to be dependent on the nucleotide state of the GTPase. GMAP-210 would only bind to Rab1 in its GTP-bound, active, not in its GDP-bound, inactive state. The pulldown experiment was repeated with the GDP-locked, inactive (Rab1S25N) mutant in comparison to the GTP-locked, active mutant of Rab1 (Rab1Q70L) (Fig.34, p.62). The difference in phenotype after siRNA knockdown (2.3, p.48*ff*) in HeLa L compared to *hTERT*-RPE1 cells showed, that there seemed to be a difference in GMAP-210 function in these two cell types. To be sure, that the different behaviour of GMAP-210 is not related to different interactions partners, cell extracts from both cell lines were tested in this pulldown experiment. The experiment (Fig.34, p.62), however, showed no difference in binding behaviour or efficiency between HeLa L- and *hTERT*-RPE1-derived GMAP-210. Rab1 could pull down GMAP-210 from cell extract only in its GTP-locked, active mutant form. The GDP-locked version did not bind to GMAP-210. The coomassie stained SDS-PAGE depicted below the Western blots showed efficient coupling of the recombinant Rab1 proteins to the beads. GMAP-210 bound specifically to active Rab1 but not to inactive, GDP-bound Rab1. This was independent of cell type used.

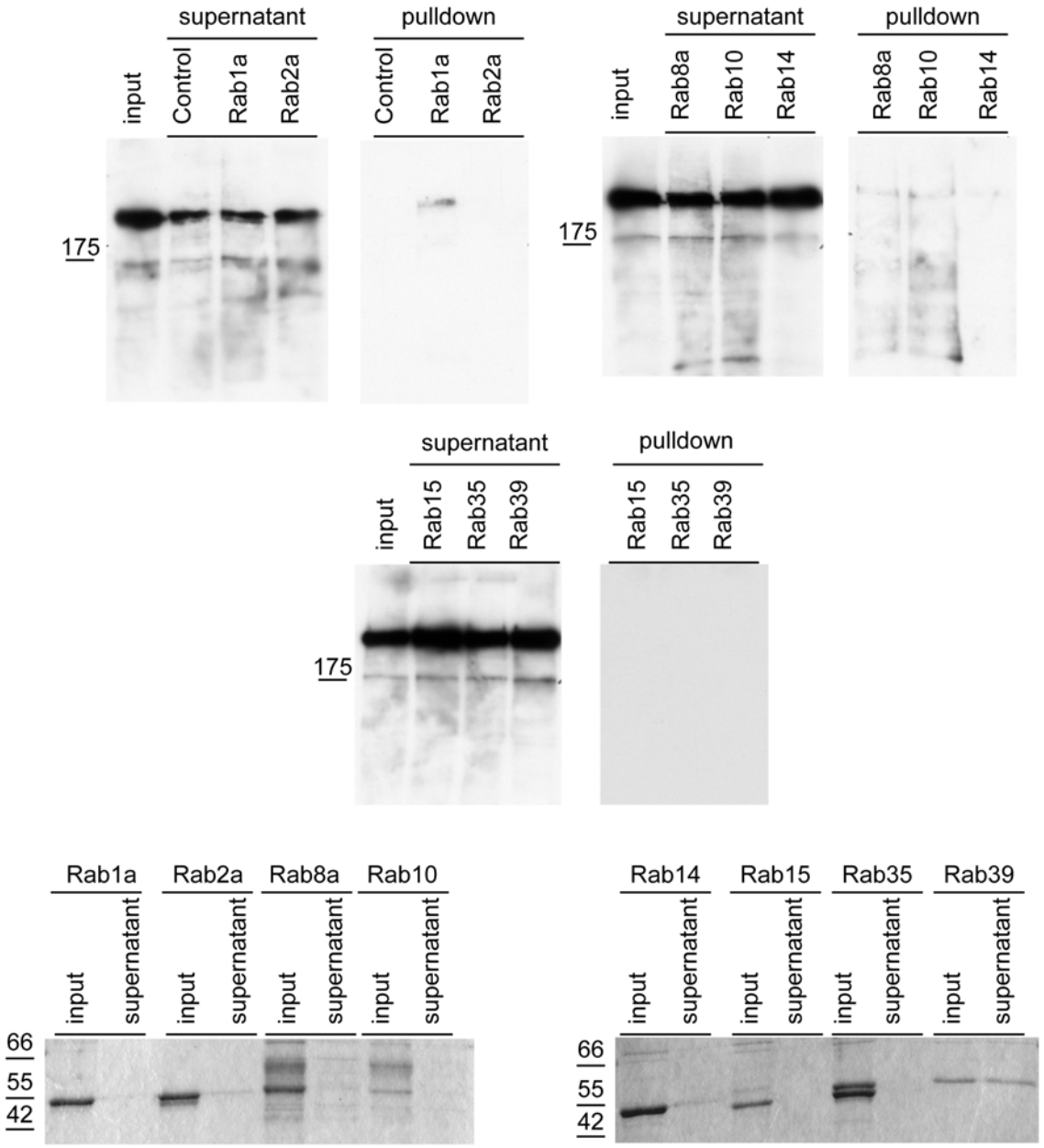

Figure 33: **Recombinant Rab GTPase Pulldown Of GMAP-210.** A HeLa L extract was made with NL100 buffer and incubated with the respective recombinant, GST-tagged Rab GTPase, pre-coupled to glutathione-sepharose in the presence of 100 μM GTP; beads were extracted with NE200 buffer and TCA precipitated; protein was analysed on Western blot from 6% SDS-PAGE gels, for protein detection rabbit anti GMAP-210 antibody (1:500) and HRP donkey anti rabbit (1:1000) secondary antibody were used (upper row); lower gels show coomassie stained 10% SDS-PAGE gels loaded with about 1 μg recombinant Rab GTPase input and the same amount of supernatant from above the glutathione-sepharose after pre-binding to monitor coupling efficiency.

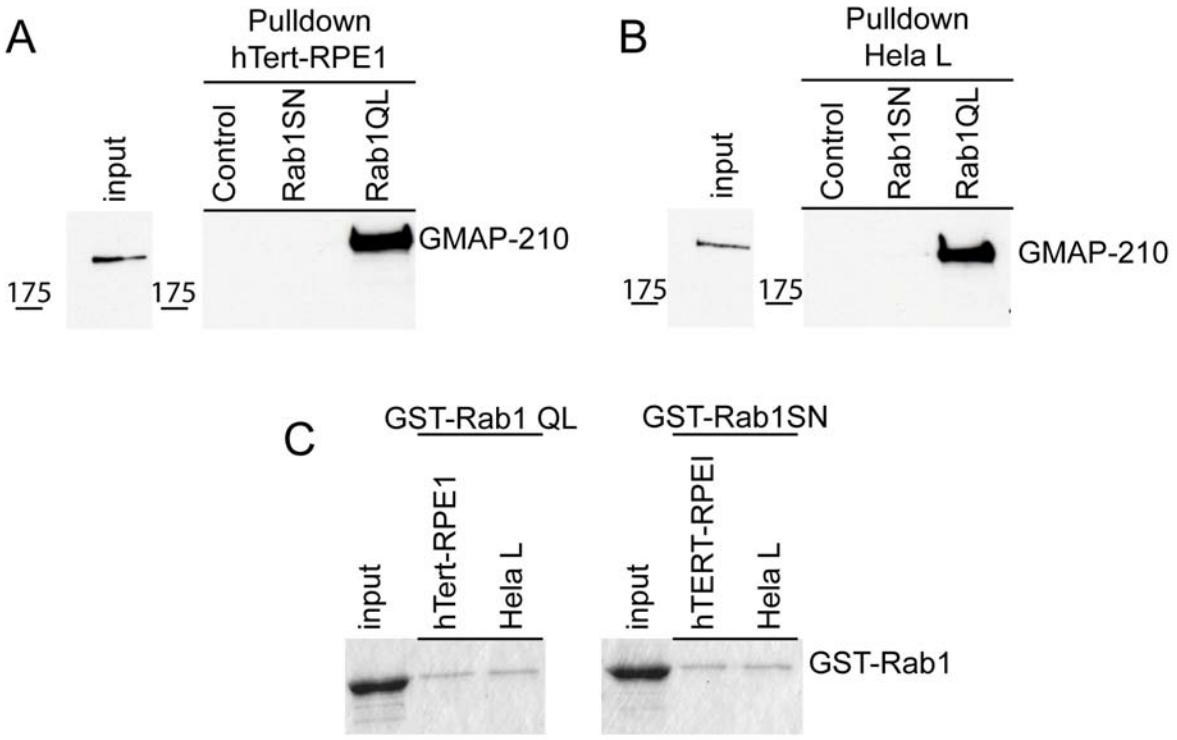

Figure 34: **Dependency Of The GMAP-210 Pulldown On The Nucleotide State Of Rab1.**
A: HeLa L or B: *hTERT*-RPE1 extract was made with NL100 buffer and incubated with recombinant, GST-tagged, mutant Rab1, pre-coupled to glutathione-sepharose in the presence of 100 μM GTP (for Q-L mutant) or 100 μM GDP (for S-N mutant); Rab1 was either used in its active, GTP-bound form (Q-L) or in its inactive, GDP-bound form (S-N); beads were boiled in SDS sample buffer and samples analysed by Western blotting from 6% SDS-PAGE gels; protein was detected with rabbit anti GMAP-210 primary antibody (1:500) and HRP donkey anti rabbit secondary antibody; C: shows coupling efficiency of recombinant protein to glutathione-S-sepharose; 1 μg recombinant Rab1 input and supernatant were loaded and stained with coomassie brilliant blue.

2.4.3 GMAP-210 Overlaps With The COPII Complex On A Subpopulation Of Vesicular Structures

As interactor of Rab1, which is found in the early secretory pathway (Cao *et al.*, 1998; Allan *et al.*, 2000), GMAP-210 was likely to be a player in the ER-to-Golgi trafficking. Thus, it might interact with other components of the early secretory pathway.
The first candidates tested were the coatomer complexes COPI and COPII. In Fig.35 HeLa L cells had been transfected with siRNA against GMAP-210 3'-UTR for 72 h and then stained for the coatomer I component βCOP or the coatomer II component Sec31. βCOP was concentrated at the Golgi apparatus and stained vesicular structures in the cell periphery. These vesicular structures did not co-localise with GMAP-210 vesicular-tubular structures observed (close-up in Fig.35). Upon depletion of GMAP-210, the peripheral COPI vesicles were widely unchanged, the Golgi localised pool remained and appeared more concentrated on the collapsed structure as observed for GM130 (Fig.24, p.49). The COPII signal localised to the perinuclear region and overlapped with the signal for GM130. COPII also showed staining on vesicular structures in the cell periphery. Upon depletion of GMAP-210 by siRNA, vesicular structures were unchanged, however Golgi localised signal concentrated on the now compacted Golgi. Again the signal was stronger. In order to examine the COPII vesicles for co-localisation with GMAP-210, the pEGFPN3-GMAP-210 plasmid was transfected into HeLa L cells for 24 h. After fixing, cells were co-stained with the antibody against COPII. Several vesicles positive for GFP signal also showed staining for COPII (Fig.35, white arrowheads). There were still discrete tubular structures showing GFP and distinct COPII carrying vesicles.

2.4.4 Peripheral GMAP-210 Signals Overlap With ERGIC53

GMAP-210 partially co-localised with COPII on vesicles. This made it likely that GMAP-210 could also be found on ER-Golgi-Intermediate-Compartments. This was tested by co-staining for the ER-Golgi-Intermediate-Compartment protein of 53 kDa (ERGIC53). HeLa L and *hTERT*-RPE1 cells were fixed and co-stained with antibodies against ERGIC53 and GMAP-210 (Fig.36, p.65). In both cell types, HeLa L and *hTERT*-RPE1, some overlap of ERGIC53 and the GMAP-210 signal could be observed on vesicular structures (Fig.36, p.65, "Control" and arrows in close-ups).
When GMAP-210 was depleted by siRNA treatment, ERGIC53 distribution was not disturbed. The Golgi localised ERGIC53 pool remained while in HeLa L cells the signal got stronger, due to the effect of a compact Golgi.
As ERGIC53 partially co-localised with GMAP-210, constructs for expression of GMAP-

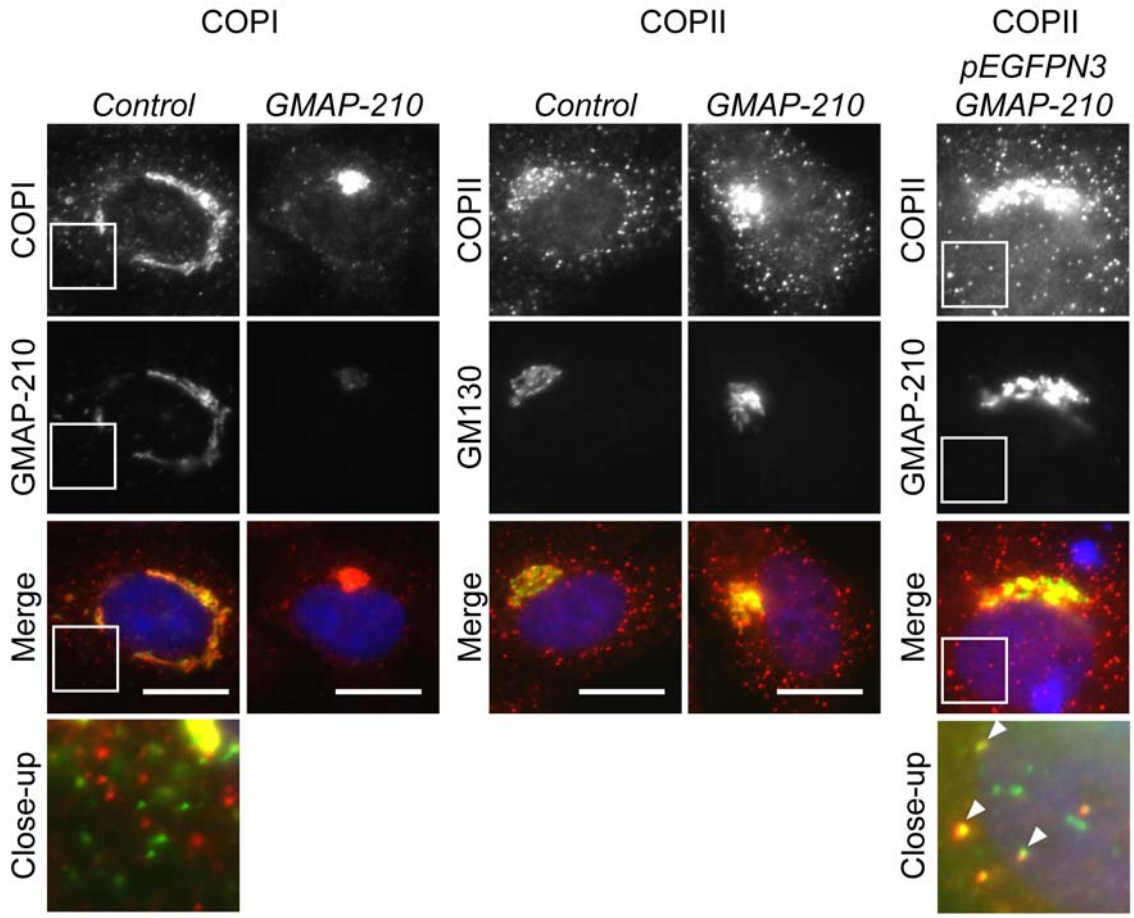

Figure 35: **Coatomer Proteins And GMAP-210.** HeLa L cells were transfected with an siRNA oligo against GMAP-210 3'-UTR or GL2 (control) for 72 h, fixed and stained with either rabbit anti GMAP-210 (green, 1:500, left) or mouse anti GM130 (green, 1:500, middle) and mouse anti βCOP (red, 1:500, left) or rabbit anti COPII (red, 1:500, middle); right panel shows pictures of cells transfected for 24 h with a vector for expression of GMAP-210 full-length with a C-terminal enhanced GFP-Tag (green) and co-stained with the rabbit anti COPII (red, 1:500) antibody; blue channel: DAPI staining; Bar=5 μm.

210 were transfected into HeLa L and *hTERT*-RPE1 cells and, after fixing, co-stained with the antibody against ERGIC53 (Fig.37, p.66). The constructs transfected were full-length GMAP-210, amino acids 1683-1875 (GRAB domain), amino acids 1598-1979 and amino acids 1-1712 (full-length without GRAB domain). Again the GMAP-210-GFP signal and ERGIC53 signal overlapped on some vesicles in the cell periphery. Obviously full-length GMAP-210 shared some structures with ERGIC53 in both cell types (pEGFPN3-GMAP-210). GRAB domain showed no overlap (pEGFPC2-GMAP-210 1683-1875), C-terminus (pEGFPC2-GMAP-210 1598-1979) had some co-localisation and full-length protein without GRAB domain (pEGFPC2-GMAP-210 1-1712) shared some structures

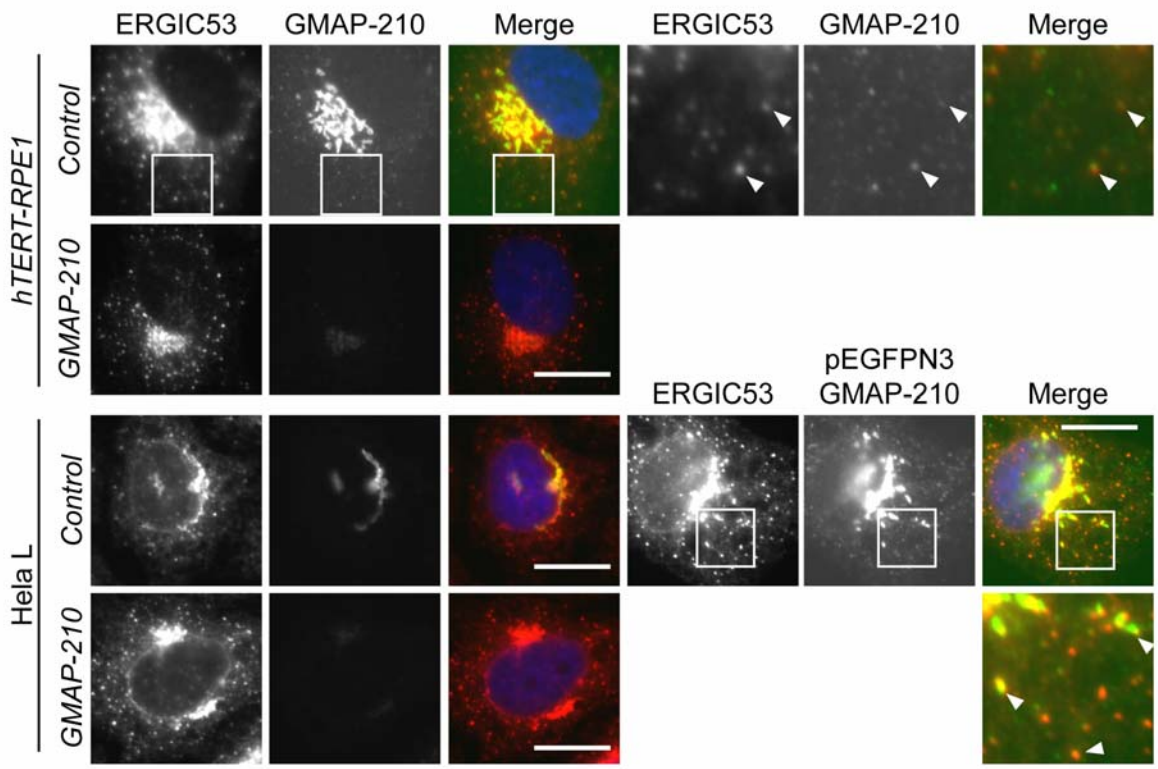

Figure 36: **GMAP-210 And The ER-Golgi-Intermediate Compartment.** *hTERT*-RPE1 (top) or HeLa L (bottom) cells were transfected with an siRNA oligo against GMAP-210 3'-UTR or GL2 (control) for 72 h and then fixed and stained with rabbit anti GMAP-210 (green, 1:500) and mouse anti ERGIC53 (red, 1:1000); right panel shows close-up of the peripheral cell region indicated by boxes; for *hTERT*-RPE1 cells; HeLa L cells were transfected for 24 h with the pEGFPN3-GMAP-210 construct for 24 h (green), fixed and stained with antibodies against ERGIC53 (red) as described above; close-up (bottom right) shows cell periphery indicated by boxes; arrow indicate structures with overlapping signals; blue channel: DAPI staining; Bar=5 μm.

with ERGIC53, but only in HeLa L cells.

2.4.5 Summary

GMAP-210 was tested for interaction with several different components of the ER-to-Golgi and intra-Golgi trafficking pathways. None of the tested markers changed localisation significantly after depletion of GMAP-210. Yeast 2-Hybrid interaction studies with the Rab family of small GTPases identified several Rab proteins as possible interaction partners. Pulldown experiments showed that only Rab1 could bind to GMAP-210 *in vitro* and did so depending on its nucleotide state. Mapping of the interaction domain within GMAP-210, identified amino acids 855 to 1332 as interaction domain.

Co-staining of GMAP-210 with antibodies against a COPII component or the ER-Golgi intermediate compartment marker ERGIC53, showed several instances of overlapping sig-

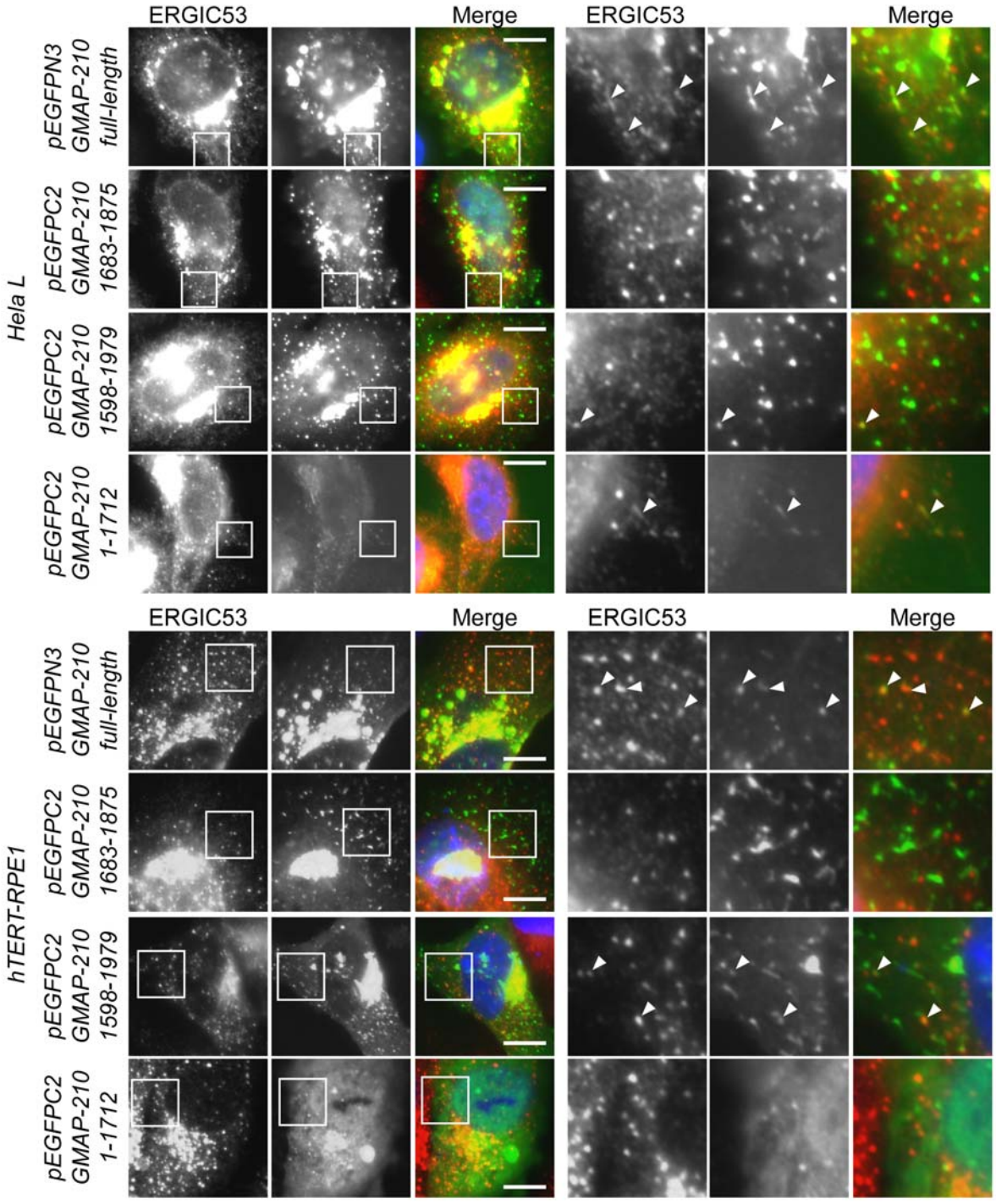

Figure 37: **GMAP-210 And The ER-Golgi Intermediate Compartment.** HeLa L (top) and *hTERT*-RPE1 (bottom) cells were transfected with the indicated constructs for 24 h and then fixed with paraformaldehyde and stained with the mouse anti ERGIC53 antibody (red, 1:1000); the right side shows close-ups of highlighted areas from cells depicted on the left side; arrows indicate structures with co-localising signals; blue channel: DAPI staining; Bar=5 μm.

nals on vesicular structures. It could also be shown, that the GMAP-210 GRAB domain did not co-localise with ERGIC53, although it was needed for Golgi binding (2.1.2, p.29).

2.5 GMAP-210 siRNA Depletion Does Not Impair VSV-G Or Shiga Toxin B Subunit Trafficking

Because of its association with Rab1, COPII and ERGIC53 and its cis-Golgi localisation, it is quite likely, that GMAP-210 is involved in ER-to-Golgi or Golgi-to-ER trafficking. This was tested with two different experiments examining anterograde and retrograde trafficking after knockdown of GMAP-210.

2.5.1 Vesicular Stomatitis Viral G-Protein Is Transported To The Plasma Membrane At Normal Rates In GMAP-210 Knock-Down Cells

The Vesicular Stomatitis Virus is a member of the Rhabdoviridae family. Its G-Protein is a ready tool in cell biology to examine transport from the ER to the plasma membrane. Usage of its temperature sensitive mutant, VSV-G^{ts045}, allows it to be retained in the ER by culturing cells at 39.5°C. Refolding happens upon incubation on ice and transport is started when cells are brought to 32°C (Bergmann, 1989).
HeLa L cells were treated with GMAP-210 siRNA or GL2 control siRNA for 72 h. 14 h prior to the VSV-G transport assay, the cells were also transfected with a plasmid encoding the temperature sensitive mutant of the vesicular stomatitis viral G-protein (VSV-G^{ts045}) fused to an N-terminal, enhanced GFP tag and incubated at normal growth conditions at 37°C for 2 h. The cells were cultured for 12 h under restrictive conditions and then incubated on ice to allow refolding of the protein. Shifting the cells to the permissive temperature of 32.5°C started the export of VSV-G^{ts045}. Cells were fixed and stained with an antibody against the lumenal domain of VSV-G, which is exposed to the cell's outside when the protein reaches the plasma membrane (Fig.38). Cells were, however, not permeabilised prior to staining. In control cells the GFP-signal of the transfected VSV-G protein could be followed from the endoplasmic reticulum, to the Golgi after 30 min. After 60 min the protein reached the plasma membrane localisation but had still a Golgi localised pool. The antibody against the lumenal domain of VSV-G only stained the plasma membrane after 60 min, seldomly already after 30 min and marked the completion of VSV-G transport through the cell. HeLa L cells depleted of endogenous GMAP-210 also showed a GFP signal in the endoplasmic reticulum at the start of the transport, Golgi was reached after 30 min and plasma membrane localisation was visible after 60 min. In order to quantify the transport efficiency of GFP-VSV-G, signal intensity

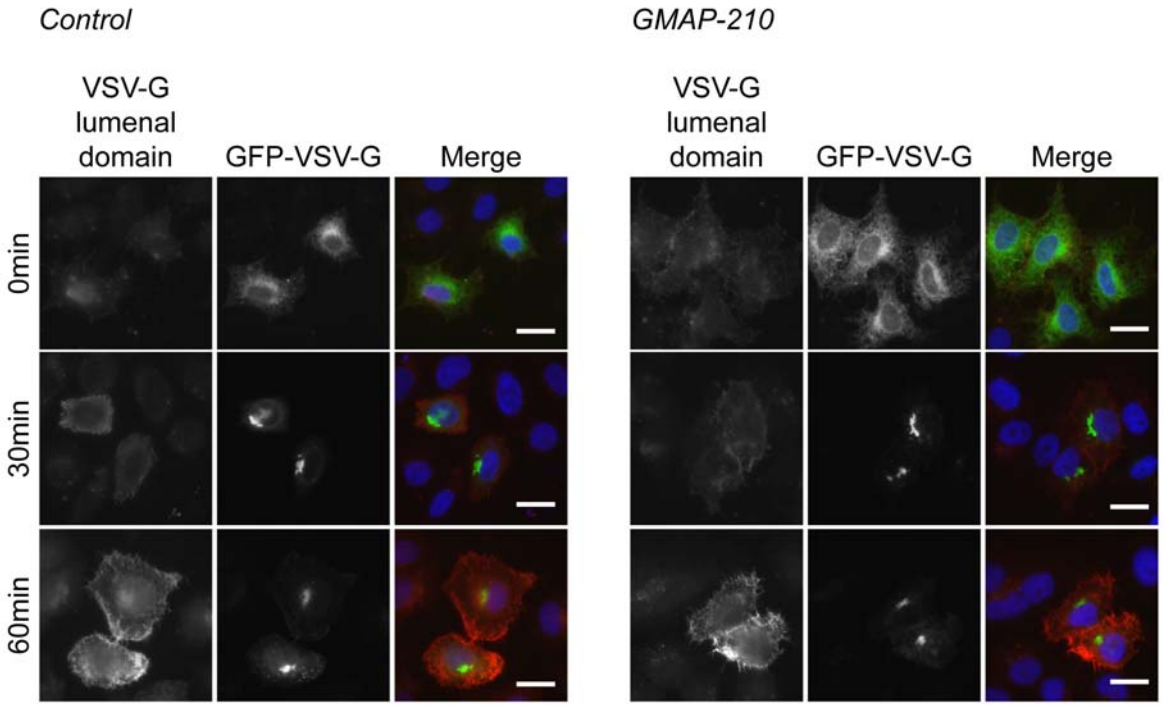

Figure 38: **VSV-G Transport After GMAP-210 Depletion.** HeLa L cells were transfected with siRNA oligo against GL2 (control) or GMAP-210 3'-UTR for 72 h; 14 h before the experiment, the cells were additionally transfected with a GFP-tagged vesicular stomatitis viral G-protein and incubated for 2 h at 37°C; cells were then shifted to 39.5°C overnight; after incubation for 30 min on ice, cells were further incubated at 32.5°C and fixed with paraformaldehyde at the indicated time-points, but without permeabilising; staining was done with a mouse antibody against the lumenal domain of the VSV-G protein (red, 1:20); blue channel: DAPI staining; Bar=10 μm.

in the green and red channel after 60 min were measured with the MetaVue Software and after correction for background the ratio of red signal to green signal (thus signal of transported protein to overall protein) calculated and presented graphically in Fig.39. Obviously the ratio of transported to overall protein was the same in control (4.8+/-0.9) and GMAP-210 siRNA treated cells (4.5+/-0.8). Transport of VSV-G is not impaired by GMAP-210 depletion.

2.5.2 Shiga Toxin B Subunit Is Internalised And Transported At Normal Rates In GMAP-210 siRNA Treated Cells

Shiga toxin is a tool to study endocytosis and subsequent transport, via early and recycling endosomes, to the Golgi apparatus and the endoplasmic reticulum (Johannes and Goud, 1998). Transport of the toxin holoenzyme is coordinated by the B-subunit, whereas the A-subunit is responsible for toxicity.

For testing uptake of the shiga toxin B subunit labelled with Cy3-fluorescent dye (Fuchs

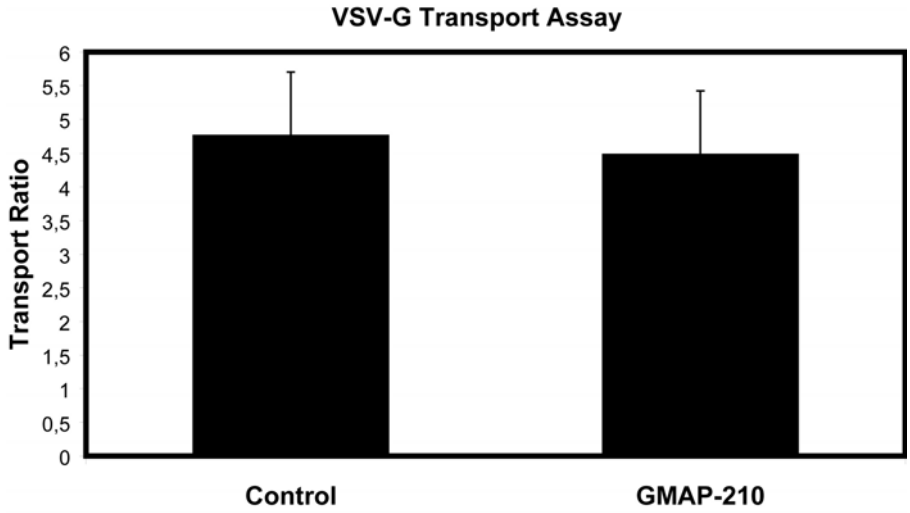

Figure 39: **Graphical Quantification Of VSV-G Transport Efficiency.** The VSV-G transport assay was performed as described above; the digital pictures were analysed with the MetaVue software for measuring the intensity of red and green staining; background was subtracted and the ratios of red to green calculated for both conditions; about 15 cells expressing the VSV-G protein were used for measurement under each condition; Ratio GL2 4.8+/-0.9; Ratio GMAP-210 4.5+/-0.8.

et al., 2007), HeLa L cells were transfected for 72 h with siRNA against GL2 as control or GMAP-210 before incubating the coverslips on ice for 30 min in a solution containing Cy3-shiga toxin B subunit. After shifting the cells to normal growth conditions at 37°C, they were fixed and stained with the Golgi marker GM130 at different time-points up to 240 min (Fig.40). In control cells shiga toxin B subunit bound to the cell surface during incubation on ice, entered the cells and showed up in vesicular structure within the first 10 min. After 60 min, the signal still localised in vesicular structures throughout the cell but also clearly in a perinuclear area co-stained for GM130. After 120 min the perinuclear signal became brighter, but a signal on vesicular structures started to reappear, which was also seen after 240 min at which time the perinuclear signal became weaker again, although it did not disappear entirely.

In cells transfected for 72 h with an siRNA oligo against GMAP-210, the shiga toxin B subunit bound to the cell surface as seen in controls and entered the cell within the first 10 min. The toxin appeared in the perinuclear region within 60 min after incubation

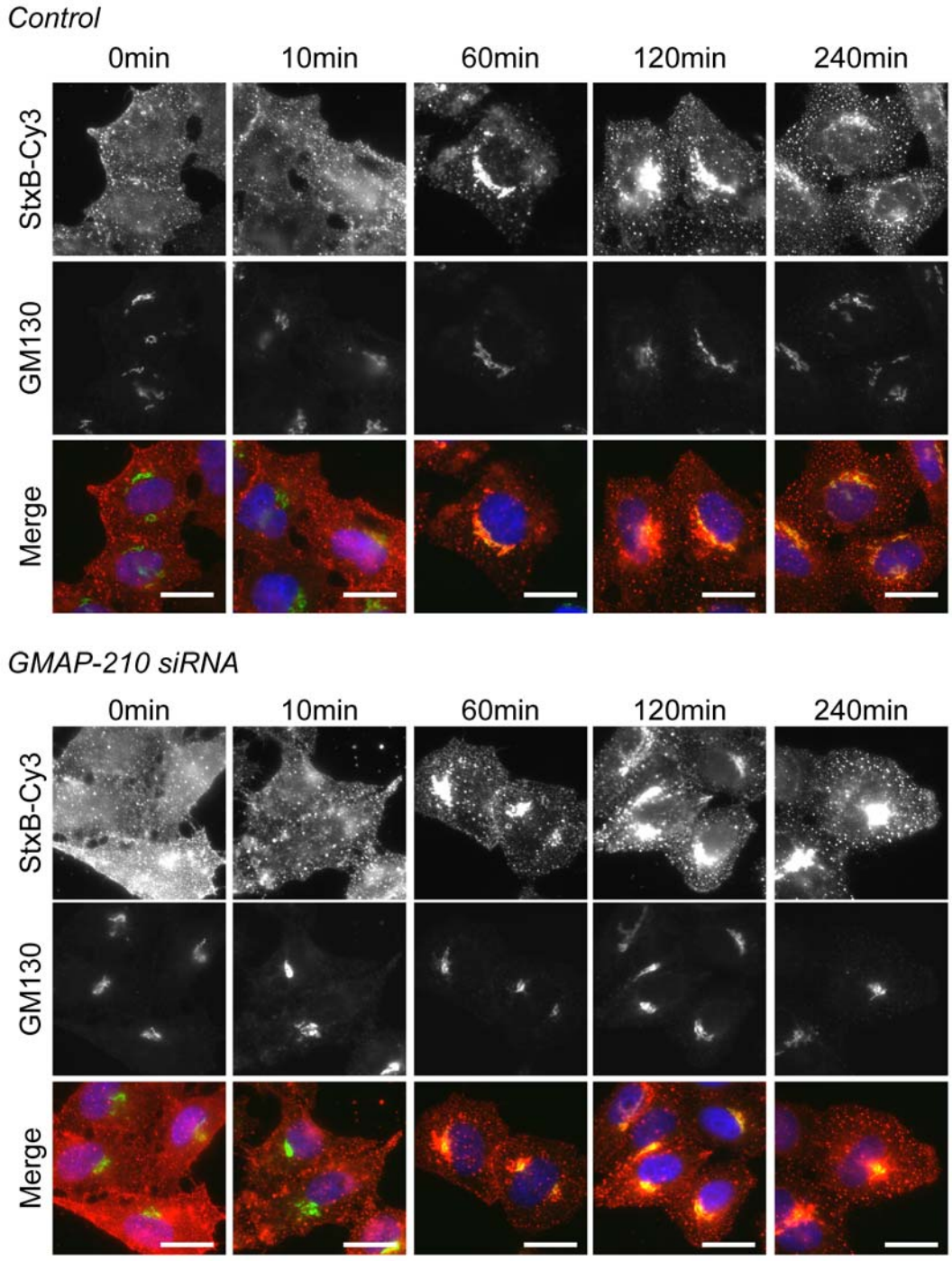

Figure 40: **Shiga Toxin Uptake After GMAP-210 Depletion.** HeLa L cells were transfected with an siRNA oligos against GL2 (control) or GMAP-210 3'-UTR for 72 h before incubating the cells in a Cy3-shiga toxin B subunit solution (red, 1:2500) on ice; cells were washed with 37°C growth medium, incubated at normal growth conditions and fixed at the given time-points with paraformaldehyde; cells were stained with mouse anti GM130 antibody (green; 1:500); blue channel: DAPI staining; Bar=10 μm.

and became stronger within another 60 min. At this time vesicular structures, containing shiga toxin, started to appear. The signal in the perinuclear region was not lessened after a total of 240 min, which might have been due to the compaction of the Golgi (2.3, p.48*ff*) observed in HeLa L cells. This might have masked the effect of reduction of signal at the Golgi apparatus.

2.5.3 Summary

GMAP-210 was describe to disturb anterograde and retrograde trafficking after overexpression of the full-length protein (Pernet-Gallay *et al.*, 2002). In these experiments, GMAP-210 was depleted by siRNA and the effects on anterograde and retrograde traffic evaluated by VSV-G transport and uptake of shiga toxin B subunit. VSV-G was transported to the plasma membrane at equal rates in control cells and cells depleted of GMAP-210. Anterograde transport was unhindered. The uptake rate of the shiga toxin B subunit was equal until it reached the Golgi apparatus. The rate of retrograde traffic between the Golgi apparatus to the ER was, however, difficult to compare, as Golgi morphology had changed after GMAP-210 depletion and the compacted Golgi showed a much higher signal intensity, than the Golgi in control cells.

2.6 GMAP-210 Remains On Golgi Remnants After Brefeldin A Treatment And GMAP-210 Depletion Does Not Change Brefeldin A Effect On Cells

2.6.1 Brefeldin A Effect On GMAP-210 Localisation

The fungal metabolite Brefeldin A (BFA) binds to the interface of interaction between the Arf-GEF GBF (Kawamoto *et al.*, 2002; Zhao *et al.*, 2002; Garcia-Mata *et al.*, 2003) or BIG (Shinotsuka *et al.*, 2002) with the GDP-bound Arf1 and creates a stable GEF-GDP-Arf complex (Sciaky *et al.*, 1997), making the GEF unavailable for activating any Arf1. The Golgi subsequently breaks down and most membranes fuse with the ER. Most Golgi localised proteins, like mannosidase II redistribute to the ER (Klausner *et al.*, 1992) whereas others stay in distinct Golgi fragments, like the golgin GM130 (Nakamura *et al.*, 1995). The coatomer complex subunits redistribute to the cytoplasm. GMAP-210 was described to act like other Golgi matrix proteins and localise to the small Golgi fragments near the ER-exit sites (Rios *et al.*, 1994). However, the homologue of GMAP-210 in *S.cerevisiae*, Rud3p, is dependent on Arf1 to localise to the Golgi apparatus (Gillingham *et al.*, 2004). So far interaction of GMAP-210 with Arf1 could not be proven, but if GMAP-210 really

relies on Arf1 for its Golgi localisation, it should be removed from Golgi membranes upon Arf1 inactivation by Brefeldin A. First, HeLa L cells were cultured for 24 h under standard conditions and then treated for 10 min with 5 μg/ml Brefeldin A (Fig.41; left side). After Brefeldin A treatment, most of the Golgi had disassembled into small fragments distributed throughout the cell. These fragments are positive for GM130 as indicated by antibody staining. GMAP-210, like GM130 (Nakamura *et al.*, 1995), could be found on small vesicular structures, matching BFA Golgi remnants. Although there were vesicular structures, which stained for GM130 and GMAP-210 at the same time, there were others with clear and distinct signals for only one of the two golgins.

Thus, full-length localisation of GMAP-210 does not depend on the active form of Arf1. Still it was possible, that GMAP-210 had additional Golgi localisation motives, which kept it bound to the Golgi, even after blocking the activation of Arf1 using BFA. If GRAB domain interaction with Arf1 was correct, a construct only expressing the GMAP-210 GRAB domain should no longer be able to bind to the Golgi apparatus when Arf1 is

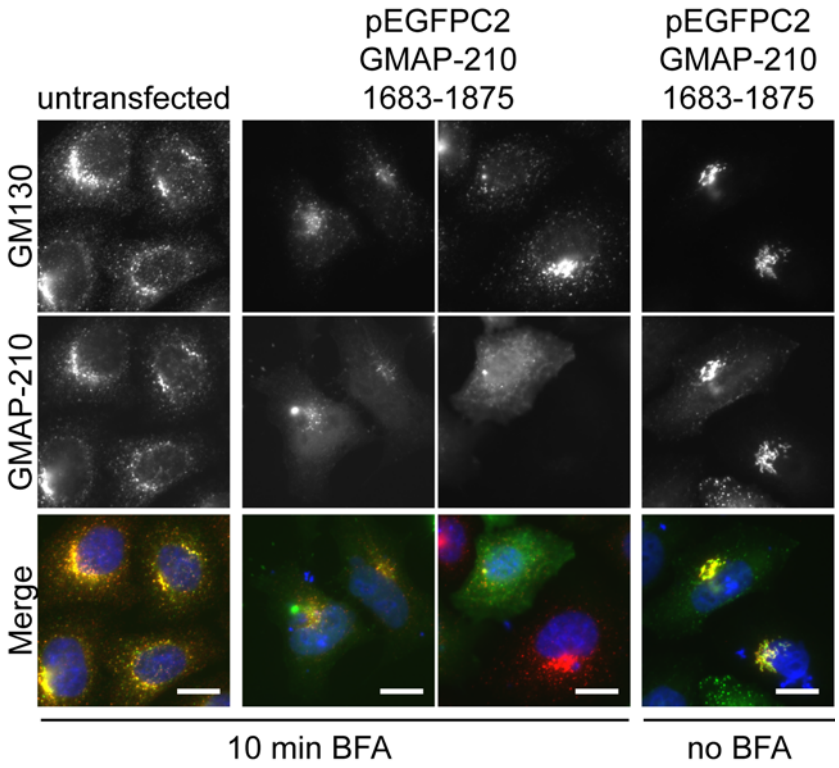

Figure 41: **Brefeldin A Induced Golgi Disassembly And Effect On The GMAP-210 GRAB Domain**. HeLa L cells were transfected for 24 hours with GMAP-210 GRAB domain (amino acids 1683-1875) with an N-terminal, enhanced GFP-Tag (green); control cells were grown untransfected; cells were fixed with paraformaldehyde either after 10 min of treatment with 5 μg/ml Brefeldin A or untreated as indicated; cells were stained with mouse anti GM130 (red, 1:500) and, in the case of untransfected cells, with rabbit anti GMAP-210 (green, 1:500); blue channel: DAPI staining; Bar=10 μm.

inactivated by Brefeldin A.
HeLa L cells, which expressed pEGFPC2-GMAP-210(1683-1875) for 24 h, were treated with Brefeldin A for 10 min. After fixing they were stained for GM130 or GM130 and GMAP-210 for control cells (Fig.41). In cells not treated with Brefeldin A, transfected GRAB domain localised to the perinuclear region on the same structure as GM130. After 10 min of BFA treatment, the Golgi apparatus started to fragment as seen by GM130 staining. GMAP-210 GRAB domain still localised to the GM130 positive fragments, although the diffuse cytosolic staining increased, indicating a loss of binding to the Golgi apparatus. Therefore the GRAB domain does appear to target due to Arf1, while full-length GMAP-210 must possess additional targeting information.

2.6.2 Brefeldin A Induced Golgi Assembly and Disassembly After GMAP-210 Depletion

In this context, it was not only interesting if GMAP-210 localisation was influenced by Brefeldin A treatment, but also, if GMAP-210 had any function in the processes of Golgi fragmentation and redistribution of certain Golgi components to the endoplasmic reticulum. Thus, Brefeldin A induced Golgi breakdown and the subsequent Golgi reassembly after washout of the compound were analysed in the presence and absence of GMAP-210.
HeLa L cells were transfected with siRNA oligos against GL2 control and GMAP-210 3'-UTR for 72 h and then treated with 5 μg/ml Brefeldin A. Cells were fixed and stained with antibodies against βCOP and GM130 at different time-points. Control and GMAP-210 depleted cells were compared (Fig.42). In HeLa L cells, which were treated with Brefeldin A, βCOP lost its Golgi localisation within the first 10 minutes and showed diffuse cytosolic distribution. In cells treated with GMAP-210 siRNA, COPI was also lost from the Golgi within 10 min. GM130 staining monitored the Golgi breakdown, which occurred within 30 min in control cells. In GMAP-210 knockdown cells, the breakdown took longer. Even after 45 min GM130 could be seen concentrated in the perinuclear region, although the cisternal stacks of the Golgi had broken into vesicular structures. In this regard it is important to remember, that the Golgi apparatus collapsed upon GMAP-210 depletion and started out from a much more compacted state than in control cells, which could cause the slower spreading of the Golgi remnants after Brefeldin A treatment.
For reassembly studies, HeLa L cells, treated with siRNA and Brefeldin A for 20 min, were washed and incubated at normal growth conditions. At 30 min, 60 min and 90 min after washout, the cells were fixed and stained for GM130 and βCOP (Fig.43). After Brefeldin A induced Golgi disassembly and washout of the compound, the Golgi ap-

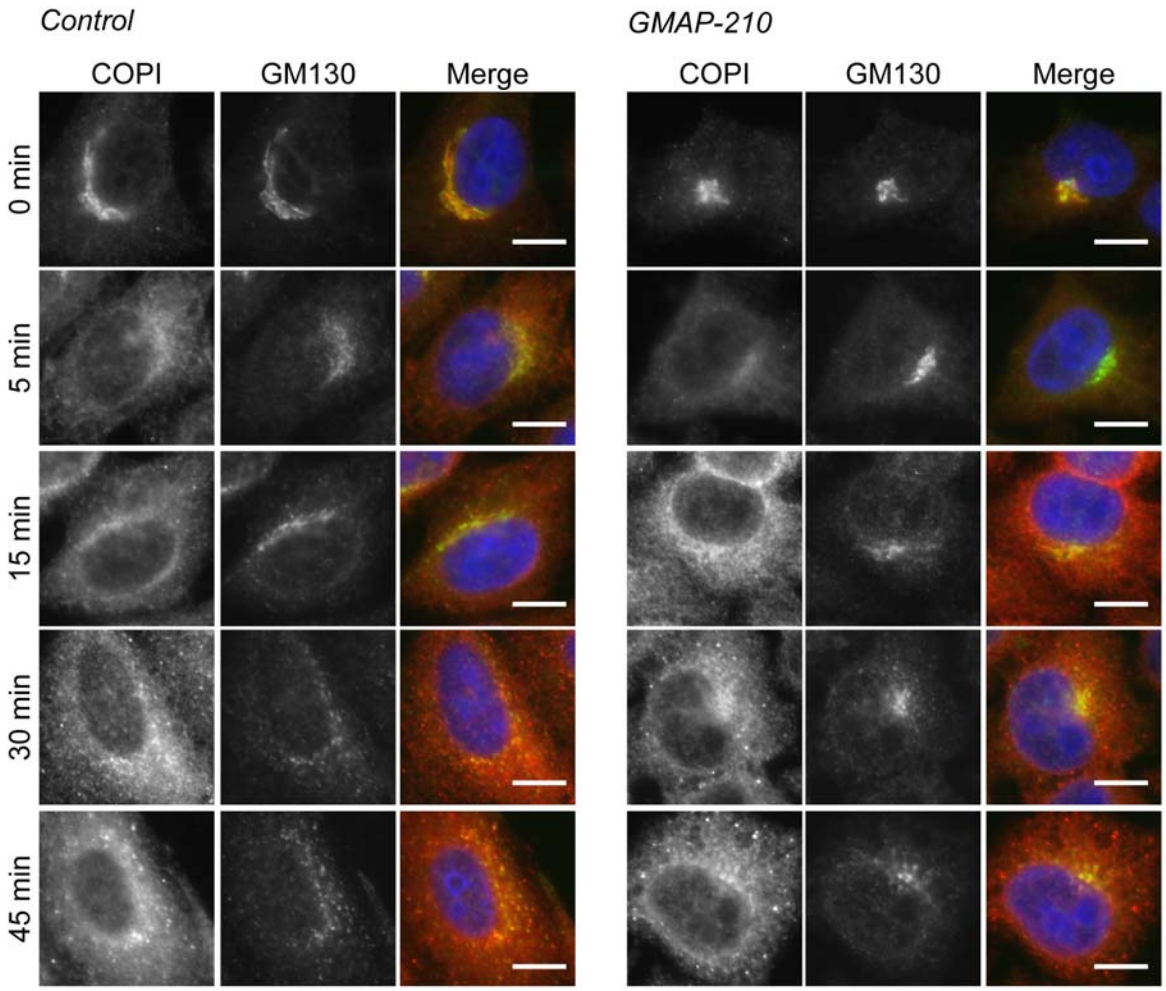

Figure 42: **Effect Of GMAP-210 Depletion Upon BFA Induced Golgi Disassembly.** HeLa L cells were transfected with an siRNA oligo against GMAP-210 3'UTR or GL2 (control) for 72 hours; for Brefeldin A treatment, growth medium was replaced by growth medium supplemented with 5 μg/ml Brefeldin A; coverslips were fixed in Methanol at the indicated time-points; for staining mouse anti βCOP (red, 1:500) and sheep anti GM130 (green1:500) antibodies were used; blue channel: DAPI staining; Bar=5 μm.

paratus began to reform. GM130 staining showed, that the Golgi remnants started to concentrate in a juxtanuclear position within 30 min and subsequently formed the Golgi typical stacked cisternae. COPI was recruited to the remnants more slowly, but appeared weakly 30 min after removal of Brefeldin A. After 90 min COPI showed its typical Golgi localisation. In GMAP-210 siRNA treated cells, the Golgi reassembly started out from an already more concentrated cluster of Golgi remnants (compare 42, p.74), which fused quicker to form a Golgi apparatus with stacked cisternae. COPI already appeared 30 min after compound removal at the Golgi. This may again have been an effect of the collapsed and concentrated Golgi and might be only indirectly related to the depletion of GMAP-210.

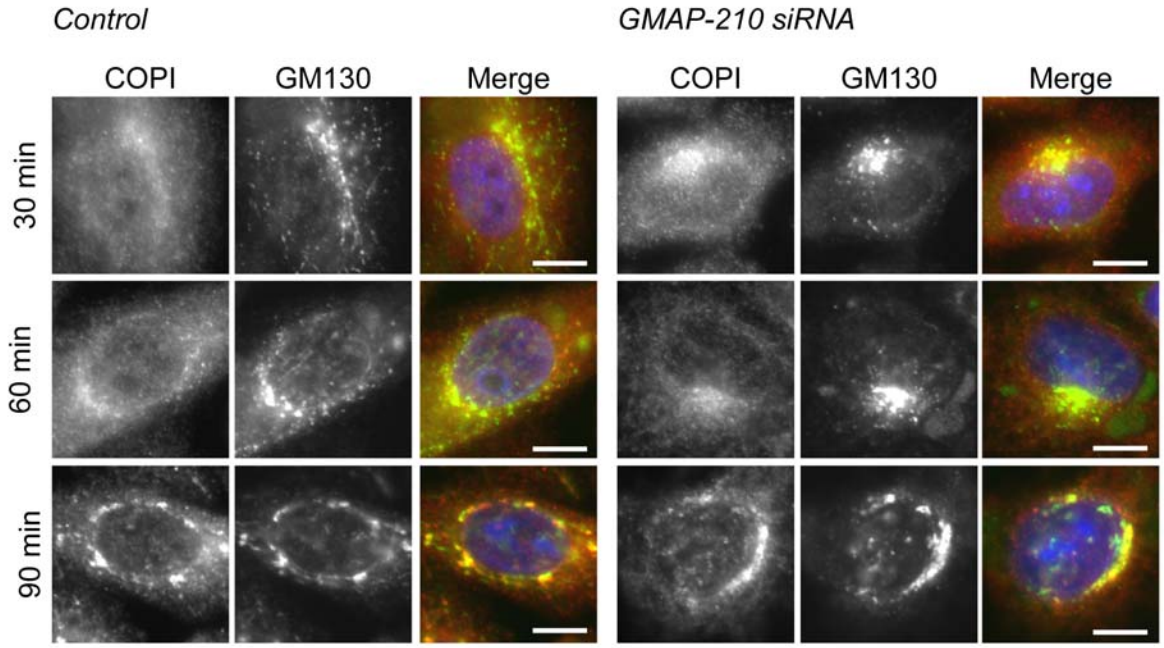

Figure 43: **Golgi Reassembly After BFA Wash-Out.** HeLa L cells were transfected with an siRNA oligo against GMAP-210 3'-UTR or GL2 (control) for 72 hours; for Brefeldin A treatment, growth medium was replaced by growth medium supplemented with 5 μg/ml Brefeldin A; after 30 min of incubation, cells were washed five times with growth medium and fixed with methanol after the indicated times; for staining mouse anti COPI (red, 1:500) and sheep anti GM130 (green, 1:500) were used as antibodies; blue channel: DAPI staining; Bar=5 μm.

hTERT-RPE1 cells did not show the compaction of the Golgi after GMAP-210 depletion and thus Brefeldin A induced dis- and reassembly was expected to be easier to examine. *hTERT*-RPE1 cells were treated for 72 h with GL2 control oligo or GMAP-210 siRNA oligo. For disassembly the growth medium was replaced with growth medium containing 5 μg/ml Brefeldin A and fixed after 0 min, 20 min and 30 min. Then the cells were washed and coverslips were fixed after 30 min, 60 min and 90 min. The cells were stained with antibodies against GM130 and GMAP-210 (Fig.44). The Golgi apparatus of *hTERT*-RPE1 cells dispersed within 20 min of Brefeldin A treatment. GMAP-210 and GM130 stayed on the Golgi remnants and were not redistributed to the endoplasmic reticulum, thus *hTERT*-RPE1 control cells behaved similarly to HeLa L cells. In *hTERT*-RPE1 cells treated with siRNA oligos against GMAP-210, the Golgi dispersed like in control cells. No difference in localisation of GM130 or GMAP-210 or disassembly kinetics could be observed.

After washout of Brefeldin A, the Golgi started to reassemble and already after 30 min the Golgi formed long ribbons. After 60 min the Golgi had reached its wild-type structure, although it was still slightly disordered. This did not change after 90 min. GMAP-210

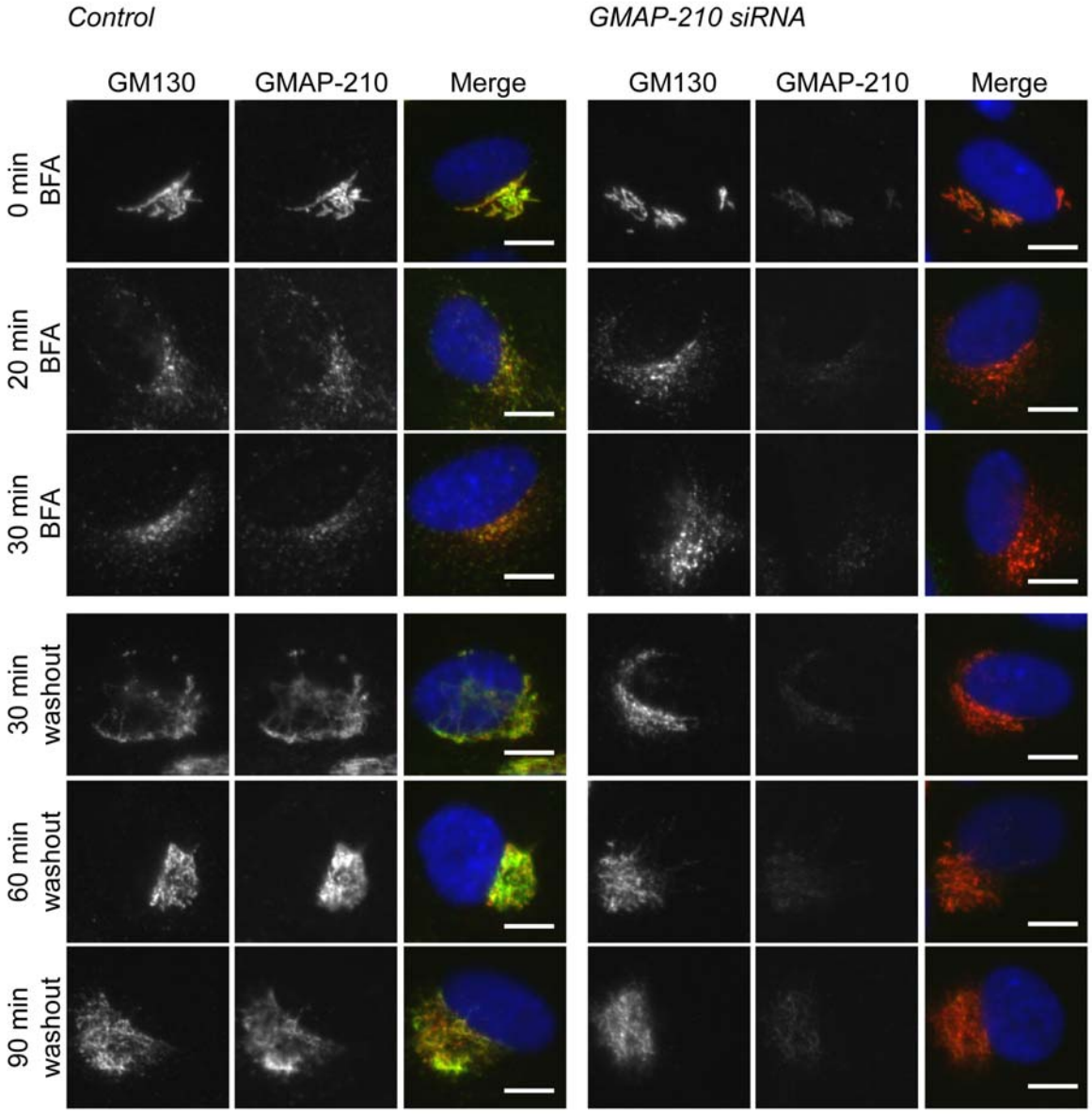

Figure 44: **Brefeldin A Dis- And Reassembly In *hTERT*-RPE1 cells.** *hTERT*-RPE1 cells were transfected with an siRNA oligo against GMAP-210 3'-UTR or GL2 (control) for 72 hours; for Brefeldin A disassembly, growth medium was replaced by growth medium supplemented with 5 μg/ml Brefeldin A and coverslips were fixed in paraformaldehyde at the indicated time-points; after 30 min the cells were washed 3 times with growth medium and incubated for another 30, 60 and 90 min and fixed as described above; for staining mouse anti GM130 (red, 1:500) and rabbit anti GMAP-210 (green, 1:500) were used; blue channel: DAPI staining; Bar=5 μm.

siRNA treated cells showed the same behaviour and speed of reassembly after Brefeldin A washout.

2.6.3 Summary

GMAP-210 reacted to Brefeldin A treatment of cells (Rios *et al.*, 1994) as described, being localised at small stacked Golgi remnants (Klausner *et al.*, 1992). A transfected GRAB domain construct also localised to the Golgi apparatus, although Brefeldin A induced inactivation of Arf1 caused reduced Golgi localisation of these constructs. Following kinetics of Golgi disassembly by Brefeldin A treatment showed a slower dispersal speed of the Golgi fragments in GMAP-210 depleted cells in comparison to control cells. The reassembly of Golgi after Brefeldin A washout was also faster, starting out from less dispersed fragments. In *hTERT*-RPE1 cells, where no change in morphology by GMAP-210 depletion could be observed, Brefeldin A induced disassembly, and later reassembly, showed no different kinetics.

2.7 GMAP-210 Shows No Microtubule Interaction

In the literature, GMAP-210 is reported to not only localise to the Golgi apparatus, but also to interact directly with microtubule minus-ends by its C-terminus (Infante *et al.*, 1999). Although it had been shown, that the C-terminus comprises the Golgi interacting GRAB domain (see Gillingham *et al.* (2004) and 2.1.2 in this work p.29*ff.*), it is still possible, that GMAP-210 binds to microtubule minus-ends as described. Overexpression of GMAP-210 is also supposed to disrupt the microtubule network in COS cells (Infante *et al.*, 1999). Microtubules do no longer show a spindle-like formation around the centrosome, but rather a diffuse centre at the Golgi apparatus. Overexpression of a construct missing the microtubule binding domain still localises to the Golgi apparatus, but does not disturb the morphology of the microtubule network. Furthermore, GMAP-210 is also described to bind γ-tubulin-containing complexes (γ-TCCs) and to recruit γ-tubulin to the Golgi apparatus upon its overexpression (Rios *et al.*, 2004).

2.7.1 Transfection Of GMAP-210 Constructs Does Not Change The Microtubule Network In HeLa L

Discovery of GMAP-210 interaction with minus-ends of stable microtubules, was a surprise (Infante *et al.*, 1999), as this result would make GMAP-210 a very important golgin, involved in Golgi morphology and would further prove, that microtubules could also be

anchored to the Golgi rather than the centrosome (Rios and Bornens, 2003). Overexpression of GMAP-210 disturbed the arrangement of centrosomal microtubules in COS cells. Whether or not GMAP-210 is involved in anchoring or nucleating microtubules at the Golgi apparatus had to be elucidated.

For this HeLa L cells were transfected with various N- and C-terminal constructs of GMAP-210 tagged with enhanced GFP and co-stained for α-tubulin, to show effects on the microtubule network (Fig.45 left panel). As shown before (2.1.2, p.29*ff*), localisation of N- and C- terminus contradicted Infante *et al.* (1999). The N-terminus (pEGFPC2-GMAP-210 1-375) localised diffusely in the cytosol of HeLa L cells, whereas the C-terminus (pEGFPC2-GMAP-210 1598-1979) localises to the perinuclear Golgi apparatus (Fig.11, p.34). Examining the microtubule network and their centrosomal origin, showed, in cells

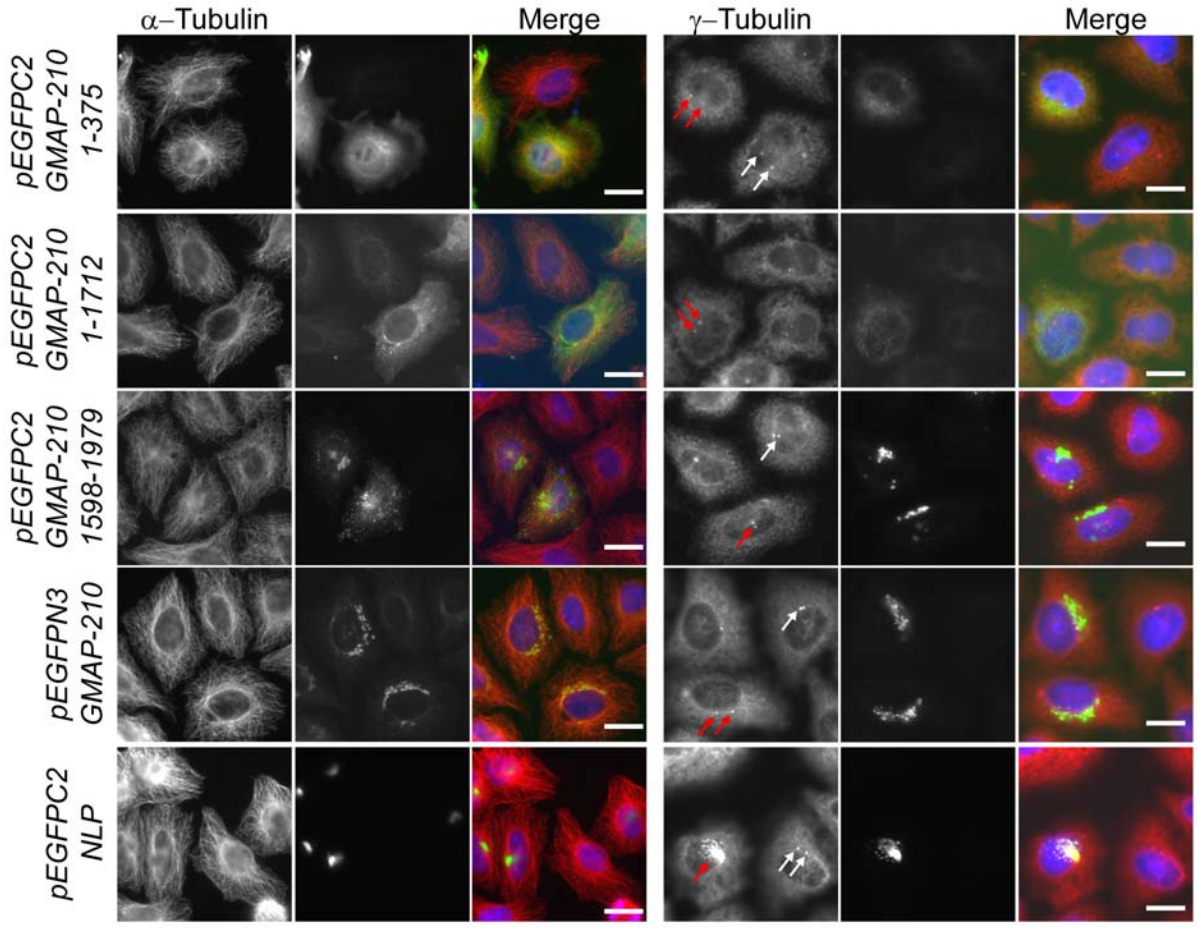

Figure 45: **α- and γ-Tubulin In GMAP-210 Transfected HeLa L Cells.** HeLa L cells were transfected with the indicated GMAP-210 constructs or NLP with an enhanced GFP-Tag for 24 h (green) and fixed with paraformaldehyde for staining with mouse anti α-tubulin DM1A (red, 1:1000, left) or methanol for staining with mouse anti γ-tubulin (red, 1:1000, right); arrows indicate γ-tubulin at the centrosomes in untransfected (white arrow) or transfected (red arrow) cells; contrast enhanced for better visibility; blue channel: DAPI staining; Bar=10 μm.

expressing the very N-terminus of GMAP-210(pEGFPC2-GMAP-210 1-375), a difference between transfected and untransfected cells. However, the microtubule aster's centre seemed to be more defined than in untransfected cells, rather than more diffuse (Infante *et al.*, 1999). The effect was only marginally and GMAP-210 N-terminus showed no localisation on microtubules. A construct missing the C-terminus (pEGFPC2-GMAP-210 1-1712), showed no effect on the microtubule network, but in contrast to Infante *et al.* (1999), the construct did not localise to the Golgi apparatus. It rather localised in the cytoplasm and stained some vesicular-tubular structures. C-terminus (pEGFPC2-GMAP-210 1598-1979) and full-length constructs of GMAP-210 did also not alter the morphology of the microtubule network (Fig.45).

2.7.2 GMAP-210 Depletion Does Not Disturb The Microtubule Network In HeLa L Cells

As overexpression does not disturb the microtubule network the effect of GMAP-210 depletion on microtubules had to be examined. In HeLa L cells the Golgi apparatus was shown to fragment and scatter upon siRNA treatment against GMAP-210 (Rios *et al.*,

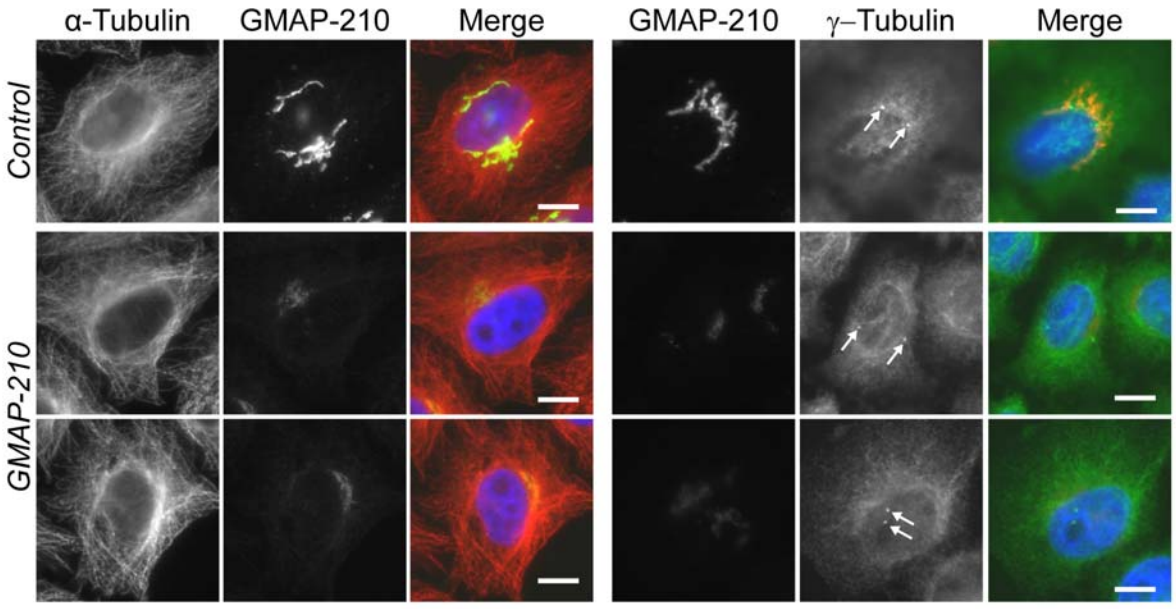

Figure 46: **α- and γ-Tubulin In GMAP-210 Depleted HeLa L Cells.** HeLa L cells were transfected with siRNA oligos against GL2 (control) or GMAP-210 3'-UTR for 72 h, fixed with paraformaldehyde and stained with mouse anti tubulin DM1A (red, 1:1000, left) or methanol for staining with mouse anti γ-tubulin (red, 1:1000, right), arrows indicate centrosome localised γ-tubulin; contrast enhanced for better visibility; both experiments were co-stained with rabbit anti GMAP-210 (green, 1:500); blue channel: DAPI staining; Bar=5 μm.

2004). The results in 2.3 (p.48) proved, however, that, although the Golgi apparatus fragmented (Fig.26, p.52), the fragments remained in a very tight cluster, smaller than the Golgi apparatus in control cells (Fig.24, p.49).
HeLa L cells were treated for 72 h with siRNAs against GMAP-210 and GL2 as control, fixed and stained for GMAP-210 and α-tubulin (Fig.46). After knockdown of GMAP-210 in HeLa L cells the microtubule network was unchanged. Some cells concentrated more tubulin in the perinuclear region and the microtubules looked more organised in an aster-like fashion with many microtubules originating from a point in the perinuclear region. This was, however, within the normal range of variation for HeLa L cells and thus could not be seen as a specific effect of GMAP-210 knockdown.

2.7.3 GMAP-210 Does Not Interact With Taxol Stabilised Microtubules *in vitro*

Further characterisation of GMAP-210 effect on microtubules could be tested in *in vitro* experiments with taxol stabilised microtubules. For this N- and C-terminus of GMAP-

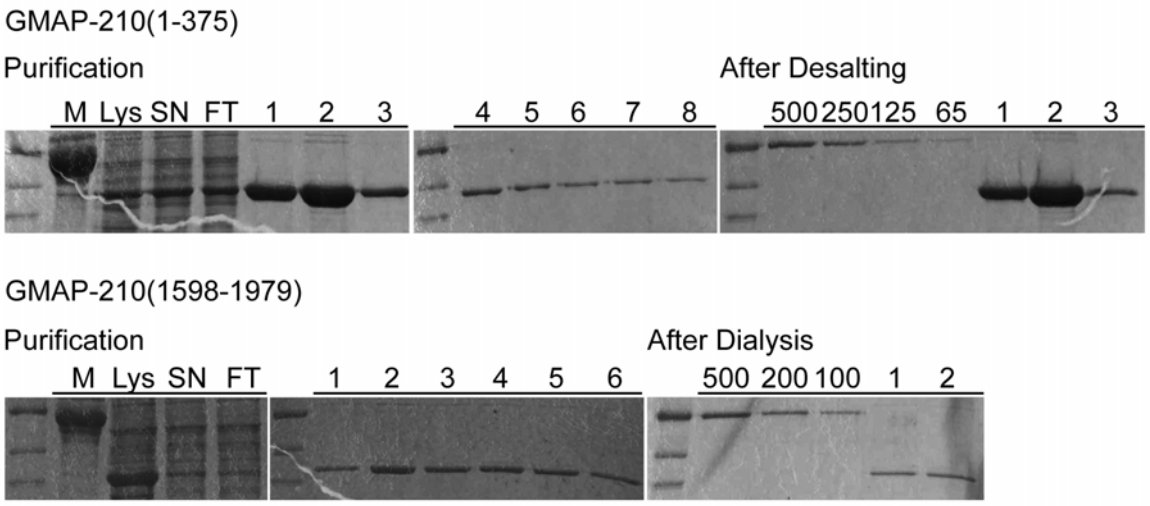

Figure 47: **Purification Of GMAP-210 N- And C-Terminus From Sf9 Cells.** Coomassie blue stained SDS-PAGE gels of the purification process of GMAP-210 amino acids 1-375 and GMAP-210 amino acids 1598-1979 from Sf9 cells infected with a recombinant Baculovirus; proteins were purified with Ni-NTA agarose and in IMAC200 buffer eluted fractions were either desalted and eluted into PBS (GMAP-210 1-375, upper gels, fractions 1, 2, 3) or dialysed overnight against PBS (GMAP-210 1598-1979, lower gels, fractions 1, 3-6 & 2); 10 μl per sample were loaded; M: cell free culture medium after harvesting Sf9 cells; Lys: crude lysate; SN: cleared lysate; FT: flow through after incubation with Ni-NTA agarose; numbers show fractions eluted from beads or fraction pools after dialysis/desalting; 500/250/200/125/100/65: show μg pure BSA to judge protein concentration of samples; 10 μl of each sample were loaded.

210 (GMAP-210 1-375 and GMAP-210 1598-1979) were expressed and purified from Sf9 cells with the Baculovirus system. Fig.47 shows the quality and concentration of both preparations used in the biochemical assays. Both constructs showed one distinct band with little degradation. After desalting, the pooled and desalted or dialysed fractions were estimated by comparison to BSA standards. GMAP-210 N-terminus concentrations were 200 μg/ml, 400 μg/ml and 100 μg/ml μg/ml. The GMAP-210 C-terminus concentrations were lower, 10 μg /ml and 20 μg/ml.

GMAP-210 N- And C-Terminus Do Not Bundle Microtubules *in vitro* Proteins binding to microtubules can organise and bundle them. Thus, to show binding of GMAP-210 to microtubules, the bundling capability of the recombinant GMAP-210 fragments was tested *in vitro*, comparing it to the known microtubule bundling protein Prc1sp2 (splice variant 2) (Mollinari *et al.*, 2002) also purified from Sf9 cells (Neef *et al.*, 2007).

Rhodamine labelled, *in vitro* grown and taxol stabilised microtubules were incubated with 400 ng recombinant protein (GMAP-210 amino acids 1 to 375, GMAP-210 amino acids 1598 to 1979 or Prc1sp2) for 20 min. Microtubules were analysed by epifluorescence at a 40x magnification. Fig.48 shows unordered microtubules in the negative control (first image) and highly ordered microtubules bundled by Prc1sp2 (second image). In comparison neither the N-terminus nor the C-terminus of GMAP-210 show any propensity to order the microtubules into bundles and microtubules look similar to the control. Neither N- nor C-terminus of GMAP-210 have microtubule bundling capability.

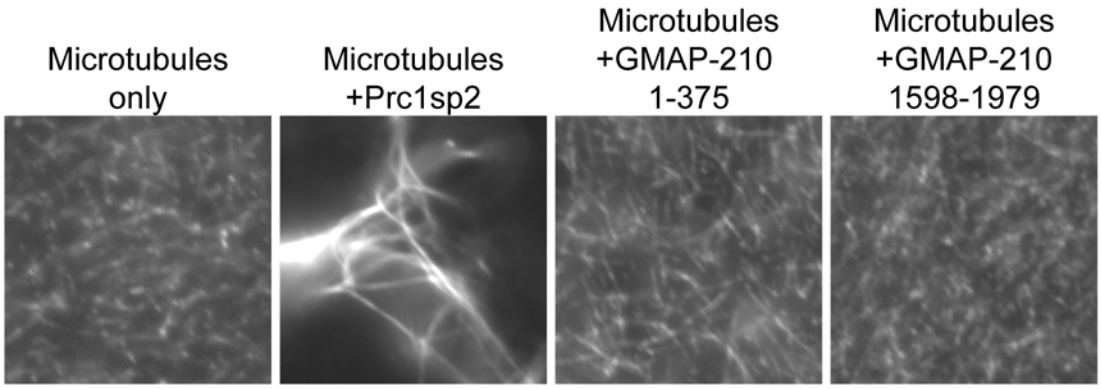

Figure 48: **Microtubule Bundling Assay With GMAP-210 N- And C-Terminus.** Rhodamine labelled microtubules, prepared *in vitro*, were incubated with buffer or 400 ng recombinant Prc1sp2, GMAP-210 N- or C-terminus (all three prepared from Sf9 cells) for 20 min at room temperature and analysed by fluorescence microscopy at 40x magnification; contrast enhanced for better visibility.

GMAP-210 Does Not Associate With Microtubules In Microtubule Spin-Down Assays Another possibility to identify microtubule association of proteins is the microtubule spin-down assay. Taxol stabilised microtubules from pig brain were incubated *in vitro* with 400 ng recombinant protein. After incubation at room temperature, the microtubules were centrifuged through a glycerol cushion and the pellet analysed by Western blotting and coomassie brilliant blue stained SDS-PAGE. Apart from GMAP-210 amino acid 1 to 375 and 1598 to 1979, Prc1sp2, as positive control, was tested for microtubule binding (Fig.49). Microtubule pellets were dissolved in sample buffer and analysed by SDS-PAGE. The coomassie blue stained SDS-PAGE gels (Fig.49, lower row) showed good microtubule recovery under all conditions. Western blots treated with 6xHis-Tag or Prc1 antibodies, showed protein presence or absence in the microtubule pellet. Prc1sp2 was found in the pellet with the taxol stabilised microtubules, but no protein was detected in pellets without microtubules. The GMAP-210 N-terminus (amino acids 1 to 375) showed some faint, unspecific precipitation with and without microtubules, whereas

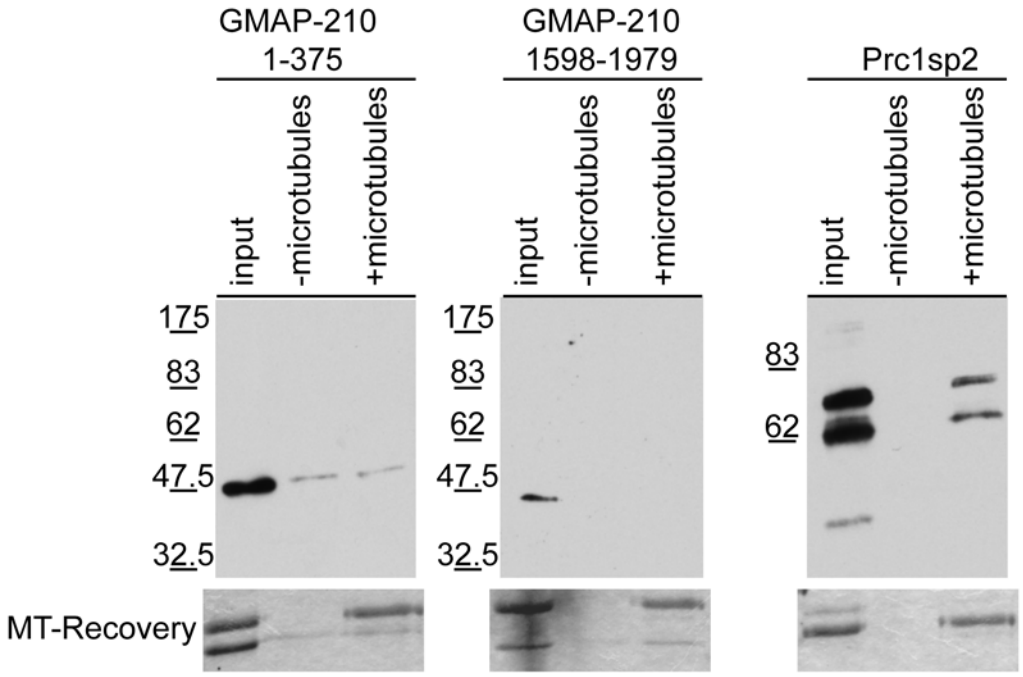

Figure 49: **Microtubule Spin-Down Of Recombinant GMAP-210 N- And C-Terminus.** Microtubules grown *in vitro* were incubated with 400 ng recombinant GMAP-210 N- or C-terminus or Prc1sp2 (all prepared from Sf9 cells) for 20 min; microtubule pellets were dissolved in SDS-PAGE sample buffer and subjected to coomassie stained SDS-PAGE to check for microtubule recovery ($5/6^{th}$ of sample) or Western blot ($1/6^{th}$ of sample); proteins were detected by rabbit anti Prc1 (right, 1:500) and HRP donkey anti rabbit (left and middle, 1:1000) or mouse anti 6xHis (1:1000) and HRP donkey anti mouse antibodies.

the GMAP-210 C-terminus (amino acids 1598 to 1979) was not detected in the pellet, irrespective of absence or presence of microtubules.
Recombinant GMAP-210 N- and C-terminus did not interact with microtubules *in vitro*.

2.7.4 GMAP-210 Has No Effect On Golgi Reassembly After Nocodazole Treatment

The drug nocodazole depolymerises microtubules in cells, disturbing the cytoskeleton. Apart from arresting the cells in G2-M phase, cells treated for a short period, lose their Golgi integrity as a consequence of microtubule depolymerisation (Thyberg and Moskalewski, 1999). The Golgi fragments and forms small Golgi stacks distributed throughout the cell (Ho *et al.*, 1989). Removal of the agent, allows microtubules to repolymerise and the Golgi reassembles in its perinuclear position. Rios *et al.* (2004) show, that nocodazole treatment of HeLa L depleted of GMAP-210, does not change Golgi fragmentation, overexpression of GMAP-210, however, disturbs recovery of microtubule asters.

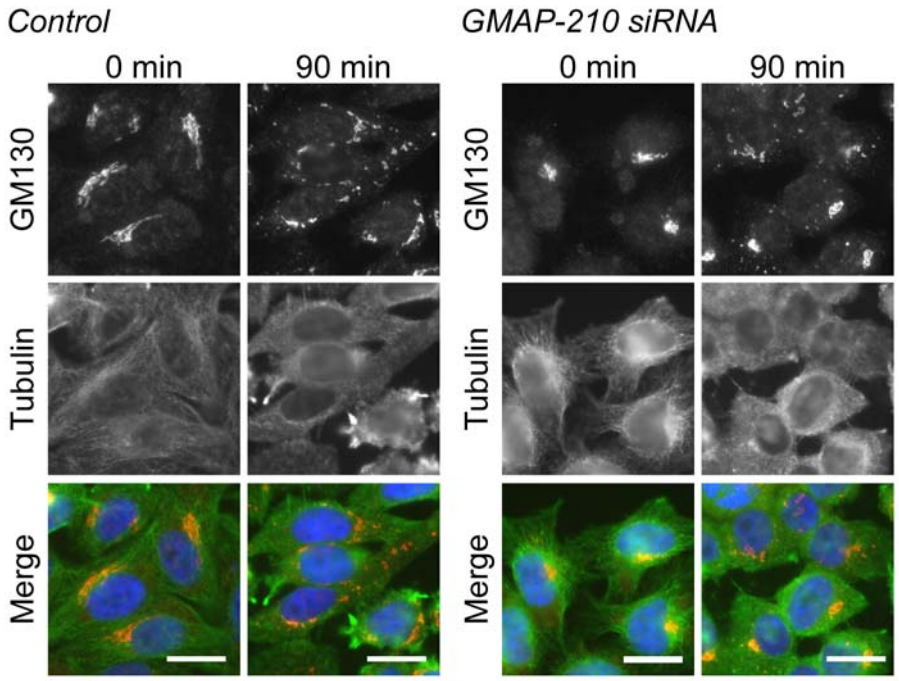

Figure 50: **Nocodazole Induced Golgi Disassembly In HeLa L Cells After GMAP-210 Depletion.** HeLa L cells were transfected with an siRNA oligo against GMAP-210 3'UTR or GL2 (control) for 72 hours; growth medium was then replaced by growth medium containing 200 μg/ml nocodazole and coverslips fixed at the indicated time-points with paraformaldehyde and stained with sheep anti GM130 (red, 1:500) and mouse anti α-tubulin (green, DM1A 1:2000); blue channel: DAPI staining; Bar=10 μm.

The phenotype observed by Rios *et al.* (2004) is completely different from the phenotype seen with the siRNA oligo used for this work (2.3, p.48), Golgi is fragmented (Rios *et al.*, 2004), instead of compacted. This makes it necessary to examine microtubules and Golgi morphology after nocodazole treatment of GMAP-210 depleted cells. HeLa L cells were treated with an siRNA oligo against GMAP-210 3'-UTR or GL2 control for 72 h. Cells were then treated with 200 μg/ml Nocodazole for 90 min, fixed and stained with antibodies against GM130 and α-tubulin. (Fig.50). After 72 h siRNA treatment against GMAP-210, the Golgi showed the compacted morphology observed before (Fig.24, p.49). The microtubule network was not influenced by absence of GMAP-210 (compare 2.7.2, p.79). After 90 min of nocodazole treatment, cells showed a diffuse, cytoplasmic α-tubulin staining, as microtubules were completely depolymerised. This effect could be seen in control cells and in cells depleted of GMAP-210 alike. The Golgi apparatus was fragmented in control cells and fragments could be found throughout the cell periphery, although a big perinuclear clustering of fragments, reminiscent of Golgi, still existed. In cells depleted of GMAP-210, small Golgi fragments were seen in the cell periphery after 90 min of nocodazole treatment. The biggest part of GM130 staining was found on a prominent structure near the nucleus. This big structure looked like Golgi in GMAP-210 depleted cells before nocodazole treatment. It was, however, impossible to say, if this concentration of Golgi membranes near the nucleus was due to a direct effect of GMAP-210 depletion. It was also possible, that the compact Golgi, after microtubule depolymerisation, diffused more slowly in the cell, because of purely kinetic reasons.

One possible theory could be, that GMAP-210 helps to link the Golgi apparatus to microtubules (Infante *et al.*, 1999) and thus helps to position it near the centrosome in a juxtanuclear position. If this was true cells depleted of GMAP-210 and treated with nocodazole should face problems in reassembly and repositioning of the Golgi apparatus after washout of the drug.

In order to test this, *hTERT*-RPE1 cells were treated with siRNA against GMAP-210 or GL2 control for 72 h. Cells were incubated on ice for 60 min and treated with 200 μg/ml nocodazole at 37°C to depolymerise microtubules. Cells were then fixed and stained for GM130 and α-tubulin 0 min, 5 min, 15 min and 30 min after nocodazole washout (Fig.51). *hTERT*-RPE1 cells were used to circumvent the effect of Golgi compaction, which has proven to make comparison of changes at the Golgi apparatus more difficult. *hTERT*-RPE1 control cells showed a fragmented and scattered Golgi after treatment with nocodazole for 60 min. This was also true for cells depleted of GMAP-210. Thus, the starting point for reassembly was equal for GMAP-210 siRNA treated cells and control cells. 5 min after nocodazole washout, the microtubules began to condense under both conditions. The Golgi still remained fragmented. After 15 min, the microtubule net-

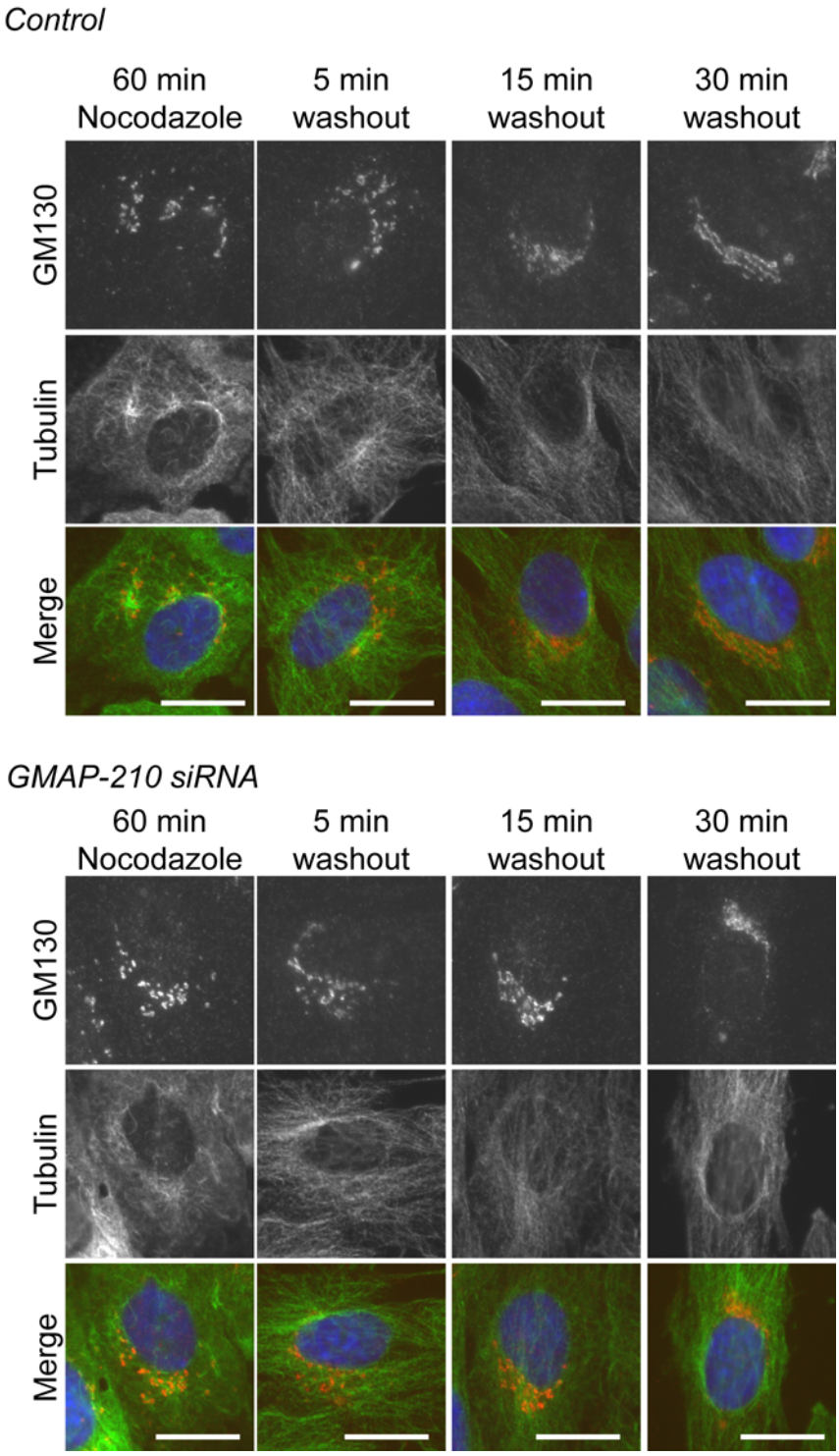

Figure 51: **Nocodazole Induced Golgi Disassembly In HeLa L Cells After GMAP-210 Depletion.** *hTERT*-RPE1 cells were transfected with an siRNA oligo against GMAP-210 3'-UTR or GL2 (control) for 72 hours; the cells were then incubated on ice for 60 min prior to exchange of the growth medium with growth medium containing 200 μg/ml nocodazole; after 60 min, coverslips were washed 3 times with growth medium and fixed at the indicated time-points with paraformaldehyde and stained with sheep anti GM130 (red, 1:500) and mouse anti α-tubulin (green, 1:1000); blue channel: DAPI staining; Bar=10 μm.

work was re-established and the Golgi fragments started to concentrate in the perinuclear region. After 30 min the Golgi had mostly reformed its ribbon-like structure of stacked cisternae and thus had regained its normal morphology. No difference in Golgi reassembly could be observed between control cells and cells missing GMAP-210.
Depletion of GMAP-210 had no effect on microtubules or Golgi morphology during nocodazole treatment and subsequent repolymerisation of microtubules and reassembly of the Golgi.

2.7.5 GMAP-210 Is Not Associated With γ-Tubulin

In Rios *et al.* (2004) GMAP-210 was shown to recruit γ-tubulin containing complexes (γ-TCCs) to the Golgi apparatus of Cos-7 cells. Overexpression of a full-length construct of GMAP-210 caused strong staining for γ-tubulin on the Golgi. A construct missing the C-terminus did not cause such an effect. Due to the confusion about the interaction and targeting domains of GMAP-210 in the literature (compare Infante *et al.* (1999) and Gillingham *et al.* (2004) and 2.1.2, p.29*ff.*) it was verified if this effect could be reproduced with the described or a different domains of GMAP-210.

HeLa L cells were transfected for 24 h with GFP-tagged constructs for GMAP-210 N-terminus (pEGFPC2-GMAP-210 1-375 and pEGFPC2-GMAP-210 1-1712), GMAP-210 full-length or GMAP-210 C-terminus (pEGFPC2-GMAP-210 1598-1979). The cells were fixed and stained for γ-tubulin and analysed by epifluorescence microscopy (Fig.45, p.78, right panel). As positive control the N-terminal 702 amino acids of the ninein-like

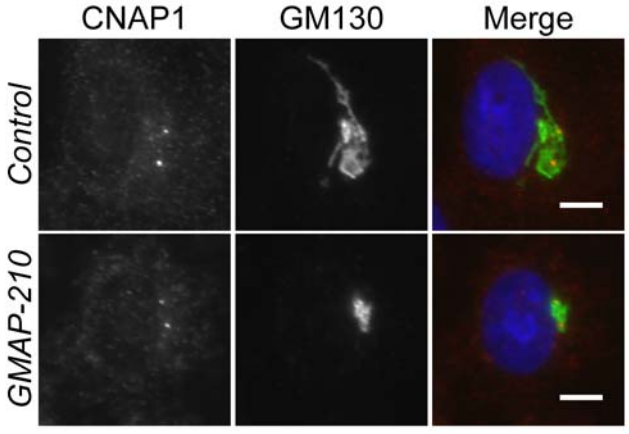

Figure 52: **Golgi Positioning Near The Centrosome After GMAP-210 Depletion.** HeLa L cells were transfected with siRNA oligos against GL2 (control) or GMAP-210 3'-UTR for 72 h and fixed with methanol; cells were stained with mouse anti CNAP-1 (red, 1:1000) and sheep anti GM130 (green, 1:500) antibodies; blue channel: DAPI staining; Bar=5 μm.

protein (NLP) were transfected into HeLa L cells (gift from M. Casenghi). NLP was described to recruit γ-tubulin ring complexes (γ-TuRCs) upon overexpression (Casenghi *et al.*, 2003).

In untransfected cells, γ-tubulin staining could be found on two dots in the perinuclear region, the centrosomes of G2 phase cells. Also diffuse cytoplasmic staining could be seen. Cells transfected with the N-terminus of NLP could easily be identified by aggregates of GFP, which at the same time stained for γ-tubulin. When GMAP-210 full-length was transfected, GFP stained the Golgi apparatus. γ-tubulin still localised to the centrosomes and could not be found co-localising with GMAP-210. The Golgi apparatus still localised near the centrosome as normal. Overexpression of either N-terminus or C-terminus did also not recruit γ-tubulin to the Golgi apparatus in HeLa L cells. As a side note, overexpressed NLP did not disturb the microtubule network of interphase cells (Fig.45, p.78 bottom left).

It was furthermore tested if the loss of GMAP-210 in HeLa L cells disturbed the γ-tubulin distribution or positioning of the Golgi apparatus in relation to the microtubule organising centre. For this, HeLa L cells were treated with siRNA against GMAP-210 or GL2 control for 72 h, fixed and either co-stained for GMAP-210 and γ-tubulin (Fig.46, p.79) or GM130 and the centrosomal protein CNAP1 (Fig.52). After depletion of GMAP-210 the antibody against γ-tubulin still stained two dots in the perinuclear region as expected. CNAP1 staining on the centrosomes was also unchanged. GM130 staining monitors the Golgi positioning. After GMAP-210 siRNA, the Golgi apparatus compacted (see 2.3, p.48) but remained adjacent to the CNAP1 staining in the perinuclear region. Golgi positioning near the centrosome was not dependent on GMAP-210.

If GMAP-210 interacted with γ-tubulin, then a high concentration of γ-tubulin in the cell, should recruit at least some GMAP-210. γ-tubulin recruitment could be achieved by overexpression of the NLP N-terminus (Casenghi *et al.*, 2003), as shown in Fig.45 (p.78).

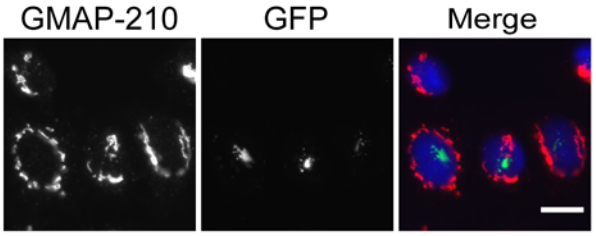

Figure 53: **GMAP-210 Localisation In NLP Transfected Cells.** HeLa L cells were transfected with a construct for expression of N-terminally GFP-tagged NLP (green) for 24 hours and fixed with paraformaldehyde; cells were stained with rabbit anti GMAP-210 (red, 1:500); blue channel: DAPI staining; Bar=10 μm.

HeLa L cells were transfected with a GFP-tagged version of NLP amino acids 1-702 for 24 h, fixed and stained for GMAP-210 (Fig.53). Overexpression of the N-terminal half of NLP caused aggregates of GFP to show up in HeLa L cells. These aggregates stained strongly for γ-tubulin. The staining for GMAP-210, however, could only be found on perinuclear Golgi membranes like in untransfected cells.
GMAP-210 is not recruited to strong concentrations of γ-tubulin.

2.7.6 Summary

GMAP-210 interaction with microtubules was tested by different methods. First the effect of GMAP-210 overexpression and depletion on the microtubule network of HeLa L cells was examined. Overexpression of different N- and C- terminal constructs gave no hint at disturbance of microtubules, neither at their origin, the centrosome, nor in the cell periphery. Slight changes were observed, when a short N-terminal construct (GMAP-210 1-375) was expressed. The microtubules looked more concentrated at the MTOC. Depletion of GMAP-210 had also no effect on microtubules.
Recombinant N- and C-terminal protein, purified from Sf9 cells, were tested for their capability to bind to taxol stabilised microtubules. Bundling of microtubules by these proteins was examined. Microtubules incubated with fragments of GMAP-210 were not bundled, in contrast the microtubule binding protein Prc1sp2 easily organised tubules. Microtubules were also incubated with recombinant N- and C-terminus of GMAP-210 and tested in a spin-down assay. In the microtubule pellet no GMAP-210 C-terminus and only little, precipitated N-terminus could be found. Prc1sp2 bound microtubules *in vitro*. Furthermore, the effect of GMAP-210 depletion on nocodazole induced Golgi fragmentation was tested. In HeLa L cells, Golgi fragments remained more concentrated in the perinuclear region in cells depleted of GMAP-210, if compared to control cells. In *hTERT*-RPE1 cells, this effect was not observed. Reassembly of the Golgi after nocodazole washout proceeded with similar kinetics in control cells and cells depleted of GMAP-210. γ-Tubulin localisation was also unchanged, when GMAP-210, full-length or fragments, were overexpressed. Ninein-like protein, however, recruited γ-tubulin visibly upon overexpression, but did not recruit GMAP-210 to these accumulations of γ-tubulin. GMAP-210 depletion also had no influence on the localisation of γ-tubulin and the Golgi remained near the microtubule organising centre. In any case, γ-tubulin was found on Golgi membranes.
Neither GMAP-210 interaction with microtubules nor with γ-tubulin could be proven.

2.8 GMAP-210 Recruits The Intraflagellar Transport Protein IFT20 To The Golgi Apparatus

IFT20 is an essential component of the intraflagellar transport machinery and is needed to build cilia and flagella (Rosenbaum and Witman, 2002). It directly interacts with the heterotrimeric kinesin II subunit Kif3B (Baker *et al.*, 2003). Surprisingly, it is also found at the Golgi apparatus (Follit *et al.*, 2006). Thus, IFT20 is an interesting candidate for a protein linking Golgi membranes to microtubules and thus might participate in the function of GMAP-210 and influence Golgi morphology. The reason for IFT20's presence on the Golgi apparatus is only speculated about (Follit *et al.*, 2006), and its function in primary cilium formation of *hTERT*-RPE1 cells and the function at the Golgi were examined.

2.8.1 Tools For IFT20

IFT20: Cloning In a first step, the NCBI database (www.ncbi.nlm.nih.gov) was searched for the human version of the *Chlamydomonas reinhardtii* IFT20. Four version of this protein were found in the human genome (Fig.54). A fifth version was deduced from the database sequences by adding the sequence for the elongated N-terminus to the sequence of BC002640. This construct was later amplified successfully (BC002640+ in Fig.54) from HeLa L cDNA.

The clone EAW51075, which has an alternative C-terminus, was only added recently to the database and thus not examined in this work. It has the same sequence as BC002640 but replaces the last two amino acids by a 20 amino acids long sequence, which could be identified as a flagellar P-ring protein domain by Pfam database search. These proteins are part of the bacterial flagellum. The other four versions differ by either their N-terminus, which is elongated by 26 amino acids, or their alternatively spliced C-terminus after amino acid 96 or 70 respectively. Amino acids 27 to 96 or 1 to 70 (in versions with the short N-terminus) are identical in all five versions and represent the IFT20 core domain. Primers were designed to amplify four of the five variants (see Tab.1). These IFT20 clones were named after the primers used in their amplification for easy reference. They are summarized in Tab.2 (p.91), together with the respective template DNA used or their amplification.

Database Information The IFT20 gene maps to chromosome 17 locus 17q11.2. It is a protein of 18.1 kDa and is expressed in a wide variety of tissues, especially in soft tissue, the uterus and the umbilical cord. It was also found in all states of human development

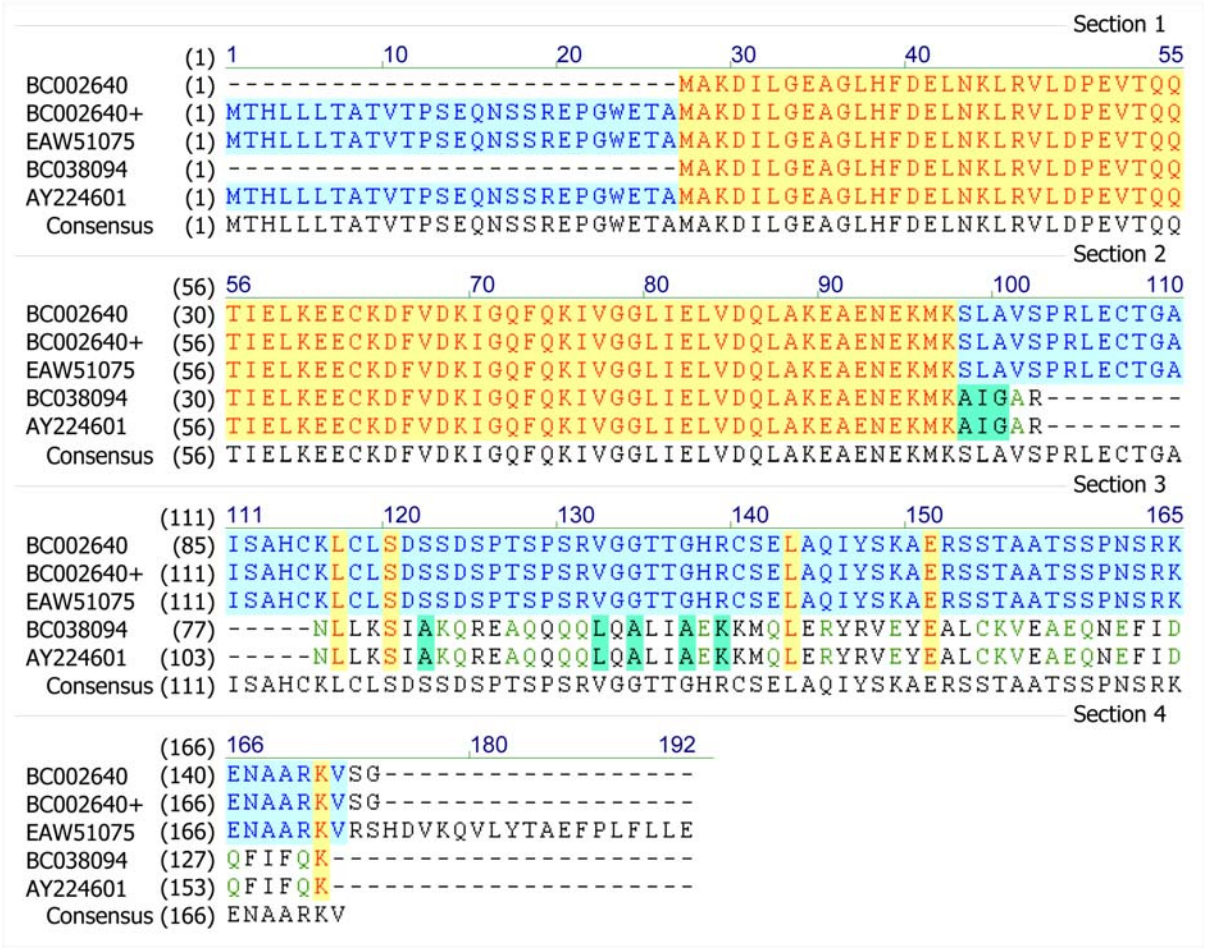

Figure 54: **Alignment Of The Five Identified Variants Of Human IFT20.** Alignment performed by VectorNTI10 (Invitrogen); yellow: identity of all sequences; blue: identity in a subset of sequences; green: similarities;

Table 1: Primers used for amplification of different variants of the human IFT20 coding sequence; forward primers inserted BamHI, reverse primers SalI restriction sites.

Primer Name	**DNA Sequence**	**Description**
IFT20-F2	GGGATCCCCATGGCCAAGGACATCCTGGGTGAAGCAGG	5' short N-terminus
IFT20-R2	GGTCGACTCAACCCGATACCTTTCTAGCTGC	3' short C-terminus
IFT20-F3	GGGATCCCCATGACACACCTCCTCCTGACTGCC	5' long N-terminus
IFT20-R3	GGTCGACTCATTTCTGAAAAATAAATTGGTC	3' long C-terminus

Table 2: Overview of IFT20 variants; primers as listed in table 1; Source: DNA template used for amplification; EAW51075 was not amplified, but F3 primer could have been used besides an applicable reverse primer; aa: number of amino acids.

Accession No.	**Primer Pair**	**Protein Length**	**Source**
AY224601	F3R2	158 aa	Fetus cDNA
BC038094	F2R2	132 aa	F3R2 clone
BC002640+	F3R3	174 aa	HeLa L cDNA
BC002640	F2R3	148 aa	F3R3 clone
EAW 51075	F3–	192 aa	—-

rather equally except in embryo and juvenile (where it seems to be not present at all). As this data was achieved by EST expression profile (www.ncbi.nlm.nih.gov; UniGene; HS696090), it was not possible to deduce possible differences in the expression pattern of the different IFT20 variants. This also goes beyond the scope of this work and is not further examined.

Polyclonal Antibodies Against IFT20 Polyclonal antibodies were raised against the shortest version of IFT20 (F2R2). Recombinant protein was expressed in *E.coli* transformed with the pQE32-vector and purified. Overexpression of IFT20 was achieved at 37°C with 3 h of induction. Purified protein was dialysed against 25 mM Tris/HCl pH 7.4 and 300 mM NaCl.
Immunisation of two rabbits (#5917 and #5918) was performed by Biogenes (Berlin, Germany) with a total amount of 2 mg recombinant protein for both rabbits. Testbleeds were evaluated at 1 month intervals and one month after the 3rd testbleed, rabbits were bled out and about 50 ml antiserum per rabbit collected.
Affinity purification of the bleedout of rabbit #5917 was performed with 6x-His-IFT20 (F2R2 variant), purified under denaturing conditions. The antibody specificity was evaluated for immuno-staining of fixed cells and Western blot experiments.

IFT20 siRNA And Antibody Specificity For knockdown of IFT20 in cell culture, an siRNA oligo was designed (Tab.5, p.122), which specifically targets the core domain of IFT20, which all five variants have in common (Fig.54).
hTERT-RPE1 cells were transfected with the siRNA oligo against IFT20 or GL2 control for 72 h. Cells were subsequently starved by removing growth medium and replacing it with growth medium devoid of FCS for 48 h to stimulate primary cilium growth, while

adding the respective siRNA oligos anew. Cells were incubated for 1 h on ice, fixed with methanol and stained with the purified antibodies against IFT20 (Fig.55). Co-staining was done with an antibody against acetylated tubulin. In control cells the IFT20 antibody stained two structures. One was situated in the perinuclear region, which was shown to co-stain with the Golgi localised GMAP-210 (Fig.56). The second structure detected with the IFT20 antibody is the primary cilium as shown by acetylated tubulin staining. Upon treatment with the specific IFT20 siRNA oligo, the staining for IFT20 completely disappeared from the Golgi complex and the primary cilium.

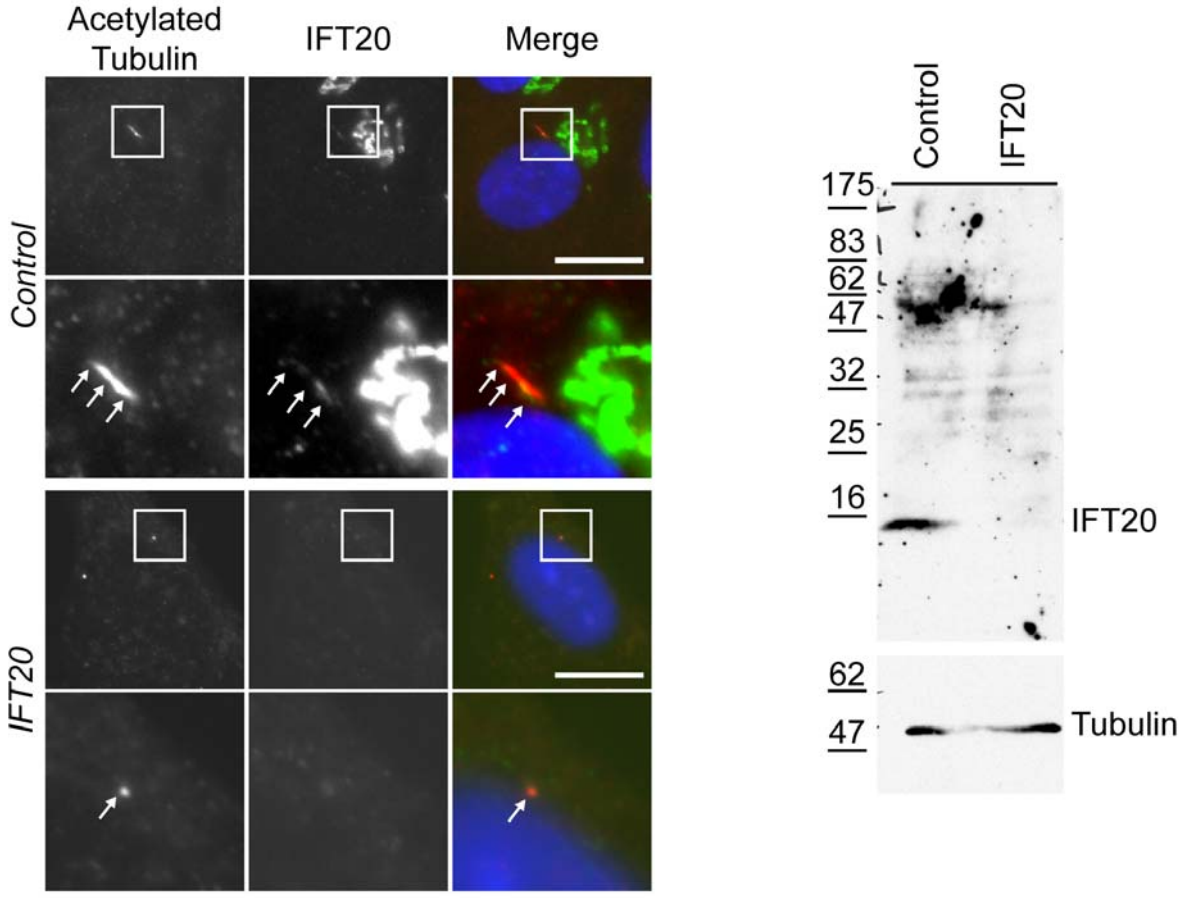

Figure 55: **Immunofluorescence And Western Blotting Of *hTERT*-RPE1 Cells Treated With IFT20 siRNA.** *hTERT*-RPE1 cells were treated for 72 h with an siRNA oligo targeting the core domain of IFT20 or GL2 (control) and subsequently starved for 48 h by culturing in growth medium without FCS whereas siRNA treatment was repeated; cells were then put on ice for 1 h, fixed in methanol and stained with mouse anti acetylated tubulin (red, 1:1000) and rabbit anti IFT20 (green, 1:500); blue channel: DAPI staining; Bar=10 μm; lower pictures show close-up of the indicated region in pictures above; arrows indicate primary cilium or centrosome, respectively; Western blotting (right) was done by lysing cells, treated with siRNA against IFT20 or GL2, for 30 min on ice in mammalian lysis buffer and analysing 20 μg protein extract on 12.5% SDS-PAGE; protein was detected with rabbit anti IFT20 (1:250) and HRP donkey anti rabbit antibodies, detection with mouse anti α-tubulin antibodies shows equal loading of both lanes.

Depletion of IFT20 was also shown by Western blot (Fig.55). *hTERT*-RPE1 cells were treated as described above, but instead of fixing, the cells were collected and lysed. The lysate was subjected to SDS-PAGE and Western blotting. Protein was revealed with the affinity purified antibody (2.8.1, p.91). A second SDS-PAGE gel loaded with the same amount of protein was subjected to Western blotting. An antibody against α-tubulin, showed equal loading.
The α-tubulin signal proved, that equal amounts of protein were loaded in each lane. A distinct band below the 16 kDa marker revealed IFT20 protein in control cells, whereas the band was completely absent from cell extracts treated with siRNA against IFT20. The affinity purified antibody detected IFT20 in immunofluorescence and Western blotting. The designed siRNA oligo results in the loss of the IFT20 protein from cells.

2.8.2 IFT20 Depletion Prevents Primary Cilium Formation

IFT20 is an important part of the intraflagellar transport complex, linking it to the heterotrimeric kinesin II subunit Kif3B ((Baker *et al.*, 2003)). Its depletion prevents primary cilium formation in cells.
It was tested if depletion of IFT20 with the designed oligo had the described effect on cilium formation. *hTERT*-RPE1 cells were transfected with the siRNA oligo against

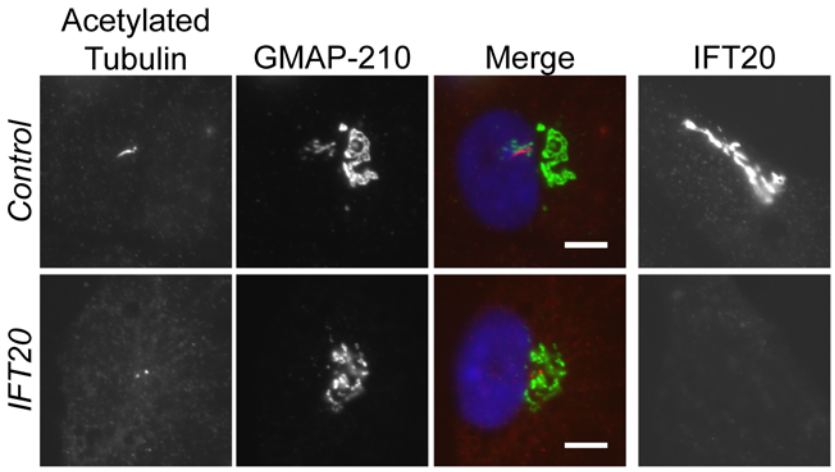

Figure 56: **GMAP-210 Localisation After IFT20 siRNA.** *hTERT*-RPE1 cells were treated with siRNA oligos against IFT20 or GL2 (control) for 72 h; cells were subsequently starved by replacing growth medium with medium devoid of FCS for another 48 h, while retransfecting siRNA as before; cells were incubated on ice for one hour and fixed with methanol and stained with antibodies against acetylated tubulin (red; mouse; 1:500) and GMAP-210 (green; rabbit; 1:500); cells treated in parallel were stained for IFT20 (rabbit; 1:500) to show depletion (right column); blue channel: DAPI staining; Bar=5 μm.

IFT20 or the control GL2, starved for 48 h to stimulate cilium growth and analysed by staining with antibodies against acetylated tubulin and IFT20 (Fig.55, p.92 and Fig.56). IFT20 is depleted efficiently from *hTERT*-RPE1 cells by the siRNA oligo. In control cells the primary cilium was stained by acetylated tubulin. In cells depleted of IFT20 the acetylated tubulin antibody only labelled two dots representing the centrosomes. No primary cilium was formed.
IFT20 was also localised on the Golgi apparatus. Its function is not elucidated yet, but due to its direct link with the motor protein Kif3B (Baker *et al.*, 2003) it could be involved in establishing Golgi morphology. Thus, the effect of IFT20 depletion upon the Golgi apparatus was examined. Cells treated with siRNA against IFT20 or the control GL2 were stained with an antibody against GMAP-210 (Fig.56). IFT20 staining of cells prepared in parallel showed depletion of IFT20. Acetylated tubulin staining showed the loss of the primary cilium. Only the centrosomes were stained. The Golgi, however, was still labelled by the GMAP-210 antibody. Neither Golgi morphology nor Golgi position were changed after IFT20 knockdown.

2.8.3 GMAP-210 Depletion Prevents IFT20 Golgi Localisation

As Golgi localised protein, which also links to the microtubule network by binding to a kinesin (Baker *et al.*, 2003), IFT20 is a possible interaction partner of GMAP-210. As shown in 2.4 (p.55) all examined Golgi localised components of the secretory pathway stayed attached to the Golgi apparatus, even when it collapsed after GMAP-210 depletion in HeLa L cells. Testing the behaviour and localisation of IFT20 after GMAP-210 knockdown will give insight into IFT20's relation to GMAP-210.
hTERT-RPE1 and HeLa L cells were treated with siRNA against GMAP-210 or the control GL2, fixed and stained for IFT20 and GM130 (Fig.57). As GM130 staining showed, Golgi in HeLa L cells collapses and the GM130 signal became more intense on the smaller Golgi. In *hTERT*-RPE1 cells Golgi morphology was rather unchanged. The IFT20 antibody labelled clearly the Golgi apparatus in *hTERT*-RPE1 control cells. In HeLa L the signal was rather weak. When GMAP-210 was depleted, IFT20 antibody staining of Golgi was significantly reduced in both cell types.
Either IFT20 did no longer bind to the Golgi apparatus and was thus localised elsewhere, probably in the cytosol or on vesicles, or IFT20 was degraded or its expression reduced. In order to test this, a Western blot experiment was performed to show IFT20 protein levels in the cells.
hTERT-RPE1 cells were treated with siRNA against GMAP-210, IFT20 or GL2 for 72 h. Cells were then collected and lysed. Equal amounts of extracts were loaded to 12.5%, 10%

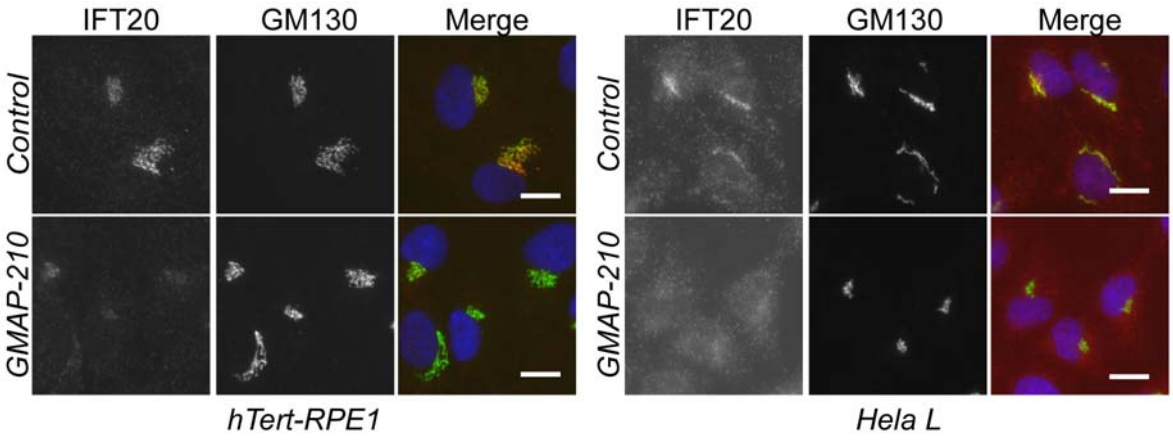

Figure 57: **IFT20 Localisation After GMAP-210 siRNA.** *hTERT*-RPE1 (left) and HeLa L (right) cells were treated for 72 h with siRNA against GMAP-210 3'-UTR or GL2 (control), fixed in paraformaldehyde and stained with rabbit anti IFT20 (red, 1:500) and mouse anti GM130 (green, 1:500); blue channel: DAPI staining; Bar=10 μm.

and 6% SDS-PAGE gels and subjected to Western blotting. Protein was detected with IFT20, α-tubulin or GMAP-210 antibodies (Fig.58). The α-tubulin antibody confirmed equal loading for all three conditions. GMAP-210 and IFT20 antibodies showed depletion of the proteins in the respective siRNA experiments. Depletion of GMAP-210 did not change the protein levels of IFT20, neither did IFT20 depletion change the expression level of GMAP-210. This proved, that IFT20 lost its capability to bind to the Golgi

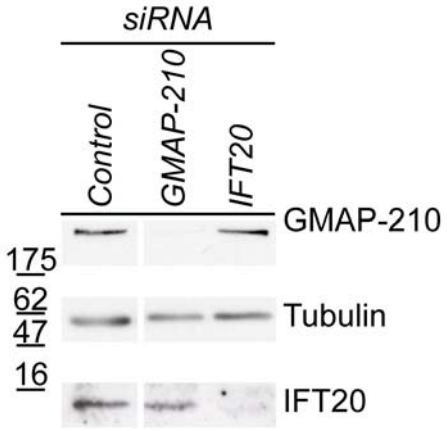

Figure 58: **Protein Levels Of GMAP-210 And IFT20 After siRNA.** *hTERT*-RPE1 cells were transfected with siRNA against GL2 (control), GMAP-210 3'-UTR or IFT20 core domain for 72 h; cells were lysed in mammalian lysis buffer for 30 min on ice and 20 μg of each extract analysed by Western blotting; proteins were detected with rabbit anti GMAP-210 (1:500) or rabbit anti IFT20 (1:250); detection with mouse anti α-tubulin antibody DM1A (1:4000) was used as control for equal loading.

apparatus when GMAP-210 was not present, rather than showing a reduced protein level in the cell.

2.8.4 GMAP-210 Does Not Localise On The Primary Cilium

IFT20 localises to the Golgi apparatus and also interacts with GMAP-210. Thus, it is possible, that GMAP-210 is actually involved in primary cilium formation and is localised on the cilium or at the basal body. In fact, GMAP-210 could be observed near the cilium. It is, however, unclear if this was a GMAP-210 bearing Golgi fragment localised coincidentally near the cilium or if it was specific targeting of GMAP-210 to the cilium. In order to answer this question, *hTERT*-RPE1 cells were starved for 48 h and then stained for acetylated tubulin, GMAP-210 and GM130, after incubation on ice and methanol fixation (Fig.59). In this experiment, the blue channel was not used for DAPI staining of DNA, but for AMCA secondary antibody, detecting rabbit anti GMAP-210. In the close-up of Fig.59 a primary cilium with nearby GMAP-210 staining is shown. This pool of GMAP-210 co-localised with GM130, which confirmed Golgi-localisation of GMAP-210. Consequently, GMAP-210 did not localise to the primary cilium, but only to the Golgi apparatus.

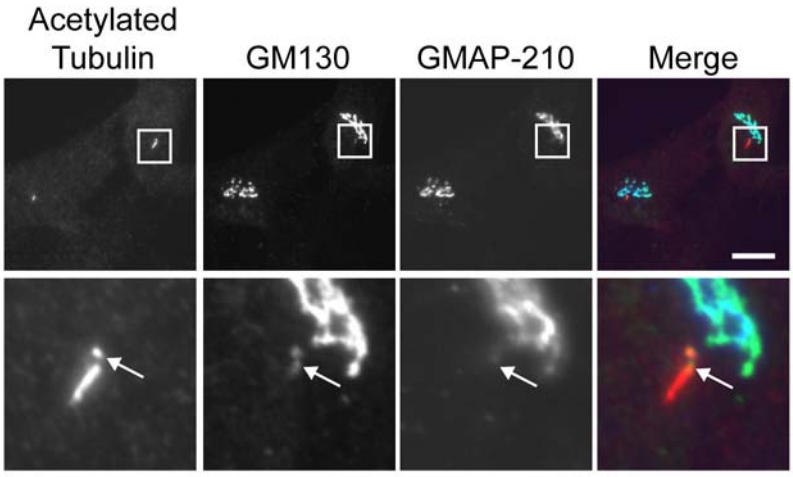

Figure 59: **Localisation Of GMAP-210 And The Primary Cilium.** *hTERT*-RPE1 cells were starved for 48 h by growth in culture medium without FCS and then incubated for 1 h on ice; after fixing with methanol, cells were stained with mouse anti acetylated tubulin (red, 1:500), sheep anti GM130 (green, 1:500) and rabbit anti GMAP-210 (blue, 1:500); close-up of primary cilium region shown, arrows indicate GMAP-210 and GM130 signal at the cilium base; Bar=10 μm.

2.8.5 GMAP-210 siRNA Does Not Inhibit Primary Cilium Formation

GMAP-210 knockdown inhibits IFT20 targeting to the Golgi complex. IFT20 is necessary for primary cilium formation. If GMAP-210 was also involved in primary cilium formation, its depletion would interfere with the cells capability to form a cilium. It will now be examined if GMAP-210 knockdown has an effect on intraflagellar transport and primary cilium formation.

(Fig.60). *hTERT*-RPE1 cells were treated for 72 h with siRNA against GL2 control or GMAP-210. They were then starved for 48 h while still keeping up siRNA conditions by retransfecting the oligos. Cells were incubated on ice for 1 h, fixed with methanol and stained for acetylated tubulin and IFT20.

In control cells acetylated tubulin stained the primary cilium growing from the centrosome. IFT20 localised on the Golgi apparatus in the juxtanuclear region and co-localised with acetylated tubulin on the primary cilium. After GMAP-210 siRNA the IFT20 antibody only labelled the primary cilium as did the antibody against acetylated tubulin.

Obviously, IFT20 was removed only from the Golgi apparatus, but was still localised at the primary cilium. The cilium still formed normally.

In order to quantify the capability of *hTERT*-RPE1 cells to form primary cilia under various conditions, cells were treated with siRNA against GL2, GMAP-210 or IFT20 for 72 h, and starved for 48 h before incubating them for 1 h on ice, fixing them with methanol and staining for acetylated tubulin. Cells were then counted and overall number of cells

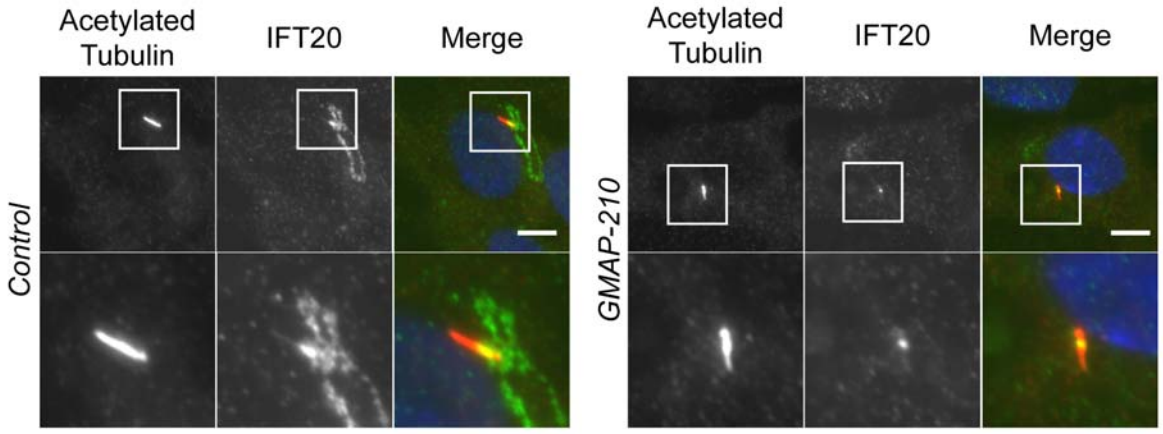

Figure 60: **Primary Cilium Formation In GMAP-210 Depleted Cells.** *hTERT*-RPE1 cells were transfected with siRNA oligos against GMAP-210 3'-UTR or GL2 (control) for 72 h and then cultured an additional 48 h in growth medium without serum, whereas siRNA oligos were retransfected as before; coverslips were placed on ice for 1 h, fixed in methanol and stained with mouse anti acetylated tubulin (red, 1:1000) and rabbit anti IFT20 (green, 1:500); pictures in the lower row show close-ups of indicated regions in the upper row pictures; blue channel= DAPI staining; Bar=5 μm.

compared to the number of cells forming a primary cilium. For each condition, about 200 cells from three independent experiments were counted (Fig.61). In control cells 80% (+/-8.8%) developed a primary cilium. After GMAP-210 knockdown 71% (+/-9.3%) and after IFT20 knockdown 31% (+/-5.9%) of the cells were able to form a primary cilium. GMAP-210 siRNA did not impair cilium formation at a significant level, whereas IFT20 siRNA reduced the capability of *hTERT*-RPE1 cells to form primary cilia by more than 60%.

2.8.6 GMAP-210 Directly Interacts With IFT20

IFT20 does not localise to the Golgi in absence of GMAP-210. Hence, direct interaction of IFT20 and Golgi-localised GMAP-210 is likely. To prove direct interaction, yeast 2-hybrid and co-immunoprecipitation experiments were performed.

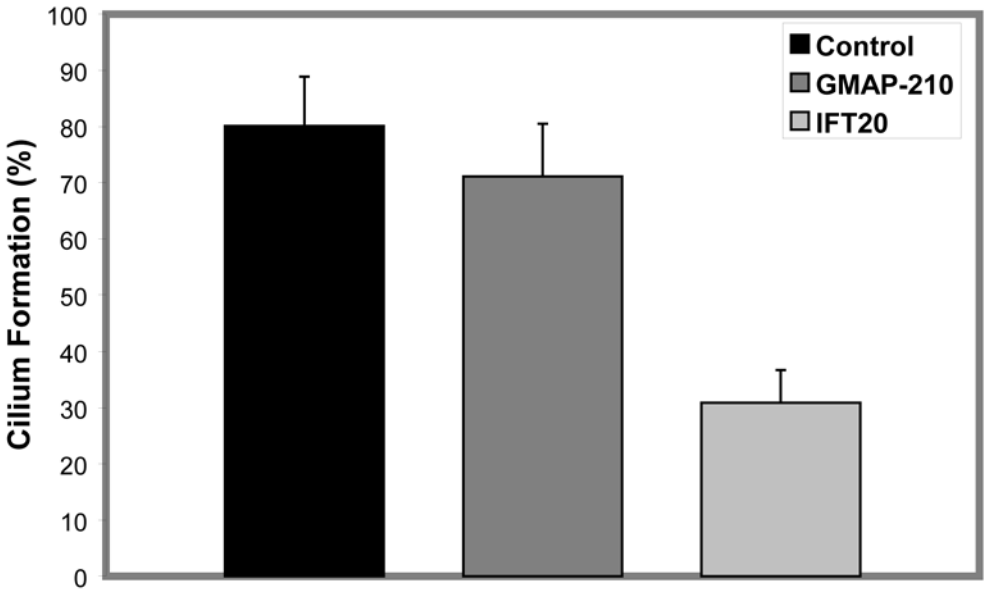

Figure 61: **Graphical Representation Of GMAP-210 And IFT20 siRNA Effect On Primary Cilium Formation.** *hTERT*-RPE1 cells were transfected for 72 h with siRNA oligos against GMAP-210 3'-UTR, IFT20 core domain or GL2 (control) and subsequently incubated for 48 h at normal growth conditions in serum without FCS, whereas siRNA was retransfected; cells were incubated on ice for 1 h, fixed with methanol and stained with mouse anti acetylated tubulin (red; 1:500) and sheep anti GM130 (green, 1:500); cells with primary cilia were counted against total cell number; GL2 80% +/-8.8; GMAP-210 71% +/-9.3; IFT20 31% +/-5.9; (n=3); 200 cells counted per condition.

IFT20 Interacts With A Coiled-Coil Region Of GMAP-210 In Yeast 2-Hybrid IFT20 was tested in yeast 2-hybrid interaction studies against GMAP-210. Two other golgins, human Golgin-84 and mouse GM130, were also tested as controls. The shortest version of IFT20 (F2R2) was transfected as a pFBT9 construct and tested as bait against the golgins as prey (Fig.62, left). Additionally, all four variants of IFT20 available were tested as bait against full-length GMAP-210 (Fig.62, right).
IFT20(F2R2) only interacted with the full-length GMAP-210 construct. There was a slight interaction with mouse GM130, but Golgin-84 did not react with IFT20. All of the IFT20 variants interacted with GMAP-210. Thus, the shortest version could be used in all further experiments.
To map the exact interaction domain of GMAP-210, fragments of GMAP-210 were used as prey in a yeast 2-hybrid experiments with IFT20(F2R2) (Fig.63). IFT20 interacted with full-length GMAP-210, the C-terminal 382 amino acids (GMAP-210 1598-1979) and the middle part, amino acids 855 to 1712, whereas only the amino acids 855 to 1332 and not 1333 to 1712 showed interaction. The N-terminal fragments, amino acids 1 to 375 and 618 to 803, did not bin. IFT20 interacted with GMAP-210 in yeast 2-hybrid, in a stretch in the middle of GMAP-210 (GMAP-210 855-1332) and in the C-terminus (GMAP-210 1598-1979).

IFT20 Co-Precipitates With GMAP-210 Better proof for direct interaction of IFT20 with GMAP-210 is co-immunoprecipitation of endogenous IFT20 and GMAP-210. A cell extract from *hTERT*-RPE1 cells was prepared and incubated with Protein-G sepharose and antibodies against IFT20 (5 μl), GMAP-210 (20 μl) or the preimmune serum of rabbit #6130 (1 μl). The beads were extracted in SDS-PAGE sample buffer and

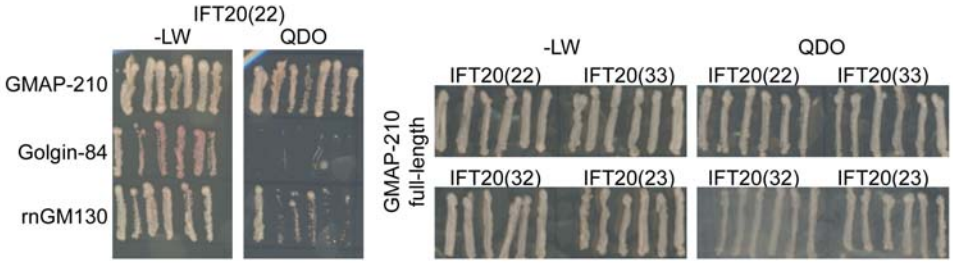

Figure 62: **Yeast 2-Hybrid Interaction Of IFT20 With Various Golgins.** Yeast 2-Hybrid interaction experiment, testing GMAP-210, Golgin-84 and mouse GM130 in pAct2 vector against IFT20(F2R2) in the pFBT9 vector (left); Yeast 2-Hybrid interaction experiment between full-length GMAP-210 in pAct2 and the various splice variants of IFT20 (F2R2, F3R3, F3R2, F2R3) in pFBT9; -LW: leucine and tryptophane deficient medium (growth control); QDO: leucine, tryptophane, histidine and alanine deficient medium.

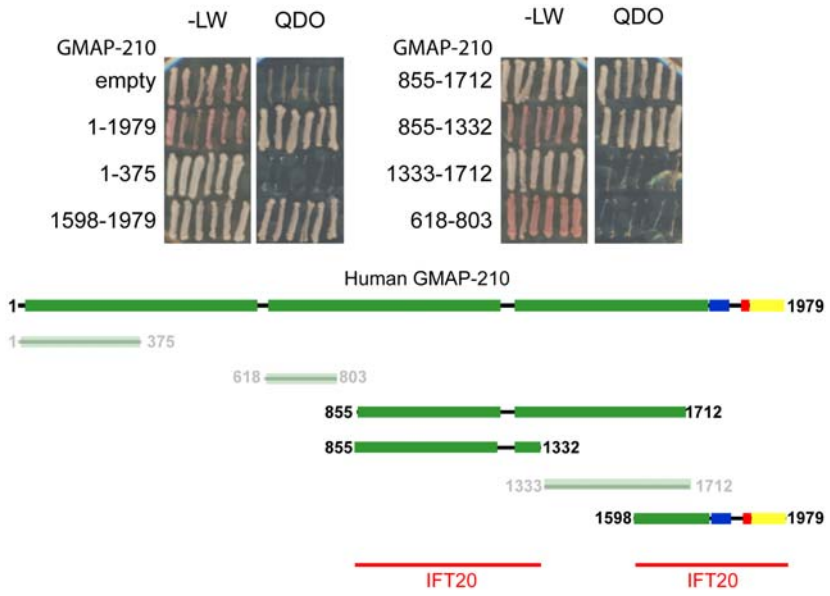

Figure 63: **Yeast 2-Hybrid Mapping Of IFT20 Interaction Site In GMAP-210.**
Yeast 2-Hybrid interaction experiment, testing the indicated fragments of GMAP-210 in pAct2 vector against IFT20(F2R2) in pFBT9 vector; -LW: leucine and tryptophane deficient medium (growth control); QDO: leucine, tryptophane, histidine and alanine deficient medium.

subjected to Western blotting. Proteins were detected with antibodies against IFT20 or GMAP-210. HRP-coupled Protein A was used for chemiluminescence detection, in order to reduce the background signal of the antibody light chain (Fig.64). The GMAP-210 antibody efficiently immunoprecipitated the protein and also co-precipitated IFT20. The IFT20 antibody precipitated the protein from the *hTERT*-RPE1 extract and also co-precipitated endogenous GMAP-210 protein. The pre-immune serum did not show any affinity for either GMAP-210 or IFT20. Thus, GMAP-210 and IFT20 interact specifically and directly *in vitro*.

2.8.7 Heterotrimeric Kinesin II Is Not Associated With IFT20 On The Golgi Apparatus

IFT20 links the intraflagellar transport complex to the heterotrimeric kinesin II component Kif3B (Baker *et al.*, 2003) and thus is supposed to link the IFT complex to microtubules and give it mobility. It is possible, that IFT20 and Kif3B link the Golgi apparatus, via GMAP-210, to the microtubule network.

Overexpressed Kif3B Does Not Localise To The Golgi Apparatus There is some evidence, that Kif3B is localised at the Golgi Apparatus (Hirokawa, 1998). Pres-

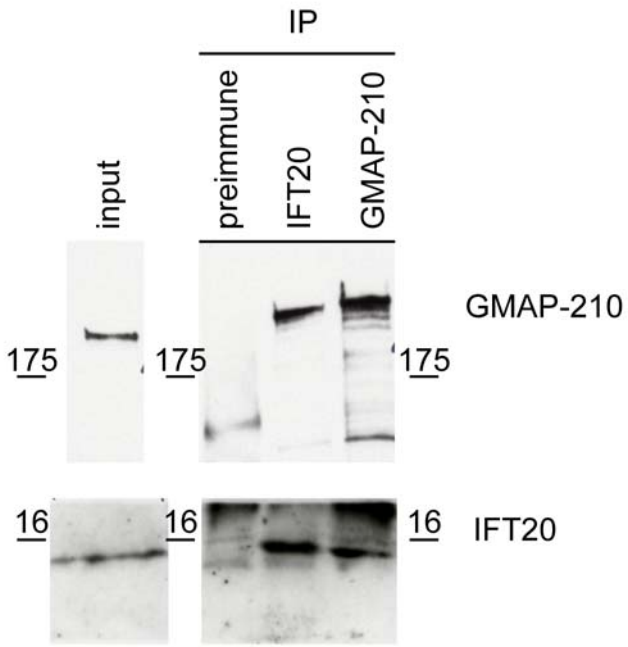

Figure 64: **Co-Immunoprecipitation Of GMAP-210 And IFT20.** *hTERT*-RPE1 cells were lysed in TNTE buffer and incubated with rabbit anti GMAP-210 antibody, rabbit anti IFT20 antibody or #6130 pre-immune serum (rabbit prior to injection with GMAP-210 antigen) and Protein-G-sepharose; beads were boiled in SDS sample buffer and analysed by Western blotting from 6% and 12.5% SDS-PAGE gels; proteins were detected with rabbit anti GMAP-210 (1:500) or rabbit anti IFT20 antibody.

ence at the Golgi apparatus would be a first hint to its function and maybe the function of IFT20. Kif3B targeting was tested with overexpressed proteins.
Full-length and C-terminal (aa 592-747) Kif3B were amplified from HeLa L cDNA. The C-terminal fragment consisted of the globular tail domain and did not interact with IFT20 (Baker *et al.*, 2003). *hTERT*-RPE1 cells, starved for 48 h, were transfected with the various constructs for 24 h and their localisation examined. The cells were co-stained with an antibody against acetylated tubulin to locate the primary cilium (Fig.65). Overexpressed full-length Kif3B localised only to the primary cilium, to the nucleus and diffusely in the cytoplasm in *hTERT*-RPE1 cells. The globular tail domain was also seen at the primary cilium, co-localising with acetylated tubulin, and in the cytoplasm. Kif3B, localised on the cilium, decorated the base of the cilium, although, due to high background in the cytosol, a weak signal on the primary cilium itself would be lost. Kif3B was not found on the Golgi apparatus in any case.

Kif3B Depletion Does Not Change Golgi Morphology The Effect of Kif3B knockdown was examined by using siRNA. For this a SmartPool designed by Dharmacon/Perbio

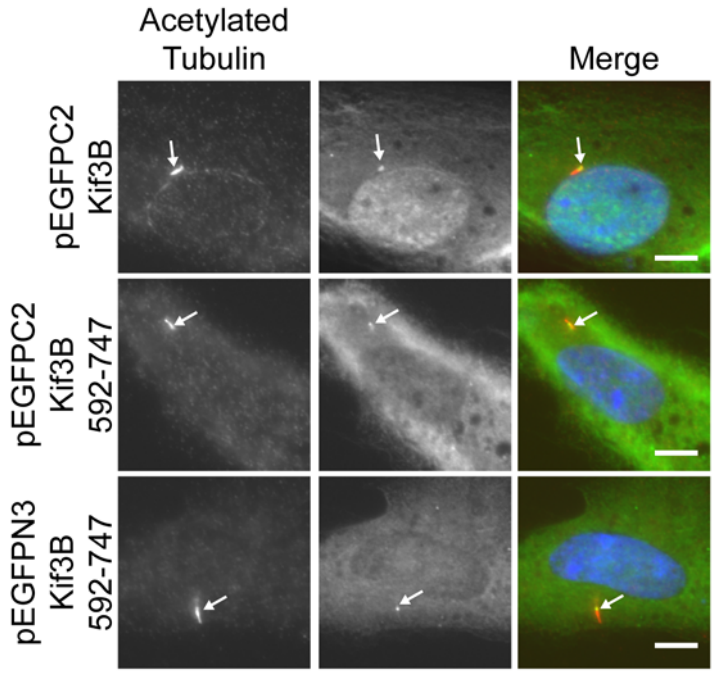

Figure 65: **Localisation Of Kif3B.** *hTERT*-RPE1 cells were cultured for 24 h with growth medium without FCS, transfected with the indicated constructs for Kif3B full-length and C-terminal amino acids 592 to 747 (green) and cultured for another 24 h; cells were incubated for 1 h on ice, fixed with methanol and stained with mouse anti acetylated tubulin (red, 1:500); arrows indicate primary cilium and basal body; blue channel= DAPI staining; Bar=5 μm.

was used, which included four different siRNA oligos targeting the same gene (Tab.5, p.122). *hTERT*-RPE1 cells were transfected with the siRNA SmartPool against Kif3B or a pool against GL2 control. After 48 h the cells were transfected with a construct for expression of GFP tagged full-length Kif3B to monitor depletion efficiency. 24 h after the transfection of the construct, the cells were fixed with paraformaldehyde and stained with an antibody against IFT20 (Fig.66). Furthermore, cells treated in the same way were collected before fixation and extracted. Cell extracts of control and Kif3B siRNA treated cells were loaded to SDS-PAGE and examined by Western blotting. Exogenously expressed protein was detected with a sheep anti GFP antibody or an antibody against α-tubulin (Fig.66). Immunofluorescence and Western blotting showed, that the expression of the GFP-tagged Kif3B protein was completely abolished by treatment with the siRNA SmartPool. Localisation of IFT20 on the Golgi apparatus was not changed by the absence of Kif3B in immunofluorescence.

If Kif3B was involved in Golgi positioning and morphology by its putative link with IFT20 and GMAP-210, its depletion would change the Golgi apparatus.

hTERT-RPE1 cells were treated for 72 h with the siRNA SmartPool against GL2 or Kif3B and subsequently starved for another 48 h under siRNA conditions. Cells were incubated

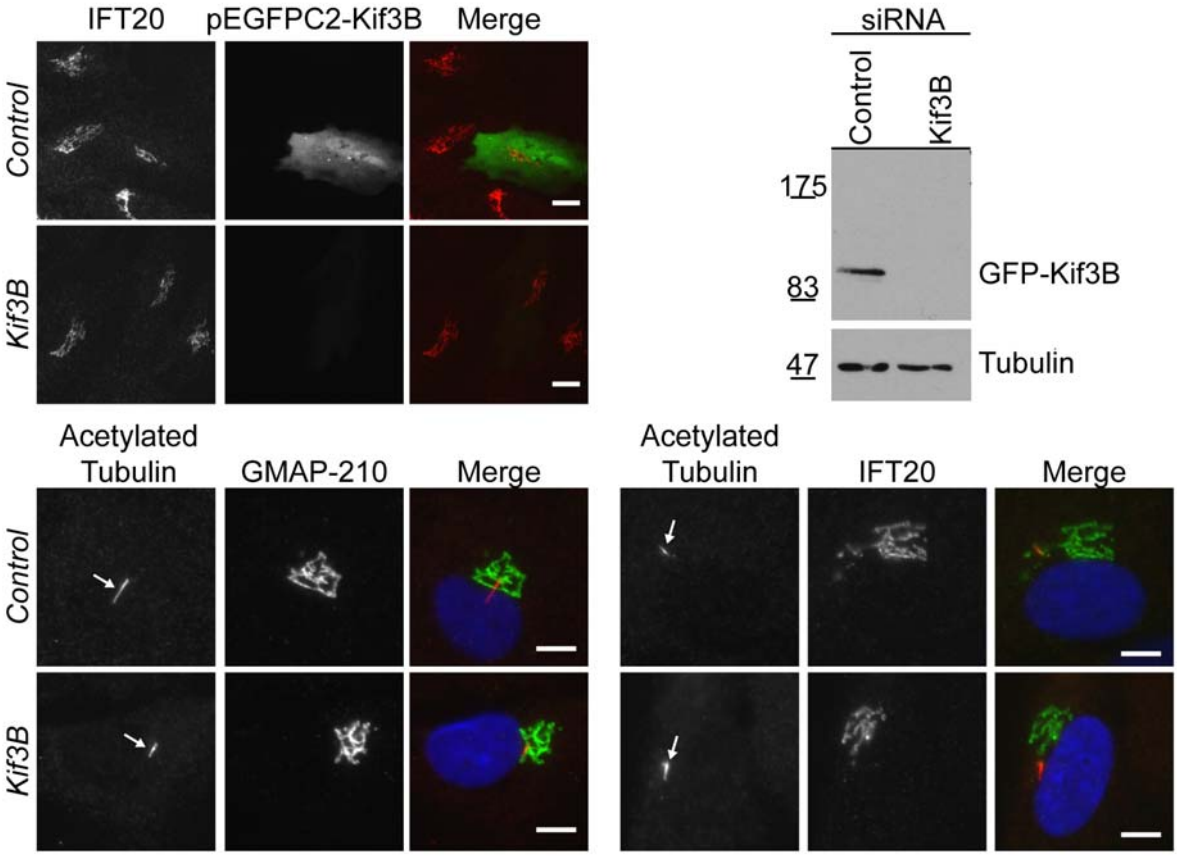

Figure 66: **Effects Of Kif3B siRNA Treatment In *hTERT*-RPE1 Cells.** *hTERT*-RPE1 cells were transfected with an siRNA SmartPool against Kif3B or GL2 (control) for 72 h; after 48 h the cells were also transfected with a construct for expression of full-length Kif3B with an N-terminal, enhanced GFP-tag for 24 h (green) without removing the siRNA; cells were fixed with paraformaldehyde and stained with rabbit anti IFT20 (red, 1:500) antibody (upper left panel). From the same cells an extract was made by lysis in mammalian lysis buffer on ice; 20 μg were applied to a 6% SDS-PAGE gel and analysed by Western blotting; protein was detected with sheep anti GFP antibody (1:1000); the mouse anti α-tubulin antibody controlled equal loading (upper right panel). *hTERT*-RPE1 cells were transfected with an siRNA SmartPool against Kif3B or GL2 (control) for 72 h after which the cells were cultured for another 48 h in growth medium without FCS; siRNA was retransfected; cells were incubated on ice for 1 h, fixed with methanol and stained, as indicated, with mouse anti acetylated tubulin (red, 1:500) and rabbit anti GMAP-210 (green, 1:500, left) or rabbit anti IFT20 (green, 1:500, right) antibodies (lower left and right panel); arrows indicate the primary cilium; blue channel= DAPI staining; Bar=5 μm.

on ice for 1 h, fixed with methanol and stained for acetylated tubulin and GMAP210 (Fig.66, lower left). After depletion of Kif3B, GMAP-210 was still localised on the Golgi apparatus in *hTERT*-RPE1 cells and Golgi morphology was not changed. Acetylated tubulin still stained the cilium, positioned near the Golgi apparatus.
The influence of Kif3B depletion on primary cilium formation was further examined. Cells were treated as described above, but stained for acetylated tubulin and IFT20 instead (Fig.66, lower right). In cells depleted of Kif3B, a primary cilium had, nevertheless, formed and was stained by the acetylated tubulin and IFT20 antibody. IFT20 was also found at the Golgi apparatus.
Depletion of Kif3B by siRNA did not inhibit primary cilium formation in *hTERT*-RPE1 cells and IFT20 localises normally.

2.8.8 Summary

The intraflagellar transport protein IFT20 was localised on the Golgi apparatus and the primary cilium. When IFT20 was depleted from starved *hTERT*-RPE1 cells, their ability to form a primary cilium was significantly impaired and only about 30% of cells formed a cilium, in comparison to 80% in control cells. Depletion of GMAP-210 removed IFT20 from the Golgi apparatus, but not from the primary cilium. Western blotting of cells, depleted of GMAP-210, showed, that protein levels of IFT20 were the same as in control cells. Direct interaction of GMAP-210 and IFT20 was proven by yeast 2-hybrid and co-immunoprecipitation studies. GMAP-210 localisation and Golgi morphology, however, were not changed by IFT20 depletion. GMAP-210 itself was not involved in primary cilium formation. No GMAP-210 was found at the centrosome and depletion of GMAP-210 inhibited primary cilium formation only slightly (71% of cells instead of 80% in controls).
The IFT20 associated subunit Kif3B of the heterotrimeric kinesin II was not associated with Golgi localised IFT20, although GFP-tagged Kif3B protein was found at the basal body of the primary cilium in *hTERT*-RPE1 cells. Depletion of Kif3B with an siRNA SmartPool, did neither change Golgi morphology, nor localisation of IFT20. Primary cilium formation was also not inhibited.

3 Discussion

In this work, I studied the localisation of the protein GMAP-210. I examined its targeting motives and tried to elucidate its function in the cell. To this end I set out to discover interaction partners of GMAP-210 and studied the effects of overexpression and knockdown on Golgi morphology, transport pathways and behaviour to treatment with different drugs.

3.1 GMAP-210 Localises To The Golgi Apparatus And Vesicular Tubular Structures Of The Early Secretory Pathway

3.1.1 The C-Terminal GRAB Domain Is The Golgi Targeting Domain Of GMAP-210

The golgin GMAP-210 was discovered by screens with antisera from patients with the Sjoegren's autoimmune disorder (Rios *et al.*, 1994). GMAP-210 localises to the cis-Golgi apparatus and has extensive coiled-coil structural elements. Treatment of cells with the fungal compound Brefeldin A displaces GMAP-210 to Golgi mini-stacks near the ER-exit sites (Fig.41, p.72). Consequently, GMAP-210 qualifies as a golgin (Barr and Short, 2003; Gillingham and Munro, 2003). Publications on GMAP-210 are, however, contradictory in regards to its Golgi localising domain. Infante *et al.* (1999) describe the N-terminus as Golgi binding portion, others claim the C-terminus to target to Golgi membranes (Chen *et al.*, 1999; Gillingham *et al.*, 2004).

Studies on Rud3p, the *S.cerevisiae* homologue of human GMAP-210, revealed a putative binding domain in the C-terminus (Gillingham *et al.*, 2004) of all Rud3p homologues, which was termed GRAB domain. This domain is reminiscent of the GRIP domain, which mediates recruitment of certain golgins to the trans-Golgi by binding to Arl1 (Panic *et al.*, 2003b; Wu *et al.*, 2004). The GRAB domain from *S.cerevisiae* Rud3p interacts with the small GTPase Arf1p and disruption of the GRAB domain, by mutation of the essential residues aspartate 407 and leucine 410, prevents interaction with Arf1p and abolishes Golgi binding of Rud3p.

To identify the GMAP-210 Golgi targeting motif (Fig.67, p.106), overexpression experiments were performed with fragments of GMAP-210. N-terminal fragments and fragments from the GMAP-210 middle-part display only weak Golgi binding, if any (Fig.11, p.34). C-terminal fragments transfected into HeLa L cells show Golgi localisation (Fig.8, p.29), whereas targeting depends on the GRAB domain (amino acids 1757-1875). Constructs which only contain the GRAB and GA1 domain, however, (aa 1757-1979, aa 1778-1979)

target less clearly (Fig.6, p.23), also showing a diffuse cytosolic localisation. Mutation of the essential aspartate and leucine residues (D1780 and L1783) inhibits Golgi binding significantly (Fig.9, p.30). The minimal GRAB domain without a coiled-coil element (aa 1757-1875) shows a diffuse cytosolic signal apart from Golgi targeting. Adding a coiled-coil element (GMAP-210 1683-1875) improves targeting. In analogy to GRIP domain (Fig.4, p.15), the coiled-coil structure seems to enable the GRAB domain to dimerise, which is necessary for binding the Golgi localised recruitment factor.

This proves without any doubt, that the C-terminal GRAB domain of GMAP-210 is the domain, which targets the protein to the Golgi apparatus. Weak Golgi targeting of N-terminal constructs (Fig.11, p.34) could partially explain results from Infante *et al.* (1999), but how they missed Golgi targeting of their C-terminal fragments is not easily explained. In HeLa L, GMAP-210 fragments containing the amino acids 855 to 1332 are found at Golgi membranes after depletion of endogenous GMAP-210 (Fig.27, p.53). The same fragment of GMAP-210 (Fig.67) binds to Rab1 in *in vitro* pulldown assays and in yeast 2-hybrid studies (2.4.2, p.56*ff*).

GMAP-210 is targeted by its C-terminal GRAB domain to the cis-Golgi (Fig.67). A second targeting signal, which interacts with the small GTPase Rab1 can be found in the middle part of GMAP-210, although Golgi targeting is conditional as this fragment binds only weakly to Golgi in HeLa L cells and is recruited to the Golgi only when endogenous GMAP-210 is depleted.

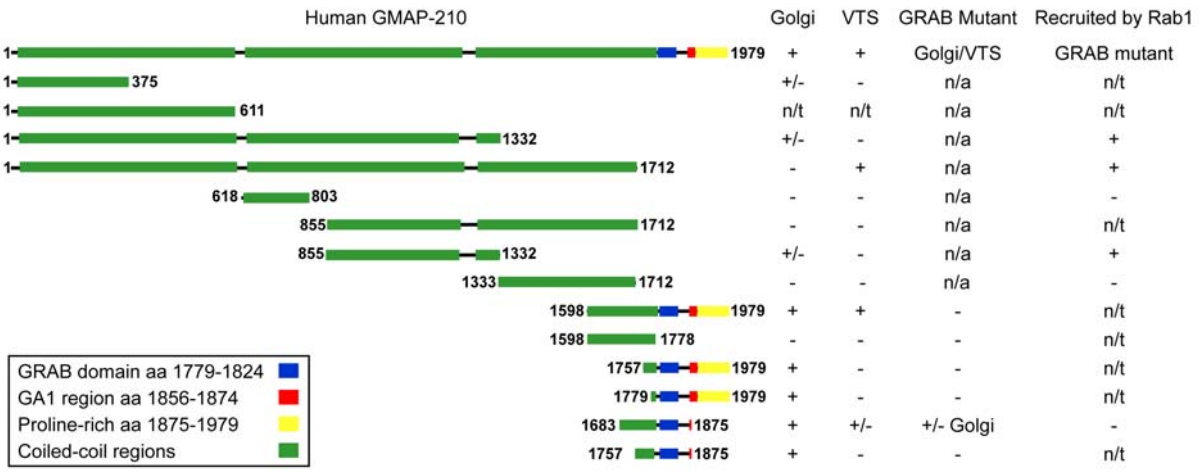

Figure 67: **GMAP-210 Fragments And Their Localisation In HeLa L.** Overview of the complete array of tested constructs and their localisation to different compartments and interaction with Rab1 (after GMAP-210 depletion). VTS= vesicular tubular structures; "+" = does localise, "-" = does not localise; GRAB mutant = localisation of the construct with mutated GRAB domain; n/a = not applicable; n/t = not tested; data compiled from Fig.8, 9, 10, 11 and section 2.3.4.

3.1.2 GMAP-210 Localises To Vesicular Tubular Structures

Staining of endogenous GMAP-210 and transfection of various constructs shows signals for GMAP-210 on vesicular tubular structures in the cell periphery (2.1.2, p.29*ff*). Especially D1780A L1783A mutations of GMAP-210 or fragments without the GRAB domain target to vesicular tubular structures, which are more pronounced than those seen with staining of endogenous GMAP-210 (Fig.9, p.30). Constructs expressing the C-terminus (GMAP-210 1598-1979) or the GRAB domain and some adjacent coiled-coil structure (GMAP-210 1683-1875) can also be found on vesicular structures (Fig.67).
Most Golgi markers tested, like GM130 and p115, do not overlap with GMAP-210 on these structures (Fig.7, p.28 and Fig.29, p.57). Two markers from the ER-to-Golgi secretory pathway partially co-localise with GMAP-210 on the vesicular tubular structures (Fig.35, p.64 and Fig.36, p.65): the coat protein complex COPII (1.2.2, p.8) and the cargo receptor ERGIC53 (1.2.2, p.9). Nevertheless, there are discrete structures, stained for GMAP-210 but not for COPII or ERGIC53.

3.1.3 Conclusion

GMAP-210 is a Golgi localising protein, which is targeted to the Golgi by the GRAB domain in its C-terminus. Two residues in the GRAB domain, D1780 and L1783, are necessary for this interaction (Fig.10, p.32). Dimerisation of GMAP-210, comparable to the GRIP domain, is also necessary for GRAB domain targeting. Without dimerisation, the GRAB domain has only a weak affinity for the Golgi apparatus. The N-terminus shows only weak Golgi targeting capability, which is probably due to dimerisation with coiled-coil domains of endogenous protein and not due to a specific targeting motif. The middle-part of GMAP-210 binds to Golgi localised Rab1.
GMAP-210 is also found at vesicular tubular structures, which are distributed throughout the cell. GMAP-210 targets to these tubules independently of the GRAB domain, and the structures get more pronounced if GMAP-210, without a GRAB domain or with a mutant GRAB domain, is transfected. Some of the GMAP-210 positive structures are also positive for ERGIC53 or the coat protein COPII. This is consistent with data from *D.melanogaster* (Friggi-Grelin *et al.*, 2006), where dGMAP co-localises with Sec23 at ER exit sites in electron microscopy studies. This and the interaction of Rud3p with Arf1p (and the putative interaction of GMAP-210 and Arf1) imply GMAP-210's involvement in the early secretory pathway.

3.2 GMAP-210 Depletion Does Not Block Intracellular Transport

GMAP-210 localises at the cis-Golgi (Rios *et al.*, 1994) and on vesicular tubular structures, which are partially labelled for markers of the ER-to-Golgi pathway. It was described, that overexpression of GMAP-210 blocks the anterograde transport of C-terminally truncated, secreted alkaline phosphatase (Pernet-Gallay *et al.*, 2002), and also transport of influenza virus hemagluttinin A between the ER and cis-Golgi. Furthermore, retrograde transport of the shiga toxin subunit B, containing a KDEL signal for effective export from the Golgi apparatus, is also inhibited and shiga toxin is trapped in GMAP-210 positive Golgi fragments.

Here, VSV-G anterograde trafficking was tested (Fig.38, p.68) in GMAP-210 depleted cells. Transport rates do not change after GMAP-210 siRNA, as measured by comparing the signal of VSV-G transported to the plasma membrane against total signal of VSV-G in the cell (Fig.39, p.69). To test retrograde transport, the uptake efficiency of shiga toxin B subunit and its transport to the ER was monitored in GMAP-210 depleted cells (Fig.40, p.70). The uptake of shiga toxin B subunit and its transfer to the Golgi is not impaired. Retention in the Golgi apparatus is hard to evaluate, as the signal intensity in the collapsed Golgi is stronger than in control cells with normal Golgi ribbons. This is consistent with results from Kim (2003), which show that depletion of the *S.cerevisiae* homologue of GMAP-210, Rud3p, does not block intracellular trafficking. Its deletion from *S.cerevisiae* causes glycosylation defects, implying that Rud3p is necessary for Golgi function.

3.3 GMAP-210 And The Microtubule Network

3.3.1 GMAP-210 Does Not Bind Directly To Microtubules

GMAP-210 is also described as microtubule associated protein (Infante *et al.*, 1999), which binds to microtubule minus-ends, probably even nucleating them at the cis-Golgi by its capability to recruit γ-tubulin containing complexes (Rios *et al.*, 2004). Extensive studies in this work, however, do not reveal any direct association of GMAP-210 with the microtubule network.

In vitro binding assays do not uncover interactions of the GMAP-210 N- or C-terminus, purified from Sf9 cells, with microtubules (Fig.49, p.82) and neither are these protein fragments able to bundle taxol stabilised microtubules (Fig.48, p.81). GMAP-210 full-length and fragments overexpressed in HeLa L cells do not disturb the microtubule network sig-

nificantly (Fig.45, p.78). Disturbances of centrosomal microtubules, as shown by Infante *et al.* (1999), cannot be seen. Cos-7 cells were used in this previous study instead of HeLa L cells, and since these show a more defined microtubule network, subtle changes in microtubule organisation might be more readily visible. Also knockdown of GMAP-210 with siRNA does not change the microtubule network in HeLa L cells (Fig.46, p.79).

3.3.2 Nocodazole Induced Disassembly Of The Golgi Is Only Slightly Altered By GMAP-210 Depletion

Depolymerisation of the microtubule network by the drug nocodazole causes reversible Golgi fragmentation and dispersal of Golgi mini-stacks. These are still able to fulfil intracellular transport as normal (Thyberg and Moskalewski, 1999). Washout of the drug allows the Golgi apparatus to reform in the perinuclear region. These effects are linked to the microtubule network and a disturbance of the link between Golgi and microtubules should change the progress of dis- and reassembly. GMAP-210 depletion in HeLa L cells causes the Golgi apparatus to collapse, becoming more compact and lose its ribbon-like structure. Treatment with nocodazole for 90 min fragments the Golgi and disperses it in control cells. In GMAP-210 depleted cells, the Golgi dispersal is slower and after 90 min there is still a cluster of Golgi fragments in the perinuclear region, which greatly resembles the compacted Golgi apparatus before treatment (Fig.50, p.83). In *hTERT*-RPE1 cells no compacted Golgi is observed and treatment with Nocodazole fragments the Golgi apparatus at equal rates in control and GMAP-210 depleted cells (Fig.51, p.85). Reassembly is also not changed by GMAP-210 depletion. This hints at the fact, that GMAP-210 function is possibly different in the two cell types. *hTERT*-RPE1 cells might also be less sensitive to depletion of GMAP-210.

3.3.3 GMAP-210 Is Not A γ-Tubulin Binding Protein

Rios *et al.* (2004) show, that GMAP-210 can recruit γ-tubulin to the Golgi apparatus upon overexpression. Furthermore, GMAP-210 localises to the centrosome itself, when its Golgi localising domain is removed. This displaces the pericentriolar marker CTR453 from the centrosome, which is attributed to interaction of γ-tubulin with GMAP-210. A model is presented, where GMAP-210 recruits γ-tubulin and short, stable microtubules to the Golgi apparatus and nucleates microtubules on that organelle.
As no γ-tubulin has been found at the Golgi apparatus before (Murphy *et al.*, 1998; Khodjakov and Rieder, 1999), constructs of GMAP-210 were transfected into HeLa L cells and γ-tubulin distribution was examined. γ-Tubulin is not recruited to the Golgi

apparatus, but antibodies against γ-tubulin stain two dots in the perinuclear region. No construct of GMAP-210 localises at the two centrosomal dots stained with γ-tubulin. However, overexpression of the N-terminus of the ninein-like protein readily accumulates γ-tubulin (Casenghi *et al.*, 2003), but no GMAP-210 or Golgi membranes (Fig.45, 53, p.78 and 87).

3.3.4 Conclusion

This shows, that GMAP-210 is unlikely to be involved in microtubule nucleation at the Golgi apparatus. First, no *in vitro* interaction of GMAP-210 with microtubules can be detected. Secondly, the microtubule network of HeLa L cells is not disturbed by GMAP-210 overexpression or depletion. Third, no link to γ-tubulin, which is necessary for microtubule nucleation, can be established and endogenous GMAP-210 does not co-localise with γ-tubulin under any circumstances. It is possible, that GMAP-210 attaches the Golgi apparatus to the microtubule network by mediating the interaction between a motor protein and Golgi membranes. This would explain the morphological changes visible after depletion and overexpression of GMAP-210 in HeLa L cells. The impaired dispersal of Golgi fragments after GMAP-210 depletion could also hint at a function of GMAP-210 in mediating Golgi microtubule interaction. However, GMAP-210 does not have the properties expected of a Golgi MAP.

3.4 GMAP-210 Shows Interaction With Several Golgi Localised Proteins

Not much is known about GMAP-210 interactors. The *S.cerevisiae* homologue of GMAP-210, Rud3p, is shown to bind to the Golgi apparatus via its interaction with the small GTPase Arf1p (Gillingham *et al.*, 2004).

3.4.1 Binding Of The GRAB Domain To Arf1 Is Regulated

The whole family of small ADP-ribosylation factor and ribosylation factor-like proteins was tested for interaction in yeast 2-hybrid experiments (Fig.13, p.37). Full-length GMAP-210 interacts with the small GTPases Arl4A, B and C and Arl16. Arl16 does not interact with the GMAP-210 GRAB domain, but Arl4A, B and C do and the interaction is abolished by the mutation of the two essential residues aspartate and leucine in the GRAB domain (Fig.14, p.38). However, further studies reveal, that the Arl4 family does not localise to the Golgi apparatus, but is found on the plasma membrane (Fig.16, p.40)

(Hofmann *et al.*, 2007). Arl4 recruits the guanine nucleotide exchange factor cytohesin and thus activates Arf6. Pulldown experiments with recombinant Arl4 (Fig.18, p.43) and immunoprecipitation (Fig.19, p.44) show no binding of GMAP-210 and Arl4. Surprisingly, the active mutant of Arf1 interacts in yeast 2-hybrid with a fragment, which contains only the GMAP-210 GRAB domain and mutation of the GRAB domain abolishes this. Arf1 does, however, not interact with full length GMAP-210 (Fig.12, p.35). Yeast 2-hybrid mapping of GMAP-210 shows, that Arf1 interaction is inhibited by a part N-terminally from the GRAB domain (Fig.22, p.47). This hints at regulation of Arf1 binding to the GMAP-210 GRAB domain in full-length GMAP-210. The GRAB domain is activated for Arf1 binding upon interaction with a yet unidentified factor.

3.4.2 GMAP-210 Interacts With The Small GTPase Rab1

Rab GTPases are involved in all transport steps and give identity to membrane compartments (Pfeffer, 2001; Zerial and McBride, 2001; Short *et al.*, 2005). They are essential components of intracellular trafficking. GMAP-210 was screened against a yeast 2-hybrid library of the complete Rab GTPase family (Fig.30, p.58). Several Rab GTPases show interaction with GMAP-210, including Rab1 and Rab2. Rab1 co-localises with GMAP-210 on the cis-Golgi of HeLa L cells (Fig.31, p.59), Rab2 is clearly localised on a different compartment, the medial Golgi (Short *et al.*, 2001). Pulldown experiments with all positive Rab GTPases found in the yeast 2-hybrid screen (Fig.33, 34, p.61, 62) confirm, that Rab1 interacts with GMAP-210 in a nucleotide dependent manner. Yeast 2-Hybrid experiments were further used to map down the interaction domain for Rab1 on GMAP-210 (Fig.32, p.59). Amino acids 855 to 1332 can bind Rab1. Interaction with Rab2 is stronger, but due to the localisation of Rab2 and its inability to pull down GMAP-210, this is likely of no importance. Even more interesting is the fact, that GRAB mutant GMAP-210 is recruited to the Golgi of HeLa L cells, when endogenous GMAP-210 is depleted by siRNA. This targeting capability also maps to the same fragment as Rab1 binding (Fig.27, p.53). It is thus possible, that GMAP-210 binds to Rab1, but only in combination with GRAB domain targeting (Fig.68). Without the GRAB domain binding signal, the Rab1 interaction domain is too weak or structurally blocked for bringing GMAP-210 to the membrane. Alternatively, it is competed by endogenous GMAP-210. Depletion of endogenous GMAP-210 frees Rab1 for binding mutant GMAP-210. However, this effect is not visible in *hTERT*-RPE1 cells.

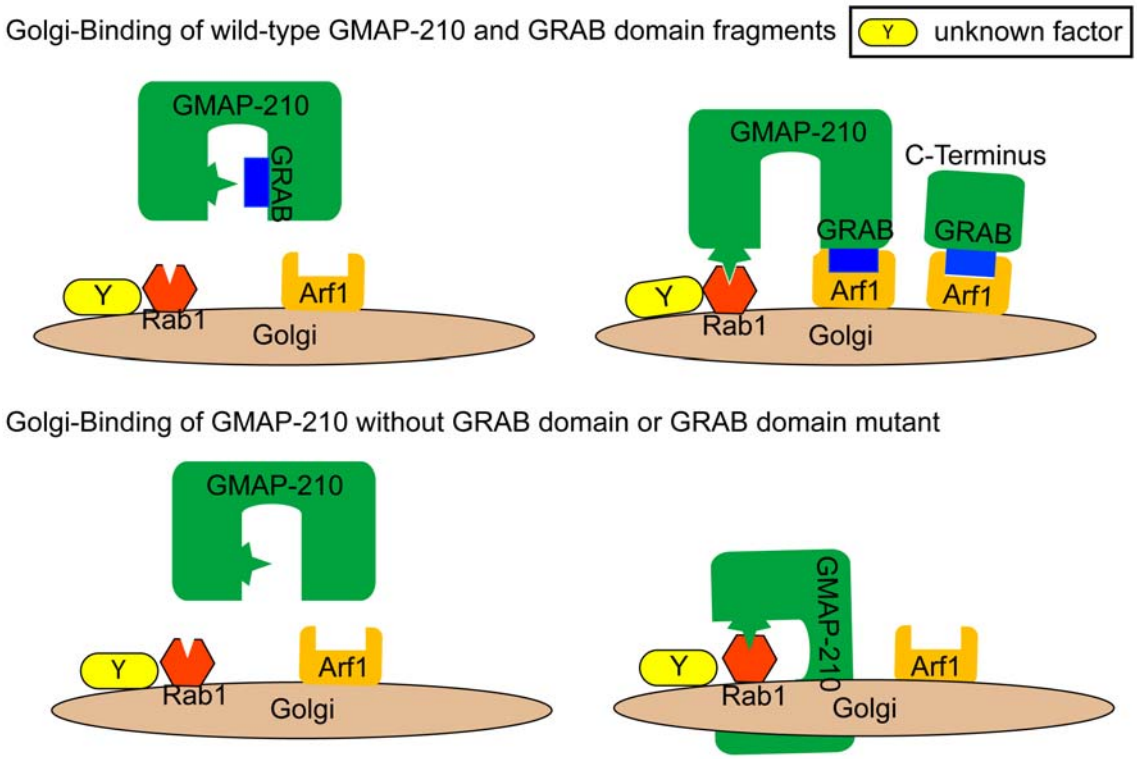

Figure 68: **Model Of Competition Between Endogenous And GRAB Domain Mutant GMAP-210 For Rab1 Binding On The Golgi Apparatus.** Endogenous GMAP-210 binds the GRAB domain binding factor "X" (allegedly Arf1), which causes a conformational change in GMAP-210 and enables Rab1 binding. Exogenously expressed GMAP-210 is sterically hindered to bind Rab1, but can do so, if no endogenous GMAP-210 is present to compete for Rab1 on the Golgi apparatus. A factor "Y" might label a GMAP-210 specific pool of Rab1; not drawn to scale.

3.4.3 Conclusion

GMAP-210 is a large coiled-coil domain protein targeted to the Golgi apparatus by its C-terminal GRAB domain (Fig.69). Studies in *S.cerevisiae* show, that the GRAB domain of Rud3p binds to Arf1p on the Golgi apparatus. In this work, no interactor from the Arf- and Arl-family could be identified for GMAP-210 with certainty. Candidates from a yeast 2-hybrid screening with all Arf family members are not Golgi proteins but are found at the plasma membrane or do not interact with the GRAB domain. Pulldown experiments do also not confirm interaction. Arf1, however, interacts with the GMAP-210 GRAB domain, when the minimal domain is tested in yeast 2-hybrid. This raises the possibility, that binding of Arf1 to GMAP-210 is regulated by different factors, which induce a structural change in GMAP-210 and thus expose the GRAB domain for Arf1 interaction.

A screen with the Rab GTPase family identifies Rab1 as a small GTPase binding GMAP-

210 (Fig.69). In HeLa L cells GRAB mutant GMAP-210 is recruited to the Golgi apparatus, when endogenous GMAP-210 is depleted. It is further shown, that this recruitment is mediated by the same region Rab1 binds to. It is thus possible, that GMAP-210 interacts with a small GTPase by its GRAB domain and with Rab1 by a domain in the middle part in a synergistic way. GRAB mutants cannot compete with endogenous GMAP-210 for Rab1 binding (Fig.68). Only in the absence of endogenous GMAP-210, these GRAB mutants are recruited to the Golgi. For interaction of GMAP-210 and Arf1 a regulation of the binding domain could likewise be proposed. GMAP-210 can only interact with Arf1 when an additional factor causes a conformational change and exposes the GRAB domain for binding. This could explain, why Arf1 cannot interact with full-length GMAP-210 *in vitro*, but shows up in a yeast 2-hybrid experiment, which uses the minimal GRAB domain. Further testing will be necessary.

3.5 IFT20: An Unexpected GMAP-210 Interactor

3.5.1 GMAP-210 Interacts With IFT20 But Is Not Involved in Primary Cilium Formation

The most surprising interaction partner of GMAP-210 discovered in this work is IFT20. IFT20 is described as Golgi localising protein of the intraflagellar transport machinery (Follit *et al.*, 2006). Depletion of GMAP-210 and staining for IFT20 shows a loss of the protein from the Golgi apparatus (Fig.57, p.95). This effect is clearly visible in *hTERT*-RPE1 cells, but also in HeLa L cells, which have only very little IFT20. The overall amount of IFT20 in the cell, after it is lost from the Golgi apparatus, is not changed (Fig.58, p.95) and IFT20 depletion by siRNA has no effect on Golgi morphology or localisation of GMAP-210 (Fig.56 p.93). However, loss of IFT20 significantly reduces the ability of the cell to form a primary cilium. When IFT20 is depleted from the cell, 60% less primary cilia are observed in *hTERT*-RPE1 cells in comparison to control cells. De-

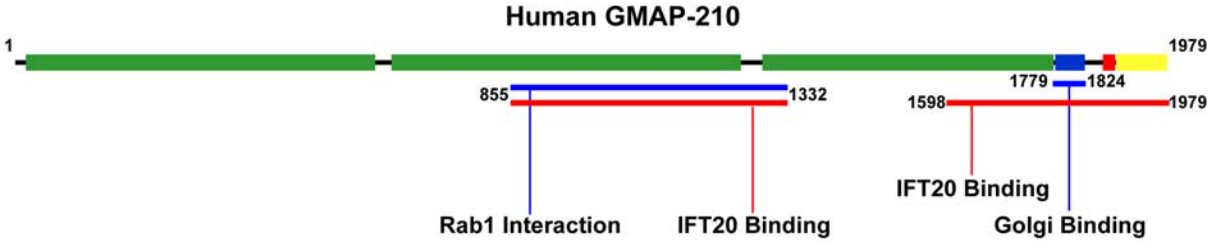

Figure 69: **Binding Domains Of GMAP-210 Interaction Partners.** Identified domains in GMAP-210 and their recruited binding partners; green: coiled-coil; blue: GRAB domain; red: GA1 domain; yellow: proline rich sequence.

pletion of GMAP-210 and the subsequent loss of IFT20 from the Golgi apparatus does not significantly alter the capability of *hTERT*-RPE1 cells to grow a primary cilium, indicating, that the Golgi localisation of IFT20 is not necessary for primary cilium formation. IFT20 interacts directly with GMAP-210 in yeast 2-hybrid (Fig.62, p.99), but not with other golgins. Endogenous IFT20 is also co-immunoprecipitated with GMAP-210 antibodies from *hTERT*-RPE1 extract and vice versa (Fig.64, p.101). Mapping of the interaction domain of GMAP-210 by yeast 2-hybrid (Fig.63, p.100) identifies two regions of GMAP-210, which bind to IFT20: the middle part, amino acids 855 to 1332, and the C-terminus, amino acids 1598 to 1979 (Fig.69). Rather than binding to two separate regions in GMAP-210, it can be expected, that the tertiary structure of GMAP-210 brings these two regions closely together for binding of IFT20.
IFT20 interacts with the kinesin Kif3B subunit of the heterotrimeric kinesin. This kinesin is responsible for microtubule plus-end directed motility within the primary cilium. Although it is described to localise to the Golgi apparatus, protein can only be found at the primary cilium when overexpressed in *hTERT*-RPE1 cells (Fig.65, p.102). Depletion of Kif3B by an siRNA gene pool does neither alter IFT20 nor GMAP-210 localisation at the Golgi (Fig.66, p.103). Cilia form normally, although Kif3B function in intraflagellar transport would indicate otherwise (Kozminski *et al.*, 1995).

3.5.2 Conclusion

The IFT complex particle IFT20 is essential for formation of flagella and cilia and is required for cargo transport within the cilium (Baker *et al.*, 2003). Its localisation at the Golgi apparatus is unexplained. Follit *et al.* (2006) observed a stream of IFT20 particles from the Golgi apparatus to the cilium and moderate knockdown of IFT20 significantly reduces the levels of the transmembrane protein polycystin-2 in the primary cilium. GMAP-210 depletion removes the Golgi localised pool of IFT20 from the organelle, but does not prevent primary cilium formation in *hTERT*-RPE1 cells. This raises the question of IFT20 function at the Golgi apparatus and the involvement of GMAP-210 in the intraflagellar transport. From the collected data we propose the following model about IFT20 and GMAP-210 function in transport of cargo to the cilium. The cargo transported to the cilium by this means is not needed for assembly of the cilium itself, but for the function of this structure, for example components of cellular signalling localised to the primary cilium (Scholey and Anderson, 2006).
The IFT-cargo is exported from the ER exit sites in GMAP-210 positive COPII vesicles (Fig.70), which travel to cis-Golgi. IFT20 particles are recruited and the IFT-cargo is “handed over” by GMAP-210, which dissociates from the complex. The IFT-cargo

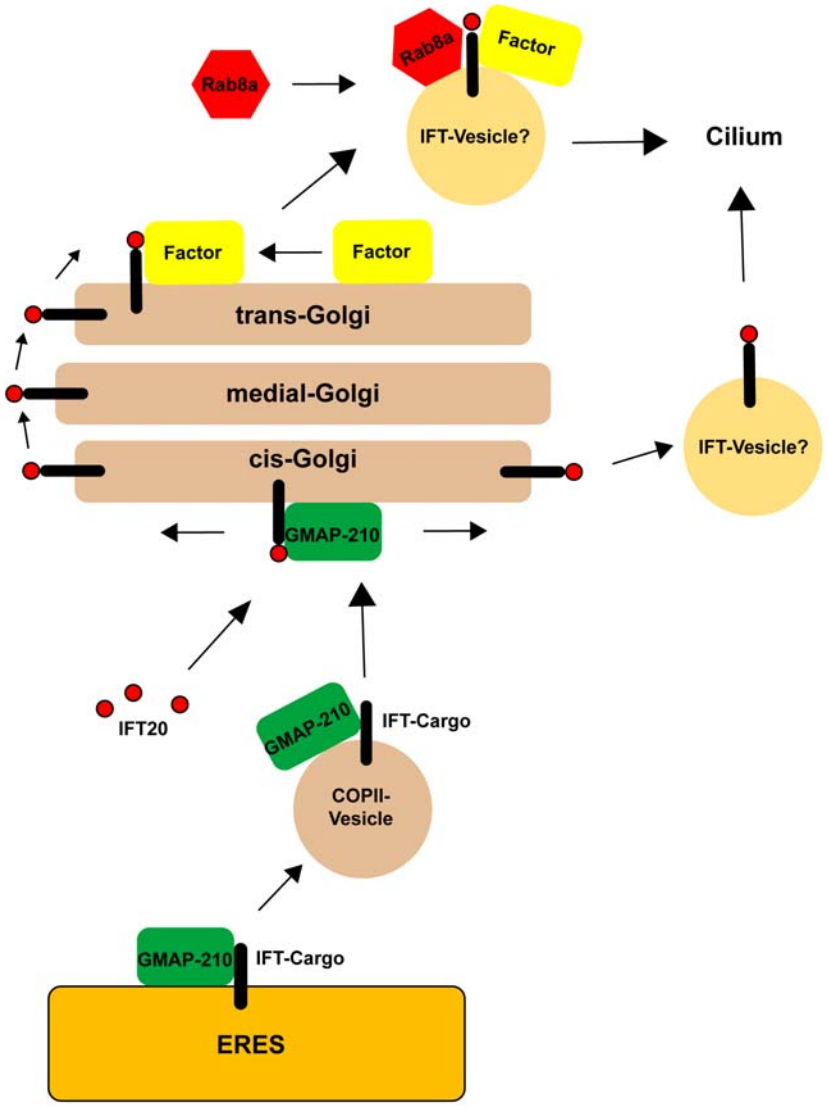

Figure 70: **Model For Functions Of Golgi Localised IFT20 And Its Interaction With GMAP-210.** Cargo destined to the cilium leaves the ER exit sites (ERES) in specialised COPII vesicles, on cis-Golgi GMAP-210 recruits IFT20 and performs a "hand-over" of the IFT-cargo to IFT20; the IFT-cargo-IFT20 complex travels through the Golgi stack and is packed into vesicles destined to the cilium, maybe assisted by Rab8a; alternatively, the IFT-cargo-IFT20 complex leaves the cis-Golgi in special IFT-vesicles after dissociation from GMAP-210 and travels directly to the cilium.

proceeds through the Golgi stack and is transported to the cilium by vesicles, maybe with assistance of Rab8a (Nachury *et al.*, 2007; Yoshimura *et al.*, 2007) and other factors. As IFT20 is only proven to localise to the cis-Golgi by its interaction with GMAP-210 (Rios *et al.*, 1994; Friggi-Grelin *et al.*, 2006), another possible pathway can be proposed. The IFT-cargo-IFT20 complex would leave the Golgi by vesicles budding directly from the cis-Golgi. This would be necessary if the transported cargo does not need medial- and trans-Golgi processing. In this scenario, IFT20 and GMAP-210 could even function as

cargo receptor and coat protein as it has been hypothesised, that IFT evolved from the clathrin- and COPI-coat systems (Jekely and Arendt, 2006). To verify either of the two hypotheses, the exact cisternal localisation of IFT20 on the Golgi needs to be determined. Furthermore, identification of a specific cargo of this transport pathway and examination of its glycosylation pattern would help much to pin down the exact function of GMAP-210 and IFT20 in the intraflagellar transport.
It is however obvious, that there is more to GMAP-210 than its role in intraflagellar transport. HeLa L cells express only little IFT20 in comparison to *hTERT*-RPE1 cells and HeLa L cells are also not able to grow a primary cilium, which is consistent with their lack of IFT20. Nevertheless, they express a significant amount of GMAP-210 and its depletion changes Golgi morphology. Furthermore, organisms without cilia, like *S.cerevisiae* and plants, have homologues to GMAP-210, but supposedly none to IFT20.

3.6 GMAP-210 And Golgi Morphology

3.6.1 Golgi Grows Tubules Upon GMAP-210 Overexpression

Overexpression of a wide array of N- and C-terminal constructs of GMAP-210 has no effect on Golgi morphology (Fig.8, 9, 11, p.29*ff*). After overexpression of full-length GMAP-210 in HeLa L, however, tubules grow from the Golgi (Fig.8, p.29). These structures are part of the Golgi membrane, as they also stain for GM130.

3.6.2 GMAP-210 Depletion Shrinks Golgi In HeLa L

The phenotype of GMAP-210 overexpression is consistent with the effect of GMAP-210 depletion by siRNA (2.3, p.48*ff*). A siRNA oligo was designed, which targets a sequence in the 3'-untranslated region of the human GMAP-210 gene. In HeLa L cells, depletion of GMAP-210 causes the Golgi apparatus to shrink to about half its normal size (Fig.25, p.50) and to lose its ribbon-like structure (Fig.24, p.49). All Golgi markers tested remain at the Golgi apparatus (Fig.29, p.57) and, although the volume of Golgi membranes is decreased, staining of Golgi resident proteins increases in intensity, signifying, that Golgi resident proteins are concentrated on a smaller amount of Golgi membranes (Fig.29, p.57). ERGIC53 and COPII are affected in the same way (Fig.35 and 36, p.64 and 65). The distribution of the vesicles, they localise to, is not altered significantly, although this is not surprising as co-localisation with GMAP-210 is only partial and depletion of GMAP-210 would only affect a subset of COPII- and ERGIC53-positive vesicular structures. Of course it is impossible to follow the fate of vesicular tubular structures after GMAP-210

depletion, until a unique marker for these is identified. Electron microscopical analysis of the Golgi apparatus in HeLa L cells treated with siRNA against GMAP-210 reveals, that the Golgi remains in the perinuclear region, but fragments into swollen compartments, which show neither stacking of cisternae nor a Golgi ribbon (Fig.26, p.52). Strangely enough, in *hTERT*-RPE1 cells the Golgi apparatus is not at all affected by GMAP-210 siRNA (Fig.24 and Fig.25, p.49*f*), although the protein is depleted, as shown by Western blotting (Fig.23, p.49). This could be due to two reasons. Either GMAP-210 depletion in HeLa L cells is more effective than in *hTERT*-RPE1 cells and even undetectable levels of GMAP-210 can keep up Golgi morphology or *hTERT*-RPE1 cells are able to compensate for the loss of GMAP-210 by a different, unknown factor, which is not available to HeLa L cells. Total Golgi fragmentation as observed by Rios *et al.* (2004) was not caused by a more effective depletion of GMAP-210 from HeLa L cells, as their Western blots and immunofluorescence images show incomplete depletion of GMAP-210 from cells. Additionally, they see different populations of cells, some have reduced levels of GMAP-210, others are unaffected by the siRNA. The siRNA oligo against the 3'-UTR of GMAP-210 used in this work gives a complete knockdown in all cells. The Golgi dispersal witnessed by Rios *et al.* (2004) could be due to off-target effects, which often cause Golgi dispersal (*AH, SY, JE, FAB, personal observation*).

3.6.3 Conclusion

GMAP-210 overexpression and depletion has consistently opposite effects in HeLa L cells. Whereas GMAP-210 overexpression causes the Golgi membranes to grow out into fine tendrils, depletion of the protein collapses the Golgi and it concentrates in the perinuclear region. EM studies make it likely that the Golgi is fragmented into swollen vesicles. This could indicate one of two functions for GMAP-210 in Golgi: Either GMAP-210 tethers incoming vesicles (Fig.71A) or it links the Golgi to the cytoskeleton by plus-end directed microtubule motors (Fig.71B). As a tether, GMAP-210 could capture vesicles of the early secretory pathway, being recruited by Rab1 and binding to their membrane with the proposed ALPS (ArfGAP1 lipid packing sensor) domain. The GRAB domain would be protected against Arf1 binding until it is released by a yet unknown factor. The GRAB domain then tethers the vesicle to the Golgi for subsequent membrane fusion by SNARE proteins. Overexpression improves capturing, thus building tubules made from freshly fused vesicles. When GMAP-210 is depleted, capturing is impaired, and Golgi volume decreases. However, to cause such a severe effect, GMAP-210 had to be involved in an important transport pathway and the decrease of Golgi material would also

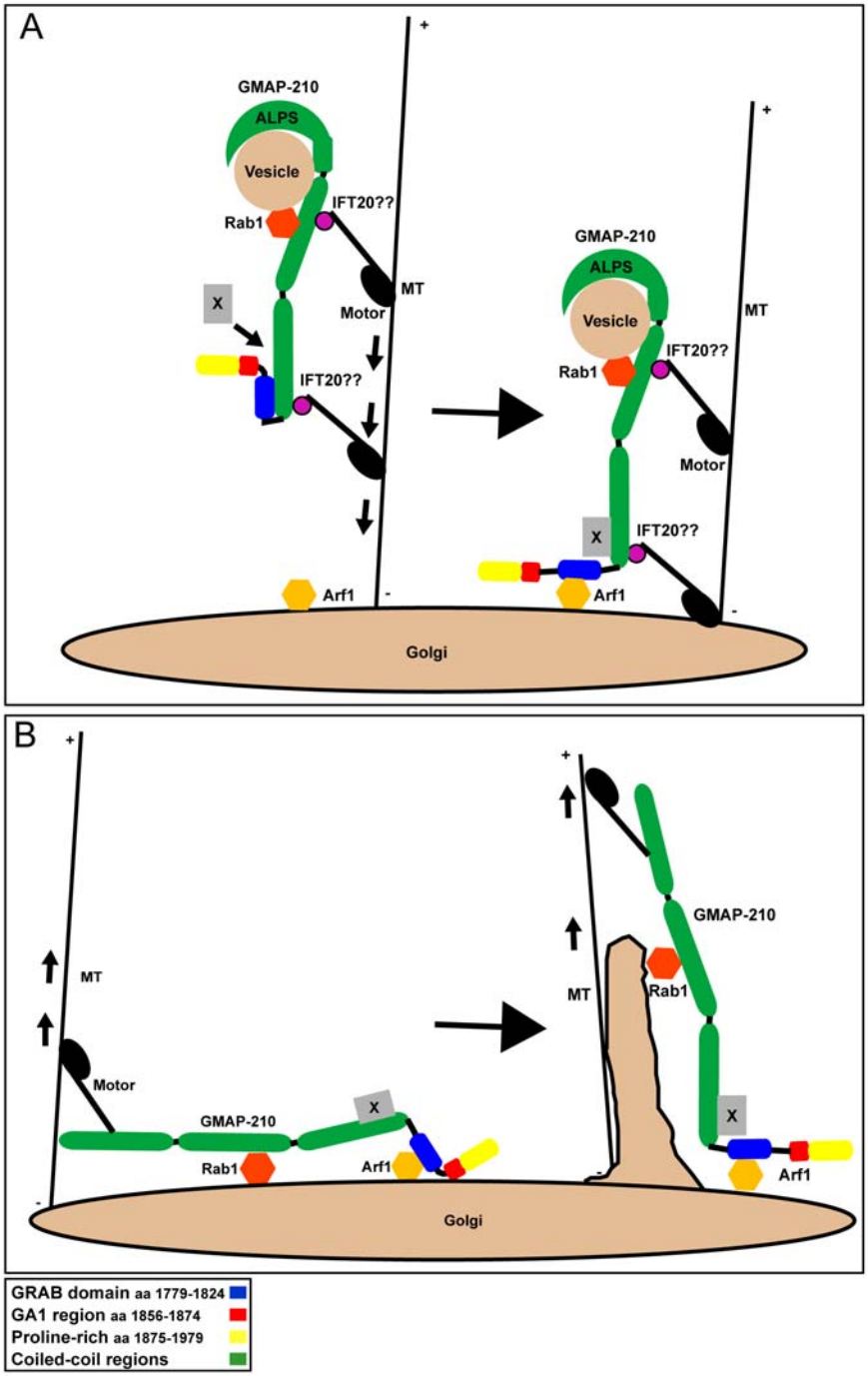

Figure 71: **Models for Molecular Function Of GMAP-210 At The Golgi Apparatus.**
A: GMAP-210 as tethering factor. GMAP-210 binds vesicles with its alleged ALPS domain at the C-terminus after being recruited by Rab1. The GRAB domain is blocked until the factor "X" frees it for binding to Arf1 on the Golgi membrane. IFT20 could link to a microtubule minus-end directed motor protein and cause vesicle movement. Cartoon not drawn to scale. B: GMAP-210 as microtubule linker protein. GMAP-210 binds to Golgi membranes by its Rab1 and Arf1 interaction and links Golgi membranes to the microtubule network by microtubule plus-end directed motor proteins. This causes enlargement of the Golgi apparatus. Position of interaction of the motor with GMAP-210 chosen arbitrarily. Not drawn to scale.

decrease the amount of Golgi resident proteins, as they are transported to the ER and cannot return. This would result in a phenotype reminiscent of Brefeldin A treatment. Additionally, depletion of GMAP-210 has little effect on intracellular transport (Powers and Barlowe, 1998) and does not alter VSV-G transport rates (2.5.1, p.67). Thus, GMAP-210 is most likely not involved in basal protein transport, but rather in a specialised transport pathway as proposed for flagellar cargo transport (3.5, p.113). Another possible function of IFT20, which might even be independent of flagellar cargo transport, could be imagined (Fig.71A). Binding of IFT20 to GMAP-210 could link the protein and the bound vesicle to microtubule minus-end directed motors, thus enabling the complex to travel to the Golgi apparatus. This would, however, make it necessary, that IFT20 is able to bind to two different motor proteins, plus-end directed Kif3B in intraflagellar transport and a microtubule minus-end directed protein for vesicle transport to the Golgi. Due to the small size of IFT20 this is unlikely.

Thus, the second model for GMAP-210 function is more compelling. GMAP-210 might set up a link to the microtubule network (Fig.71B), probably via plus-end directed motor proteins. A likely candidate could be the kinesin Kif5B, as its depletion also causes Golgi collapse (Feiguin *et al.*, 1994), although in astrocytes, which show a different wild-type Golgi morphology. Upon overexpression of GMAP-210 Golgi membranes would be drawn along microtubules, thus forming the Golgi tubules observed (Fig.8, p.29). In this model, Rab1 and Arf1 play the role of anchoring points for GMAP-210 and could regulate Golgi size and position, by regulated release of GMAP-210 from the membranes.

3.7 Outlook

This work settles some important questions about GMAP-210 localisation at the Golgi apparatus. It identifies binding partners and implies it in different functions in Golgi morphology and intracellular trafficking. But all these findings raise further questions about GMAP-210.

How is it involved in intracellular trafficking? Is this role linked to primary cilium formation and function or does its interaction with IFT20 serve a completely different purpose? If not, why is this protein conserved, even in plants, which do not have cilia? What role does it fulfil in formation of cilia and flagella?

GMAP-210 might not to be essential for survival of cells in cell culture, but in multicellular organisms things might look different and the next step in unravelling GMAP-210's elusive purpose should not in the least be to study its function *in vivo* beyond the test tube and cell culture.

4 Materials And Methods

4.1 Materials And Reagents

Buffers and general solutions were prepared by Marianne Siebert from the Department of Cell Biology. Suppliers for commercially available chemicals, reagents and materials were Amersham Pharmacia (Freiburg, Germany), Becton Dickinson (Heidelberg, Germany), Invitrogen (Paisley, UK), Merck (Darmstadt, Germany), Nunc (Wiesbaden, Germany), Qiagen (Hilden, Germany), Roche/Boehringer (Mannheim, Germany), Roth (Karlsruhe, Germany) and Sigma (Taufkirchen, Germany). Oligonucleotides were obtained from Metabion (Martinsried, Germany). DNA sequencing was done by Medigenomix (Martinsried, Germany) or the core facility of the Max-Planck-Institute for Biochemistry in Martinsried. Restriction enzymes and buffers were obtained from New England Biolabs (NEB) (Frankfurt, Germany). Commercial antibodies were purchased from Abcam plc. (Cambridge, UK), Cell Signaling Technology (Frankfurt, Germany), Dianova (Hamburg, Germany), NEB (Frankfurt, Germany), Santa Cruz Biotech (Heidelberg, Germany), Sigma-Aldrich (Taufkirchen, Germany) and Upstate Biotechnologies (Biomol, Hamburg, Germany).
Often used buffers are summarised in Tab.3.

Table 3: General buffer solutions used

Solution	**Composition**
DNA Loading Dye (6x)	0.25%(w/v) bromophenol blue, 40%(w/v) sucrose, in TE
LB	10 g/l Bacto-tryptone, 5 g/l Bacto-yeast extract, 10 g/l NaCl
LB-Agar	LB plus 15 g/l Bacto-agar
Milk-PBS (Blocking Buffer)	4% (w/v) milk powder in PBS plus 0.2%(w/v) Tween-20
PBS	8 g/l NaCl, 0.2 g/l KCL , 1.44 g/l Na_2HPO_4, 0.24 g/l KH_2PO_4, pH 7.4
SDS-PAGE Lower Buffer (4x)	181.72 g/l Tris, 4 g/l Sodiumdodecylsulphate
SDS-PAGE Running Buffer (10x)	30.2 g/l Tris, 188 g/l glycine, 10 g/l Sodiumdodecylsulphate
SDS-PAGE Sample Buffer (3x)	2.3 g Tris/HCl pH 6.9, 9.0 g Sodiumdodecylsulphate, 50 mg bromophenol blue in 100 ml; 10% β-mercaptoethanol

continued next page

Solution	Composition
SDS-PAGE Upper Buffer (4x)	60.6 g/l Tris, 4 g/l Sodiumdodecylsulphate
TAE(50x)	242.4 g/l Tris, 57.2 ml/l glacial acetic acid, 100 ml/l 0.5 M EDTA pH 8.0
TE	10 mM Tris/HCl pH 7.4 , 1 mM EDTA

4.1.1 Vectors And Plasmids

Parental Vectors The vectors used for this study are all based on commercially available vectors which were modified as appropriate. Modifications were done by Francis A. Barr (pFAT2, pMAL-Tev, pAcHis and pFBT9), Herman Silljé (pcDNA3.1-MycA), Xiumin Yan (pcDNA3.1+ cFLAG) and myself (pFBT10). The parental vectors used are listed in Tab.4.

Table 4: Parental Vectors (*Amp = Ampicilin; Kan = Kanamycin*)

Vector Name	Organism	Description(resistance/selection)
pCRIITOPO	*E.coli*	Topoisomerase cloning (*Amp, Kan*)
pFAT2	*E.coli*	N-terminal 6xHis-GST-Tag for bacterial expression (*Amp*)
pQE32Tev	*E.coli*	N-terminal 6xHis-Tag for bacterial expression, Tev-cleavage site in front of MCS (*Amp*)
pMAL-Tev	*E.coli*	N-terminal MBP-Tag for bacterial expression, Tev cleavage site in front of MCS (*Amp*)
pAcHis	*E.coli*, insect cells	N-terminal 6xHis-Tag for expression in insect cells (Sf9) (*Amp*)
pcDNA3.1+	*E.coli*, mammalian cells	Mammalian expression (*Amp*)
pcDNA3.1+ cFLAG	*E.coli*, mammalian cells	C-terminal FLAG-Tag, Mammalian expression (*Amp*)
pEGFPC2	*E.coli*, mammalian cells	N-terminal, enhanced GFP-Tag, Mammalian expression (*Kan*)
pEGFPN3	*E.coli*, mammalian cells	C-terminal, enhanced GFP-Tag, Mammalian expression (*Kan*)
pcDNA3.1+ MycA	*E.coli*, mammalian cells	N-terminal *myc*-Tag, mammalian expression *Amp*

continued on next page

Vector Name	Organism	Description(resistance/selection)
pAct2	*E.coli*, *S.cerevisiae*	Yeast 2-hybrid Gal4 transactivator domain fusion (Leu)
pFBT9	*E.coli*, *S.cerevisiae*	Yeast 2-hybrid Gal4 DNA binding domain fusion on N-terminus of MCS (Trp)
pFBT10	*E.coli*, *S.cerevisiae*	Yeast 2-hybrid Gal4 DNA binding domain fusion on C-Terminus of MCS (Trp)

Plasmids The Plasmids used for these studies were created by the methods described in section 4.4.1 (p.130), using the parental vectors in Tab.4. Vectors named "pJE" were done by myself, vectors named differently were created by the respective person (see Appendix A, p.148*ff*).

4.1.2 siRNA Oligos

The siRNA oligos used to deplete specific mRNAs were synthesised by Dharmacon Inc. Their names and the target sequence are listed in Tab.5. They were designed with a sequence, following: NN(N19)dTdT, with the sense oligo reading (N19)dTdT and the antisense reading (N19 reverse complemented)dTdT (Elbashir *et al.*, 2001).

Table 5: siRNA oligonucleotides

Target Gene	Target Sequence
Human Lamin A	*AACTGGACTTCCAGAAGAACATC*
GL2	*AACGUACGCGGAAUACUUCGAUU*
siGENOME SMARTpool GL2	*sequences not published by supplier*
Human GMAP-210 3'-UTR	*AAGCCAGAGACAATCTAGCAC*
Human IFT20# 1	*NNGGAAGAGTGCAAAGACTTT*
siGENOME SMARTpool Human Kif3B	*sequences not published by supplier*

4.1.3 Antibodies

Primary Antibodies In Tab.6 the primary antibodies used for immunofluorescence, immunoprecipitation and/or Western blotting are listed.

Table 6: Primary Antibodies used; aa = amino acids; Sα = Sheep anti; Rα = Rabbit anti; Mα = Mouse anti;

Name	**Description**	**Organism**	**Dilution**		**Supplier**
			IF	WB	
RαGMAP-210	polyclonal antibody against human 6xHis-GMAP-210 aa 1-375; affinity purified from bleedout animal # 6130; purified with native GST-6xHis-GMAP-210 1-375	Rabbit	1:500	1:500	Biogenes, Berlin
RαIFT20(1.2)	polyclonal antibody against human 6xHis-IFT20; denatured in 8M Urea; affinity purified from bleedout animal # 5918	Rabbit	1:500	1:250	Biogenes, Berlin
RαPrc1	–	Rabbit	–	1:500	R. Neef
FAB35	6xHis-GFP affinity purified	Sheep	1:2000	1:1000	FAB, ICRF
FAB36	human Golgin-97 aa 589-769 affinity purified	Sheep	1:500	1:500	FAB, ICRF
FAB37	6xHis-rat p115 aa 772-959, serum	Sheep	1:500	1:500	FAB, ICRF
FAB40	6xHis-rat GM130 serum or affinity purified	Sheep	1:500	1:500	FAB, ICRF
9E10	c-myc, affinity purified	Mouse	1:1000	1:1000	-
DM1A	α-tubulin, affinity purified	Mouse	1:1000	1:4000	Sigma-Aldrich
MαGolgin-97 clone CDF4	unknown	Mouse	1:1000	–	Dianova
SαTGN46	polyclonal human TGN46, affinity purified	Sheep	1:2000	–	AbD Serotec

continued on next page

Name	Description	Organism	Dilution		Supplier
			IF	WB	
MαLAMP1 CD107a	human LAMP1, affinity purified	Mouse	1:250	–	Becton-Dickinson
MαGM130 clone 35	rat GM130 aa, affinity purified 869-98	Mouse	1:250	1:250	Becton-Dickinson
MαGolgin-84 clone 26	human Golgin-84 aa 510-713 affinity purified	Mouse	–	1:500	Becton-Dickinson
MαGS15 clone 19	rat GS15 aa 1-85, affinity purified	Mouse	1:100	–	Becton-Dickinson
MαGS27 clone 25	human GS27 aa 5-124, affinity purified	Mouse	1:500	–	Becton-Dickinson
MαGS28 clone 1	rat GS28 aa 3-108, affinity purified	Mouse	1:500	–	Becton-Dickinson
Mαp115 clone 15	rat p115 aa 843-955, affinity purified	Mouse	1:50	–	Becton-Dickinson
Mαp230 clone 15	human p230 aa 2063-2179, affinity purified	Mouse	1:250	–	Becton-Dickinson
MαSyntaxin 6 clone 30	rat Syntaxin 6 aa 6-136, affinity purified	Mouse	1:2500	–	Becton-Dickinson
MαVti1a clone 45	mouse Vti1a aa 114-217, affinity purified	Mouse	1:500	–	Becton-Dickinson
MαVti1b clone 7	mouse Vti1b aa 9-121, affinity purified	Mouse	1:500	–	Becton-Dickinson
Mα Histidine	6xHis-Tag clarified ascites fluid	Mouse	–	1:5000	GE Healthcare
MαVSV-G	lumenal domain of the vesicular stomatitis virus G-protein	Mouse	1:20	–	Ira Mellmann
MαEEA1 clone 14	human EEA1 aa 3-281	Mouse	1:50	–	Becton-Dickinson
MαCaveolin clone 56	purified	mouse	1:100	–	Becton-Dickinson
Mα-βCOP clone maD	–	mouse	1:500	–	Sigma

continued on next page

Name	Description	Organism	Dilution		Supplier
			IF	WB	
MαSec31a clone 32	–	mouse	1:250	–	Becton-Dickinson
RαCOPII	sec31	rabbit	1:500	–	ABR/Abcam
MαKDEL-R KR-10	peptide from bovine KDEL sequence	mouse	1:500	–	Stressgen (USA)
MαRab1 1E7	–	mouse	1:5	–	Weide *et al.* (1999)
RαRab2	Peptide of c-terminus	rabbit	1:500	–	Santa Cruz
MαERGIC53	human ERGIC53	mouse	1:1000	–	Alexis Biochemicals
Mα-acetylated Tubulin 6/11B/1	acetylated α-tubulin from the outer arm of sea urchin sperm axonemes	Mouse	1:500	–	Sigma-Aldrich
RαCNAP1	clone 2-6	Rabbit	1:1000	–	E.A. Nigg
Mα-γ-tubulin GTU88	synthetic peptide aa 38-53	Mouse	1:1000	–	Sigma-Aldrich
ShαGolgin-84	–	Sheep	1:500	–	Martin Lowe

Secondary Antibodies The conjugated antibodies listed in Tab.7) were used for immunofluorescence and Western blotting studies.

Table 7: Secondary Antibodies used

Name	Antigen	Organism	Dilution		Supplier
			IF	WB	
Alexa-488 α-mouse	Mouse IgG	Donkey	1:1000	–	Molecular Probes(dye)/ Jackson Laboratories
Alexa-488 α-rabbit	Rabbit IgG	Donkey	1:1000	–	Molecular Probes(dye)/ Jackson Laboratories
Alexa-488 α-sheep	Sheep IgG	Donkey	1:1000	–	Molecular Probes(dye)/ Jackson Laboratories
Cy2-α-sheep	Sheep/Goat IgG	Donkey	1:1000	–	Jackson Laboratories
Cy3-α-mouse	Mouse IgG	Donkey	1:1000	–	Jackson Laboratories
Cy3-α-rabbit	Rabbit IgG	Donkey	1:1000	–	Jackson Laboratories
Cy3-α-sheep	Sheep/Goat IgG	Donkey	1:1000	–	Jackson Laboratories

continued on next page

Name	Description	Antigen	Dilution		Supplier
			IF	WB	
HRP-α-mouse	Mouse IgG	Donkey	–	1:1000	Jackson Laboratories
HRP-α-rabbit	Rabbit IgG	Donkey	–	1:1000	Jackson Laboratories
HRP-α-sheep	Sheep/Goat IgG	Donkey	–	1:1000	Jackson Laboratories
HRP-ProteinA	Mouse/Rabbit IgG	–	–	1:1000	Amersham-Pharmacia

4.2 Bacterial Methods

4.2.1 Growth And Maintenance Of *E.coli* Bacteria

The bacterial strain *Escherichia coli* was grown in LB medium supplemented with the proper amount of antibiotics (100μg/ml Ampicilin, 50μg/ml Kanamycin or 100 μg/ml Ampicilin plus 34 μg/ml Chloramphenicol) depending on the resistance marker of the transformed plasmids. Short-term storage of transformed bacteria was done at 4°C on LB-agar with antibiotics.

4.2.2 Bacteria Strains

The *Escherichia coli* strains used in this work and their genotypes are listed in Tab.8.

4.2.3 Expression And Purification of Recombinant Protein From *E.coli*

Culturing Of *E.coli* *Escherichia coli* strain JM109 or BL21pRIL were grown in LB medium supplemented with antibiotics suitable for selecting the transformed plasmid. For BL21pRIL chloramphenicol had to be added to select for the pRIL plasmid. pMAL-transformed bacteria were cultured in presence of 0.2% Glucose. Bacteria cultures were inoculated with either a 25 ml overnight culture, grown at 37°C in the appropriate medium or with a single colony picked from an LB-agar plate. The cultures were grown under constant shaking at a rate of 180 rpm. The culture was induced at an OD_{600} of 0.5-0.8 with 0.5 mM Isopropyl β-D-thiogalactoside (IPTG) and then grown for 2-4 h at 37°C or 14-18 h at 18°C. The bacteria were harvested at 3000 *g* (Sorval RC5C) at a temperature of 4°C for 20 min. The supernatant was discarded and the pellet either processed immediately or frozen on dry ice and kept at -20°C.

Purification Of Recombinant, His-Tagged Protein Under Native Conditions The cell pellet was resuspended in chilled IMAC5 buffer (all buffers used are listed in

Table 8: E.coli strains and function.

Strain	**Genotype**	**Description**
XL1-blue	F'::Tn proA$^+$B$^+$ lacI^q Δ(lacZ)M15/ recA1 endA1 gyrA96 (NaI^r) thi hsdR17 ($r_K^- m_K^+$) glnV44 relA1 lac	General cloning
GM2163	F$^-$ ara-14 leuB6 fhuA31 lacY1 tsx78 glnV44 galK2 galT22 mcrA dcm-6 hisG4 rfbD1 rpsL136 dam13::Tn9 xy1A5 mtl-1 thi-1 mcrB1 hsdR2	Cloning of non-methylated DNA for digestion with Dam or Dcm-sensitive restriction enzymes
BL21(DE3)[a]	F$^-$ ara-14 leuB6 fhuA31 lacY1 tsx78 glnV44 galK2 galT22 mcrA dcm-6 hisG4 rfbD1 rpsL136 dam13::Tn9 xylA5 mtl-1 thi-1 mcrB1 hsdR2	Recombinant protein expression
JM109 [a]	F' traD36 proA$^+$B$^+$ lacI^q Δ(lacZM15/ Δ(lac-proAB) thi hsdR17	Recombinant protein expression
TOP10	F' mcrA Δ (mrr-hdsRMS-mcrBC) Φ80 lacZΔlacX74 recA1 deoR araD139 Δ(ara-leu)7697 galU galK rpsL (Str^R) amdA1 nupG	TA-cloning of PCR products

[a] sometimes transformed with the pRIL plasmid (Stratagene), which provides tRNAs for rare codons: arginine, isoleucine and leucine, selective marker: chloramphenicol

Tab.9, p.128) supplemented with 0.5 mg/ml Lysozyme (Amersham, Freiburg), 1mM PMSF (Sigma, Taufkirchen) and 1 tablet/10 ml Protease Inhibitor Cocktail (Roche, Mannheim). The suspended bacteria were incubated for 10 min at 37°C to lyse the cells. The lysate was sonicated at 4°C four times 30 s with 30 s rest periods in between with a Bandelin Sonopuls sonicator (Bandelin, Berlin). In order to clear the lysate of cell debris ultracentrifugation was performed in a Beckman Optima LE-80K Ultracentrifuge (Beckman, USA) with a SW28 or SW40 rotor at 27000rpm and 4°C for 35 min. The cleared lysate was incubated with 0.5 ml Ni-NTA Agarose (Qiagen, Hilden) per 1 l of original culture in an empty 50 ml Falcon tube for 2 h at 4°C. The Ni-NTA agarose was pelleted for 5 min at 400 *g* and 4°C and washed four times in batch with IMAC20-TX supplemented with 1 mM ATP and 1 mM $MgCl_2$ (Tab.9). Resident Triton-X100 was removed by washing with IMAC20. The beads were transferred to a column with a volume of 3 ml. The protein was eluted from the beads with IMAC200 while collecting fractions of 0.5 ml-1 ml. Protein yield was analysed by SDS-PAGE and Coomassie blue staining and peak fractions dialysed overnight against 5 l of an appropriate buffer at 4°C. The dialysed protein was

frozen at -80°C.

Table 9: Buffers used for native recombinant protein purification with Ni-NTA-Agarose

Buffer	**Composition**
IMAC5	20 mM Tris/HCl pH 8.0, 300 mM NaCl, 5 mM Imidazole
IMAC20	20 mM Tris/HCl pH 8.0, 300 mM NaCl, 20 mM Imidazole
IMAC20-TX	20 mM Tris/HCl pH 8.0, 300 mM NaCl, 20 mM Imidazole, 0.1% Triton-X100
IMAC200	20 mM Tris/HCl pH 8.0, 300 mM NaCl, 200 mM Imidazole

Purification Of Recombinant, His-Tagged Protein Under Denaturing Conditions Bacteria were grown as described. The pellet was re-suspended in 8 M Urea (in PBS pH 8.0) at room temperature. The suspension was sonicated 3 times for 1 min and then centrifuged at 27000 rpm for 45 min in a SW28 or SW40 rotor (Beckmann, USA) at room temperature. The supernatant was then incubated for 2 h under constant rotation with 1 ml Ni-NTA-agarose beads per 1 l of original bacteria culture. The beads were transferred to a 3 ml column, washed with 40 ml 8 M Urea and then eluted with 8 M Urea and 200 mM Imidazole in PBS. Five 1.5 ml fractions were collected and analysed with SDS-Page and Coomassie staining. Peak fractions were pooled and dialysed overnight at room temperature against PBS with 0.1% Sodium-Dodecylsulphate (SDS).

Purification of Recombinant Protein With GST- Or MBP-Tag The Purification of these proteins was analogous to purification of 6xHis-tagged proteins except for the usage of different buffers and affinity beads. Lysis buffer was PBS supplemented with 0.5 mg/ml lysozyme and protease inhibitor cocktail. After sonication and ultracentrifugation different resins were added to the cleared bacterial lysate. For GST-tagged proteins 0.5 ml glutathione-sepharose (GE Healthcare, Sweden or Amersham, Freiburg) per 1 l of original culture, for MBP-tagged proteins 5 ml amylose resin (NEB, Frankfurt) per 30 ml lysate were used. Binding was allowed for 2 h at 4°C. The resin was washed once in batch with wash solution (PBS + 1 mM ATP + 1 mM $MgCl_2$) and then transferred to a new column. After washing 4 times with wash buffer, GST-tagged proteins were eluted with GST-elution buffer (100 mM Tris/HCl pH 7.4 + 150 mM NaCl + 15 mM reduced glutathione) and collected in 1 ml fractions. MBP-tagged proteins were eluted with 20 mM maltose in PBS and collected in 500 μl fractions. After analysis on Coomassie stained SDS-PAGE, the most concentrated fractions were pooled and dialysed against PBS or 10 mM Tris/HCl pH 7.5 at 4°C. After dialysis overnight, protein was aliquoted, shock frozen on dry ice and stored at -80°C.

4.3 Yeast Methods

4.3.1 Yeast Strain, Growth Medium and Culture

The *Saccharomyces cerevisiae* strain PJ69-4A was used for all experiments in this work (James *et al.*, 1996).

Genotype of PJ69-4A
MATα, trp1-901, leu2-3, 112, ura3-52, his3-200, gal4Δ, gal80Δ, LYS2::GAL1$_{UAS}$-GAL1$_{TATA}$-HIS3, GAL2$_{UAS}$-GAL2$_{TATA}$-ADE2, MEL1 *met*2=GAL7-*lac*Z

Yeast were grown at 30°C on one of two media, depending on experimental purpose. Either YPDA or SC dropout medium, which selects for the appropriate transformed plasmids, was used. YPDA medium includes 10 g/l yeast extract, 20 g/l peptone (both Difco/Becton-Dickinson, Heidelberg) and 20 g/l glucose (20 g/l Bacto-agar was added for solid medium plates). After dissolving the components, the media was sterilised at 121°C for 20 min, cooled down to 55°C and sterile filtered adenine hemisulphate 0.2% (w/v)was added before plates were poured.

Amino acid base(-Leu/-Trp/-His/-Ura) for SC medium was prepared by mixing 20 g of each alanine, arginine, asparagine, aspartic acid, cysteine, glutamine, glutamic acid, glycine, inositol, isoleucine, lysine, methionine, phenylalanine, proline, serine, threonine, tyrosine and valine with 5 g adenine and 2 g p-aminobenzoic acid. For the dropout mix, 36.7 g of amino acid base were supplemented with either 2 g histidine, 4 g leucine, 2 g tryptophane or 2 g uracil, depending on the desired selectivity of the medium. SC medium included 6.7 g/l yeast nitrogen base (Difco), 2 g/l of the appropriate dropout mix and 20 g/l glucose (and 20 g/l Bacto-agar for solid medium plates). The pH was adjusted to 6.5 and buffered with 20 mM Tris/HCl. Autoclaving and pouring of the plates was performed as described above for YPDA medium, whereas Adenine was only added, if not used as selectivity marker.

4.3.2 Transformation Of Yeast By The Frozen Cell Method

Competent yeast cells were prepared by picking several colonies from a freshly grown plate. From these, overnight cultures of liquid YPDA medium were grown at 30°C under shaking. The overnight culture was then diluted to an OD_{600} of 0.15 in fresh YPDA medium and grown to an OD_{600} of 0.6 (i.e. 1.2-1.5x10^7 cells). After harvesting at 3000 rpm for 2 min at room temperature the cells were washed in half a culture volume of sterile dH_2O and spun again. The pellet was resuspended in $1/8^{th}$ of the original culture volume of Lithium-Sorbitol: 100 mM LiOAc, 10 mM Tris/HCl pH 8.0, 1 M Sorbitol (molecular biology grade;

filter sterilized) and incubated for 5 min at room temperature. All resident Lithium-Sorbitol was removed by centrifuging twice as described above. The pellet was again resuspended in Lithium-Sorbitol (600 μl per 100 ml of original culture) and 10 mg/ml salmon sperm DNA (Gibco) were added as carrier DNA. After heat-treatment at 95°C for 5 min, the yeast was aliquoted and stored at -80°C until used.
For transformation, the competent yeast cells were thawed at room temperature and mixed with 0.2 μg plasmid DNA per 10 μl of yeast. Each reaction was overlaid with 150 μl Lithium-Polyethylenglycol (LiPEG: 100 mM LiOAc pH 8.0, 1 mM EDTA pH 8.0, 40% PEG3350, filter sterilised) and mixed by vortexing for 5 s. After 20 min of incubation at room temperature, 17.5 μl Dimethylsulfoxide (DMSO) were added, mixed again by vortexing and incubated for 15 min at 42°C. The reaction mix was centrifuged for 3 min at 400g, the supernatant removed and the cell pellet resuspended in 200 μl sterile dH_2O. 100 μl were then plated onto the appropriate selective media and incubated for 3-4 days at 30°C.

4.3.3 Yeast 2-Hybrid Method

For yeast 2-hybrid experiments, PJ69-4A yeast was transformed with bait and prey plasmids as described above and grown on SC-Leu/-Trp medium plates. Colonies were picked and restreaked on quadruple dropout medium plates (SC-Leu/-Trp/-His/-Ade) and grown for another 2-3 days at 30°C. Growth on selective medium indicated interaction. Its strength could be estimated by colour.

4.4 DNA Methods

Standard work with DNA, especially agarose gel electrophoresis and restriction digest were performed as described (Sambrook *et al.*, 1989). Preparation of DNA from bacteria by the Mini-, Midi or Maxiprep method and extraction of DNA from agarose gels was performed using the kit systems provided by Qiagen(Hilden) according to the manufacturer's instructions.

4.4.1 Cloning Strategies

Whenever applicable, a standard cloning strategy was used. This strategy is called the "Shortway"-system and provides PCR-products, which could be subcloned into a wide variety of vectors (all vectors on Tab.4, p.121 are compatible to this system). For this strategy, a BamHI, BglII or BclI restriction site on the 5'-end and a SalI or XhoI re-

striction site on the 3'-end were generated during amplification of the gene by PCR. The ATC-Sequence of the BamHI/BglII/BclI restriction site was designed to be in frame with the start codon of the insert as shown here:

GGG ATC CCC *ATG* BamHI
GAG ATC TCC *ATG* BglII
GTG ATC ACC *ATG* BclI

The restriction site is underlined and the start codon in italics. The PCR product was TA-TOPO cloned (see 4.4.3, p.132) into the pCRIITOPO-vector (Invitrogen). The insert was then sequenced and subcloned into the respective shortway vectors (Tab.4, p.121). For vectors which add a C-terminal tag to the insert, a clone without a stop codon was amplified. In the rare case that the amplified sequence included one of the mentioned restriction sites either an individual cloning strategy had to be devised or the restriction site was removed by silent mutation (see 4.4.4, p.132).

4.4.2 Polymerase Chain Reaction (PCR)

For Polymerase Chain Reaction either *Pfu* Turbo Polymerase (Stratagene, Amsterdam) or the KOD-Hotstart-Polymerase (Novagene, Darmstadt) were used. The reaction was performed in a volume of 50 μl. The reaction mixture composition is given on Tab.10.

Composition in regard to $MgSO_4$, Polymerase, DMSO and dNTPs concentrations could be varied, depending on the template, its size and its GC-content. Buffers were provided

Table 10: Reaction mix composition for PCR

PCR from cDNA library			
***Pfu* Turbo Polymerase**		**KOD Hotstart Polymerase**	
Volume	**Component**	**Volume**	**Component**
5 μl	marathon-ready cDNA library Clontech, Palo Alto, CA, USA	5 μl	marathon-ready cDNA library Clontech, Palo Alto, CA, USA
2.5 μl	4 μM Forward Primer	3 μl	5 μM Forward Primer
2.5 μl	4 μM Reverse Primer	3 μl	5 μM Reverse Primer
5 μl	10x Pfu-Buffer	5 μl	10x Buffer
		2 μl	25 mM $MgSO_4$
1 μl	10 mM dNTPs(NEB)	5 μl	2 mM dNTPs(Novagene)
1 μl	*Pfu* Turbo Polymerase	1 μl	KOD Hotstart Polymerase

with the enzymes from the respective supplier, primers were synthesised by Metabion (Martinsried).
Usually a second round of PCR was performed, substituting the cDNA with the purified PCR product of the first run as template. Different PCR programs were used for the two different polymerases:

Pfu **Polymerase**		**KOD Polymerase**		
Time	Temperature	Time	Temperature	
30 s	94°C	120 s	94°C	1 cycle
30 s	94°C	15 s	94°C	25 cycles
60 s	55°C[a]	30 s	60°C[a]	25 cycles
2 min/1kb	68°C	30 sec/1kb	72°C	25 cycles
2 min/1kb	68°C	30 sec/1kb	72°C	1 cycle

[a] The annealing temperature could be changed for GC-rich templates

The reaction was performed in a GeneAmp PCR System 2400 thermocycler (Perkin-Elmer, USA). PCR products were either purified with the Qiagen PCR product purification protocol or subjected to agarose gel electrophoresis.

4.4.3 TA-TOPO Cloning

After Polymerase Chain Reaction and agarose gel electrophoresis, the amplified DNA was extracted from the gel with the QiaQuick Gel Extraction Kit (Qiagen, Hilden). The PCR product was inserted into the pCRIITOPO vector by using the TA-TOPO cloning system (Invitrogen, UK). A single adenosine overhang was added to the 3'-ends of the DNA double-strand. To this end the extracted PCR product (50 μl volume) was incubated with 1 μl Taq Polymerase (NEB, Frankfurt) at 72°C for 30 min in the presence of 5 μl buffer as provided by the manufacturer (10x concentration) and 0.25 mM dNTPs. 2 μl of the mix were added to 0.5 μl TA-TOPO cloning mix and incubated for 5 min at room temperature. The complete reaction mix was then transformed into TOP10 bacteria (Tab.8, p.127).

4.4.4 Site-Specific Mutagenesis

Quickchange mutagenesis was used to introduce a 1-3 basepair mutation into a DNA sequence. For this the Quickchange protocol from Stratagene was used in combination with *Pfu*-Turbo-Polymerase or KOD-Hotstart-DNA-Polymerase (Novagene, Darmstadt). 33 basepairs long forward and reverse primers were designed, in which the changed codon

was in the centre, flanked by 15 nucleotides on both sides. For the reaction 30 ng template DNA, 1 pM of each primer, 0.25 μM dNTPs, 5 μl 10x Pfu-Buffer and 1 μl (2.5U) *Pfu* turbo polymerase (both Stratagene) or KOD Polymerase (Novagene, Darmstadt) were mixed in a total volume of 50 μl. The PCR cycling programs were as follows:

Pfu **Polymerase**		**KOD Polymerase**		
Time	Temperature	Time	Temperature	
30 s	94°C	120 s	94°C	1 cycle
30 s	94°C	15 s	94°C	18 cycles
60 s	55°C[a]	30 s	60°C[a]	18 cycles
2 min/1kb	68°C	30 sec/1kb	72°C	18 cycles
2 min/1kb	68°C	30 sec/1kb	72°C	1 cycle

[a] The annealing temperature could be changed for GC-rich templates

After that, 1 μl restriction enzyme DpnI was added and the mix incubated for one hour at 37°C, which totally degraded the methylated template DNA. 5-10 μl of the mix were then transformed into XL1-blue bacteria and plated on the appropriate selective plates.

4.5 Protein Methods

4.5.1 Determination of Protein Concentration

For determining of protein concentration the BioRad Protein Assay Kit (BioRad, Munich) was used. It uses a modified Bradford assay protocol. The dye reagent was diluted 1:5 with water and 1 ml mixed with 10 μl protein solution. After vortexing, the mixture was incubated for 5-10 min at room temperature, transferred to disposable 1 ml cuvettes and absorption at 595 nm measured in an Ultrospec 3000 Pro spectrophotometer (Amersham Pharmacia, Freiburg). Samples of bovine serum albumin (BSA) (Sigma, Taufkirchen) with known concentrations were recorded as standard curve.

4.5.2 Protein Precipitation

For protein precipitation trichloroacetic acid (TCA) was used. Protein solutions were diluted to 500 μl with water, if necessary, then mixed with 50 μl 0.15% sodium-deoxycholate and vortexed thoroughly. After 5 min of incubation at room temperature, 100 μl of 72% TCA were added, the mix vortexed and incubated on ice for 60 min. The precipitated protein was pelleted by centrifugation at 20000 *g* for 5 min. The pellet was washed twice with 1 ml Acetone pre-cooled to -20°C. It was then redissolved in an appropriate amount

of SDS-PAGE sample buffer, wherein a small amount of 1 M Tris/HCl pH 8.5 was added for neutralising resident acid.

4.5.3 SDS-PAGE (Polyacrylamide Gel Electrophoresis)

Small SDS polyacrylamide gels (8x6.5 cm) were prepared. SDS-PAGE sample buffer was added to the samples and boiled for 5 min at 95°C. Gels were run in a BioRad Mini Protean II or III gel chamber (BioRad, Munich) in SDS-PAGE running buffer at 180 V and 50 mA per two gels for 1 h.

4.5.4 Coomassie Staining of SDS-PAGE Gels

Staining of SDS-PAGE gels was done by immersion for 15 min in fresh 0.01% Coomassie Brilliant Blue R-250 in 50% Methanol, 10% acetic acid, while rocking. The gels were destained in 20% iso-propanol and 20% acetic acid. In order to estimate protein masses, an NEB Protein Broad Range Marker (NEB, Frankfurt) was run side-by-side with protein samples.

4.5.5 Western Blotting

Proteins were separated on SDS-PAGE gels and subsequently transferred to 45 μm Hybond-C Extra Nitrocellulose (Amersham, Freiburg) by semi-dry blotting in transfer buffer (SDS-PAGE running buffer with 10% methanol). This was done on a Trans-Blot SD Transfer Cell (BioRad, Munich) at 15 V and 200 mA for 40 min. The membranes were then blocked in milk solution (4% milk powder (w/v) in PBS with 0.1% Tween-20) for 1-2 h at room temperature or alternatively overnight at 4°C. After blocking, the primary antibody was applied for 1-2 h at room temperature or overnight at 4°C. The membranes were subsequently washed 5 times in milk solution for 3-5 min and then treated with the secondary antibody for 1 h at room temperature. Antibodies were diluted in milk solution. Membranes were again washed three times in milk solution and three times in PBS. The bound depletion can interfere with the cells capability to form a cilium.antibodies were detected by chemiluminescence, using ECL Western Blot Detection Reagent (Amersham, Freiburg) or SuperSignal West Femto Maximum Sensitivity Substrate (Pierce Biotechnology, Bonn) for higher sensitivity (at 30-100% concentration), according to the manufacturers' instructions. The membranes were exposed to Kodak X-Omat XAR-5 film (Sigma-Aldrich) until a clear signal could be detected. The films were developed with the Kodak X-OMAT 2000 Processor developer. For estimation of protein masses, an NEB Protein Prestained Marker

or Protein Broad Range Marker were run side-by-side with protein samples.

4.5.6 Antibody Production And Purification

In the course of this work, two antibodies were raised. Immunisation and preparation of test serums were done by Biogenes (Berlin) in two rabbits.
For affinity purification of antibodies, 1 mg of recombinant protein was coupled to 1 ml of Affigel-15 (BioRad, Munich) in an appropriate volume of PBS and incubated for 2 h at 4°C. The resin was then washed three times in 10-15 ml PBS and subsequently in 15 ml 0.2 M glycine pH 2.8, followed by another three washes with PBS. The coupling efficiency was analysed on coomassie stained SDS-PAGE gels.
5-10 ml of antiserum were then incubated with the prepared Affigel-15 for 2 h at 4°C, washed four times in PBS and transferred to a fresh column. The isolated antibody was eluted with 10 times 1 ml 0.2 M glycine pH 2.8 and analysed on 10% coomassie stained SDS-PAGE. Most concentrated fractions were pooled and dialysed overnight at 4°C against PBS. Dialysed antibodies were collected and frozen on dry ice and stored at -80°C.

4.6 Cell Culture Methods And Microscopy

4.6.1 Mammalian Cell Culture

Cell Lines For this work the following cell lines were used:

- HeLa L, cervix adenocarcinoma, adherent
- HeLa S3, cervix adenocarcinoma, grown in suspension
- HS68, human foreskin fibroblast, adherent, propagate for 40 passages
- *hTERT*-RPE1, human retinal pigment epithelial, immortalized with telomerase reverse transcriptase, adherent, Clontech
- Sf9, *Spodoptera frugiperda* (fall armyworm) ovary, adherent, for Baculovirus expression

All cell lines, except *hTERT*-RPE1 were obtained from the American Type Culture Collection (ATCC).

Cell Growth Conditions And Growth Media HeLa and HS68 cell lines were cultured at 37°C and 5% CO_2 atmosphere in Dulbecco's Modified Eagle Medium (DMEM) with 10% foetal calf serum (FCS). 100 U/ml penicillin and 100 μg/ml Streptomycin (all Invitrogen, Gibco, UK) could be added during transfections. *hTERT*-RPE1 cells were grown at the same environmental conditions, but in a 1:1 mixture of Dulbecco's Modified Eagle Medium (DMEM) with HAM's F-12 Nutrient Mix, 10% foetal calf serum (FCS), 2.5 mM L-glutamine and 1.2 g/l sodium bicarbonate. For serum starvation the same medium without foetal calf serum was used and the adherent cells were washed three times with the serum-free medium. For splitting cells, old medium was removed and the cells washed with PBS, then incubated for 15 min at 37°C and 5% CO_2 in PBS and 1 mM EDTA (HeLa L and RPE1) or 0.25% trypsin with 1 mM EDTA (HS68 cells) (Invitrogen, Gibco, UK). Cells not detached after this treatment were suspended by rinsing the culture dish several times by pipetting up and down. The cell suspension was then added to fresh medium in a fresh or rinsed recycled culture dish.
Sf9 cells were cultured in TC100 insect cell medium (Pan, Aidenbach) containing 10% foetal calf serum, 100 U/ml penicillin and 100 μg/ml Streptomycin (Invitrogen, Gibco, UK) at 27°C. Splitting was done by gentle rinsing the culture dish with the resident medium. Detached cells were added to fresh medium on a fresh culture dish.

4.6.2 Transient Transfection Of DNA Into Mammalian Cells

HeLa L and *hTERT*-RPE1 cells were transiently transfected with DNA constructs for expression in mammalian cells (Tab.4, p.121) by a lipid based method. As transfection reagent FUGENE 6 (Roche, Mannheim) or TransIt-Lt1 (Mirus Bio Corporation, USA) were used. The reagents were applied following the manufacturers' protocols. In short a 6-well plate (Corning, Falcon or Nunc) with 50000-100000 cells per well in 2 ml of growth medium were prepared 24 h in advance. For one well on a 6-well plate, 97 μl Optimem (Invitrogen, Gibco, UK) were mixed with 3 μl transfection reagent and incubated at room temperature for 5-10 min. After addition of 0.5 μg to 1 μg plasmid DNA, the mix was incubated for another 20 min and then added drop-wise to the cells. They were then grown for 24-36 h. For larger culture dishes, the protocol was scaled up in relation to the increased amount of culture medium used.

4.6.3 RNA Interference

Specific knockdown of protein expression levels was obtained by transfecting small interfering RNA oligonucleotide duplexes (siRNA) into HeLa L or *hTERT*-RPE1 cells as described

(Elbashir *et al.*, 2001). The siRNA oligo sequence was chosen to lie in the coding region, more than 100bp downstream of the start codon, or the 3'-UTR and followed the sequence $NN(N_{19})dTdT$, so that sense and antisense strand had an overlap of 21 nucleotides and a 2 nucleotide overhang on the 3'-end (Tab.5, p.122). siGENOME SmartPools were designed by the rules devised by the supplier Dharmacon (Perbio, Bonn). Some single oligo duplexes were designed with a software provided on their homepage (www.dharmacon.com). BLAST searches Altschul *et al.* (1997) made sure, that the siRNA oligo sequence was specific for the intended target mRNA.

If not supplied already pre-annealed, oligos were diluted to a concentration of 20 μM (15 μM for GMAP-210 3'-UTR) in a volume of 100 μl with provided buffer and RNAse-free water also provided by the supplier. For annealing, the mix was heated to 90°C for 1 min and then incubated for 60 min at 37°C. The annealed oligos were stored at -80°C.

For transfection of HeLa L or *hTERT*-RPE1 cells, 20000-40000 cells were plated per well of a 6-well plate (Corning, Falcon or Nunc) 24 h prior to transfection. In sterile and RNAse free plastic test tubes, 200 μl Optimem (Invitrogen, Gibco, UK) were mixed with 3 μl Oligofectamine (Invitrogen, UK) and incubated for 10 min at room temperature. In the meantime, 50 μl Optimem were mixed with 3 μl annealed siRNA duplex or siGENOME SmartPool. After combining both volumes and 20 min of incubation at room temperature, 38 μl Optimem were added and everything added drop-wise onto the 2 ml culture medium in the well. After 24 -96 h of culturing the transfected cells were processed further for immunofluorescence (see 4.6.4, p.137) or lysed for Western blotting (see 4.5.5, p.134).

4.6.4 Indirect Immunofluorescence

For immunofluorescence microscopy cells were grown on glass coverslips, sterilised by flaming with ethanol in 6-well plates (Falcon, Nunc or Corning). Cell numbers plated depended on cell line and time until fixation. Cells were fixed in either paraformaldehyde (PFA) or methanol.

Paraformaldehyde Fixation PFA(4%) was prepared by dissolving 4 g PFA in 100 ml PBS at 80°C in a fume hood under continuous stirring. 10 μl 1 M $CaCl_2$ and 10 μl 1 M $MgCl_2$ were added before cooling to room temperature. The pH was adjusted to 7.4 and the clear solution vacuum filtered through a 0.45 μm filter.

The cells on coverslips were either washed three times with PBS or fixed immediately. The coverslips were incubated for 20 min at room temperature in 4% paraformaldehyde and then washed and quenched for 10 min with 50 mM NH_4Cl (prepared freshly in PBS). The coverslips were then washed three times with PBS and permeabilised with 0.1-0.2%

Triton-X100 in PBS for 5 min at room temperature. Triton-X 100 was removed by washing three times with PBS.

Methanol Fixation The coverslips were either washed three times with PBS or fixed immediately with methanol pre-cooled to -20°C. The fixation was performed for 4 min in a -20°C freezer and the cells washed afterwards.

PTEMF Fixation The coverslips were washed three times with PBS and then fixed and permeabilised at the same time with 50 mM PIPES buffer pH 6.8, 0.2% Triton X-100, 1 mM $MgCl_2$, 10 mM EGTA and 4%(w/v) formaldehyde for 15 min at room temperature. Cells were washed again three times with PBS.

Antibody Labelling Of Fixed Cells After washing, the coverslips were removed from the wells, excess liquid removed with 3MM filterpaper and put upside down onto 50 μl drops of antibody solution in PBS on parafilm (American Can Company, USA). The antibody was centrifuged hard (20000 g, 3 min) and the parafilm stuck flat to the working surface with a water-film. The coverslips were incubated with the antibody for 45-90 min in a dark moisture chamber. The coverslips were transferred back to the culture dish and washed three times with PBS. Then incubation with secondary antibody was performed identically to the procedure described above. After another 45-90 min the coverslips were transferred back and washed again for three times with PBS and then mounted on 10 μl Mowiol mounting medium (containing, in most cases, 1 μg/ml DAPI for DNA staining) on glass slides for microscopy and left to dry in a dark place for several hours.
Mowiol was prepared by mixing 2.4 g 4-88 Mowiol to 6 g of analytical grade glycerol under continuous stirring. 6 ml of dH_2O were added and the mixture left for 2 h at room temperature. After addition of 12 ml of 0.2 M Tris/HCl pH 8.5 it was heated to 50°C for 10 min and centrifuged for 15 min at 3000 g.

Immunofluorescence Microscopy Images were collected with an Axioskop-2 with a 63x Plan Apochromat oil immersion objective of NA 1.4, standard filter sets (Carl Zeiss GmbH, Jena), a 1300 by 1030 pixel cooled-CCD camera model CCD-1300-Y (Princeton Instruments, USA) and MetaVue software (Visitron Systems GmbH, Puchheim). Images were cropped in Adobe Photoshop CS2 then sized and placed in figures using Adobe Illustrator CS2 (Adobe Systems Inc., USA).

Delta Vision Microscope Cell samples prepared as described above (see 4.6.4, p.137) were processed with an APPLIED PRECISION DeltaVision RT Life Cell Imaging System with a 60x Olympus PlanApo objective (Aperture 1.4 with immersion oil). Images were processed with the softWoRx software (Applied Precision, USA). Stacks of 20-40 pictures were taken and deconvolved in 10 cycles with standard parameters and merged into a single picture. Cropping and placing of images was done using the Adobe Creative Suite 2 (Adobe Systems Inc., USA).

4.6.5 Electron Microscopy

Fixing of cells, embedding and imaging was done by Dr. Thomas Keil (Department of Molecular Biology, Max-Planck-Institute of Biochemistry, Martinsried). Cells were treated with siRNA as described above (see 4.6.3, p.136). For fixing, the growth medium was exchanged for 37°C-warm PBS and 1 mM EDTA for 15 min at 37°C. The cell suspension was collected and pelleted at 400 *g*. The cell pellet was then washed twice in PBS (first warm then room temperature) and fixed in 2.5% glutaraldehyde in 0.1 M cacodylate buffer containing 5% sucrose, pH 7.1-7.2, at room temperature for 30-40 min. The cells were then incubated in the same fixative containing 1% tannic acid at 4°C for 30-60 min, postfixed in 1% OsO_4 for 1-2 h, stained en bloc in 1% aqueous uranyl acetate at 60°C overnight and dehydrated in ethanol and then embedded in Spurr's medium. Thin sections were taken on a Leica Ultracut with a Diatome diamond knife and investigated in a Philips (FEI) CM 12 operated at 120 kV.

4.6.6 Transport Assays

For transport assays, cells were grown and transfected as described (4.6.2, p.136 and 4.6.3, p.136).

VSV-G Transport Assay For vesicular stomatitis virus G-protein transport, cells were transfected as described (4.6.2, p.136) with a construct expressing a GFP-tagged version of the VSV-G^{ts45} protein (Bergmann, 1989) 14 h before the experiment. The transfected cells were grown for 2 h at normal cell culture conditions and then shifted to 39.5°C and 5% CO_2. After 12 h the culture medium was replaced by ice-cold medium and the cells were placed on ice for 30 min. While a set of coverslips was fixed with PFA (see 4.6.4, p.137), the cells were shifted to 32°C (medium replaced with 32°C pre-warmed medium) and 5% CO_2 for 30 min and 60 min, when additional sets of coverslips were fixed. Fixing by PFA was done as described (see 4.6.4, p.137), whereas the cells were

not permeabilised with Triton-X100. The antibody against the lumenal domain of the VSV-G-Protein (Tab.6, p.123*ff*) revealed protein transported to the plasma membrane (incubation time for both antibodies was 30 min). Pictures were taken and the ratio of transported protein (red channel) against overall GFP-tagged protein (green channel) was measured with the MetaVue Software (Visitron Systems GmbH, Puchheim).

Shiga Toxin Uptake Cells were cultured and prepared as described above. For shiga toxin uptake, the cells were first washed three times in ice-cold PBS and then transferred upside down onto 50 μl of shiga toxin mix on a parafilm on ice. The incubation was performed in the dark and prior to incubation, excess liquid was removed with 3MM filter paper. The shiga toxin mix was composed of 2% BSA (ultra-pure, Jackson Immunoresearch, UK) and 25 mM Hepes-KOH pH 7.2 in DMEM (Invitrogen, Gibco, UK) mixed with Cy3 conjugated, recombinant B subunit of *Shigella sp.* toxin at a dilution of 1:1000. After incubation with labelled shiga toxin B-subunit, the coverslips were transferred back to the culture wells and washed three times with ice-cold PBS. The first time-point was fixed with PFA as described and the rest of the coverslips washed three times with 37°C pre-warmed DMEM and put back to normal culture conditions. Further time-points were fixed after 10, 30, 60, 120 and 240 min (Fuchs *et al.*, 2007).

4.6.7 Drug Treatment

Cells were grown on coverslips for 24 h before transfection and further growth for an appropriate amount of time (see 4.6, p.135). Drug treatment was performed by removing growth medium and replacing it by washing three times with growth medium supplemented with the appropriate amount of the respective drug. Cells were then put back to standard culture conditions.

Drug	**Concentration**	**Supplier**
Brefeldin A	5 μg/ml	Sigma-Aldrich, Taufkirchen
Nocodazole	200 ng/ml	Calbiochem, Darmstadt

For washout experiments, culture wells were washed 3-5 times with drug-free culture medium and put back to normal culture conditions. A set of coverslip was fixed at appropriate time-points.

4.7 Mammalian Biochemical Methods

4.7.1 Protein Expression And Purification From Sf9 Cells With The Baculovirus System

This method consists of two steps, first the preparation of the recombinant baculovirus in Sf9 cells and second the infection of Sf9 cells with the recombinant virus and subsequent purification of the recombinant protein.

For the generation of the virus the BaculoGold Kit from Pharmingen (Becton-Dickinson, Heidelberg) was used. 0.25 μg BaculoGold DNA (2.5 μl) were mixed with 2.5 μg pAcHis vector construct for expression of the appropriate protein (see Tab.4, p.121). While incubating for 5 min, the growth medium on a 3 cm culture dish with $5{\cdot}10^5$ Sf9 cells, prepared 6-24 h before, was replaced by 0.5 ml buffer A (included in the kit). Then 0.5 ml buffer B were added to the DNA and the mixture added drop-wise to the cells under continuous rocking. After incubation for 4 h at 27°C, the culture dish was washed once with TC100 and the cells grown in 2.5 ml TC100 at 27°C.

After 5 days the supernatant was taken and centrifuged for 5 min at 1000 *g* at room temperature. The supernatant (P_0-virus) was kept for further amplification.

Next, 200 μl of P_0 mixed with 1 ml TC100 were used to infect a 10 cm dish of $5{\cdot}10^6$ Sf9 cells. The cells were incubated for 1 h at 27°C and then the infection mix was replaced by 10 ml TC100 and the cells grown for 4 days. The supernatant was collected as described above (P_1-virus) and stored at 4°C. For amplifying the P_1-virus, 500 μl were mixed with 1 ml TC100 and $5{\cdot}10^6$ cells on a 10 cm dish infected for 1 h and, after replacing the virus with 10 ml TC100, grown for 4 days. The P_2-virus was recovered like the P_1-step. In order to get the final P_3-virus, $2{\cdot}10^7$ cells on a 15 cm culture dish were infected with 100 μl P_2-virus, diluted in 3 ml TC100, for 1 h. The cells were then grown in 25 ml TC100 for 4 days and the virus was collected, when cell lysis reached 50%. The P_3-virus was stored at 4°C in the dark. After each step, the cells were collected and the protein expression assayed by Western blot and coomassie stained SDS-PAGE.

For protein expression ten 15 cm dishes with $2{\cdot}10^7$ Sf9 cells were each infected with 1 ml P_3-virus in 2 ml TC100 each. After 1 h, 30 ml TC100 were added. Three days later, cells were harvested by pipetting up and down in the culture medium. The cell suspension was then centrifuged at room temperature for 8 min at 400 *g*. The pellet was washed in 200 ml PBS and after centrifugation as above lysed for 30 min on ice in 20 ml lysis buffer (IMAC5, Protease Inhibitor Cocktail, 0.2 mM PMSF, 0.1% Triton-X100, see 4.2.3, p.126 for IMAC5). The crude lysate was ultracentrifuged for 35 min at 27000 rpm and 4°C in a SW40 rotor (Beckman Optima LE-80K) and the supernatant

applied to 300 μl Ni-NTA-Agarose (Qiagen, Hilden). After incubation for 2 h at 4°C and constant rolling, the beads were pelleted at 1000 *g* and washed in 20 ml lysis buffer before they were transferred to a 3 ml disposable column. The beads were then washed again with IMAC20-TX and IMAC20. The protein was eluted with three times 1 ml of IMAC200 buffer into 8 fractions. After analysis on coomassie stained SDS-PAGE, fractions with highest concentrations were pooled as appropriate and dialysed (see 4.2.3, p.126) or desalted.

For desalting, a desalting column was prepared by piercing the bottom of an Eppendorf tube with a syringe needle and filling it with 100 μl glasswool. This was overlaid with desalting Gel P-6 DG (BioRad, Munich) in several steps of centrifugation (1500 *g*, 2 min, 4°C) and addition of gel until the Eppendorf tube was filled up to the 1 ml marking. The desalting column was then washed four times with PBS and the protein solution was applied. Elution was done with the same volume of the appropriate buffer. Protein was frozen in liquid Nitrogen and stored at -80°C.

4.7.2 Preparation Of Rat Liver Golgi Membranes

The preparation of rat liver Golgi membranes was done as described in Hui *et al.* (1998). In brief, three 2-3 months old male or female Wistar rats (Chbb: THOM, MPI for Biochemistry, Martinsried) were anaesthetised with CO_2 gas and killed by breaking their necks. The liver tissue (between 45 g and 60 g in total) was removed with surgeon scissors at 4°C and placed into ice-cold 0.5 M K/S (K/S buffer: 0.1 M potassium phosphate pH 6.7, 5 mM $MgCl_2$, varied Molarity of sucrose as indicated), supplemented with EDTA-free Protease Inhibitor Cocktail (Roche Diagnostics, Mannheim). The liver tissue was cut to small pieces with surgeon scissors and subsequently forced through a 150 μm steel mesh sieve. The homogenate was transferred to 14 ml Beckman centrifuge tubes. Each of the 6 tubes used was filled with 6.5 ml 0.86 M K/S and overlaid with 4 ml of the liver homogenate in 0.5 M K/S. A layer of 2 ml 0.25 M K/S was applied on top. The gradient was centrifuged for 60 min at 29000 rpm at 4°C in a SW40 rotor in a Beckman Optima LE-80K Ultracentrifuge (Beckman, USA). The cloudy interphase (crude Golgi fraction) at the border of the 0.5 M K/S and 0.86 M K/S layer was collected for further processing. The 0.5 M K/S fraction contained the cytosol. The crude Golgi fraction was adjusted to a sucrose concentration of 0.25 M with 0.1 M Potassium phosphate pH 6.7, 5 mM $MgCl_2$ and placed on top of a cushion of 1.3 M K/S in a fresh 14 ml Beckman centrifuge tube. The mixture was centrifuged for 20 min at 7000 rpm at 4°C (SW40, Beckman Optima LE-80K). The Golgi membranes could be collected from the top of the cushion and were frozen in aliquots on dry ice and stored at -80°C. The quality and yield of the prepara-

tion process was assayed by spectroscopic methods (see 4.5.1, p.133) and Western blot with 10 μg of each homogenate, rat liver cytosol, interphase and purified membranes for enrichment and possible degradation of GM130.
For experiments, Golgi membranes were often extracted with detergents. Golgi membranes were thawed on ice and then centrifuged for 5 min at 20000 g and 4°C and the sucrose containing buffer removed. The pelleted Golgi membranes were then resuspended in extraction buffer (50 mM Hepes/KOH pH 7.2, 200 mM NaCl, 0.5% Triton-X100 + Protease Inhibitor Cocktail, Roche) for 30 min on ice and then centrifuged for 15 min at 20000 g and 4°C.

4.7.3 Preparation Of Mammalian Cell Extracts

For mammalian cell extracts, cells were grown on 15 cm culture dishes to 80-90% confluency and, after washing with PBS, either scraped with a silicon cell scraper into 5-10 ml ice-cold PBS or detached by 15 min of treatment with PBS/1 mM EDTA at 37 °C. The cell suspension was centrifuged at 400 g at 4°C for 5 min and the cell pellet resuspended in the appropriate buffer (see Tab.11) for 30 min on ice for lysis. The cell extract was centrifuged for 15 min at 20000 g, 4°C in order to remove cell debris. The protein concentration in the supernatant was assayed (see 4.5.1, p.133).

Alternatively, cell extracts could be fractionated into membrane and cytosolic fraction. For this cells were harvested as described above and resuspended into TMK-buffer (25 mM Tris/HCl pH 7.3, 130 mM KCl, 5 mM $MgCl_2$ + Inhibitor Cocktail), centrifuged again and resuspended again in TMK. The cell suspension was passed through a 27 Gauge syringe needle 20 times and centrifuged for 5 min at 20000 g and 4°C. The supernatant was ultracentrifuged in a Beckman TLA55 rotor at 50000 rpm and 4°C for 30 min. The supernatant comprised the cytosolic fraction, the pellet the membranous fraction. The

Table 11: List of Lysis Buffers used

Buffer	**Composition**
TNTE	10 mM Tris/HCl pH 7.5, 150 mM NaCl, 0.3% Triton-X100, 5 mM EDTA
RIPA	10 mM Tris/HCl pH 7.5, 150 mM NaCl, 1% Triton-X100, 0.1% SDS, 1% sodium deoxycholate
Mammalian Lysis Buffer	50 mM Tris/HCl pH 7.5, 150 mM NaCl, 0.1% Triton X-100

membranes were then extracted for 30 min on ice in TMK plus 1% Triton-X100 and processed as described above.

4.7.4 Preparation Of Tubulin From Pig Brain

As raw material about 25-50 fresh pig brains were acquired from the slaughter house and transported in ice-cold PBS until further processing. The preparation of the brain homogenate was done in the cold room at 4°C. As a first step, the blood vessels and brain skin were removed with normal paper towels and a scalpel. The brain matter was weighed and the same volume of depolymerisation buffer added. Then the brain was mixed harsh in a standard kitchen mixer to homogenise the tissue. The homogenate was cleared by centrifugation in an SLA 1500 rotor at 13600 rpm for 1 h at 4°C (Sorval RC3-C, Thermo Scientific, USA). The supernatant was collected in a 5 l Erlenmeyer tube and the same amount of HMPB (pre-warmed to 37°C), 0.8265 mg/ml final volume ATP, 0.262 mg/ml final volume GTP and 1 g/ml starting volume Glycerol were added and polymerisation was allowed for 1 h in a 37°C water bath with gentle shaking every 15 min. The mixture was centrifuged at 37°C in a Ti45 rotor at 44000 rpm for 30 min (Beckmann Optima LE-80K). The pellets were collected in 100 ml/kg brain of depolymerisation buffer and kept for 30 min at 4°C. The next centrifugation step was done again in the Ti45 rotor pre-cooled to 4°C, at 30000 rpm for 30 min. The supernatant was mixed with its volume 37°C-warm HMPB, 0.8265 mg/ml final volume ATP, 0.262 mg/ml final volume GTP and 1 g/ml starting volume Glycerol and incubated for 30 min at 37°C with gentle shaking every 5 min. The polymerised tubulin solution was again centrifuged for 30 min in a Ti45 rotor at 44000 rpm (151000 g) at 35°C. The pellet was resuspended in 15 ml/kg brain ice-cold BRB80 buffer and incubated on ice for 30 min. The last centrifugation step was carried out twice in a TLA100.4 rotor for 10 min, 4°C at 49000 rpm. The supernatant was pooled, its concentration assayed by OD_{280} measurement and coomassie blue SDS-PAGE, aliquoted and snap-frozen on dry-ice.

4.8 General Biochemical Methods

4.8.1 Small GTPase Effector Pulldown From Cell Extracts

For pulldown experiments a protein was immobilized on resin and incubated with cell extract. Bound proteins were analysed by Western blotting. The methods used were different for Rab-effectors and Arl-/Arf-effectors as described below. Pulldown experiments for Rab-effectors followed the description of Christoforidis and Zerial (2000), pulldown

Table 12: Buffers for Tubulin Preparation from Pig Brain

Buffer	**Composition**
Depolymerisation Buffer	50 mM MES/KOH pH 6.6; 1 mM $CaCl_2$
HMPB (High Pipes)	1 M Pipes/KOH pH 6.9; 10 mM $MgCl_2$; 20 mM EGTA
5xBRB80 (Brinkley BR buffer 1980)	400 mM Pipes/KOH pH 6.8; 5 mM $MgCl_2$; 5 mM EGTA

with Arl-/Arf-GTPases followed Panic *et al.* (2003a) and Lu *et al.* (2005).

Rab Effector Pulldown 500 μg of GST-6xHis-tagged Rab protein was coupled to 50 μl of glutathione-S-sepharose beads (GE Healthcare, Sweden) in a volume of 500 μl PBS for 1 h at 4°C. Then, beads were washed three times in 500 μl NE100 buffer (20 mM HEPES/NaOH pH 7.5, 100 mM NaCl, 10 mM EDTA, 0.1% Triton-X100); centrifugation was done at 400 *g*, 4°C for 5 min. In the meantime, the cell extract was prepared as described (see 4.7.3, p.143), whereas NL100 buffer (20 mM HEPES/NaOH pH 7.5, 100 mM NaCl, 5 mM $MgCl_2$, 0.1% Triton-X100) was used for lysis. Cell extract (1-5 mg protein) and glutathione-S-sepharose bound Rab-proteins were mixed and GDP or GTP was added to a concentration of 100 μM and incubated for 2 h at 4°C under constant rolling. The beads were washed three times in NL100 buffer (centrifugation at 400 *g*, 4°C, 5 min) and then either boiled in 50 μl SDS-sample buffer or extracted with 500 μl NE200 buffer (20 mM HEPES/NaOH pH 7.5, 200 mM NaCl, 20 mM EDTA, 0.1% Triton-X100) for 10 min at 4 °C. The beads were centrifuged (400 *g*, 4°C, 5 min) and the supernatant was treated with fresh glutathione-S-sepharose beads for 10 min at 4°C. This step was repeated up to three times. The cleared supernatant was then TCA-precipitated (see 4.5.2, p.133) and analysed by Western blotting (see 4.5.5, p.134).

Arf-/Arl-Effector Pulldown For Arf-/Arl-Effector Pulldown, 100 ml *E.coli* transformed with the appropriate pFAT2-construct were grown and induced with IPTG for 2 h at 22 °C. The bacteria were harvested, lysed (PBS, 5 mM $MgCl_2$, 5 mM βMercaptoethanol, 200 μM GTP or GDP, 1% Triton-X100 and PIC) and bound for 30 min to 200 μl glutathione-S-sepharose beads as described in 4.2.3 (p.126). The beads were washed three times in wash buffer (lysis buffer w/o Triton-X100) and then the cell extract (see 4.7.3, p.143) was directly applied to 50 μl of protein bound to beads and supplemented with 200 μM GDP or GTP. After 2 h of incubation at 4 °C and constant rolling, the beads

were washed three times in lysis buffer containing 200 μM GDP or GTP and then boiled in 50 μl SDS-PAGE sample buffer.

4.8.2 Co-Immunoprecipitation From Cell Extracts

A cell extract was prepared as described (see 4.7.3, p.143) and mixed with 2-20 μl of the appropriate antibody (depending on antibody concentration and affinity) or 2 μl of pre-immune serum as control and 20 μl packed Protein-A- or Protein-G-sepharose beads (Amersham, Freiburg) The mix was incubated for 2 h at 4°C under constant rolling. The beads were centrifuged for 5 min at 400 *g* and 4°C in order to pellet the beads. The beads were washed three times with 500 μl lysis buffer and then boiled for 5 min in 30 μl SDS-sample buffer and analysed by Western blotting (4.5.5, p.134).

4.8.3 Microtubule Assays

Microtubules were grown *in vitro* from tubulin purified from pig brain (see 4.7.4, p.144).

In vitro Preparation Of Microtubules 25 μl tubulin from pig brain (4 mg/ml; 40 μM) were mixed with 43.1 μl BRB80 buffer (Tab.12) containing 10 μM Taxol and with 3.1 μl 100 mM $MgCl_2$, 3.1 μl 100 mM GTP and 3.7 μl DMSO and incubated for 30 min at 37°C. The polymerised microtubules were then pipetted on top of a 40% glycerol cushion (in BRB80 buffer) in a TLA100 rotor centrifuge tube (Beckman, USA) and centrifuged in a Beckman Optima TLX-120 microcentrifuge for 15 min at 55000 rpm and 35°C. The supernatant was removed and the pellet washed with 50 μl BRB80 and 10 μM Taxol and centrifuged again for 10 min. The pellet was then resuspended in 50 μl BRB80 buffer and 50 μM Taxol by incubating for 30 min at room temperature and subsequent gentle pipetting. The final microtubule concentration was 20 μM (2 mg/ml).

Microtubule Bundling For microtubule bundling experiments, microtubules were prepared as described above whereas 1.5 μl rhodamine-labelled tubulin was added. For bundling, 400 ng of purified, recombinant protein were incubated for 20 min at room temperature with 1 μl rhodamine-labelled microtubules in BRB80 buffer and 10 μM Taxol. One drop of the mixture was then applied to an objective slide, covered with a glass cover slip and examined under an Axioskop-2 with a 40x Plan Apochromat objective of NA 1.3, standard filter sets (Carl Zeiss GmbH, Germany), a 1300 by 1030 pixel cooled-CCD camera model CCD-1300-Y (Princeton Instruments, USA) and MetaVue software (Visitron

Systems GmbH, Puchheim). Images were cropped in Adobe Photoshop CS2 then sized and placed in figures using Adobe Illustrator CS2 (Adobe Systems Inc., USA).

Microtubule Spin-Down Assays 400 ng of purified, recombinant protein were mixed with 2 μl (4 μg) microtubules and 5 μl BRB80 buffer containing 50 μM Taxol in a total volume of 20 μl. The mix was incubated for 20 min at room temperature and then centrifuged in a Beckman Optima TLX-120 (Beckman, USA) in a TLA100 rotor at 55000 rpm, 25 °C for 20 min. A 75 μl 40% glycerol cushion was used to improve separation. The pellet was washed with 50 μl BRB80 buffer and 50 μM Taxol and centrifuged again for 20 min. The pellet was resuspended in 30 μl SDS-PAGE sample buffer and analysed on coomassie stained SDS-PAGE (24 μl) and Western blotting (6 μl).

A Plasmids Used

Table 13: Plasmids used; abbreviations: pAH=*Alexander Haas*, pBS=*Benjamin Short*, pCP=*Christian Preisinger*, pEF=*Evelyn Fuchs*, pFB=*Francis Barr*, pRK=*Robert Kopajtich*

pFB #	Creator #	Short Name	Description
		GMAP-210 Constructs	
pFB2037	pJE001	pCRIITOPO-GMAP210	human GMAP210, BamHI-EcoRI/EcoRI-XhoI has BamHI site in sequence (Nr.2)
pFB2037	pJE002	pCRIITOPO-GMAP210	human GMAP210, BamHI-EcoRI/EcoRI-XhoI has BamHI site in sequence (Nr.11) K1827G version
pFB2040	pJE004	pCRIITOPO-GMAP210(1-375)	human GMAP210 N-Term aa 1-375, BamHI-XhoI; derived from pFB2037
pFB2041	pJE005	pCRIITOPO-GMAP210(1598-1979)	human GMAP210 C-Term aa 1598-1979, BamHI-XhoI; S1827G version
pFB2215	pJE014	pCRIITOPO-GMAP210(618-803	Human GMAP210 aa 618-803 with STOP codon, BamHI-XhoI, derived from pFB2037
pFB2216	pJE015	pCRIITOPO-GMAP210(855-1712)	Human GMAP210 aa 855-1712 with STOP codon, BglII-XhoI, derived from pFB2037
pFB2232	pJE031	pCRIITOPO-GMAP210(855-1332)	Human GMAP210 aa 855-1332 with STOP codon; BglII-XhoI, derived from pFB2037
pFB2233	pJE032	pCRIITOPO-GMAP210(1333-1712)	Human GMAP210 aa 1333-1712 with STOP codon; BamHI-XhoI, derived from pFB2037
pFB2710	pJE092	pCRIITOPO-GMAP210(1-375)'	human GMAP210 aa 1-375; no stop codon; BamHI XhoI
pFB2711	pJE093	pCRIITOPO-GMAP210(1598-1979)'	human GMAP210 aa 1598-1979; no stop codon; BamHI XhoI
pFB2712	pJE094	pCRIITOPO-GMAP210'	human GMAP210; no stop codon, BamHI XhoI
pFB2713	pJE095	pCRIITOPO-GMAP210(1598-1778)	human GMAP210 aa 1598-1778; BamHI XhoI
pFB2714	pJE096	pCRIITOPO-GMAP210(1779-1979)	human GMAP210 aa 1779-1979, BamHI XhoI
pFB2717	pJE099	pCRIITOPO-GMAP210(1598-1979) D1780A L1783A	human GMAP210 aa 1598-1979; D1780A and L1783A mutation; BamHI XhoI; S1827G
pFB2721	pJE103	pCRIITOPO-GMAP210(1779-1838)	human GMAP210 aa 1779-1838, BamHI XhoI
pFB2849	pJE143	pCRIITOPO-GMAP210 D1780A L1783A	human GMAP210; mutation D1780A and L1783A; BamHI-EcoRI/EcoRI-XhoI
pFB2857	pJE151	pCRIITOPO-GMAP210(1757-1979)	human GMAP210 aa 1757-1979; BamHI XhoI
pFB2858	pJE152	pCRIITOPO-GMAP210(1757-1838)	human GMAP210 aa 1757-1838; BamHI XhoI
pFB3019	pJE154	pCRIITOPO-GMAP210(1757-1875)	human GMAP210 aa 1757-1875; BamHI XhoI
pFB3291	pJE225	pCRIITOPO-GMAP-210(1598-1979)	human GMAP-210 aa 1598-1979; S1827 version; BamHI XhoI
pFB3292	pJE226	pCRIITOPO-GMAP-210(1598-1979)DALA	human GMAP-210 aa 1598-1979; D1780A L1783A mutant; S1827 version; BamHI XhoI
pFB4183	pJE292	pCRIITOPO-GMAP-210ΔBamHI	human GMAP-210 without BamHI (silent mutation) in the sequence; BamHI XhoI
pFB4184	pJE293	pCRIITOPO-GMAP-210(1-1712)	human GMAP-210 aa 1-1712 (PCR from pFB4183; no internal BamHI); BamHI XhoI
pFB4185	pJE294	pCRIITOPO-GMAP-210(1683-1875)	human GMAP-210 aa 1683-1875; BamHI XhoI; GRAB domain plus coiled-coil
pFB4364	pJE316	pCRIITOPO-GMAP-210(1-1332)	human GMAP-210 aa 1-1332; BamHI XhoI; has internal BamHI: cut BamHI-EcoRI EcoRI-XhoI
pFB2226	pJE025	pAct2-GMAP210	Human GMAP210; BamHI-XhoI, derived from 2037
pFB2227	pJE026	pAct2-GMAP210(1-375)	Human GMAP210 aa 1-375 with STOP codon, BamHI-XhoI, derived from pFB2040

continued on next page

pFB #	Creator #	Short Name	Description
pFB2228	pJE027	pAct2-GMAP210(1598-1979)	Human GMAP210 aa 1598-1979 with STOP codon, BamHI-XhoI, derived from pFB2041; S1827G
pFB2229	pJE028	pAct2-GMAP210(855-1712)	Human GMAP210 aa 855-1712 with STOP codon, BglII-XhoI, derived from pFB2037
pFB2230	pJE029	pAct2-GMAP210(618-803)	Human GMAP210 aa 618-803 with STOP codon, BamHI-XhoI, derived from pFB2037
pFB2234	pJE033	pAct2-GMAP210(855-1332)	Human GMAP210 aa 855-1332 with STOP codon; BglII-XhoI, derived from pFB2037
pFB2235	pJE034	pAct2-GMAP210(1332-1712)	Human GMAP210 aa 1333 712 with STOP codon; BamHI-XhoI, derived from pFB2037
pFB2737	pJE119	pAct2-GMAP210(1779-1979)	human GMAP210 aa 1779-1979, from pFB2714
pFB2844	pJE138	pAct2-GMAP210(1598-1979) D1780A L1783A	human GMAP210 aa 1598-1979; D1780A and L1783A mutation; from pFB2717; S1827G
pFB3361	pJE242	pAct2-GMAP210(1598-1979) S1827	human GMAP210 aa 1598-1979; derived from pFB3291
pFB3362	pJE243	pAct2-GMAP210(1598-1979) D1780A L1783A S1827	human GMAP210 aa 1598-1997; D1780A L1783A mutant; from pFB3292
pFB4472	pJE334	pAct2-GMAP-210(1683-1875)	human GMAP-210 aa 1683-1875; from pFB4185
pFB4473	pJE335	pAct2-GMAP-210(1683-1875)D1780A L1783A	human GMAP-210 aa 1683-1875; GRAB mutant
pFB2043	pJE006	pQE32Tev-GMAP210(1-375)	human GMAP210 N-Term aa 1-375, BamHI-XhoI; derived from pFB2040 ; expression in JM109; protein insoluble
pFB2739	pJE121	pFAT2-GMAP210(1-375)	human GMAP210 aa 1-375, from pFB2040
pFB2846	pJE140	pAcHis-GMAP210	human GMAP210; from pFB2037; sequenced
pFB3295	pJE229	pAcHis-GMAP-210(1-375)	human GMAP-210 aa 1-375; from pFB2040; sequenced
pFB3352	pJE233	pAcHis-GMAP210(1598-1979) S1827	human GMAP210 aa 1598-1979; derived from pFB3291
pFB2220	pJE019	pEGFPC2-GMAP210(1598-1979)	Human GMAP210 aa 1598-1979 with STOP codon, BamHI-XhoI, derived from pFB2041; S1827G
pFB2221	pJE020	pEGFPC2-GMAP210d(1-375)	Human GMAP210 aa 1-375 with STOP codon, BamHI-XhoI, derived from pFB2040
pFB2740	pJE122	pEGFPN3-GMAP210	human GMAP210; from pFB2712
pFB2746	pJE128	pEGFPC2-GMAP210(1779-1979)	human GMAP210 aa 1779-1979; from pFB2714
pFB2747	pJE129	pEGFPN3-GMAP210(1-375)	human GMAP210 aa 1-375; from pFB2710
pFB2748	pJE130	pEGFPN3-GMAP210(1598-1979)	human GMAP210 aa 1598-1979; from pFB2711
pFB3145	pJE206	pEGFPC2-GMAP210/1757-1979)	human GMAP210 aa 1757-1979; from pFB2857
pFB3149	pJE210	pEGFPC2-GMAP210(1757-1838)	human GMAP210 aa 1757-1838; from pFB2858
pFB3159	pJE220	pEGFPC2-GMAP210(1757-1875)	human GMAP210 aa 1757-1875 from pFB3019
pFB4186	pJE295	pEGFPC2-GMAP-210(1598-1979) DALA	human GMAP-210 C-Terminus aa 1598-1979; D1780A L1783A mutation;
pFB4187	pJE296	pEGFPN3-GMAP-210 DALA	human GMAP-210 D1780A L1783A mutation
pFB4188	pJE297	pEGFPC2-GMAP-210	human GMAP-210; derived from pFB4183
pFB4189	pJE298	pEGFPC2-GMAP-210(1757-1875) DALA	human GMAP-210 aa 1757-1875; GRAB domain with D1780A L1783A mutation
pFB4190	pJE299	pEGFPC2-GMAP-210(1-1712)	human GMAP-210 aa 1-1712; dervied from pFB4184
pFB4366	pJE318	pEGFPC2-GMAP-210(1598-1778)	human GMAP-210 aa 1598-1778; derived from pFB2713

continued on next page

pFB #	Creator #	Short Name	Description
pFB4367	pJE319	pEGFPC2-GMAP-210(1683-1875)	human GMAP-210 aa 1683-1875; GRAB domain plus coiled-coil; derived from pFB4185
pFB4372	pJE324	pEGFPC2-GMAP-210(855-1712)	human GMAP-210 aa 855-1712; derived from pFB2216
pFB4469	pJE331	pEGFPC2-GMAP-210(1598-1979)S1827	human GMAP-210 aa 1598-1979; S1827 variant; derived from pFB3291
pFB4470	pJE332	pEGFPC2-GMAP-210(1-1332)	human GMAP-210 aa 1-1332; derived from pFB4364
pFB4471	pJE333	pEGFPC2-GMAP-210(1683-1875)D1780A L1783A	human GMAP-210 aa 1683-1875; D1780A L1783A mutant; GRAB mutant
pFB4820	pJE418	pdsRed-GMAP-210	human GMAP-210; derived from pFB4183; weak exp. in HeLaL
pFB4821	pJE419	pdsRed-GMAP-210(1-1712)	human GMAP-210; aa 1-1712; derived from pFB4184; weak exp. in HeLaL
pFB4822	pJE420	pdsRed-GMAP-210(1683-1875)	human GMAP-210; aa 1683-1875; coiled-coil plus GRAB; derived from pFB4185; weak exp. in HeLaL
pFB4970	pJE472	pEGFPC2-GMAP-210(618-803)	human GMAp-210; aa 618-803; derived from pFB2215
pFB4971	pJE473	pEGFPC2-GMAP-210(855-1332)	human GMAP-210; aa 855-1332; derived from pFB2232
pFB4972	pJE474	pEGFPC2-GMAP-210(1333-1712)	human GMAP-210; aa 1333-1712; derived fom pFB2233
		Rud3p Constructs	
pFB391	pCRII-GRP1	G RP1/RUD3 fl	Full length GRP1/RUD3 (yeast golgin-160 homologue) BamHI cassette
pFB393	pACT2 GRP1.1	Gal4AD GRP1.1	Gal4AD full-length GRP1/RUD3 fusion
pFB3153	pJE214	pCR2.1TOPO-Rud3	S.cerevisiae Rud3p; BamHI SalI
pFB3351	pJE232	pAct2-Rud3	S.cerevisiae Rud3p from pFB3153
pFB4192	pJE301	pMyc-Rud3	S.cerevisiae Rud3; derived from pFB3153
		Golgins	
pFB2722	pJE104	pCRIITOPO-Golgin97	human Golgin97, BclI SalI; from dam+ bacteria (BclI resistant)
pFB2856	pJE150	pCRIITOPO-Golgin97 Y697A	human Golgin97 Y697A GRIP mutation; BclI/SalI
pFB3436	pJE247	PCRIITOPO-Golgin-84	human Golgin-84; with stop codon; BamHI SalI
pFB2845	pJE139	pAct2-Golgin97	human Golgin97; from pFB2722
pFB3141	pJE202	pAct2-Golgin97Y697A	human Golgin97 GRIP Arl1 binding mutation pFB3020
pFB3441	pJE252	pAct2-Golgin-84	human Golgin-84; from pFB3436
		Golgin-84	
pFB3436	pJE247	PCRIITOPO-Golgin-84	human Golgin-84; with stop codon; BamHI SalI
pFB3441	pJE252	pAct2-Golgin-84	human Golgin-84; from pFB3436
		IFT20 Constructs	
pFB2048	pJE011	pCRIITOPO-IFT20	human IFT20, BamHI-SalI; only bp 1-213(aa 1-71), then gap and frame-shift, seems to exist, with longer 3'-end; seems to function in plasmids with stop-codon!

continued on next page

pFB #	Creator #	Short Name	Description
pFB4889	pJE437	pCRIITOPO-IFT20(F2R2)	human IFT20; F2 R2 Primer used; BamHI SalI
pFB4890	pJE438	pCRIITOPO-IFT20(F2R2)'	human IFT20; nostop; F2 R2' Primer used; BamHI SalI
pFB4891	pJE439	pCRIITOPO-IFT20(F2R3)	human IFT20; F2 R3 Primer used; BamHI SalI
pFB4892	pJE440	pCRIITOPO-IFT20(F2R3)'	human IFT20; nostop; F2 R3' Primer used; BamHI SalI
pFB4893	pJE441	pCRIITOPO-IFT20(F3R3)	human IFT20; F3 R3 Primer used; BamHI SalI
pFB4894	pJE442	pCRIITOPO-IFT20(F3R3)'	human IFT20; nostop; F3 R3' Primer used; BamHI SalI
pFB4895	pJE443	pCRIITOPO-IFT20(F3R2)	human IFT20; F3 R2 Primer used; BamHI SalI
pFB4896	pJE444	pCRIITOPO-IFT20(F3R2)'	human IFT20; nostop; F3 R2' Primer used; BamHI SalI
pFB4957	pJE459	pAct2-IFT20old	human IFT20; derived from pFB2048
pFB4952	pJE454	pFBT10-IFT20(33)'	human IFT20; F3 R3' primer used; derived from pFB4894
pFB4953	pJE455	pFBT9-IFT20(32)	human IFT20; F3 R2 Primer used; derived from pFB4895
pFB4954	pJE456	pFBT9-IFT20(23)	human IFT20; F2 R3 Primer used; derived from pFB4891
pFB4955	pJE457	pFBT9-IFT20(33)	human IFT20; F3 R3 Primer used; derived from pFB4893
pFB4956	pJE458	pFBT9-IFT20old	human IFT20; derived from pFB2048
pFB2049	pJE012	pQE32Tev-IFT20	human IFT20, BamHI-SalI; expresses in JM109 only 3h/37Â°C; dialyse protein in Tris/300mM NaCl; derived from pFB2048
pFB2051	pJE013	pEGFPC2-IFT20	human IFT20, BamHI-SalI, derived from pFB2048
pFB4943	pJE445	pEGFPC2-IFT20(22)	human IFT20; F2 R2 Primer used; derived from pFB4889
pFB4944	pJE446	pEGFPN3-IFT20(22)'	human IFT20; F2 R2' Primer used; derived from pFB4890
pFB4945	pJE447	pEGFPC2-IFT20(23)	human IFT20; F2 R3 Primer used; derived from pFB4891
pFB4946	pJE448	pEGFPN3-IFT20(23)'	human IFT20; F2 R3' Primer used; derived from PFB4892
pFB4947	pJE449	pEGFPC2-IFT20(32)	human IFT20; F3 R2 Primer used; derived from pFB4895
pFB4948	pJE450	pEGFPN3-IFT20(32)'	human IFT20; F3 R2' Primer used; derived from pFB4896
pFB4949	pJE451	pEGFPC2-IFT20(33)'	human IFT20; F3 R3' Primer used; insert has no stop codon, but vector; derived from pFB4894
pFB4950	pJE452	pEGFPN3-IFT20(33)'	human IFT20; F3 R3' Primer used; derived from pFB4894
pFB4951	pJE453	pEGFPC2-IFT20(33)	human IFT20; F3 R3 Primer used; derived from pFB4893
		Heterotrimeric Kinesin II Kif3B	
pFB4877	pJE425	pCRIITOPO-Kif3B	human Kif3B; BclI XhoI
pFB4879	pJE427	pCRIITOPO-Kif3B'	human Kif3B; nostop; BclI XhoI
pFB4885	pJE433	pCRIITOPO-Kif3B(592-747)	human Kif3B; aa 592-747; BclI XhoI
FB4887	pJE435	pCRIITOPO-Kif3B(592-747)'	human Kif3B; aa 592-747; nostop; BclI XhoI
pFB4963	pJE465	pEGFPN3-Kif3B'	human Kif3B; derived from pFB4880
pFB4967	pJE469	pEGFPN3-Kif3B(592-747)'	human Kif3B; aa 592-747; derived from pFB4888

continued on next page

pFB #	Creator #	Short Name	Description
pFB4962	pJE464	pEGFPC2-Kif3B	human Kif3B; derived from pFB4878
pFB4966	pJE468	pEGFPC2-Kif3B(592-747)	human Kif3B; aa 592-747; derived from pFB4886
		ADP-Ribosylation Factor Constructs	
pFB2191	pRK	pCRIITOPO-Arf1	Human Arf1, BamHI+XhoI
pFB3619	pJE264	pCRIITOPO-Arf1ΔN14Q71L	human Arf1; deleted AA 1-14; GTP-locked; BamHI XhoI
pFB3635	pJE280	pCRIITOPO-Arf1Q71A	human Arf1; GTP-locked by Q to A mutation; BamHI XhoI
pFB4195	pJE304	pCRIITOPO-Arf1ΔN14	human Arf1; without aa 1-14; BamHI XhoI
pFB4195	pJE304	pCRIITOPO-Arf1ΔN14	human Arf1; without aa 1-14; BamHI XhoI
pFB2192	pRK	pCRIITOPO-Arf3	human Arf3, BamHI+XhoI
pFB2273	pRK	pCRIITOPO-Arf3Q71L	Human Arf3, BamHI+XhoI, GTP mutant, derived from pFB2192
pFB2193	pRK	pCRIITOPO-Arf4	human Arf4, BamHI+XhoI
pFB2274	pRK	pCRIITOPO-Arf4Q71L	Human Arf4, BamHI+XhoI, GTP mutant, derived from pFB2193
pFB2194	pRK	pCRIITOPO-Arf5	human Arf5, BamHI+XhoI
pFB2275	pRK	pCRIITOPO-Arf5Q71L	Human Arf5, BamHI+XhoI, GTP mutant, derived from pFB2194
pFB2195	pRK	pCRIITOPO-Arf6	human Arf6, BglII+XhoI
pFB2276	pRK	pCRIITOPO-Arf6Q67L	Human Arf6, Bgl II+XhoI, GTP mutant, derived from pFB2195
pFB2282	pRK	pFBT9-Arf1Q71L	Human Arf1, BamHI+XhoI, GTP mutant, derived from pFB2272
pFB2571	pRK	pFBT9-Arf1wt	Human Arf wt, derived from pFB 2191
pFB4200	pJE309	pFBT9-Arf1Q71A	human Arf1; GTP-locked (QA); derived from pFB3635
pFB4204	pJE313	pFBT9-Arf1ΔN14 Q71L	human Arf1; GTP-locked (QL); without aa 1-14; derived from pFB3619
pFB2283	pRK	pFBT9-Arf3Q71L	Human Arf3, BamHI+XhoI, GTP mutant, derived from pFB2273
pFB2572	pRK	pFBT9-Arf3wt	Human Arf wt, derived from pFB 2192
pFB2284	pRK	pFBT9-Arf4Q71L	Human Arf4, BamHI+XhoI, GTP mutant, derived from pFB2274
pFB2573	pRK	pFBT9-Arf4wt	Human Arf wt, derived from pFB 2193
pFB2285	pRK	pFBT9-Arf5wt	Human Arf5, BamHI+XhoI, derived from pFB2275
pFB2574	pRK	pFBT9-Arf5QL	Human Arf Q71L, derived from pFB 2275
pFB2286	pRK	pFBT9-Arf6Q67L	Human Arf6, Bgl II+XhoI, GTP mutant, derived from pFB2276, same as pFB2410
pFB2409	pRK	pFBT9-Arf6 wt	Human Arf6 wt, derived from pFB2195
pFB3624	pJE269	pFAT2-Arf1	human Arf1; dervied from pFB2191
pFB3625	pJE270	pFAT2-Arf1Q71L	human Arf1; GTP-locked; derived from pFB2272
pFB4202	pJE311	pFAT2-Arf1Q71A	human Arf1; GTP-locked (QA); derived from pFB3635
FB4203	pJE312	pFAT2-Arf1ΔN14 Q71L	human Arf1; GTP-locked (QL); without aa 1-14; derived from pFB3619
pFB4363	pJE315	pFAT2-Arf1ΔN14	human Arf1; without aa 1-14; derived from pFB4195
pFB4817	pJE415	pFAT2-Arf3	human Arf3; derived from pFB2192
pFB4716	pJE381	pFAT2-Arf6	human Arf6; derived from pFB2195
pFB4717	pJE321	pFAT2-Arf6QL	human Arf6; GTP-locked; derived from pFB2276

continued on next page

pFB #	Creator #	Short Name	Description
pFB2400	pRK	pEGFPN3-Arf1 wt	Human Arf1 wt, derived from pFB2390
pFB2405	pRK	pEGFPN3-Arf1 Q71L	Human Arf1 Q71L, GTP mutant, derived from pFB2395
pFB2401	pRK	pEGFPN3-Arf3 wt	Human Arf3 wt, derived from pFB2391
pFB2406	pRK	pEGFPN3-Arf3 Q71L	Human Arf3 Q71L, GTP mutant, derived from pFB2396
pFB2402	pRK	pEGFPN3-Arf4 wt	Human Arf4 wt, derived from pFB2392
pFB2403	pRK	pEGFPN3-Arf5 wt	Human Arf5 wt, derived from pFB2393
pFB2407	pRK	pEGFPN3-Arf5 Q71L	Human Arf5 Q71L, GTP mutant, derived from pFB2398
pFB2404	pRK	pEGFPN3-Arf6 wt	Human Arf6 wt, derived from pFB2394
pFB2408	pRK	pEGFPN3-Arf6 Q67L	Human Arf6 Q67L, GTP mutant, derived from pFB2399
pFB4115	pAH600	pCRIITOPO-Sar1a WT	Human Sar1a WT from HeLa cDNA, BamHI, XhoI
pFB4116	pAH601	pCRIITOPO-Sar1a H79G	Human Sar1a H79G, GTP locked, from pFB4115, BamHI, XhoI
pFB4119	pAH604	pFBT9-Sar1a H79G	Human Sar1a H79G, GTP locked, from pFB4116.
pFB3021	pJE156	pCRIITOPO-ScArf1	yeast Arf1; BamHI XhoI
pFB3037	pJE168	pCRIITOPO-ScArf1Q71L	S.cerevisiae Arf1 with Q71L mutation GTP-locked; BamHI XhoI
pFB3294	pJE228	pCRIITOPO-ScArf1ΔN14	S.cerevisiae Arf1 deleted aa 1-14; BamHI XhoI
pFB3443	pJE254	pCRIITOPO-ScArf1Q71LΔN14	S.cerevisiae Arf1 deleted aa 1-14; GTP-locked; BamHI XhoI
pFB3617	pJE262	pCRIITOPO-ScArf1Q71L'	S.cerevisiae Arf1; GTP-locked; no stop codon; BamHI XhoI
pFB3618	pJE263	pCRIITOPO-ScArf1'	S.cerevisiae Arf1; no stop codon; BamHI XhoI
pFB3038	pJE169	pFBT9-ScArf1Q71L	S.cerevisiae Arf1 with Q71L mutation GTP-locked; BamHI XhoI; sequenced
pFB3085	pJE191	pFBT9-ScArf1	S.cerevisiae Arf1 wt; from pFB3021;
pFB3444	pJE255	pFBT9-ScArf1Q71LΔN14	S.cerevisiae Arf1 deleted aa 1-14; GTP-locked; from pFB3443
pFB3147	pJE208	pFAT2-ScArf1	S.cerevisiae Arf1 wt; from pFB3021;
pFB3148	pJE209	pFAT2-ScArf1QL	S.cerevisiae Arf1 GTP-locked; from pFB3037
pFB3359	pJE240	pFAT2-ScArf1ΔN14	S.cerevisiae Arf1 deleted aa 1-14; from3294
pFB3446	pJE257	pFAT2-ScArf1Q71LΔN14	S.cerevisiae Arf1 deleted aa 1-14; GTP-locked; from pFB3443
pFB4193	pJE302	pEGFPN3-ScArf1	S.cerevisiae Arf1; derived from pFB3618
pFB4194	pJE303	pEGFPN3-ScArf1QL	S.cerevisiae Arf1; GTP-locked; derived from pFB3617
		ADP-Ribosylation Factor-Likes Constructs	
pFB2623	pJE035	pCRIITOPO.Arl1	Human Arl1, BamHI XhoI
pFB2626	pJE038	pCRIITOPO.Arl1Q71L	human Arl1Q71L, GTP-locked BamHI XhoI
pFB3293	pJE227	pCRIITOPO-Arl1ΔN14	human Arl1 deleted aa 1-14; BamHI XhoI
pFB3442	pJE253	pCRIITOPO-Arl1Q71LΔN14	human Arl1 deleted aa 1-14; GTP-locked; BamHI XhoI
pFB3616	pJE261	pCRIITOPO-Arl1'	human Arl1; BamHI XhoI; no stop codon
pFB3634	pJE279	pCRIITOPO-Arl1Q71L'	human Arl1; GTP-locked, no stop codon; BamHI XhoI
pFB3882	pJE282	pCRIITOPO-Arl1Q71A	human Arl1; GTP-locked (QA); BamHI XhoI
pFB4675	pJE340	pCRIITOPO-Arl1T31N	human Arl1 GDP-locked; BamHI XhoI; derived from pFB2623

continued on next page

pFB #	Creator #	Short Name	Description
pFB4676	pJE341	pCRIITOPO-Arl1ΔN14 T31N	human Arl1 deletion 1-14; GDP-locked; derived from pFB3293
pFB2628	pJE040	pCRIITOPO-Arl2	human Arl2, BamHI XhoI
pFB2704	pJE086	pCRIITOPO-Arl2Q70L	human Arl2, GTP-locked; BamHI XhoI
pFB4677	pJE342	pCRIITOPO-Arl2'	human Arl2 no-stop codon; derived from pFB2628
pFB4678	pJE343	pCRIITOPO-Arl2QL'	human Arl2 no-stop codon; GTP-locked; derived from pFB2704
pFB2631	pJE043	pCRIITOPO-Arl3	human Arl3, BamHI XhoI
pFB2705	pJE087	pCRIITOPO-Arl3Q71L	human Arl3, GTP-locked; BamHI XhoI
pFB4679	pJE344	pCRIITOPO-Arl3'	human Arl3 no-stop; derived from pFB2631
pFB4680	pJE345	pCRIITOPO-Arl3QL'	human Arl3 no-stop; GTP-locked; derived from pFB2705
pFB2634	pJE046	pCRIITOPO-Arl4A	human Arl4A, BamHI XhoI
pFB2635	pJE047	pCRIITOPO-Arl4A'	human Arl4A, BamHI XhoI, no stop codon
pFB2636	pJE048	pCRIITOPO-Arl4A Q79L	human Arl4A Q79L, GTP-locked, BamHI XhoI;
pFB2702	pJE084	pCRIITOPO-Arl4A Q79L'	human Arl4A, GTP-locked; no stop codon
pFB3133	pJE194	pCRIITOPO-Arl4A T34N	human Arl4 GDP-locked; BamHI XhoI
pFB4463	pJE325	pCRIITOPO-Arl4A ΔN14	human Arl4A aa 1-14 deleted, BamHI XhoI
pFB3022	pJE157	pCRIITOPO-Arl4B	human Arl4B; BamHI XhoI
pFB3032	pJE163	pCRIITOPO-Arl4B'	human Arl4B without stopcodon; BamHI XhoI
pFB2648	pJE059	pCRIITOPO-Arl4C'	human Arl4C, no stop codon, BamHI XhoI
pFB2649	pJE060	pCRIITOPO-Arl4C Q72L	human Arl4C, GTP-locked, BamHI XhoI
pFB2650	pJE061	pCRIITOPO-Arl4C Q72L'	human Arl4C, GTP-locked, no stop codon, BamHI XhoI
pFB3131	pJE192	pCRIITOPO-Arl4C T27N	human Arl4C GDP-locked, BamHI XhoI
pFB4464	pJE326	pCRIITOPO-Arl4C ΔN14	human Arl4C aa 1-14 deleted, BamHI XhoI
pFB4681	pJE346	pCRIITOPO-Arl4D	human Arl4D (ARF4L); BamHI XhoI
pFB4682	pJE347	pCRIITOPO-Arl4D'	human Arl4D no-stop; derived from pFB4681
pFB2641	pJE052	pCRIITOPO-Arl5A	human Arl5A, BamHI XhoI
pFB2706	pJE088	pCRIITOPO-Arl5A Q70L	human Arl5A, GTP-locked; BamHI XhoI
pFB4683	pJE348	pCRIITOPO-Arl5A'	human Arl5A nostop; derived from pFB2641
pFB4684	pJE349	pCRIITOPO-Arl5A QL'	human Arl5A nostop; GTP-locked; derived from pFB2706
pFB2657	pJE068	pCRIITOPO-Arl5B	human Arl5B, BamHI XhoI
pFB2708	pJE090	pCRIITOPO-Arl5B Q70L	human Arl5B, GTP-locked; BamHI XhoI
pFB2644	pJE055	pCRIITOPO-Arl6	human Arl6, BamHI XhoI
pFB2707	pJE089	pCRIITOPO-Arl6Q73L	human Arl6, GTP-locked; BamHI XhoI
pFB4685	pJE350	pCRIITOPO-Arl6'	human Arl6 nostop; derived from pFB2644
pFB4686	pJE351	pCRIITOPO-Arl6QL'	human Arl6 nostop; GTP-locked; derived from pFB2707
pFB3023	pJE158	pCRIITOPO-Arl8A	human Arl8A; BamHI XhoI
pFB3033	pJE164	pCRIITOPO-Arl8A'	human Arl8A without stopcodon; BamHI XhoI
pFB3024	pJE159	pCRIITOPO-Arl8B	human Arl8B; BamHI XhoI
pFB3034	pJE165	pCRIITOPO-Arl8B'	human Arl8B without stopcodon; BamHI XhoI
pFB2660	pJE071	pCRIITOPO-Arl11	human Arl11, BamHI XhoI; C148R mutant: EST clones exist
pFB4694	pJE359	pCRIITOPO-Arl11'	human Arl11 nostop; derived from pFB2660
pFB4689	pJE354	pCRIITOPO-Arl14	human Arl14; BamHI XhoI
pFB4690	pJE355	pCRIITOPO-Arl14'	human Arl14 nostop; derived from pFB4689
pFB4691	pJE356	pCRIITOPO-Arl15	human Arl15; BamHI XhoI

continued on next page

pFB #	Creator #	Short Name	Description
pFB4692	pJE357	pCRIITOPO-Arl15'	human Arl15 nostop; derived from pFB4691
pFB4693	pJE358	pCRIITOPO-Arl16	human Arl16; BamHI XhoI
pFB4789	pJE387	pCRIITOPO-Arl16'	human Arl16; nostop; BamHI XhoI;
pFB4785	pJE383	pCRIITOPO-ARD1'	human ARD1; nostop; BamHI XhoI, Arl-Related-Domain
pFB4786	pJE384	pCRIITOPO-ARD1	human ARD1; BamHI XhoI, Arl-Related-Domain
pFB4695	pJE360	pCRIITOPO-ARD2	human ARD2; BamHI XhoI
pFB4787	pJE385	pCRIITOPO-ARD2'	human ARD2; nostop; BamHI XhoI; Arl-Related-Domain; also Arl13B
pFB4696	pJE361	pCRIITOPO-ARD3	human ARD3; BamHI SalI
pFB4788	pJE386	pCRIITOPO-ARD3'	human ARD3; nostop; BamHI SalI; Arl-Related-Domain; also Arl13A
pFB2663	pJE074	pCRIITOPO-AFRP1	human AFRP1, BamHI XhoI
pFB2664	pJE075	pCRIITOPO-AFRP1'	human AFRP1, BamHI XhoI, no stop codon
pFB2703	pJE085	pCRIITOPO-AFRP1Q79L	human AFRP1, GTP-locked; BamHI XhoI
pFB2855	pJE149	pCRIITOPO-AFRP1Q79L'	human AFRP1 Q79L GTP-locked; no stop codon
pFB2624	pJE036	pFBT9-Arl1	human Arl1, from pFB2623
pFB2627	pJE039	pFBT9-Arl1Q71L	human Arl1Q71L, GTP-locked
pFB2661	pJE072	pFBT9-Arl11	human Arl11, from pFB2660
pFB3349	pJE230	pFBT9-Arl1ΔN14	human Arl1 deleted aa 1-14; derived from pFB3293
pFB4199	pJE308	pFBT9-Arl1Q71A	human Arl1; GTP-locked (QA); derived from pFB3882
pFB4205	pJE314	pFBT9-Arl1ΔN14 Q71L	human Arl1; without aa 1-14; GTP-locked (QL); derived from pFB3442
pFB4697	pJE362	pFBT9-Arl15	human Arl15; derived from pFB4691
pFB4811	pJE409	pFBT9-Arl14	human Arl14; derived from pFB4689
pFB4812	pJE410	pFBT9-Arl16	human Arl16; derived from pFB4693
pFB2629	pJE041	pFBT9-Arl2	human Arl2, from pFB 2628
pFB2837	pJE131	pFBT9-Arl2Q70L	human Arl2Q70L GTP-locked; from pFB2704
pFB2632	pJE044	pFBT9-Arl3	human Arl3, from pFB2631
pFB2839	pJE133	pFBT9-Arl3Q71L	human Arl3 Q71L; GTP-locked; from pFB2705
pFB2637	pJE049	pFBT9-Arl4A	human Arl4A, from pFB2634; now Arl4AW
pFB2638	pJE050	pFBT9-Arl4A Q79L	human Arl4A, from pFB2636; now Arl4AW
pFB3154	pJE215	pFBT9-Arl4A T31N	human Arl4A GDP-locked
pFB3072	pJE178	pFBT9-Arl4B	human Arl4B; from pFB3022
pFB2651	pJE062	pFBT9-Arl4C	human Arl4C, from pFB2647
pFB2696	pJE078	pFBT9-Arl4C Q72L	human Arl7, GTP-locked, from pFB2649
pFB3356	pJE237	pFBT9-Arl4C T27N	human Arl4C GDP-locked; from pFB3131
pFB4714	pJE279	pFBT9-Arl4D	human Arl4D (ARF4L); derived from pFB4681
pFB2642	pJE053	pFBT9-Arl5A	human Arl5A, from pFB2641
pFB2838	pJE132	pFBT9-Arl5A Q70L	human Arl5A Q70L; GTP-locked; from pFB2706
pFB2658	pJE069	pFBT9-Arl5B	human Arl5B, from pFB2657
pFB2841	pJE135	pFBT9-Arl5B Q70L	human Arl5B Q70L GTP-locked; from pFB2708
pFB2645	pJE056	pFBT9-Arl6	human Arl6, from pFB2644
pFB2840	pJE134	pFBT9-Arl6Q73L	human Arl6 Q73L GTP-locked; from pFB2707
pFB3073	pJE179	pFBT9-Arl8A	human Arl8A; from pFB3023
pFB3152	pJE213	pFBT9-Arl8B	human Arl8B from pFB3024
pFB2661	pJE072	pFBT9-Arl11	human Arl11, from pFB2660
pFB4811	pJE409	pFBT9-Arl14	human Arl14; derived from pFB4689
pFB4697	pJE362	pFBT9-Arl15	human Arl15; derived from pFB4691

continued on next page

pFB #	Creator #	Short Name	Description
pFB4812	pJE410	pFBT9-Arl16	human Arl16; derived from pFB4693
pFB4815	pJE413	pFBT9-ARD1	human ARD1; Arl-Related-Domain; derived from pFB4786
pFB4813	pJE411	pFBT9-ARD2	human ARD2; Arl13B; derived from pFB4695
pFB4814	pJE412	pFBT9-ARD3	human ARD3; Arl13A; derived from pFB4696
pFB2665	pJE076	pFBT9-AFRP1	human AFRP1, from pFB2663
pFB2843	pJE137	pFBT9-AFRP1Q79L	human AFRP1, GTP-locked; from pFB2703
pFB2625	pJE037	pFAT2-Arl1	human Arl1, from pFB2623
pFB2697	pJE079	pFAT2-Arl1Q71L	human Arl1, GTP-locked, from pFB2626
pFB3360	pJE241	pFAT2-Arl1ΔN14	human Arl1 deleted aa 1-14; derived from pFB3293
pFB3445	pJE256	pFAT2-Arl1Q71LΔN14	human Arl1 deleted aa 1-14; GTP-locked; from pFB3442
pFB4818	pJE416	pFAT2-Arl1T31N	human Arl1; GDP-locked; derived from pFB4675
pFB4819	pJE417	pFAT2-Arl1(d1-14)T31N	human Arl1; GDP-locked; deletion aa 1-14; derived from pFB4676
pFB2698	pJE080	pFAT2-Arl4A	human Arl4A; from pFB2634
pFB2699	pJE081	pFAT2-Arl4A Q79L	human Arl4A; GTP-locked from pFB2636
pFB4466	pJE328	pFAT2-Arl4A ΔN14	human Arl4A aa 1-14 deleted; from pFB4463
pFB2652	pJE063	pFAT2-Arl4C	human Arl4C, from pFB2647
pFB2700	pJE082	pFAT2-Arl4C Q72L	human Arl4C; GTP-locked from pFB2649
pFB4467	pJE329	pFAT2-Arl4C ΔN14	human Arl4C aa 1-14 deleted; from pFB4464
pFB3884	pJE284	pEGFPN3-Arl1Q71L	human Arl1; GTP-locked; from pFB3617
pFB4790	pJE388	pEGFPN3-Arl1	human Arl1; derived from pFB2623
pFB4700	pEJ365	pEGFPN3-Arl2	human Arl2 derived from pFB4677
FB4701	pJE366	pEGFPN3-Arl2QL	human Arl2; GTP-locked; derived from pFB4678
pFB4702	pJE367	pEGFPN3-Arl3	human Arl3; derived from pFB4679
pFB4703	pJE368	pEGFPN3-Arl3QL	human Arl3; GTP-locked; derived from pFB4680
pFB2639	pJE051	pEGFPN3-Arl4A	human Arl4A, from pFB2635
pFB2709	pJE091	pEGFPN3-Arl4A Q79L	human Arl4A, GTP-locked; from pFB2702
pFB3143	pJE204	pEGFPN3-Arl4A T34N	human Arl4A GDP-locked from pFB3133
pFB3078	pJE184	pEGFPN3-Arl4B	human Arl4B from pFB3032
pFB2653	pJE064	pEGFPN3-Arl4C	human Arl4C, from pFB2647; now Arl4C
pFB2656	pJE067	pEGFPN3-Arl4C Q72L	human Arl4C, GTP-locked, from pFB2650; now Arl4C
pFB3144	pJE205	pEGFPN3-Arl4C T27N	human Arl4C GDP-locked; from pFB3131
pFB4704	pJE369	pEGFPN3-Arl4D	human Arl4D (ARF4L); derived from pFB4682
pF4705	pJE370	pEGFPN3-Arl5A	human Arl5A; derived from pFB4683
pFB4706	pJE371	pEGFPN3-Arl5A QL	human Arl5A; GTP-locked; derived from pFB4684
pFB4709	pJE374	pEGFPN3-Arl5B	human Arl5B; derived from pFB4687
pFB4710	pJE375	pEGFPN3-Arl5B QL	human Arl5B; GTP-locked; derived from pFB4688
pFB4707	pJE372	pEGFPN3-Arl6	human Arl6; derived from pFB4685
pFB4708	pJE373	pEGFPN3-Arl6 QL	human Arl6; GTP-locked; derived from pFB4686
pFB3080	pJE186	pEGFPN3-Arl8A	human Arl8A; from pFB3033; now Arl8A
pFB3076	pJE182	pEGFPN3-Arl8B	human Arl8B from pFB3034
pFB4711	pJE376	pEGFPN3-Arl11	human Arl11; derived from pFB4694
pFB4712	pJE377	pEGFPN3-Arl14	human Arl14; derived from pFB4690
pFB4713	pJE378	pEGFPN3-Arl15	human Arl15; derived from pFB4692
pFB4793	pJE391	pEGFPN3-Arl16	human Arl16; derived from pFB4789

continued on next page

pFB #	Creator #	Short Name	Description
pFB4791	pJE389	pEGFPN3-ARD1	human ARD1; derived from pFB4785
pFB4792	pJE390	pEGFPN3-ARD3	human ARD3; Arl13A; derived from pFB4785
pFB2666	pJE077	pEGFPN3-AFRP1	human AFRP1, from pFB2664
		Additional Constructs	
pFB2723	pJE105	pCRIITOPO-NLPdC702	human NLP aa 1-702, BamHI XhoI
pFB679		VSV-G-SP-EGFP	Gift from Kai Simons. VSV-G GFP fusion ts045 folding mutant for transport studies
pFB523	pBS84	pACT2-GM130fl	pACT2 Full length rat GM130
		Rab GTPases	
pFB4770	pAH843	pFBT9-Rab1a.QA.Y40A	Human Rab1a QA GTP locked mutant, Y40A mutation to remove aromatic from GTP binding cleft
pFB4772	pAH845	pFBT9-Rab6a.QA.Y42A	Human Rab6a QA GTP locked mutant, Y42A mutation to remove aromatic from GTP binding cleft
pFB1842	pEF49	pFBT9-Rab2 Q65L	human Rab2a Q65L GTP mutant, BamHI-SalI, derived from pFB1830, + Stop codon
pFB1842	pEF49	pFBT9-Rab2 Q65L	human Rab2a Q65L GTP mutant, BamHI-SalI, derived from pFB1830, + Stop codon
pFB1842-3	pEF49-3	pFBT9-Rab2 Q65L	human Rab2a Q65L GTP mutant, BamHI-SalI, derived from pFB1830, + Stop codon
pFB2100	pEF132	pFBT9-Rab7Q67L	human Rab7, GTP, derived from pFB2091, BamHI, XhoI
pFB2102	pEF134	pFBT9-Rab8Q67L	human Rab8, GTP, derived from pFB2087, BamHI, XhoI
pFB2104	pEF136	pFBT9-Rab10Q68L	human Rab10, GTP, derived from pFB2089, BamHI, XhoI
pFB2104		pFBT9-Rab10Q68L	human Rab10, GTP, derived from pFB2089, BamHI, XhoI
pFB2294	pAH42	pFBT9-Rab11aQ69L	Human Rab 11a, GTP Mutant, BamHI SalI, derived from pFB2270
pFB2424	pEF205	pFBT9-Rab1 Q70L	mouse Rab1 GTP restricted, derived from pBS574
pFB2424		pFBT9-Rab1 Q70L	mouse Rab1 GTP restricted, derived from pBS574
pFB2425	pEF206	pFBT9-Rab6 Q72L	human Rab6 GTP restricted, derived from pBS146 NO STOP!!!
pFB2425		pFBT9-Rab6 Q72L	human Rab6 GTP restricted, derived from pBS146 NO STOP!!!
pFB2600	pRK	pFBT9-Rab1bQ67L	Human Rab1bQ67L, GTP mutant, derived from pFB2366
pFB2601	pRK	pFBT9-Rab2bQ65L	Human Rab2bQ65L, GTP mutant, derived from pFB2368
pFB2602	pRK	pFBT9-Rab3bQ81L	Human Rab3bQ81L, GTP mutant, derived from pFB2369
pFB2603	pRK	pFBT9-Rab4aQ72L	Human Rab4aQ72L, GTP mutant, derived from pFB2582
pFB2603	pRK	pFBT9-Rab4aQ72L	Human Rab4aQ72L, GTP mutant, derived from pFB2582
pFB2604	pRK	pFBT9-Rab5bQ79L	Human Rab5bQ79L, GTP mutant, derived from pFB2370
pFB2605	pRK	pFBT9-Rab6aQ72L	Human Rab6aQ72L, GTP mutant, derived from pFB2371

continued on next page

pFB #	Creator #	Short Name	Description
pFB2605	pRK	pFBT9-Rab6aQ72L	Human Rab6aQ72L, GTP mutant, derived from pFB2371
pFB2606	pRK	pFBT9-Rab8aQ67L	Human Rab8aQ67L, GTP mutant, derived from pFB2372
pFB2607	pRK	pFBT9-Rab9aQ66L	Human Rab9aQ66L, GTP mutant, derived from pFB2373
pFB2607	pRK	pFBT9-Rab9aQ66L	Human Rab9aQ66L, GTP mutant, derived from pFB2373
pFB2608	pRK	pFBT9-Rab9bQ66L	Human Rab9bQ66L, GTP mutant, derived from pFB2374
pFB2608	pRK	pFBT9-Rab9bQ66L	Human Rab9bQ66L, GTP mutant, derived from pFB2374
pFB2609	pRK	pFBT9-Rab10Q68L	Human Rab10Q68L, GTP mutant, derived from pFB2375
pFB2609	pRK	pFBT9-Rab10Q68L	Human Rab10Q68L, GTP mutant, derived from pFB2375
pFB2610	pRK	pFBT9-Rab11aQ70L	Human Rab11aQ70L, GTP mutant, derived from pFB2376
pFB2611	pRK	pFBT9-Rab13Q67L	Human Rab13Q67L, GTP mutant, derived from pFB2377
pFB2611	pRK	pFBT9-Rab13Q67L	Human Rab13Q67L, GTP mutant, derived from pFB2377
pFB2612	pRK	pFBT9-Rab14Q70L	Human Rab14Q70L, GTP mutant, derived from pFB2378
pFB2613	pRK	pFBT9-Rab18Q67L	Human Rab18Q67L, GTP mutant, derived from pFB2591
pFB2613	pRK	pFBT9-Rab18Q67L	Human Rab18Q67L, GTP mutant, derived from pFB2591
pFB2614	pRK	pFBT9-Rab23Q68L	Human Rab23Q68L, GTP mutant, derived from pFB2380
pFB2614	pRK	pFBT9-Rab23Q68L	Human Rab23Q68L, GTP mutant, derived from pFB2380
pFB2615	pRK	pFBT9-Rab27aQ78L	Human Rab27aQ78L, GTP mutant, derived from pFB2383
pFB2616	pRK	pFBT9-Rab27bQ78L	Human Rab27bQ78L, GTP mutant, derived from pFB2384
pFB2616	pRK	pFBT9-Rab27bQ78L	Human Rab27bQ78L, GTP mutant, derived from pFB2384
pFB2617	pRK	pFBT9-Rab30Q68L	Human Rab30Q68L, GTP mutant, derived from pFB2595
pFB2617	pRK	pFBT9-Rab30Q68L	Human Rab30Q68L, GTP mutant, derived from pFB2595
pFB2618	pRK	pFBT9-Rab31Q65L	Human Rab31Q65L, GTP mutant, derived from pFB2386
pFB2619	pRK	pFBT9-Rab35Q67L	Human Rab35Q67L, GTP mutant, derived from pFB2388
pFB2620	pRK	pFBT9-Rab40cQ73L	Human Rab40cQ73L, GTP mutant, derived from pFB2599
pFB2620	pRK	pFBT9-Rab40cQ73L	Human Rab40cQ73L, GTP mutant, derived from pFB2599
pFB2861		pFBT9-Rab9aQ66L	Human Rab9aQ66L, GTP-locked, derived from pFB2585, replaces previous pFB2607
pFB2861		pFBT9-Rab9aQ66L	Human Rab9aQ66L, GTP-locked, derived from pFB2585, replaces previous pFB2607

continued on next page

pFB #	Creator #	Short Name	Description
pFB3009	pRK	pFBT9-hsRab20Q61L	Human Rab20 GTP mutant, derived from pFB2928 do not use, frameshift!
pFB3009	pRK	pFBT9-hsRab20Q61L	Human Rab20 GTP mutant, derived from pFB2928 do not use, frameshift!
pFB3011	pRK	pFBT9-hsRab24S67L	Human Rab24 potential GTP mutant S67L, derived from pFB2929
pFB3011	pRK	pFBT9-hsRab24S67L	Human Rab24 potential GTP mutant S67L, derived from pFB2929
pFB3116	pAH269	pFBT9-Rab5A.QL	Human Rab5A derived from pFB3112, GTP-lock
pFB3116	pAH269	pFBT9-Rab5A.QL	Human Rab5A derived from pFB3112, GTP-lock
pFB3123	pAH276	pFBT9-Rab32.QL	Human Rab32 derived from pFB2936, GTP-lock
pFB3204	pAh297	pFBT9-Rab22a.QL	Human Rab22a GTP Lock, derived from pFB2935
pFB3246	pAH339	pFBT9-Rab5C.QL	Human Rab5C, from U2Os cDNA, Q80L GTP-Lock
pFB3346	pRK	pFBT9-hsRab19bQ79L	Human Rab19b Q79L, GTP mutant, derived from pFB3343
pFB3346	pRK	pFBT9-hsRab19bQ79L	Human Rab19b Q79L, GTP mutant, derived from pFB3343
pFB3867	pRK	pFBT9-hsRab19b.Q79A	Human Rab19b Q79A, GTP mutant, derived from pFB3346
pFB3867	pRK	pFBT9-hsRab19b.Q79A	Human Rab19b Q79A, GTP mutant, derived from pFB3346
pFB3880	pRK	pFBT9-hsRab7Q67A	Human Rab7 Q67A, GTP mutant, derived from pFB3615
pFB4764	pAH837	pFBT9-Rab4b.Q102A	Human Rab4b Q102A GTP locked mutant, derived from pFB4763.
pFB4764	pAH837	pFBT9-Rab4b.Q102A	Human Rab4b Q102A GTP locked mutant, derived from pFB4763.
pFB4773	pAH846	pFBT9-Rab6a.QA.Y42Q	Human Rab6a QA GTP locked mutant, Y42Q mutation to remove aromatic from GTP binding cleft
pFB4774	pAH847	pFBT9-Rab27a.QA.F38A	Human Rab27a QA GTP locked mutant, F38A mutation to remove aromatic from GTP binding cleft
pFB4775	pAH848	pFBT9-Rab27a.QA.F38Q	Human Rab27a QA GTP locked mutant, F38Q mutation to remove aromatic from GTP binding cleft

References

Allan, B. and Balch, W. (1999). Protein sorting by directed maturation of Golgi compartments. *Science*, **285**, 63–66.

Allan, B., Moyer, B., and Balch, W. (2000). Rab1 recruitment of p115 into a cis-SNARE complex: programming budding COPII vesicles for fusion. *Science*, **289**(5478), 444–448.

Allan, V., Thompson, H., and McNiven, M. (2002). Motoring around the Golgi. *Nat Cell Biol*, **4**, 236–242.

Altschul, S., Madden, T., Schäffer, A., Zhang, J., Zhang, Z., Miller, W., and Lipman, D. (1997). Gapped BLAST and PSI-BLAST: a new generation of protein database search programs. *Nucleic Acids Res*, **25**(1), 3389–3402.

Amor, J., Harrison, D., Kahn, R., and Ringe, D. (1994). Structure of the human ADP-ribosylation factor 1 complexed with GDP. *Nature*, **372**, 704–708.

Appenzeller, C., Andersson, H., Kappeler, F., and Hauri, H.-P. (1999). The lectin ERGIC-53 is a cargo transport receptor for glycoproteins. *Nat Cell Biol*, **1**(6), 330–334.

Appenzeller-Herzog, C. and Hauri, H. (2006). The ER-Golgi intermediate compartment (ERGIC): in search of its identity and function. *J Cell Sci*, **119**, 2173–2183.

Baker, S., Freeman, K., Luby-Phelps, K., Pazour, G., and Besharse, J. (2003). IFT20 links kinesin II with a mammalian intraflagellar transport complex that is conserved in motile flagella and sensory cilia. *J Biol Chem*, **278**(36), 34211–34218.

Balch, W., Dunphy, W., Braell, W., and Rothman, J. (1984). Reconstitution of the transport of protein between successive compartments of the Golgi meassured by the coupled incorporation of N-acetylglucosamine. *Cell*, **39**, 405–426.

Bannykh, S., Rowe, T., and Balch, W. (1996). The organization of endoplasmic reticulum export complexes. *J Cell Biol*, **135**, 19–35.

Barlowe, C. (2003). Molecular recognition of cargo by the COPII complex: a most accomodating coat. *Cell*, **114**(4), 395–397.

Barlowe, C. and Schekman, R. (1993). SEC12 encodes a guanine nucleotide exchange factor essential for transport vesicle formation form the ER. *Nature*, **365**, 347–349.

Barlowe, C., Orci, L., Young, T., Hosobuchi, M., Hamamoto, S., Salaman, N., Rexach, M., Ravazzola, M., Amherdt, M., and Schekman, R. (1994). COPII: a membrane coat formed by Sec proteins that drive vesicle budding from the endoplasmic reticulum. *Cell*, **77**(6), 895–907.

Barr, F. (1999). A novel Rab6-interacting domain defines a family of Golgi-targeted coiled-coil proteins. *Curr Biol*, **9**(7), 381–384.

Barr, F. and Egerer, J. (2005). Golgi positioning: are we looking at the right MAP? *J Cell Biol*, **168**(7), 993–998.

Barr, F. and Short, B. (2003). Golgins in the structure and dynamics of the Golgi apparatus. *Curr Opin Cell Biol*, **15**, 405–413.

Barr, F. and Warren, G. (1996). Disassembly and reassembly of the Golgi apparatus. *Sem Cell Dev Biol*, **7**, 505–510.

Barr, F., Puype, M., Vandekerckhove, J., and Warren, G. (1997). GRASP65, a protein involved in the stacking of Golgi cisternae. *Cell*, **91**, 253–262.

Barr, F., Nakamura, N., and Warren, G. (1998). Mapping the interaction between GRASP65 and GM130 components of a protein complex involved in the stacking of Golgi cisternae. *EMBO J.*, **17**, 3258–3268.

Barr, F., Preisinger, C., Kopajtich, R., and Koerner, R. (2001). Golgi matrix proteins interact with p24 cargo receptors and aid their efficient retention in the Golgi apparatus. *J Cell Biol*, **155**(6), 885–891.

Behnia, R., Panic, B., Whyte, J., and Munro, S. (2004). Targeting of the Arf-like GTPase Arl3p to the Golgi requires N-terminal acetylation and the membrane protein Sys1p. *Nat Cell Biol*, **6**, 405–413.

Bergmann, J. (1989). Using temperature-sensitive mutants of VSV to study membrane protein biogenesis. *Meth Cell Biol*, **32**, 85–110.

Bi, X., Corpina, R., and Goldberg, J. (2002). Structure of the Sec23/24-Sar1 pre-budding complex of the COPII vesicle coat. *Nature*, **419**, 271–277.

Bisgrove, B. and Yost, H. (2006). The roles of cilia in developmental disorders and disease. *Development*, **133**, 4131–4143.

Bock, J., Matern, H., Peden, A., and Scheller, R. (2001). A genomic perspective on membrane compartment organization. *Nature*, **409**, 839–841.

Bonifacino, J. and Glick, B. (2004). The Mechanisms of Vesicle Budding and Fusion. *Cell*, **116**, 153–166.

Bonifacino, J. and Lippincott-Schwartz, J. (2003). Coat proteins: shaping membrane transport. *Mol Cell Biol*, **4**, 409–414.

Brown, H., Gutowski, S., Moomaw, C., Slaughter, C., and Sternweis, P. (1993). ADP-ribosylation factor, a small GTP-dependent regulatory protein stimulates phospholipase D activity. *Cell*, **75**, 1137–1144.

Burd, C., Strochlic, T., and Gangi-Setty, S. (2004). Arf-like GTPases: not so Arf-like after all. *TRENDS in Cell Biol*, **14**(12), 687–694.

Burkhardt, J., Echeverri, C., Nilsson, T., and Vallee, R. (1997). Overexpression of the Dynamitin (p50) subunit of the Dynactin complex disrupts dynein-dependent maintenance of membrane organelle distribution. *J Cell Biol*, **139**, 469–484.

Cai, H., Yu, S., Menon, S., Cai, Y., Lazarova, D., Fu, C., Reimisch, K., Hay, J., and Ferro-Novick, S. (2007). TRAPPI tethers COPII vesicles by binding the coat subunit Sec23. *Nature*, **445**(7130), 941–944.

Cao, X., Ballew, N., and Barlowe, C. (1998). Initial docking of ER-derived vesicles requires Uso1p and Ypt1p but is independent of SNARE proteins. *EMBO J*, **17**(8), 2156–2165.

Casenghi, M., Meraldi, P., Weinhart, U., Duncan, P., Koerner, R., and Nigg, E. (2003). Polo-like Kinase 1 Regulates Nlp, a Centrosome Protein Involved in Microtubule Nucleation. *Dev Cell*, **5**(1), 113–125.

Chabin-Brion, K., Marceiller, J., Perez, F., Settegrana, C., Drechou, A., Durand, G., and Poüs, C. (2001). The Golgi Complex Is a Microtubule-organizing Organelle. *Mol Biol Cell*, **12**, 2047–2060.

Chardin, P., Paris, S., Antonny, B., Robineau, S., Beraud-Dufour, S., Jackson, C., and Chabre, M. (1996). A human exchange factor for ARF contains Sec7- and pleckstrin-homology domains. *Nature*, **384**, 481–484.

Chavrier, P. and Goud, B. (1999). The role of ARF and Rab GTPases in membrane transport. *Curr Opin Cell Biol*, **11**, 466–475.

Chen, J., Fucini, R., Lacomis, L., Erdjument-Bromage, H., Tempst, P., and Stamnes, M. (2005). Coatomer-bound Cdc42 regulates dynein recruitment to COPI vesicles. *J Cell Biol*, **169**, 383–389.

Chen, Y., Chen, P., Chen, C., Sharp, Z., and Lee, W. (1999). Thyroid hormone, T3-dependent phosphorylation and translocation of Trip230 from the Golgi complex to the nucleus. *Proc Natl Acad Sci USA*, **96**, 4443–4448.

Christoforidis, S. and Zerial, M. (2000). Purification and identification of novel Rab effectors using affinity chromatography. *Methods in Enzymology*, **20**(4), 403–410.

Clary, D., Griff, I., and Rothman, J. (1990). SNAPs, a family of NSF attachment proteins involved in intracellular membrane fusion in animals and yeast. *Cell*, **61**(4), 709–721.

Cole, D., Diener, D., Himelblau, A., Beech, P., Fuster, J., and Rosenbaum, J. (1998). *Chlamydomonas* kinesin-II-dependent intraflagellar transport (IFT): IFT particles contain proteins required for ciliary assembly in *Caenorhabditis elegans* sensory neurons. *J Cell Biol*, **141**, 993–1008.

DeMarco, V., Burkhard, P., LeBot, N., Vernos, I., and Hoenger, A. (2001). Analysis of heterodimer formation by Xklp3A/B, a newly cloned kinesin-II from *Xenopus laevis*. *EMBO J*, **20**, 3370–3379.

DeMatteis, M. and Morrow, J. (2000). Spectrin tethers and mesh in the biosynthetic pathway. *J Cell Sci*, **113**, 2331–2343.

DePina, A. and Langford, G. (1999). Vesicle Transport: The Role of Actin Filaments and Myosin Motors. *Micr Res and Tech*, **47**, 93–106.

DeRobertis, E. (1958). Morphogenesis of retinal rods: an electron microscope study. *J Biophys Biochem Cytol*, **2**, 209–216.

Diao, A., Rahman, D., Pappin, D., Lucocq, J., and Lowe, M. (2003). The coiled-coil membrane protein golgin-84 is a novel rab effector required for Golgi ribbon formation. *J Cell Biol*, **160**, 201–212.

Dominguez, M., Dejgard, K., Füllekrug, J., Dahan, S., Fazel, A., Paccaud, J.-P., Thomas, D., Bergeron, J., and Nilsson, T. (1998). gp25L/emp24/p24 protein family members of the cis-Golgi network bind both COPI and II coatomer. *J Cell Biol*, **140**, 751–765.

Drin, G., Casella, J., Gautier, R., Boehmer, T., Schwartz, T., and Antonny, B. (2007). A general amphipathic α-helical motif for sensing membrane curvature. *Nature Struct Mol Biol*, **14**(2), 138–146.

Dubois, T., Paleotti, O., Mironov, A., Fraisier, V., Stradal, T., DeMatteis, M., Franco, M., and Chavrier, P. (2005). Golgi-localized GAP for Cdc42 functions downstream of ARF1 to control Arp2/3 complex and F-actin dynamics. *Nat Cell Biol*, **7**, 353–364.

Dunphy, W. and Rothman, J. (1985). Compartment organization of the Golgi stack. *Cell*, **42**(1), 13–21.

Durfee, T., Becherer, K., Chen, P., Yeh, S., Yang, Y., Kilburn, A., and Elledge, S. (1993). The retinoblastoma protein associates with the protein phosphatase type 1 catalytic subunit. *Genes Dev*, **7**, 555–569.

Efimov, A., Kharitonov, A., Efimova, N., Loncarek, J., Miller, P., Andreyeva, N., Gleeson, P., Galjart, N., Maia, A., McLeod, I., Yates, J., Maiato, I., Khodjakov, A., Akhmanova, A., and Kaverina, I. (2007). Asymmetric CLASP-Dependent Nucleation of Noncentrosomal Microtubules at the trans-Golgi Network. *Dev Cell*, **12**, 917–930.

Egea, G., Lazaro-Dieguez, F., and Vilella, M. (2006). Actin dynamics at the Golgi complex in mammalian cells. *Curr Opin Cell Biol*, **18**, 168–178.

Elbashir, S., Harborth, J., Lendeckel, W., Yalcin, A., Weber, K., and Tuschl, T. (2001). Duplexes of 21-nucleotide RNAs mediate RNA interference in cultured mammalian cells. *Nature*, **411**, 494–498.

Farquhar, M. and Palade, G. (1998). The Golgi apparatus: 100 years of progress and controversy. *Trends Cell Biol.*, **8**(1), 2–10.

Fasshauer, D., Sutton, R., Brunger, A., and Jahn, R. (1998). Conserved structural features of the synaptic fusion complex: SNARE proteins reclassified as Q- and R- SNAREs. *Proc Natl Acad Sci USA*, **95**, 15781–15786.

Feiguin, F., Ferreira, A., Kosik, K., and Caceres, A. (1994). Kinesin-mediated organelle translocation revealed by specific cellular manipulations. *J Cell Biol*, **127**, 1021–1039.

Fiedler, K., Viet, M., Stamnes, M., and Rothman, J. (1996). Bimodal interaction of coatomer with the p24 family of putative cargo receptors. *Science*, **273**, 1396–1399.

Follit, J., Tuft, R., Fogarty, K., and Pazour, G. (2006). The intraflagellar transport protein IFT20 is associated with the Golgi complex and is required for cilia assembly. *Mol Biol Cell*, **17**(9), 3781–92.

Friggi-Grelin, F., Rabouille, C., and Therond, P. (2006). The cis-Golgi Drosophila GMAP has a role in anterograde transport and Golgi organization in vivo, similar to its mammalian ortholog in tissue culture cells. *Eur J Cell Biol*, **85**(11), 1155–1166.

Fromme, J. and Schekman, R. (2005). COPII-coated vesicles: flexible enough for large cargo? *Curr Opin in Cell Biol*, **17**, 1–8.

Fuchs, E., Haas, A., Spooner, R., Yoshimura, S.-I., Lord, J., and Barr, F. (2007). Specific Rab GTPase-activating proteins define the Shiga toxin and epidermal growth factor uptake pathway. *J Cell Biol*, **177**(6), 1133–1143.

Fukuda, M., Kuroda, T., and Mikoshiba, K. (2002). Slac2-a/melanophilin, the missing link between Rab27 and myosin Va: implications of a tripartite protein complex for melanosome transport. *J Biol Chem*, **277**, 12432–12436.

Gangi-Setty, S., Shin, M., Yoshino, A., Marks, M., and Burd, C. (2003). Golgi recruitment of GRIP domain proteins by Arf-like GTPase 1 (Arl1p) is regulated by the Arf-like GTPase 3 (Arl3p). *Curr Biol*, **13**, 401–404.

Gao, Y. and Sztul, E. (2001). A Novel Interaction of the Golgi Complex with the Vimentin Intermediate Filament Cytoskeleton. *J Cell Biol*, **152**(5), 877–893.

Garcia-Mata, R., Szul, T., Alvarez, C., and Sztul, E. (2003). ADP-ribosylation factor/COPI-dependent events at the endoplasmic reticulum-Golgi interface are regulated by the guanine nucleotide exchange factor GBF1. *Mol Cell Biol*, **14**, 2250–2261.

Gillingham, A. and Munro, S. (2003). Coiled-coil proteins and membrane traffic. *Biochim Biophys Acta*, **1641**, 71–85.

Gillingham, A. and Munro, S. (2007). The Small G Proteins of the Arf Family and Their Regulators. *Annu Rev Cell Dev Biol*, **23**, 579–611.

Gillingham, A., Tong, A., Boone, C., and Munro, S. (2004). The GTPase Arf1p and the ER to Golgi cargo receptor Erv14p cooperate to recruit the golgin Rud3p to the cis-Golgi. *J Cell Biol.*, **167**(2), 281–292.

Goldberg, J. (1999). Structural and functional analysis of the ARF1-ARFGAP complex reveals a role for coatomer in GTP hydrolysis. *Cell*, **96**, 893–902.

Golgi, C. (1898). Sur la structure des cellules nerveuses. *Arch Ital Biol*, **30**, 60–71.

Griffiths, G. and Simons, K. (1986). The trans Golgi network: sorting at the exit site of the Golgi complex. *Science*, **234**, 438–443.

Gyoeva, F., Bybikova, E., and Minin, A. (2000). An isoform of kinesin light chain specific for the Golgi complex. *J Cell Sci*, **113**(11), 2047–2054.

Haas, A., Fuchs, E., Kopajtich, R., and Barr, F. (2005). A GTPase-activating protein controls Rab5 function in endocytic trafficking. *Nat Cell Biol*, **7**(9), 887–893.

Hanson, P., Otto, H., Barton, N., and Jahn, R. (1995). The N-ethylmaleimide-sensitive fusion protein and alpha-SNAP induce a conformational change in syntaxin. *J Biol Chem*, **269**, 16955–16961.

Hanson, P., Roth, R., Morisaki, H., Jahn, R., and Heuser, J. (1997). Structure and conformational changes in NSF and its membrane receptor complexes visualised by quick-freeze/deep etch electron microscopy. *Cell*, **90**, 523–535.

Harter, C., Pavel, J., Coccia, F., Draken, E., Wegehingel, S., Tschochner, H., and Wieland, F. (1996). Nonclathrin coat protein γ, a subunit of coatomer, binds to the cytoplasmic dilysine motif of membrane proteins of the early secretory pathway. *Proc Natl Acad Sci*, **93**, 1902–1906.

Hauri, H.-P., Kappeler, F., Andersson, H., and Appenzeller, C. (2000). ERGIC-53 and traffic in the secretory pathway. *J Cell Sci*, **113**, 587–596.

Haynes, L., Thomas, G., and Burgoyne, R. (2005). Interaction of neuronal calcium sensor-1 and ADP-ribosylation factor 1 allows bidirectional control of phosphatidylinositol 4-kinase (beta) and trans-Golgi network-plasma membrane traffic. *J Biol Chem*, **280**, 6047–6054.

Hehnly, H. and Stamnes, M. (2007). Regulating cytoskeleton-based vesicle motility. *FEBS Letters*, **581**, 2112–2118.

Hirokawa, N. (1998). Kinesin and Dynein Superfamily Proteins and the Mechanism of Organelle Transport. *Science*, **279**, 519–526.

Hirokawa, N. and Takemura, R. (2004). Kinesin superfamily proteins and their various functions and dynamics. *Exp Cell Res*, **301**, 50–59.

Ho, W., Allan, V., vanMeer, G., Berger, E., and Kreis, T. (1989). Reclustering of scattered Golgi elements occurs along microtubules. *Eur J Cell Biol*, **48**, 250–263.

Hofmann, I. and Munro, S. (2006). An N-terminally acetylated Arf-like GTPase is localised to lysosomes and affects their motility. *J Cell Sci*, **119**(8), 1494–1503.

Hofmann, I., Thompson, A., Sanderson, C., and Munro, S. (2007). The Arl4 family of small G proteins can recruit the cytohesin Arf6 exchange factors to the plasma membrane. *Curr Biol*, **17**(8), 711–716.

Holleran, E., Tokito, M., Karki, S., and Holzbaur, E. (1996). Centractin (ARP1) associates with spectrin revealing a potential mechanism to link dynactin to intracellular organelles. *J Cell Biol*, **276**, 1815–1829.

Hoogenraad, C., Akhmanova, A., Howell, S., Dortland, B., DeZeeuw, C., Willemsen, R., Visser, P., Grosveld, F., and Galjart, N. (2001). Mammalian Golgi-associated Bicaudal-D2 functions in the dynein-dynactin pathway by interacting with these complexes. *EMBO J*, **20**, 4041–4054.

Hui, N., Nakamura, N., Slusarewicz, P., and Warren, G. (1998). Purification of rat liver Golgi stacks. In *Cell Biology: A Laboratory Handbook*, volume 2, pages 46–55. Academic Press.

Infante, C., Ramos-Morales, F., Fedriani, C., Bornens, M., and Rios, R. (1999). GMAP-210, A Cis-Golgi Network-associated Protein, Is a Minus End Microtubule-binding Protein. *J Cell Biol*, **145**(1), 83–98.

James, P., Halladay, J., and Craig, E. (1996). Genomic libraries and a host strain designed for highly efficient two-hybrid selection in yeast. *Genetics*, **144**, 1425–1436.

Jekely, G. and Arendt, D. (2006). Evolution of intraflagellar transport from coated vesicles and autogenous origin of the eukaryotic cilium. *BioEssays*, **28**, 191–198.

Johannes, L. and Goud, B. (1998). Surfing on a retrograde wave: how does Shiga toxin reach the endoplasmic reticulum? *Trends Cell Biol*, **8**(4), 158–162.

Johnson, K. (1995). Keeping the beat: form meets function in the *Chlamydomonas* flagellum. *BioEssays*, **17**, 847–854.

Kahn, R. and Gilman, A. (1986). The protein cofactor necessary for ADP-ribosylation of Gs by cholera toxin is itself a GTP binding protein. *J Biol Chem*, **261**, 7906–7911.

Kappeler, F., Klopfenstein, D. R., Foguet, M., Paccaud, J., and Hauri, H.-P. (1997). The recycling of ERGIC-53 in the early secretory pathway. ERGIC-53 carries a cytosolic endoplasmic reticulum-exit determinant interacting with COPII. *J Biol Chem*, **272**, 31801–31808.

Kawamoto, K., Yoshida, Y., Tamaki, H., Torii, S., Shinotsuka, C., Yamashina, S., and Nakayama, K. (2002). GBF1, a guanine nucleotide exchange factor for ADP-ribosylation factors, is localized to the cis-Golgi and involved in membrane association of the COPI coat. *Traffic*, **3**, 483–495.

Khodjakov, A. and Rieder, C. (1999). The sudden recruitment of γ-tubulin to the centrosome at the onset of mitosis and its dynamic exchange throughout the cell cycle, do not require microtubules. *J Cell Biol*, **146**, 585–596.

Kim, D. (2003). Characterization of Grp1p, a novel cis-Golgi matrix protein. *Biochem Biophys Res Com*, **303**, 370–378.

Kirchhausen, T. (2000). Three ways to make a vesicle. *Mol Cell Biol*, **1**, 187–198.

Klausner, R., Donaldson, J., and Lippincott-Schwartz, J. (1992). Brefeldin A: Insights into the Control of Membrane Traffic and Organelle Structure. *J Cell Biol*, **116**(5), 1071–1080.

Klebe, C., Prinz, H., Wittinghofer, A., and Goody, R. (1995). The kinetic mechanism of Ran–nucleotide exchange catalyzed by RCC1. *Biochemistry*, **34**(39), 12543–12552.

Koeminski, K., Johnson, K., Forscher, P., and Rosenbaum, J. (1993). A motility in the eukaryotic flagellum unrelated to flagellar beating. *Proc Natl Acad Sci USA*, **90**, 5519–5523.

Kozminski, K., Beech, P., and Rosenbaum, J. (1995). The Chlamydomonas kinesin-like protein FLA10 is involved in motility associated with the flagellar membrane. *J Cell Biol*, **131**, 1517–1527.

Lahtinen, U., Dahllof, B., and Saraste, J. (1992). Characterization of a 58 kDa cis-Golgi protein in pancreatic exocrine cells. *J Cell Sci*, **103**, 321–333.

Lazaro-Dieguez, F., Jimenez, N., Barth, G., Koster, A., Renau-Piqueras, J., Lopis, J., Burger, K., and Egea, G. (2006). Actin Filaments Are Involved in the Maintenance of Golgi Cisternae Morphology and Intra-Golgi pH. *Cell Motil Cytoskeleton*, **63**(12), 778–791.

LeBot, N., Antony, C., White, J., Karsenti, F., and Vernos, I. (1998). Role of xklp3, a subunit of the Xenopus kinesin II heterotrimeric complex, in membrane transport between the endoplasmic reticulum and the Golgi apparatus. *J Cell Biol*, **143**(6), 1559–1573.

Lederkremer, G., Cheng, Y., Petre, B., Vogan, F., Springer, S., Schekman, R., Walz, T., and Kirchhausen, T. (2001). Structure of the Sec23/24p and Sec13p/31p complex of COPII. *Proc Natl Acad Sci USA*, **98**(19), 10704–10709.

Letourneur, F., Gaynor, E., Hennecke, S., Demolliere, C., Duden, R., and Emr, S. (1994). Coatomer is essential for retrieval of dilysine-tagged proteins to the endoplasmic reticulum. *Cell*, **79**, 1199–1207.

Lewis, A. and Bridgeman, P. (1992). Nerve growth cone lamellipodia contain two populations of actin filaments that differ in organization and polarity. *J Cell Biol*, **119**, 1219–1243.

Linstedt, A. and Hauri, H. (1993). Giantin, a novel conserved Golgi membrane protein containing a cytoplasmic domain of at least 350 kDa. *Mol Biol Cell*, **4**, 679–693.

Lu, L., Tai, G., and Hong, W. (2004). Autoantigen Golgin-97, an effector of Arl1 GTPase, participates in traffic from the endosome to the trans-golgi network. *Mol Biol Cell*, **15**(10), 4426–4443.

Lu, L., Tai, G., and Hong, W. (2005). Interaction of Arl1 GTPase with the GRIP domain of Golgin-245 as assessed by GST (glutathione-S-transferase) pull-down experiments. *Methods Enzymol.*, **404**, 432–441.

Luna, E. and Hitt, A. (1992). Cytoskeleton–plasma membrane interactions. *Science*, **258**, 955–963.

Majoul, I., Straub, M., Hell, S., Duden, R., and Soling, H. (2001). KDEL-cargo regulates interactions between proteins involved in COPI vesicle traffic: Measurements in living cells using FRET. *Dev Cell*, **1**, 139–153.

Mandiyan, V., Andreev, J., and Hubbard, S. (1999). Crystal structure of the ARF-GAP domain and ankyrin repeats of PYK2-associated protein β. *EMBO J*, **276**, 6890–6898.

Marsh, B., Mastronarde, D., Buttle, K., Howell, K., and McIntosh, J. (2001). Organellar relationships in the Golgi region of the pancreatic beta cell line, HIT-T15, visualized by high-resolution electron tomography. *Proc Natl Acad Sci USA*, **98**, 2399–2406.

Marszalek, J. and Goldstein, L. (2000). Understanding the functions of kinesin-II. *Biochim Biophys Acta*, **1496**, 142–150.

Matanis, T., Akhmanova, A., Wulf, P., DelNery, E., Weide, T., Stepanova, T., Galjart, N., Grosveld, F., Goud, B., DeZeeuw, C., Barnekow, A., and Hoogenraad, C. (2002). Bicaudal-D regulates COPI-independent Golgi-ER transport by recruiting the dynein-dynactin motor complex. *Nat Cell Biol*, **4**(12), 986–992.

Matas, O., Martinez-Menarguez, J., and Egea, G. (2004). Association of Cdc42/N-WASP/Arp2/3 signaling pathway with Golgi membranes. *Traffic*, **5**, 838–846.

Maxfield, F. and McGraw, T. (2004). Endocytic Recycling. *Mol Cell Biol*, **5**, 121–132.

Miaczynska, M. and Zerial, M. (2002). Mosaic organization of the endocytic pathway. *Exp Cell Res*, **272**, 8–14.

Miki, H., Setou, M., Kaneshiro, K., and Hirokawa, N. (2001). All kinesin superfamily protein, KIF, genes in mouse and human. *Proc Natl Acad Sci USA*, **98**, 7004–7011.

Mimori-Kiyosue, Y., Grigoriev, I., Lansbergen, G., Sasaki, H., Matsui, C., Severin, F., Galjart, N., Grosveld, F., Vorobjev, I., Tsukita, S., and Akhmanova, A. (2005). CLASP1 and CLASP2 bind to EB1 and regulate microtubule plus-end dynamics at the cell cortex. *J Cell Biol*, **168**, 131–153.

Mollinari, C., Kleman, J.-P., Jiang, W., Schoehn, G., Hunter, T., and Margolis, R. (2002). PRC1 is a microtubule binding and bundling protein essential to maintain the mitotic spindle midzone. *J Cell Biol*, **157**(7), 1175–1186.

Morre, D. and Mollenhauer, H. (1964). Isolation of the Golgi Apparatus from Plant Cells. *J Cell Biol*, **23**, 295–305.

Morre, D., Hamilton, R., Mollenhauer, H., Mahley, R., Cunningham, W., Cheetham, R., and Lequire, V. (1970). Isolation of a Golgi apparatus-rich fraction from rat liver. I. Method and morphology. *J Cell Biol*, **44**, 484–491.

Moyer, B., Allan, B., and Balch, W. (2001). Rab1 interaction with a GM130 effector complex regulates COPII vesicle cis-Golgi tethering. *Traffic*, **2**(4), 268–276.

Muniz, M., Nuoffer, C., and Hauri, H.-P. (2000). The Emp24 complex recruits a specific cargo molecule into endoplasmic reticulum-derived vesicles. *J Cell Biol*, **148**, 925–930.

Munro, S. (2005). The Arf-like GTPase Arl1 and its role in membrane traffic. *Biochem Soc Trans*, **33**(4), 601–605.

Munro, S. and Nichols, B. (1999). The GRIP domain - a novel Golgi-targeting domain found in several coiled-coil proteins. *Curr Biol*, **9**, 377–380.

Murphy, S., Urbani, L., and Stearns, T. (1998). The mammalian γ-tubulin complex contains homologues of the yeast spindle pole body components spc97p and spc98p. *J Cell Biol*, **141**, 663–674.

Murshid, A. and Presley, J. (2004). ER-to-Golgi transport and cytoskeletal interactions in animal cells. *Cell Mol Life Sci*, **61**, 133–145.

Nachury, M., Lokev, A., Zhang, Q., Westlake, C., Peränen, J., Merdes, A., Slusarski, D., Scheller, R., Bazan, J., Sheffield, V., and Jackson, P. (2007). A core complex of BBS

proteins cooperates with the GTPase Rab8 to promote ciliary membrane biogenesis. *Cell*, **129**(6), 1201–1213.

Nakamura, N., Rabouille, C., Watson, R., Nilsson, T., Hui, N., Slusarewicz, P., Kreis, T., and Warren, G. (1995). Characterization of a cis-Golgi Matrix Protein, GM130. *J Cell Biol*, **131**(6), 1715–1726.

Nakamura, N., Lowe, M., Levine, T., Rabouille, C., and Warren, G. (1997). The vesicle docking protein p115 binds GM130 a cis-Golgi matrix protein, in a mitotically regulated manner. *Cell*, **89**, 445–455.

Nakamura, N., Yamazaki, S., Sato, K., Nakano, A., Sakaguchi, M., and Mihara, K. (1998). Identification of potential regulatory elements for the transport of Emp24p. *Mol Biol Cell*, **9**, 3493–3503.

Neef, R., Grueneberg, U., Kopajtich, R., Li, X., Nigg, E., Sillje, H., and Barr, F. (2007). Choice of Plk1 docking partners during mitosis and cytokinesis is controlled by the activation state of Cdk1. *Nat Cell Biol*, **9**(4), 436–444.

Nehls, S., Schnapp, E., Cole, N., Zaal, K., Kenworthy, A., Roberts, T., Ellenberg, J., Presley, J., Siggia, E., and Lippincott-Schwartz, J. (2000). Dynamics and retention of misfolded proteins in native ER membranes. *Nat Cell Biol*, **2**, 288–295.

Neu, M., Brachvogel, V., Oschkinat, H., Zerial, M., and Metcalf, P. (1997). Rab7: NMR and kinetics analysis of intact and C-terminal truncated constructs. *Proteins*, **27**, 204–209.

Nichols, B. and Pelham, H. (1997). SNAREs and membrane fusion in the Golgi apparatus. *Biochim Biophys Acta*, **13**(1404), 9–31.

Nishimura, N. and Balch, W. (1997). A di-acidic signal required for selective export from the endoplasmic reticulum. *Science*, **277**, 556–558.

Nonaka, S., Tanaka, Y., Takeda, S., and Harada, A. (1998). Randomization of the right-left asymmetry due to loss of nodal cilia generating leftward flow of extraembryonic fluid in mice lacking KIF3B motor protein. *Cell*, **95**, 829–837.

Nonaka, S., Hidetaki, S., Saijoh, Y., and Hamada, H. (2002). Determination of left-right patterning of the mouse embryo by artificial nodal flow. *Nature*, **418**, 96–99.

Novick, P., Field, C., and Schekman, R. (1980). Identification of 23 complementation groups required for post-translational events in the yeast secretory pathway. *Cell*, **21**, 205–215.

Palade, G. (1975). Intracellular Aspects of the Process of Protein Synthesis. *Science*, **189**, 867.

Pan, J. and Snell, W. (2003). Kinesin II and regulated intraflagellar transport of Chlamydomonas aurora protein kinase. *J Cell Sci*, **116**, 2179–2186.

Panic, B., Whyte, J., and Munro, S. (2003a). The ARF-like GTPases Arl1p and Arl3p act in a pathway that interacts with vesicle-tethering factors at the Golgi apparatus. *Curr.Biol.*, **13**(5), 405–410.

Panic, B., Perisic, O., Dimitry, B., Williams, R., and Munro, S. (2003b). Structural Basis for Arl1-Dependent Targeting of Homodimeric GRIP Domains to the Golgi Apparatus. *Mol Cell*, **12**, 863–874.

Pasqualato, S., Renault, L., and Cherfils, J. (2002). Arf, Arl, Arp and Sar proteins: a family of GTP-binding proteins with a structural device for 'front-back' communication. *EMBO reports*, **3**(11), 1035–1041.

Pazour, G., Wilkerson, C., and Witman, G. (1998). A dynein light chain is essential for retrograde particle movement in intraflagellar transport (IFT). *J Cell Biol*, **141**, 979–992.

Pazour, G., Dickert, B., and Witman, G. (1999). The DHC1b(DHC2) isoform of cytoplasmic dynein is required for flagellar assembly. *J Cell Biol*, **144**, 473–481.

Pellham, H. (1990). The retention signal for soluble proteins of the endoplasmic reticulum. *Trends Biochem. Sci*, **15**, 483–486.

Pereira-Leal, J. and Seabra, C. (2000). The Mammalian Rab Family of Small GTPases: Definition of Family and Subfamily Sequence Motifs Suggests a Mechanism for Functional Specificity in the Ras Superfamily. *J Mol Biol*, **301**, 1077–1087.

Perkins, L., Hedgecock, E., Thomson, J., and Culotti, J. (1986). Mutant sensory cilia in the nematode *Caenorhabditis elegans*. *Dev Biol*, **117**, 456–87.

Pernet-Gallay, K., Antony, C., Johannes, L., Bornens, M., Goud, B., and Rios, R. (2002). The Overexpression of GMAP-210 Blocks Anterograde and Retrograde Transport Between the ER and the Golgi Apparatus. *Traffic*, **3**, 822–832.

Pfeffer, S. (2001). Rab GTPases: specifying and deciphering organelle identity and function. *TRENDS Cell Biol*, **11**(12), 487–491.

Pfeffer, S. and Aivazian, D. (2004). Targeting Rab GTPases to distinct membrane compartments. *Mol Cell Biol*, **5**, 886–896.

Piperno, G., Siuda, E., Henderson, S., Segil, M., Vaananen, H., and Sassaroli, M. (1998). Distinct mutants of retrograde intraflagellar transport (IFT) share similar morphological and molecular defects. *J Cell Biol*, **143**, 1591–1601.

Porter, M. and Sale, W. (2000). The 9+2 axoneme anchors multiple inner arm dyneins and a network of kinases and phosphatases that control motility. *J Cell Biol*, **151**, 71–79.

Powers, J. and Barlowe, C. (1998). Transport of Axl2p depends on Erv14p, an ER-vesicle protein related to the *Drosophila cornichon* gene product. *J Cell Biol*, **142**, 1209–1222.

Powers, J. and Barlowe, C. (2002). Erv14p directs a transmembrane secretory protein into COPII-coated transport vesicles. *Mol Biol Cell*, **13**, 880–891.

Preisinger, C., Korner, R., Wind, M., Lehmann, W., Kopajtich, R., and Barr, F. (2005). Plk1 docking to GRASP65 phosphorylated by Cdk1 suggests a mechanism for Golgi checkpoint signalling. *EMBO J*, **24**, 753–765.

Qin, H., Diener, D., Geimer, S., Cole, D., and Rosenbaum, J. (2004). Intraflagellar transport (IFT) cargo: IFT transports flagellar precursors to the tip and turnover products to the cell body. *J Cell Biol*, **164**(2), 255–266.

Qin, H., Burnette, D., Bae, Y., Forscher, P., Barr, M., and Rosenbaum, J. (2005). Intraflagellar transport is required for the vectorial movement of TRPV channels in the ciliary membrane. *Curr Biol*, **15**, 1695–1699.

Rak, A., Pylypenko, O., Durek, T., Watzke, A., Kushnir, S., Brunsveld, L., Waldmann, L. H., Goody, R., and Alexandrov, K. (2003). Structure of Rab GDP-dissociation inhibitor in complex with prenylated YPT1 GTPase. *Science*, **302**, 646–650.

Raynaud-Messina, B. and Merdes, A. (2007). γ-tubulin complexes and microtubule organization. *Curr Opin Cell Biol*, **19**, 24–30.

Reddy, J., Burguete, A., Sridevi, K., Ganley, I., Nottingham, R., and Pfeffer, S. (2006). A Functional Role for the GCC185 Golgin in Mannose 6-Phosphate Receptor Recycling. *Mol Biol Cell*, **17**(10), 4353–4363.

Ringo, D. (1967). The arrangement of subunits in flagellar fibres. *J Ultrastruct Res*, **17**(3), 266–277.

Rios, R. and Bornens, M. (2003). The Golgi apparatus at the cell centre. *Curr Opin Cell Biol*, **15**(1), 60–66.

Rios, R., Tassin, A.-M., Celati, C., Antony, C., Boissier, M.-C., Homberg, J.-C., and Bornens, M. (1994). A Peripheral Protein Associated with the cis-Golgi Network Redistributes in the Intermediate Compartment upon Brefeldin A Treatment. *J Cell Biol*, **125**(5), 997–1013.

Rios, R., Sanchis, A., Tassin, A., Fedriani, C., and Bornens, M. (2004). GMAP-210 Recruits γ-Tubulin Complexes to cis-Golgi Membranes and Is Required for Golgi Ribbon Formation. *Cell*, **118**, 323–335.

Rojo, M., Pepperkok, R., Emery, G., Kellner, R., Stang, E., Parton, R., and Gruenberg, J. (1997). Involvement of the transmembrane protein p23 in bio-synthetic protein transport. *J Cell Biol*, **139**, 1119–1135.

Rosenbaum, J. and Witman, G. (2002). Intraflagellar Transport. *Mol Cell Biol*, **3**, 813–825.

Rothman, J. (1994). Mechanisms of intracellular protein transport. *Nature*, **372**, 55–62.

Rothman, J., Fries, E., Dunphy, W., and Urbanis, L. (1982). The Golgi apparatus, coated vesicles, and the sorting problem. *Cold Spring Harb Symp Quant Biol*, **46**, 797–805.

Sambrook, J., Fritsch, E., and Maniatis, T. (1989). *Molecular Cloning: A Laboratory Manual (Second Edition)*. Cold Spring Harbor Laboratory Press.

Sapperstein, S., Walter, D., Grosvenor, A., Heuser, J., and Waters, M. (1995). p115 is a general vesicular transport factor related to the yeast ER to Golgi transport factor Uso1p. *Proc Natl Acad Sci USA*, **92**, 522–526.

Satoh, A., Wang, Y., Malsam, J., Beard, M., and Warren, G. (2003). Golgin-84 is a rab1 binding partner involved in Golgi structure. *Traffic*, **4**, 153–161.

Scheffzek, K., Ahmadian, M., and Wittinghofer, A. (1998). GTPase-activating proteins: helping hands to complement an active site. *TRENDS Biochem Sci*, **23**(7), 257–262.

Schindler, R., Itin, C., Zerial, M., Lottspeich, F., and Hauri, H. (1993). ERGIC-53, a membrane protein of the ER-Golgi intermediate compartment, carries and ER retention motif. *Eur J. Cell Biol*, **61**, 1–9.

Scholey, J. (2003). Intraflagellar Transport. *Annu Rev Cell Dev Biol*, **19**, 423–443.

Scholey, J. and Anderson, K. (2006). Intraflagellar Transport and Cilium-Based Signalling. *Cell*, **125**, 439–442.

Schweizer, A., Fransen, J., Bächi, T., Ginsel, L., and Hauri, H.-P. (1988). Identification, by a monoclonal antibody, of a 53-kDa protein associated with a tubulo-vesicular compartment at the cis-side of the Golgi apparatus. *J Cell Biol*, **107**, 1643–1653.

Sciaky, N., Presley, J., Smith, C., Zaal, K., Cole, N., Moreira, J., Terasaki, M., Siggig, E., and Lippincott-Schwartz, J. (1997). Golgi Tubule Traffic and the Effects of Brefeldin A Visualized in Living Cells. *J.Cell.Biol.*, **139**(5), 1127–1155.

Seemann, J., Jokitalo, E., Pypaert, M., and Warren, G. (2000). Matrix proteins can generate the higher order architecture of the Golgi apparatus. *Nature*, **407**, 1022–1026.

Setty, S., Strochlic, T., Tong, A., Boone, C., and Burd, C. (2004). Golgi targeting of ARF-like GTPase Arl3p requires its Nα-acetylation and the integral membrane protein Sys1p. *Nat Cell Biol*, **6**, 414–419.

Sharer, J., Shern, J., VanValkenburgh, H., Wallace, D., and Kahn, R. (2002). ARL2 and BART enter mitochondria and bind the adenine nucleotide transporter. *Mol Biol Cell*, **13**, 71–83.

Shibata, Y., Voeltz, G., and Rapoport, T. (2006). Rough Sheets and Smooth Tubules. *Cell*, **126**, 435–439.

Shinotsuka, C., Yoshida, Y., Kawamoto, K., Takatsu, H., and Nakayama, K. (2002). Overexpression of an ADP-ribosylation factor-guanine nucleotide exchange factor, BIG2, uncouples Brefeldin A -induced adaptor protein-1 coat dissociation and membrane tubulation. *J Biol Chem*, **277**, 9468–9473.

Short, B. and Barr, F. (2004). Membrane Fusion: Caught in a Trap. *Curr Biol*, **14**, 187–189.

Short, B., Preisinger, C., Koerner, R., Kopajtich, R., Byron, O., and Barr, F. (2001). A GRASP55-rab2 effector complex linking Golgi structure to membrane traffic. *J Cell Biol*, **155**, 877–883.

Short, B., Preisinger, C., Schaletzky, J., Kopajtich, R., and Barr, F. (2002). The Rab6 GTPase regulates recruitment of the dynactin complex to Golgi membranes. *Curr Biol*, **12**(20), 1792–1795.

Short, B., Haas, A., and Barr, F. (2005). Golgins and GTPases, giving identity and structure to the Golgi apparatus. *Biochim Biophys Acta*, **1744**, 383–395.

Shorter, J. and Warren, G. (1999). A role for the vesicle tethering protein, p115, in the post-mitotic stacking of reassembling Golgi cisternae in a cell-free system. *J Cell Biol*, **146**, 57–70.

Shorter, J., Watson, R., Giannakou, M., Clarke, M., Warren, G., and Barr, F. (1999). GRASP55, a second mammalian GRASP protein involved in the stacking of Golgi cisternae in a cell-free system. *EMBO J*, **18**, 4949–4960.

Shorter, J., Matthew, B., Seemann, J., Dirac-Svejstrup, A., and Warren, G. (2002). Sequential tethering of Golgins and catalysis of SNAREpin assembly by the vesicle-tethering protein p115. *J Cell Biol*, **157**(1), 45–62.

Sivars, U., Aivazian, D., and Pfeffer, S. (2003). Yip3 catalyses the dissociation of endosomal Rab-GDI complexes. *Nature*, **425**, 856–859.

Slusarewicz, P., Nilsson, T., Hui, N., Watson, R., and Warren, G. (1994). Isolation of a matrix that binds medial Golgi enzymes. *J Cell Biol*, **124**, 405–413.

Sollner, T., Whiteheart, S., Brunner, M., Erdjument-Bromage, H., Geromanos, S., Tempst, P., and Rothman, J. (1993). SNAP receptors implicated in vesicle targeting and fusion. *Nature*, **362**, 318–324.

Sonnichsen, B., Lowe, M., Levine, T., Jamsa, E., Dirac-Svejstrup, B., and Warren, G. (1998). A role for giantin in docking COPI vesicles to Golgi membranes. *J Cell Biol*, **140**, 1013–1021.

Stamnes, M. (2002). Regulating the actin cytoskeleton during vesicular transport. *Curr Opin Cell Biol*, **14**, 428–433.

Stamnes, M., Craighead, M., Hoe, M., Lampen, N., Geromanos, S., Tempst, P., and Rothman, J. (1995). An integral membrane component of coatomer-coated transport vesicles defines a family of proteins involved in budding. *Proc Natl Acad Sci USA*, **92**, 8011–8015.

Steams, T., Willingham, M., Botstein, D., and Kahn, R. (1990). ADP-ribosylation factor is functionally and physically associated with the Golgi complex. *Proc Natl Acad Sci USA*, **87**(3), 1238–1242.

Sung, C.-H. and Tai, A. (2000). Rhodopsin trafficking and its role in retinal dystrophies. *Int Rev Cytol*, **195**, 215–267.

Sutterlin, C., Hsu, P., Mallabiabarrena, A., and Malhotra, V. (2002). Fragmentation and dispersal of the pericentriolar Golgi complex is required for entry into mitosis in mammalian cells. *Cell*, **109**, 359–369.

Svitkina, T., Neyfakh, A. A., and Bershadsky, A. (1986). Actin cytoskeleton of spread fibroblasts appears to assemble at the cell edge. *J Cell Sci*, **82**, 235–248.

Tamkun, J., Kahn, R., Kissinger, M., Brizela, B., Rulka, C., Scott, M., and Kennison, J. (1991). The arflike gene encodes and essential GTP-binding protein in Drosophila. *Proc Natl Acad Sci USA*, **88**(8), 3120–3124.

Thyberg, J. and Moskalewski, S. (1999). Role of microtubules in the organization of the Golgi complex. *Exp Cell Res*, **246**, 264–279.

Tokuyasu, K. and Yamada, E. (1959). The fine structure of the retina studied with the electron microscope. IV. Morphogenesis of outer segments of retinal rods. *J Biophys Biochem Cytol*, **6**, 225–230.

Ungar, D., Oka, T., Krieger, M., and Hughson, F. (2006). Retrograde transport on the COG railway. *Trends in Cell Biol*, **16**(2), 113–120.

Vaughan, K. (2005). Microtubule plus ends, motors, and traffic of Golgi membranes. *Biochim Biophys Acta*, **1744**, 316–324.

Vetter, I. and Wittinghofer, A. (2001). The Guanine Nucleotide-Binding Switch in Three Dimensions. *Science*, **295**(9), 1299–1304.

Walenta, J., Didier, A., Liu, X., and Krämer, H. (2001). The Golgi-associated Hook3 protein is a member of a novel family of microtubule-binding proteins. *J Cell Biol*, **152**, 923–934.

Walther, Z., Vashishtha, M., and Hall, J. (1994). The Chlamydomonas FLA10 gene encodes a novel kinesin-homologous protein. *J Cell Biol*, **26**(1), 175–188.

Wang, Q., Pan, J., and Snell, W. (2006). Intraflagellar transport particles participate directly in cilium-generated signaling in *Chlamydomonas*. *Cell*, **125**(3), 549–562.

Wang, W., Sacher, M., and Ferro-Novick, S. (2000). TRAPP stimulates guanine nucleotide exchange on Ypt1p. *J Cell Biol*, **151**(2), 289–296.

Wang, Y. (1985). Exchange of actin subunits at the leading edge of living fibroblasts: possible role of treadmilling. *J Cell Biol*, **101**, 597–602.

Ward, T., Polishchuk, R., Caplan, S., Hirschberg, K., and Lippincott-Schwartz, J. (2001). Maintenance of Golgi structure and function depends on integrity of ER export. *J Cell Biol*, **155**, 557–570.

Weber, T., Zemelman, B., McNew, J., Westermann, B., Gmachl, M., Parlati, F., Söllner, T., and Rothman, J. (1998). SNAREpins: minimal machinery for membrane fusion. *Cell*, **92**(6), 759–772.

Wedaman, K., Meyer, D., Rashid, D., Cole, D., and Scholey, J. (1996). Sequence and submolecular localization of the 115-kD accessory subunit of the heterotrimeric kinesin-II (KRP85/95) complex. *J Cell Biol*, **132**, 371–380.

Weide, T., Koster, M., and Barnekow, A. (1999). Inactive and active mutants of rab1b are not tightly integrated into target membranes. *Int J Oncol*, **15**(4), 727–736.

Weimbs, T., Low, S., Chapin, S., Mostov, K., Buchner, P., and Hofmann, K. (1997). A conserved domain is present in different families of vesicular fusion proteins a new superfamily. *Proc Natl Acad Sci USA*, **94**, 3046–3051.

Whiteheart, S., Brunner, M., Wilson, D., Wiedmann, M., and Rothman, J. (1992). Soluble N-ethylmaleimide-sensitive fusion attachment proteins (SNAPs) bind to a multi-SNAP receptor complex in Golgi membranes. *J Biol Chem*, **267**, 12239–12243.

Wieland, F. and Harter, C. (1999). Mechanisms of vesicle formation: insight from the COP system. *Curr Opin Cell Biol*, **4**, 440–446.

Wilson, D., Whiteheart, S., Wiedmann, M., Brunner, M., and Rothman, J. (1992). A multisubunit particle implicated in membrane fusion. *J Cell Biol*, **117**, 531–538.

Witman, G. (1990). *Ciliary and Flagellar Membranes*, chapter Introduction to cilia and flagella, pages 1–30. Plenum, New York.

Wu, M., Lu, L., Hong, W., and Song, H. (2004). Structural basis for recruitment of GRIP domain Golign-245 by small GTPase Arl1. *Nat Struct Mol Biol*, **11**, 86–94.

Wu, X., Rao, K., Zhang, H., Wang, F., Sellers, J., Matesic, L., Copeland, N., Jenkins, N., and Hammer, J. (2002). Identification of an organelle receptor for myosin-Va. *Nat Cell Biol*, **4**, 271–278.

Yin, G., Dai, J., Ji, C., Ni, X., Shu, G., Ye, X., Dai, J., .Wu, Q., Gu, S., Xie, Y., Zhao, R., and Mao, Y. (2003). Cloning and characterization of the human IFT20 gene. *Mol Biol Rep*, **30**, 255–260.

Yoshimura, S.-I., Egerer, J., Fuchs, E., Haas, A., and Barr, F. (2007). Functional dissection of Rab GTPases involved in primary cilium formation. *J Cell Biol*, **178**(3), 363–369.

Yoshino, A., Bieler, B., Harper, D., Cowan, D., Sutterwala, S., Gay, D., Cole, N., McCaffery, J., and Marks, M. (2003). A role for GRIP domain proteins and/or their ligands in structure and function of the trans Golgi network. *J Cell Sci*, **116**(21), 4441–4454.

Young, J., Stauber, T., DelNery, E., Vernos, I., Pepperkok, R., and Nilsson, T. (2005). Regulation of microtubule-dependent recycling at the trans-Golgi network by Rab6A and Rab6A'. *Mol Biol Cell*, **16**, 162–177.

Zerial, M. and McBride, H. (2001). Rab Proteins as Membrane Organizers. *Mol Cell Biol*, **2**, 107–119.

Zhao, L., Helms, J. B., Brunner, J., and Wieland, F. (1999). GTP-dependent binding of ADP-ribosylation factor to coatomer in close proximity to the binding site for dilysine retrieval motifs and p23. *J Biol Chem*, **274**, 14198–14203.

Zhao, X., Lasell, T., and Melancon, P. (2002). Localization of large ADP-ribosylation factor-guanine nucleotide exchange factors to different Golgi compartments: evidence for distinct functions in protein traffic. *Mol Biol Cell*, **13**, 119–133.

Publications

Parts of this work are published in:

Yoshimura, S., **Egerer, J.**, Fuchs, E., Haas, A.K., and Barr, F.A. (2007). Functional dissection of Rab GTPases involved in primary cilium formation. *J Cell Biol*, **178**, 363-369.

Reviews:
Barr, F.A. and **Egerer, J.** (2005). Golgi Positioning: are we looking at the right MAP? *J Cell Biol*, **168**, 993-998.

Acknowledgements

I would like to thank Prof. Dr. Francis A. Barr from the University of Liverpool for taking me up and providing me with this exciting and interesting topic, for continuous advice, support and teachings about cell biology. Further, I want to thank him for the many interesting discussions and amusing stories about things not directly related to science.

My special thanks go to Prof. Dr. Erich A. Nigg for his work as head of my thesis committee. Further, I want to thank him for his advice and questions during the lab meetings, which often gave a nudge into the right direction.

Furthermore, I want to thank Prof. Dr. H. MacWilliams for writing the "Zweitgutachten" for my thesis. I also thank all further members of my thesis committee.

Thanks also go to Dr. Thomas Keil for his efforts on getting an electron microscopy view of the Golgi.

Many thanks go to my colleagues from the "Barr-lab", Dr. Rüdiger Neef, Dr. Dipl.-Ing. Christian Preisinger, Dr. Ben Short, Evelyn Fuchs, Alexander Haas, Robert Kopajtich and Anna-Maria Goebel for advice, help, discussion, friendship and lots of fun in between Western blot and microscope. Thanks also go to the people from the Nigg Department for the nice time and to Dr. Eunice Chan for many strange discussions about life.

Special thanks go to Dr. Shin-ichiro Yoshimura for his teachings about cell biology, life in science and Japanese culture. Thanks for your friendship, which will hopefully last when you become a professor.

Thanks to my childhood friends, Sven, Mathias and Sebastian for keeping in touch in spite of me being far away and often unavailable. Thanks to my friends in Munich, Barbara, Oliver, Florian, Jürgen, Daniel, Michael, Imke and Andreas for making the sometimes hard periods in the lab easier by giving me a refuge to clear my head.

I want to thank Eva for being there for me through this busy time.

Finally I want to thank my parents and family for their support, help and affection. Without them this would have never been possible.

Curriculum Vitae

Personal Details:

Name	Johannes Thilo Egerer
Date of Birth	30.7.1977
Place of Birth	Marktredwitz, Germany
Nationality	German

Education:

1984-1988	Grundschule Marktredwitz II (elementary school)
1988-1997	Otto-Hahn Gymnasium Marktredwitz
	Abitur (university entrance qualification) grade 1,1
1997-1998	Obligatory social service: Gemeinde Diakonie Marktredwitz
1998-2003	University of Bayreuth: Studies of Biochemistry
	Diploma grade 1,2
April-August 2002	Universite Paris 7, Institut de Biologie Physico-Chimique
	Subject: Inhibition of Rab27 Expression in PC12 and Chromaffin Cells by RNA Interference
Nov. 2002-May 2003	Diploma Thesis at the Department for Microbiology
	with Prof. Dr. Ortwin W. Meyer
	Subject: Substratanaloge Inhibitoren der Kohlenmonoxid-Dehydrogenase von *Oligotropha carboxidovorans*
Since 2003	PhD Thesis at the Max-Planck Institute of Biochemistry
	at the independent junior research group Intracellular Protein Transport with Prof. Dr. Francis A. Barr
	Subject: The Golgin GMAP-210: Functions and Mechanisms

Additional Qualifications:

Good command of written and spoken French

Good knowledge on the Linux Operating System

Good knowledge in the LaTeX software

Good knowledge in computer hardware